PERFORMANCE OF DUAL-HOP RELAY NETWORKS WITH CO-CHANNEL INTERFERENCE AND MULTIPATH FADING

BY

ANAS M. SALHAB

A Dissertation Presented to the

DEANSHIP OF GRADUATE STUDIES

KING FAHD UNIVERSITY OF PETROLEUM & MINERALS

DHAHRAN, SAUDI ARABIA

In Partial Fulfillment of the

Requirements for the Degree of

DOCTOR OF PHILOSOPHY

In

ELECTRICAL ENGINEERING

MAY, 2013

KING FAHD UNIVERSITY OF PETROLEUM & MINERALS
DHAHRAN 31261, SAUDI ARABIA

DEANSHIP OF GRADUATE STUDIES

This thesis, written by **ANAS M. SALHAB** under the direction of his thesis adviser and approved by his thesis committee, has been presented to and accepted by the Dean of Graduate Studies, in partial fulfillment of the requirements for the degree of **DOCTOR OF PHILOSOPHY IN ELECTRICAL ENGINEERING**.

Dissertation Committee

Dr. Salam A. Zummo (Adviser)

Dr. M.-S. Alouini (Member)

Dr. Mohamed Deriche (Member)

Dr. Tareq Al-Naffouri (Member)

Dr. Ali Muqaibel (Member)

Dr. Ali A. Al-Shaikhi
Department Chairman

Dr. Salam A. Zummo
Dean of Graduate Studies

11/5/13
Date

To my parents, wife,

and

To my siblings

ACKNOWLEDGMENTS

Firstly and always I thank Allah "Lord of the Worlds" for his endless bestowal in making me live these great moments. Without his support and mercy, I would not have reached here.

My great respect and appreciation to my dear advisor Prof. Salam Zummo for his endless support and encouragement. I am greatly thankful to his way of teaching and supervision. He taught me how to think, how to be creative, and how to be in the right side of research. His rich knowledge in communications, his comments and suggestions left a great addition to my research.

I also would like to thank the committee members of my dissertation Prof. Mohamed-Slim Alouini, Dr. Mohamed Deriche, Dr. Tareq Al-Naffouri, and Dr. Ali Muqaibel for their constructive comments, suggestions, and support. My grateful thanks to my research partner my dear friend Dr. Fawaz Al-Qahtani for the great times we had together doing research.

I am greatly grateful to my parents, brothers, and sisters for their endless love, prayers, and support during my academic journey.

My loving thanks to my dear wife Ghadeer for her great support and patience during this long journey in my PhD. You deserve a part of this dissertation.

I send my great thanks to my EE department and my university KFUPM.

TABLE OF CONTENTS

LIST OF FIGURES

LIST OF ACRONYMS

AF	Amplify-and-Forward
AWGN	Additive White Gaussian Noise
BS	Base Station
CCDF	Complementary Cumulative Distribution Function
CDF	Cumulative Distribution Function
CCI	Co-Channel Interference
CSI	Channel-State Information
CTS	Clear-to-Send
DF	Decode-and-Forward
EGC	Equal-Gain Combining
e2e	End-to-End
LOS	Line-of-Sight
MGF	Moment-Generating Function
MRC	Maximal-Ratio Combining
MS	Mobile Station
PDF	Probability Density Function
RTS	Ready-to-Send

SC	Selection Combining
SEC	Switch-and-Examine Diversity Combining
SECps	Switch-and-Examine Diversity Combining with Post Examining Selection
SEP	Symbol Error Probability
SINR	Signal-to-Interference Plus Noise Ratio
SNR	Signal-to-Noise Ratio
TDMA	Time-Division Multiple-Access

THESIS ABSTRACT

NAME:	Anas M. Salhab
TITLE OF STUDY:	Performance of Dual-Hop Relay Networks with Co-Channel Interference and Multipath Fading
MAJOR FIELD:	Electrical Engineering
DATE OF DEGREE:	May 2013

Multipath fading *is one of the most challenging problems in wireless systems. It is a normal result to the multipath propagation nature of wireless channels. Relay networks in which a relay or a set of relays are employed to help a source node sending its message to destination is an efficient technique used to provide space diversity. Another critical problem in wireless channels is the* ***interference****, which is a natural result to the dense re-use of spectrum between cells. In relay networks where all relays may use the same frequency band, the interference effect could be more severe on system performance compared to the noise effect. In this thesis, we propose two low-complexity relay selection schemes. By using the moment generating function approach and the statistics of signal at the output of destination combiner, we analyze the system outage and error performance*

with these selection schemes. Also, we evaluate the interference effect on the performance of relay systems employing these relaying schemes in addition to the well-known opportunistic and N^{th}-best relaying. By employing the statistics of signals at the first hop channels of relays and the conditional statistics of signal at the output of destination combiner, we derive the outage probability of such systems. Finally, we study the impact of interference on the outage and error performance of single relay systems over various fading environments where the statistics of the signal at the destination are used to derive these measures. In most of previous analysis, the system performance is studied at high values of signal-to-noise ratio where the diversity order and coding gain are derived and analyzed.

CHAPTER 1

INTRODUCTION

1.1 Motivation

In wireless networks, the multipath propagation phenomenon of wireless channels is the main cause for signal fading. Such channel impairment can be mitigated using diversity [1]. Space or multiple antennas diversity is particularly an attractive technique to deal with such channel impairment. It relies on the principle that the signals transmitted from geographically-spaced transmitters and/or to geographically-spaced receivers, experience independent fading. Other forms of diversity, e.g., frequency and time diversity can be combined with the space diversity as a way to gain more performance enhancement. Although, dramatic performance gains can be offered by having it alone when other diversity types are not available. In conventional space diversity, a physical array of antennas is implemented on either the transmit side or the receive side, or even on both. From practical point of view, especially, in the uplink channel of a cellular system, having

multiple antennas in a mobile station (MS) is impractical due to size, complexity, and extra power they need. The idea of user cooperation came as a promising technique to solve such problem. In this technique, two users or more cooperate with each others in conducting their data transmission. A study that introduces this technique was presented in [2]. In that paper, the authors introduced the idea of user cooperation in a coded cooperative system where convolutional codes were used.

In contrast to the conventional space diversity forms, like the physical arrays [3], [4], the classical relay channel model [5] was used in [6] to provide the space diversity. In the proposed system, a collection of distributed antennas belonging to multiple terminals are exploited to provide space diversity, each terminal with its own information to transmit. This form of space diversity is also known as cooperative diversity (user cooperation diversity of [7]). This is because the terminals share their antennas and other resources to create a "virtual array" and perform their own transmissions and help in that belong to the others. Currently, several relaying schemes and protocols are being used in practice [6]. Among the relaying schemes are the amplify-and-forward (AF) and the decode-and-forward (DF) [6]. In AF scheme, the relay simply amplifies the source message before forwarding it to destination. In DF scheme, some signal processing need to be performed by the relay before the message being forwarded to destination. In general, the AF systems are classified into two subcategories, the channel-state information (CSI)-based gain relays, which use the instantaneous CSI from the previous hop,

and the fixed-gain relays, which introduce a fixed gain in forwarding the source messages. The CSI-assisted AF relay system requires a continuous estimation of the channel fading amplitudes to produce its gain and to limit the output power of the relay. In contrast, the fixed-gain relay system introduces a fixed scale to the received message regardless of the fading amplitudes which leads to a variable signal power at the relay output. This subcategory has a lower complexity compared to the former type.

In addition to the relaying schemes, several relaying protocols exist in practice [6]. They are mainly divided into three types, fixed, selection, and incremental relaying. In fixed relaying, the relays are allowed to forward the source message to destination after either amplifying it according to their power constraint, or after decoding and re-encoding operations applied on message before being forwarded. In selection relaying, the relays are chosen to be either cooperative or non-cooperative according to the signal-to-noise ratio (SNR) measurements of their channels. Finally, in incremental relaying, the relay is asked to cooperate based on a limited feedback from the destination to the source and according to the need of that cooperation. Compared to the former ones, the incremental relaying can enhance the spectral efficiency of a relay system.

Recently, several relaying schemes have been proposed, among which is the best relay or opportunistic relaying [8]. In this scheme, the relay with the best end-to-end (e2e) SNR is selected among other relays to forward the source message to destination. This scheme is optimum in the sense that the best relay is being

selected all the time. A crucial requirement for this scheme is that channels of all relays need to be estimated each time of transmission for best relay to be selected. This means a heavy load of channel estimations and hence, a highly complicated system. Another relaying scheme is the partial relaying [9]-[11]. In such scheme, a partial knowledge of the relay channels is required to perform the relay selection. Such condition is existed in ad-hoc networks where only neighboring (one hop) channel information is available to the nodes. Compared to channel estimation load in opportunistic relaying, half that load is required in the partial relaying scheme. A new relay selection scheme was presented and analyzed in [12]-[14]. This scheme is called the N^{th}-best relaying and it is efficient for situations where the best relay is involved in some scheduling or load balancing duties. In this scheme, the second or even the N^{th} best relay which has the highest e2e SNR is selected to forward the source message to destination. In this dissertation, we propose and evaluate the performance of two low-complexity relay selection schemes for dual-hop fixed gain AF relay systems. We also study the performance of such system at high SNR regime. The proposed schemes are based on the well-known switch-and-examine diversity combining (SEC) and switch-and-examine diversity combining with post examining selection (SECps) techniques. Such techniques proved their effectiveness as low-complexity antenna selection schemes in space diversity systems [15]. The aim of proposing these schemes is to reduce the required number of channels estimations compared to other relaying schemes as the opportunistic and partial relaying. In the proposed schemes, the first checked

relay whose e2e SNR satisfies a predetermined switching threshold is selected instead of the best relay to forward the source message to destination. Hence, the channels of only one relay are required to be estimated each transmission time. This saves the battery life of relays, reduces the power consumption, and hence, reducing the system complexity. Our contribution in this area of research is shown in figure 1.1.

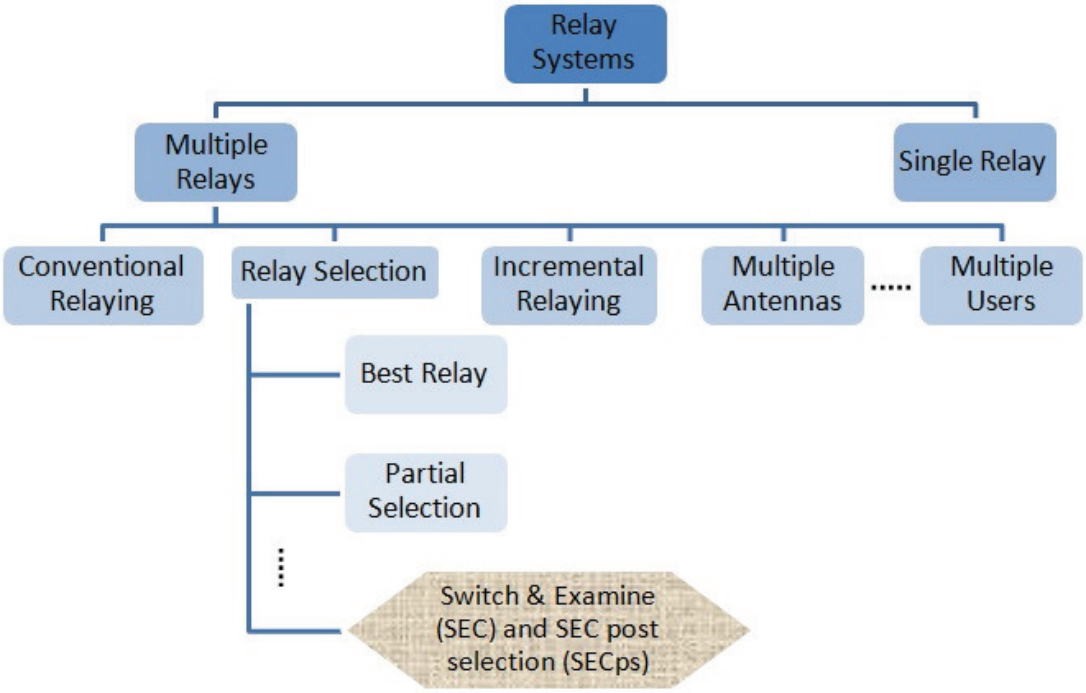

Figure 1.1: Our contribution in the area of relay selection schemes.

In general, the interference effect on the performance of relay networks with multiple relays is not widely studied. Recently, more attention has been given to evaluate such effect in multi-relay DF relay systems. In [16], the outage performance of a relay system with multiple relays and in the presence of interference at the relay and destination nodes was studied assuming Nakagami-m fading channels. Other key papers on cooperative systems with multiple relays and oppor-

tunistic relaying are the ones presented in [17], [18]. Particularly, in [17], Kim *et al.* evaluated the outage performance of an opportunistic DF relay system with interference at the relays and destination nodes. In [18], the outage and error performance of a regular DF relay system with interference at the relays and destination was evaluated assuming Rayleigh fading channels. The relays which successfully decode the source message in the first phase of communications forward it to the destination in the second phase. As mentioned before, the opportunistic relaying suffers from a heavy load of channel estimations. The lack of strong studies that evaluate the performance of multi-relay cooperative systems with interference at the relays and destination motivates us to contribute in this area of research. In this dissertation, we propose the low-complexity SEC and SECps relaying schemes for dual-hop DF relay systems with interference at the relays and destination as an alternative to the opportunistic relaying scheme. According to the proposed schemes, the first checked relay whose second hop channel's SNR satisfies a certain switching threshold is selected among other relays who successfully decode the source message in the first phase of communications to forward a re-encoded version of the message to destination in the second phase. In order to get more about system insights, we study the system performance at high SNR regime.

In this dissertation, we improve the work presented in [16] where the conventional DF relaying is extended to an opportunistic DF relaying by using different approach than the moment generating function (MGF) approach used in that paper. Using the best relay selection scheme reduces the amount of cooperation

overheads and enhances the system spectral efficiency. Furthermore, we evaluate the system behavior at the high SNR regime where more insights about the system performance like the diversity order and coding gain are provided. As mentioned before, an efficient relay selection scheme for situations where the best relay is unavailable for cooperation is the N^{th}-best relay selection scheme [12]. In this dissertation, we propose this scheme for dual-hop DF relay systems with interference at the relays and destination and evaluate the outage performance of such systems over Rayleigh fading channels. In the proposed scheme, the relay with the second or even the N^{th} best second hop SNR is selected to forward the source message to destination. This scheme simplifies to the scheme of best relay or opportunistic relaying when $N = 1$. We also analyze the system performance at high SNR regime where approximate expressions for the outage probability, diversity order, and the coding gain are provided and analyzed. Our contribution in this area of research is shown in figure 1.2.

In relay systems, considering the interference at the destination node is particularly relevant to time-division multiple-access (TDMA) systems in which a single time-slot is shared by many relays [19]. Recently, a lot of work has studied such phenomenon, among which are the papers in [20], [21]. In [20], closed-form expressions for both the outage and asymptotic outage probability of fixed-gain AF and DF relay systems in Rayleigh fading environments were evaluated. In [21], exact expressions for both the outage and asymptotic outage probability and symbol error probability (SEP) were derived with all links assumed to fol-

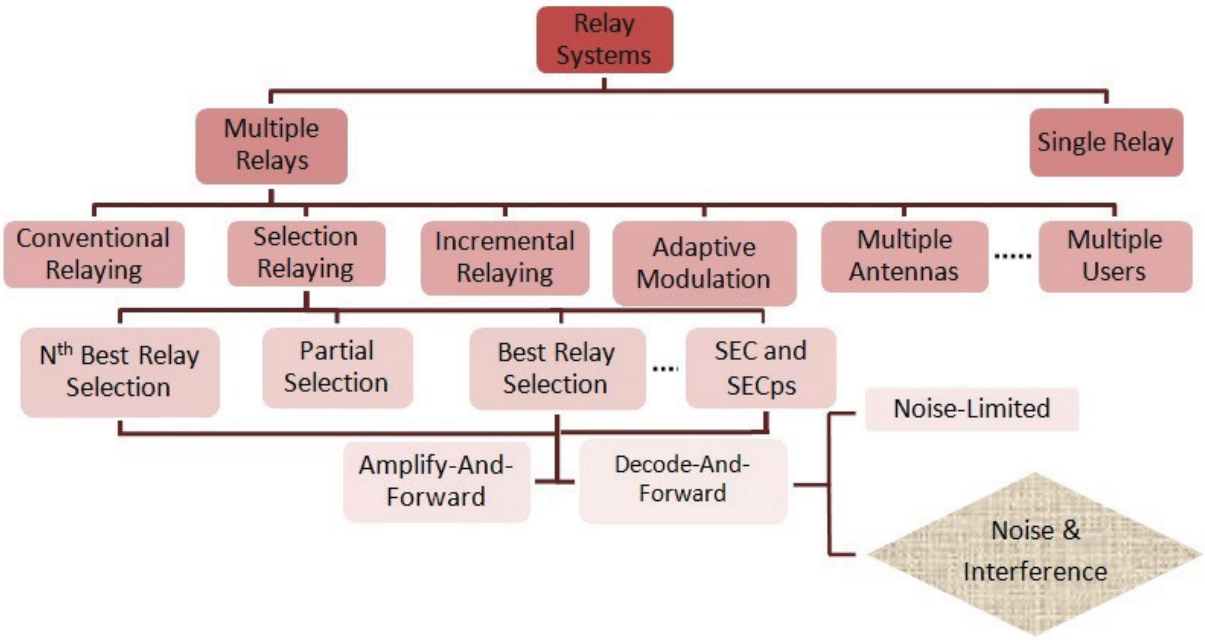

Figure 1.2: Our contribution in the area of DF relay systems with interference at the relays and destination.

low Nakagami-m distribution. Most of the research on single relay systems with interference at the destination node assumed Rayleigh or Nakagami-m fading environments. It is important to notice that in situations where line-of-sight (LOS) components exist in the system under investigation, the Rayleigh and Nakagami-m assumptions may not reflect the accurate behavior of the studied systems. In this dissertation, we evaluate the outage probability and SEP for single-relay AF systems with various fading environments, Rician/Nakagmi-m, Rician/ Rician, and Nakagami-m/Rician. Furthermore, in order to get more about the system insights, we evaluate the asymptotic system performance at high SNR values for special cases of the proposed fading scenarios. The asymptotic outage probability and SEP in addition to the diversity order and coding gain are derived and compared. Our contribution in this area of research is shown in figure 1.3.

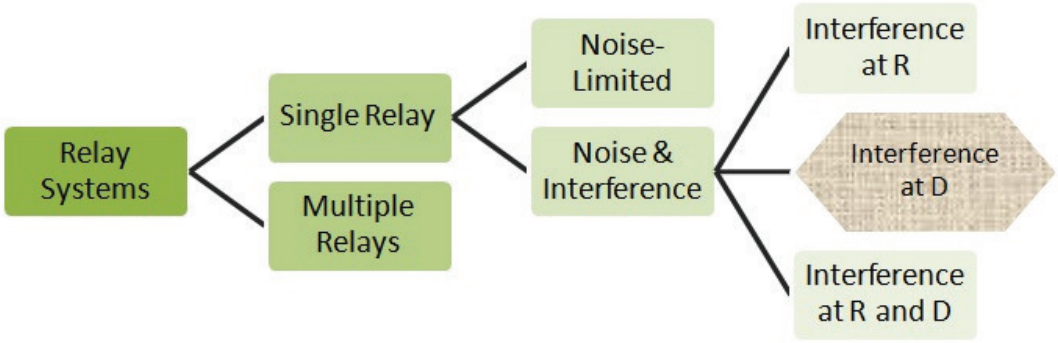

Figure 1.3: Our contribution in the area of single-relay AF relay systems with interference at the destination.

The rest of this chapter is organized as follows. The topics of multipath fading, diversity, and relay networks are briefly explained in Section 1.2. Section 1.3 explains the dissertation contributions. Finally, the dissertation outline is given in Section 1.4.

1.2 Background

1.2.1 Multipath Fading

Radiowave propagation through wireless channels is a complicated phenomenon characterized by various effects such as multipath and shadowing [22]. To deal with such effects, some statistical models and characterizations are required. If an extremely short pulse is transmitted over a time-varying multipath channel, the received signal will be a train of pulses [1]. Hence, one characteristic of a multipath medium is the time spread in the signal transmitted through that medium. A second characteristic is due to the time variations in the structure or nature of the medium. That is, if the same pulse is resent again for several

times, some changes in the received pulse train shall be observed. Such changes include, pulses size, delay between pulses, and number of pulses. This is called the impulse dispersion. The unpredictability nature of these variations bounds for a statistical modeling of the time-variant multipath channels.

As mentioned earlier, due to the multipath propagation, the received signal consists of an infinite sum of attenuated, delayed, and phase-shifted replicas of the transmitted signal, each influencing each other [23]. According to the phase of each component, the superposition can be constructive or destructive. Besides the multipath propagation, also the Doppler effect has a negative effect on the transmission characteristics of a mobile radio channel. Due to the movement of the communicating unit, the Doppler effect causes a frequency shift on each component of the received signal. When a received signal experiences a fading during its transmission, both its envelope and phase fluctuate over time. For coherent modulations, the change in signal phase can severely degrade the system performance. In such systems, some measures are taken to compensate for such effects. In systems where noncoherent modulations are used, the changes in signal phase due to fading have no effect on system performance. The coherent systems where the phase variations are assumed to be fully compensated for are called ideal coherent systems. Hence, in ideal coherent and noncoherent modulation systems, only the statistics of the fading envelope is required for evaluating the system performance.

In general, the fading can be classified in time domain into two types, slow and

fast fading. The distinction between these two types is important for the mathematical modeling of the fading channel and for evaluating the system performance. This notation is related to the coherence time, T_c, of the fading channel, which measures the period of time after which the correlation function of two samples of the channel response taken at the same frequency but different time instants drops below a certain predetermined threshold. The fading is said to be slow if the symbol time duration T_s is smaller than the channel coherence time T_c; otherwise, it is considered to be fast fading. In slow fading, any fade level will affect many successive symbols which results in burst errors; whereas, in fast fading, the fade effect will differ from one symbol to the other.

Another classification of channel fading is in the frequency domain. Here, the fading channel is classified according to its frequency selectivity characteristic to either a frequency-nonselective (flat) channel or frequency selective channel. If all frequency components of a transmitted signal are affected in the same manner, in this case, the channel is said to be frequency-nonselective or frequency-flat. This is the case for narrowband systems, where the transmitted signal bandwidth is much smaller than the channel coherence bandwidth f_c. This bandwidth measures the frequency bandwidth over which the correlation function of two samples of the channel response taken at the same time but different frequencies falls below a suitable value. On the other hand, in the case where all frequency components of a transmitted signal are affected with different amplitude gains and phase shifts, in this case, the fading channel is said to be frequency-selective. This usually

happens in the wideband systems where the bandwidth of the transmitted signal is bigger than the channel coherence bandwidth.

Due to the fast time variations in fading channel, a combination of delayed, reflected, scattered, and diffracted signal components reach the receiver. This combination could be constructive or destructive. Such type of fading is relatively fast and is therefore responsible for the short-term signal variations. Depending on the nature of the fading environment, several models are used to characterize the statistical behavior of the multipath fading envelope.

The Rayleigh distribution is usually used to model channels where there is no direct LOS path between the transmitter and the receiver [22]. In this case, the amplitude of the channel fading is a random variable and has the following probability density function (PDF)

$$f_\alpha(\alpha) = \frac{2\alpha}{\Omega} \exp\left(-\frac{\alpha^2}{\Omega}\right), \qquad \alpha \geq 0, \tag{1.1}$$

and hence, the instantaneous SNR per symbol of the channel γ has an exponential distribution given by

$$f_\gamma(\gamma) = \frac{1}{\bar{\gamma}} \exp\left(-\frac{\gamma}{\bar{\gamma}}\right), \qquad \gamma \geq 0. \tag{1.2}$$

Also, the Rayleigh fading model applies to the propagation of reflected and refracted paths through the troposphere and ionosphere, and to ship-to-ship radio links.

Nakagami-m fading PDF is in essence a chi-square distribution given by

$$f_\alpha(\alpha) = \frac{2m^m\alpha^{2m-1}}{\Omega^m\Gamma(m)}\exp\left(-\frac{m\alpha^2}{\Omega}\right), \qquad \alpha \geq 0, \tag{1.3}$$

where m is the Nakagami-m fading parameter, which ranges from $\frac{1}{2}$ to ∞. The SNR per symbol γ is distributed according to a gamma distribution given by

$$f_\gamma(\gamma) = \frac{m^m\gamma^{m-1}}{\bar{\gamma}^m\Gamma(m)}\exp\left(-\frac{m\gamma}{\bar{\gamma}}\right), \qquad \gamma \geq 0, \tag{1.4}$$

which reduces to Rayleigh fading when m=1. The Nakagami-m distribution often gives the best fit to land-mobile and indoor-mobile multipath propagation, as well as scintillating ionospheric radio links.

The Rician distribution is often used to model the propagation paths that consist of one strong direct LOS component and many random weaker components. Here, the channel fading amplitude has a distribution given by

$$f_\alpha(\alpha) = \frac{2(1+K)e^{-K}\alpha}{\Omega}\exp\left(-\frac{(1+K)\alpha^2}{\Omega}\right) I_0\left(2\alpha\sqrt{\frac{K(1+K)}{\Omega}}\right), \qquad \alpha \geq 0, \tag{1.5}$$

where I_0 is the modified Bessel function of the first type and order 0, and K is the Rician fading parameter and ranges from 0 to ∞, and it corresponds to the ratio of the power of the LOS component to the average power of the scattered component. The SNR per symbol γ has a noncentral chi-square distribution given

by

$$f_\gamma(\gamma) = \frac{(1+K)e^{-K}}{\bar{\gamma}} \exp\left(-\frac{(1+K)\gamma}{\bar{\gamma}}\right) I_0\left(2\sqrt{\frac{K(1+K)\gamma}{\bar{\gamma}}}\right), \qquad \gamma \geq 0. \quad (1.6)$$

The Rician distribution spans the range from Rayleigh fading (K=0) to no fading (constant amplitude) (K=∞). This type of fading is typically observed in the first resolvable LOS paths of microcellular urban and suburban land-mobile, picocellular indoor, and factory environments. It also applies to the dominant LOS path of satellite and ship-to-ship radio links.

1.2.2 Diversity

In wireless systems, having a transmitted signal in a deep fade increases the probability of receiving an erroneous signal at the receiver. Diversity is one way to combat such a problem by providing the receiver with multiple copies of the same transmitted signal. If p is the probability that any transmitted signal will fade below some critical value, then p^L is the probability that L independently fading replicas of the same signal will fade below that critical value.

There are several ways by which the receiver can be provided with a set of independently faded copies of the same information-bearing signal. One popular method is the frequency diversity. In this method, several copies of the signal are sent on a set of independently faded carriers with a frequency separation between any two successive carriers being larger than the channel coherence bandwidth f_c. A second method is to send multiple copies of the same signal on a set

of independently faded time slots with a time separation between the successive time slots being greater than the channel coherence time T_c. This method is called time diversity. One may view the transmission of the same information either at different frequencies or different time slots or at both as a simple form of repetition coding. The separation between carriers f_c and between time slots T_c is basically a form of block-interleaving the bits in the repetition code in an attempt to break up the error bursts and thus, to obtain independent errors. Another commonly used method is the space or antenna diversity. In this technique, two or more antennas are used to send and/or to receive multiple replicas of the same signal. It is based on the idea that sending or receiving a signal using geographically-spaced antennas will result in independently faded copies of this signal. This method can be implemented at the transmit side (transmit space diversity) or at the receive side (receive space diversity) or at both. The antenna elements must be spaced sufficiently far apart that the multipath components in the signal have significantly different propagation delay at the antennas. Usually, a separation of a few wavelengthes is required between two antennas in order to obtain signals that fade independently.

1.2.3 Relay Networks

As mentioned earlier, several methods are practically used to provide diversity in wireless systems, among which is the space diversity in which two or more antennas are implemented at either the transmit side, the receive side, or at both. From

practical point of view and, especially, in communications where a MS is involved in the communication process, having multiple antennas at the MS is impractical due to size, power, and complexity limitations. A promising technique to deal with such situation is to provide space diversity via cooperation between users. In this technique, in addition to sending their own messages, the users can utilize their antennas to help other colleagues in sending their messages. This idea is then extended to relay systems where one or more relays are used intentionally to help system users in performing their transmissions.

Recently, different topics in cooperative or relay networks have been opened for research work. Among these areas are the relaying scheme design, relaying protocols, relay selection, adaptive transmission, multiple antennas cooperative systems, multiuser cooperative networks, and combining techniques at the receive side. The most common relaying schemes are the AF and the DF relaying. Among the relaying protocols are the fixed relaying where a set of relays are used to forward the source message, the selection relaying where a relay or a number of relays are chosen to do the relaying process, and the incremental relaying where the relay or a number of relays are asked to cooperate according to the quality of the direct link. In systems where multiple relays are used, several selections schemes have been proposed. One popular scheme is the opportunistic relaying where only the best relay is chosen to do the relaying process. The relay selection criterion may depend on the quality of the first hop or the second hop, or it could depend on a certain SNR threshold. The adaptive modulation has been also introduced

in relay systems where the transmission rate is determined according the quality of system channels. Some authors have introduced the technique of multiple antennas to cooperative systems at either the source, the relay, the destination, or any combination of them. Recently, the topic of multiuser cooperative networks has been studied by many researchers. In these networks, the relays cooperate in receiving or forwarding signals to more than one node. Finally, the way the signals on the direct link and the relay pathes are combined at the destination has been studied in many papers. Among these techniques are the selection combining (SC), maximal-ratio combining (MRC), and the equal-gain combining (EGC).

1.3 Dissertation Contributions

In the area of relay selection schemes, we propose the SEC and SECps low-complexity relaying schemes. Compared to the opportunistic relaying scheme as an example, smaller number of channel estimations are required in the proposed relaying schemes. Firstly, we propose these schemes for dual-hop CSI-assisted AF relay systems where closed-form expressions for the system outage probability and SEP are derived assuming Rayleigh fading channels. In addition, the system performance is studied at high SNR regime where approximate expressions for the outage probability, diversity order, and the coding gain are evaluated and analyzed. Main results prove the effectiveness of the proposed schemes in reducing the required number of channel estimations and hence, reducing the system complexity. Also, findings show that the maximum gain achieved in system performance

happens in the range of SNR values that are comparable to the switching threshold. On the other hand, asymptotic results illustrate that the diversity order of the studied AF relay system with the proposed schemes is fixed at 2 and is not affected by the number of relays.

In the area of multi-relay dual-hop DF relay systems, we evaluate the outage performance of an opportunistic DF relay system with interference at the relays and destination assuming Nakagami-m fading environments. The main contribution of this work is that it is the first work in this area that evaluates the exact outage probability of such systems over Nakagami-m fading channels. Another contribution is that we evaluate the system behavior at the high SNR regime where more insights about the system performance like the diversity order and coding gain are provided. Main results illustrate that under the condition of finite number of interferers of finite powers, the system can still achieve full diversity order; whereas, a noise floor appears in the results and hence, a zero diversity gain is achieved when the interference power scales with SNR. Other results show that the interference at the destination is more severe on the system performance compared to that at the relay node.

Another contribution in the area of multi-relay DF relay systems with interference at the relays and destination is the proposed N^{th}-best relaying scheme. We propose and analyze the performance of this relaying scheme which is efficient in situations where the best relay is involved in some load balancing or scheduling duties in other parts of the network. We derive exact closed-form expression for

the system outage probability assuming Rayleigh fading channels. The system performance is also studied at high SNR regime. Main findings illustrate that the outage probability increases as the order of relay increases. Also, results show that the diversity order linearly increases with the number of relays and linearly decreases with the order of the relay. In addition, asymptotic results illustrate that the system is still able to achieve full diversity gain in the presence of finite number of interferers of finite powers. Finally, findings show that the diversity order linearly increases with the number of active relays although one relay is being used only.

Another addition to the area of DF relay systems with interference at the relays and destination is the proposed SEC and SECps relaying schemes to select between relays in such systems. We derive exact closed-form expression for the system outage probability assuming Rayleigh fading channels. Furthermore, we study the system performance at high SNR values where approximate expressions for the outage probability, diversity order, and the coding gain are derived and analyzed. Results show that the proposed schemes prove their effectiveness in reducing the system complexity compared to the opportunistic relaying scheme. Findings illustrate that for fixed number of interferers of fixed power or equivalently, when the interference power does not scale with SNR, the system can still achieve diversity gain; especially, in the range of SNR that is comparable to the switching threshold. Also, asymptotic results show that the system achieves the same diversity order which is 2 and approximately the same coding gain for the

cases of SEC and SECps relaying schemes. Finally, findings illustrate the severe effect of interference on the gain achieved by the SECps relaying scheme compared to the conventional SEC scheme.

The last research area we contribute in is the dual-hop fixed-gain AF relay systems with single relay and interference-limited destination. In this avenue, we evaluate the performance of such systems considering some new fading environments for the desired user channels and the interferers' channels. These scenarios are: Rician/Nakagami-m, Rician/Rician, and Nakagami-m/Rician. The considered fading scenarios are useful for situations where a LOS component is involved in the communications as in micro-cellular mobile and indoor radio systems. We derive approximate expressions for the outage probability and the SEP for all proposed fading models. Furthermore, we study the system performance of some special cases of the proposed scenarios at high SNR regime. Main results show that with different fading models for the interferers' channels, the interference is only affecting the system behavior through the coding gain without affecting the diversity order of the system. Finally, findings illustrate that approximating the Rician fading model by the Nakagami-m model does not give accurate results at least in our presented study.

1.4 Dissertation Outline

In Chapter 2, the performance of a CSI-assisted AF relay system with the SEC and SECps-based relaying schemes is evaluated assuming Rayleigh fading chan-

nels. We derive expressions for the outage probability and SEP using an upper bound on the SNR of a relay path. The asymptotic high SNR behavior of the system is also studied via deriving approximate expressions for the outage probability, diversity order, and coding gain. Furthermore, flowcharts for the proposed relaying protocols are provided in this chapter.

In Chapter 3, we propose the SEC and SECps-based relaying schemes for DF relay systems with interference at the relays and destination. We derive exact closed-form expression for the outage probability assuming Rayleigh fading channels for all links in the system. Furthermore, we study the system performance at high SNR values where approximate expressions for the outage probability, diversity order, and the coding gain are derived and analyzed. Flowcharts for the proposed relaying protocols are also provided and explained. The special case where there is no interference is also considered in this chapter where closed-form expression for the system outage probability is derived.

Chapter 4 studies the interference effect at both the relay and destination nodes on the performance of an opportunistic best relay DF relay system assuming Nakagami-m fading channels. Also, we study the system behavior at high SNR values and derive approximate expressions for the outage probability, diversity order, and coding gain of the system. Both non-identical and identical cases of interferers' channels are considered in the analysis.

In Chapter 5, we evaluate the outage performance of an opportunistic N^{th}-best relay DF relaying system with interference at the relay and destination nodes. We

derive exact closed-form expression for the outage probability assuming Rayleigh fading environments. Furthermore, we evaluate the system performance at the high SNR regime where approximate expressions for the outage probability, diversity order, and coding gain are provided and analyzed. Both, non-identical and identical cases of interferers' channels are considered in the analysis of this chapter.

In Chapter 6, we propose and evaluate the performance of three fading models for fixed-gain AF relay systems with interference-limited destination. The considered fading scenarios are: Rician/Nakagami-m, Rician/Rician, and Nakagami-m/Rician. Approximate expressions for the outage probability and SEP are derived. Also, we derive approximate expressions for the outage probability and SEP at high SNR values for some special cases of the considered fading scenarios.

Finally in Chapter 7, we briefly summarize the main conclusions of the dissertation and point out possible future research directions.

CHAPTER 2

AF RELAY SELECTION USING SWITCH-AND-EXAMINE IN NOISE-LIMITED CHANNELS

2.1 Introduction

In this chapter, we present a low-complexity relay selection scheme for CSI-assisted dual-hop AF cooperative systems. The scheme is mainly based on the switch-and-examine diversity combining and switch-and-examine diversity combining with post examining selection techniques in which a relay is selected out of multiple relays to forward the source message to destination. The selection process is performed such that the selected relay SNR satisfies a predetermined switching threshold instead of best relay. Such a relay that satisfies this threshold will be chosen instead of the best relay. In the analysis, we use an upper bound on the

e2e SNR of the selection scheme and derive the PDF and the cumulative distribution function (CDF) of this SNR assuming Rayleigh fading channels. These statistics are then used to derive accurate approximations for both the e2e outage probability and SEP where the direct link is considered. We assume that MRC is used at the destination to combine the signals through the relay and the direct link. To get more about system insights, the outage performance is studied at high SNR regime where approximate expressions for the outage probability as well as the diversity order and coding gain are derived and analyzed. Monte-Carlo simulations are provided to illustrate the validity of the analytical results and to show the tightness of the used SNR bound. Results illustrate the effectiveness of the proposed relaying schemes in reducing the required number of channel estimations compared to the opportunistic relaying. Furthermore, results show the gain achieved in system performance, especially, at low to medium SNR values when the SECps selection scheme is used compared to the conventional SEC relaying. Finally, findings show that the system with the SEC and the SECps relaying schemes has the same diversity order of 2 and the same coding gain.

The rest of this chapter is organized as follows. Section 2.2 reviews related literature. Section 2.3 explains the system model. The performance analysis of the SEC and SECps relaying schemes is conducted in Section 2.4 and Section 2.5, respectively. Section 2.6 gives a simple method for calculating optimum switching threshold. In Section 2.7, some numerical results are discussed. Finally, some conclusions are provided in Section 2.8.

2.2 Literature Review

In last few years, several relay selection schemes were proposed and being used in multi-relay cooperative systems. In [8], the authors proposed the opportunistic relay selection scheme where the relay with the strongest e2e SNR is selected to forward the source message. This scheme is optimal in the sense that in each transmission period the relay with the strongest e2e SNR is selected to forward the source message. On the other hand, this scheme suffers from a heavy load of channel estimations where all relays channels are required to be estimated first before the best relay being selected. Some papers on the performance of relay systems with opportunistic relaying are presented in [25], [26]. In these studies, in order for a destination or a central unit to select the best relay among all other relays, the channels of all relays need to be estimated first.

A partial relay selection scheme for AF relay systems was proposed in [13]. In this scheme, the relay with the best first hop is chosen to forward the source message to destination. The partial relaying schemes are useful for certain practical situations in ad-hoc networks where only the first hop channels of relays are available to the source. In [12], Ikki *et al.* presented a new relay selection scheme where the relay with the second or even the N^{th}-best e2e SNR is selected to forward the source message to destination. This scheme is useful in situations where the best relay may not be available to cooperate due to some scheduling or load balancing conditions. Some relay selection schemes that are based on certain functions of the two hops SNRs like the modified harmonic mean were presented

and evaluated in [27].

A key study that presents new relaying scheme in which the selection criterion is based on the magnitudes of the relays channels and not on the channels SNRs was presented in [28]. The authors claimed that these selection schemes are less complicated if compared with the schemes where the channels SNRs are required to be estimated in the relay selection process. Three energy-fair decentralized relay selection techniques in wireless sensor networks whose nodes are uniformly distributed according to a two-dimensional homogeneous Poisson process were proposed in [29]. The importance of these schemes is that they take the network topological structure into consideration. A partial relay selection scheme was proposed in [30]. This protocol is based on the DF relaying where the relay with a first hop SNR larger than a constant switching threshold is chosen to forward the source message only if its second hop SNR exceeds the same switching threshold. The authors considered the case of identical relay paths and the switching threshold was assumed to be constant in the analysis. Furthermore, the outage and the bit error probabilities were numerically evaluated and no closed-from expressions were provided. A study on the performance of some relaying schemes like selection relaying and switched relaying was presented in [31]. The direct link was ignored in the analysis and the switching threshold was assumed to be fixed. Also, only the case of identical relay paths was presented and the performance measures were numerically evaluated without providing any analytical expressions.

Recently, a new relay selection scheme was presented in [32] assuming Rayleigh

faded channels. The authors called it switch-and-stay partial relay selection. They implemented their scheme only on the first hop channels of the two relays. It works as follows, the first hop channel of the active relay is compared with a certain SNR threshold. If it is larger, then this relay continues forwarding the source message to destination in the next transmission period. If not, the second idle relay is asked by the source to do the cooperation process in the next transmission time slot. This relaying scheme reduces the complexity of the other relaying schemes which require the channels of both relays to be estimated each transmission period. On the other hand, a drawback of this scheme is that it does not consider the second hop channels of relays in the selection process. Also, this scheme is limited to the practical situation where two relays are being utilized. In addition, the authors assumed no existence of the direct link between the source and the destination in their analysis. Most recently, a paper on switched relay selection schemes for AF relay systems has been presented in [33]. The authors utilized some switched selection schemes for AF relay systems with multiple antennas. The performance measures were numerically computed and no closed-form expressions were provided. Also, the direct link was ignored in the analysis and the switching threshold was assumed to be constant.

As can be seen, most of the relay selection schemes in the aforementioned studies suffer from a heavy load of channel estimations. As an example, the best relay selection scheme requires that channels of all relays be estimated each transmission time. On the other hand, in the partial relaying scheme, half this

estimation load is required each time. This means more power consumption, low battery life, and high system complexity. As known, in most wireless systems like the sensor and ad-hoc networks, once the minimum requirements of the system performance are achieved, no more operations that increase the system complexity need to be conducted. This shows the significant need for new relay selection schemes with low implementation complexity and adequate system performance.

Motivated by the above discussion, we propose a low-complexity suboptimal relay selection scheme for CSI-assisted dual-hop AF relay systems. This scheme is based on the SEC and SECps techniques. The need for channels to be estimated in CSI-based AF relay systems motivated us to consider such a type and not the fixed-gain AF relaying where fixed relay scales are usually used. The contributions of our analysis over the existing studies are summarized in the following points: *i*) in contrast to [30] where constat switching threshold was assumed, the switching threshold is evaluated to minimize the SEP at the output of the MRC combiner and thus giving optimum performance; *ii*) our proposed analysis is a non-trivial extension of [32] where switch-and-stay was employed using two relays only; *iii*) we present a comprehensive study for the outage performance of both relaying schemes at high SNR regime where the diversity order and coding gain are derived and analyzed, *iv*) due to its importance, the direct link is considered in all our derivations in contrast to that presented in [32]; and *v*) closed-form expressions for both the outage probability and SEP of the generic independent non-identical distributed (i.n.d.) and independent identical distributed (i.i.d.) cases of relay

paths are provided in our study in contrast to [30] where only the i.i.d. case was considered. In the proposed scheme, only the first checked relay whose e2e SNR exceeds the switching threshold is selected to forward the source message to destination. Thus, in contrast to the aforementioned relay selection schemes, the channels of only an arbitrary relay are required to be estimated each time of data transmission. In this case, the other relays remain silent and do not need to operate as channel estimators. This results in a noticeable reduction in the required number of channel estimations and saves the power of these relay and hence, reducing the system complexity. In the analysis of this chapter, we first derive the PDF and the CDF of the SNR at the output of the selection scheme. Then, we consider the existence of the direct link and derive closed-form expression for the CDF and hence, the outage probability of the e2e SNR at the output of the MRC combiner. Finally, we evaluate closed-form expression for the SEP of the whole system. An upper bound on the SNR of the relay path is used in the analysis. The asymptotic behavior is derived in the same manner.

2.3 System Model

The system under investigation is shown in Figure 2.1. In this system, a source node (S) communicates with a destination node (D) through the direct link and a relay path. At the guard period of each transmission, a ready-to-send (RTS) packet and a clear-to-send (CTS) packet are sent from the source and the destination, respectively. From these signals, an arbitrary relay out of M relays

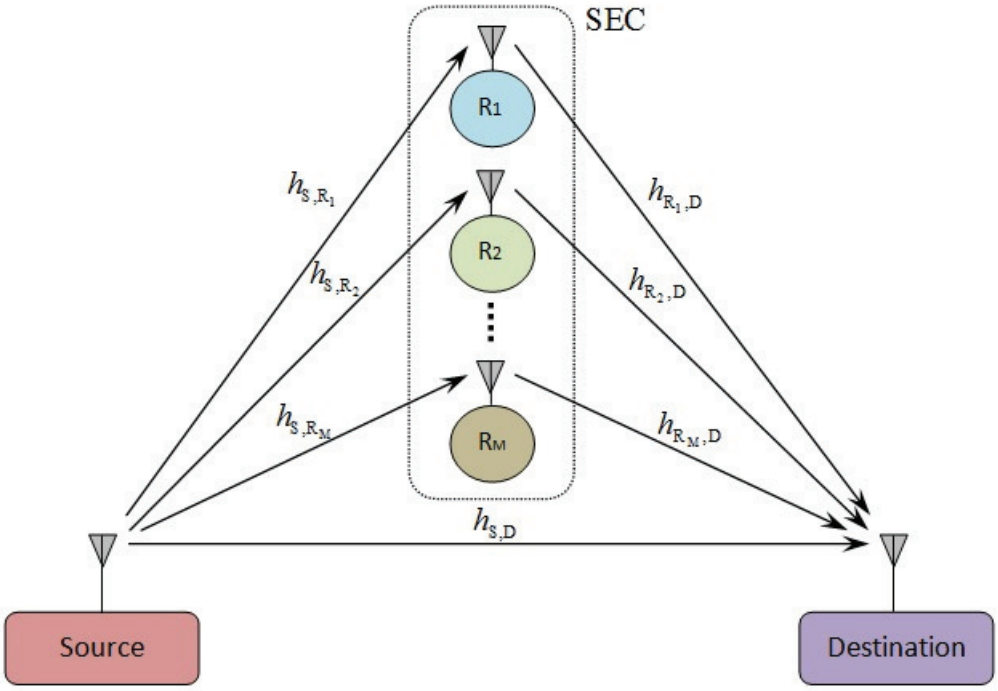

Figure 2.1: A schematic diagram for dual-hop AF relay system with SEC relay selection scheme and MRC at destination.

estimates its instantaneous channels. Then, the minimum magnitude of the two hops is compared with a predetermined switching threshold. If this minimum is larger than the switching threshold, then this relay is selected to forward the source message and a short duration flag packet is sent from this relay to the other relays signalling its presence. Otherwise, a flag packet is sent from this relay to other relay asking it to estimate its channels to be compared then with the switching threshold. This process continues until a relay satisfying the switching threshold is found or reaching the last relay. At this case, the last relay is chosen to forward the source message. As an enhancement on the SEC-based relaying scheme, we also propose the SECps relay selection scheme. This scheme shares all operation steps of the SEC-based relaying and only differs in the last step where

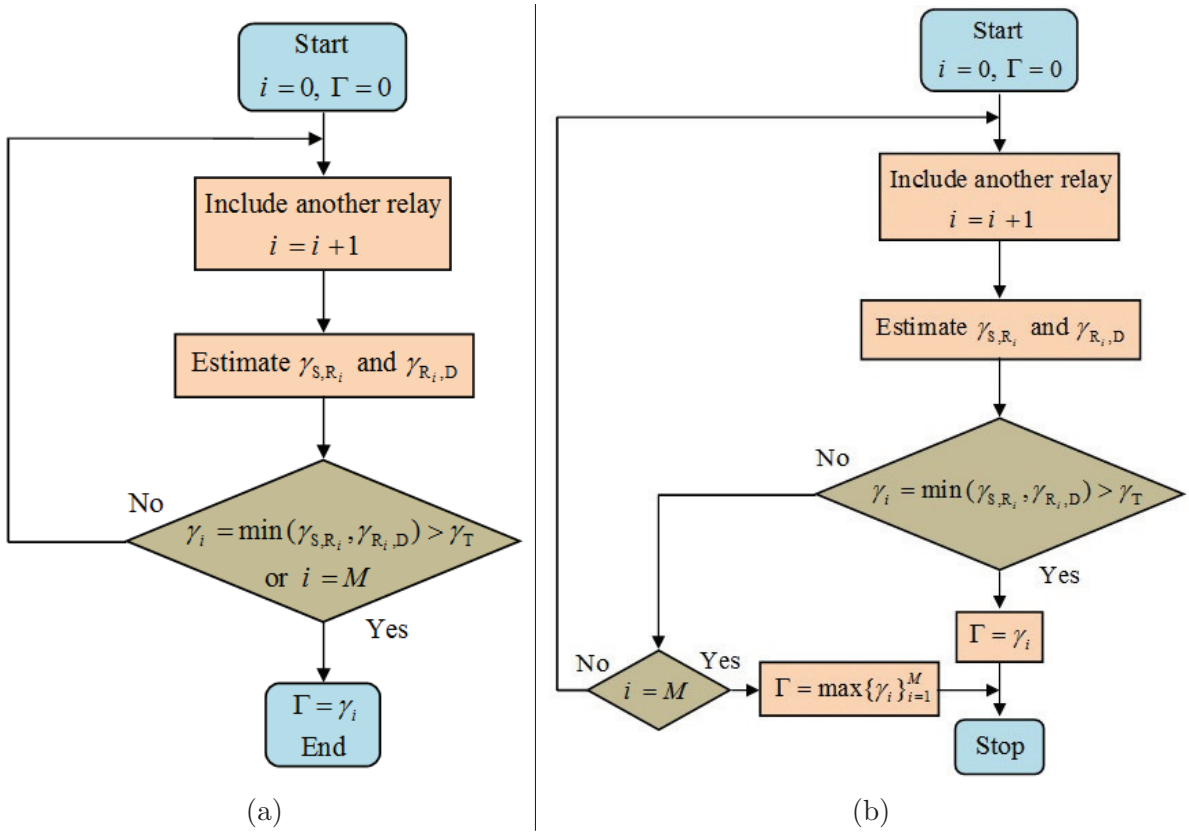

Figure 2.2: Flowcharts for the proposed relaying schemes, (a) SEC relaying, (b) SECps relaying.

the last relay is reached and found unacceptable. In this case, the SECps scheme selects the best relay among all relays to forward the source message to destination. This results in a noticeable enhancement in system performance compared to the SEC relaying scheme as will be shown in our results. In calculating the switching threshold, the SNRs of both the first hop and second hop channels of the selected relay are required at the destination node. These SNR values along with the direct link SNR are then used in calculating the switching threshold in such a way the e2e SEP is minimized. Flowcharts for the proposed relaying schemes are shown in Figure 2.2.

At the destination, MRC is used to combine the signal on the direct path

with that through the relay. The channel coefficients between the source and the i^{th} relay R_i ($h_{\mathsf{S},\mathsf{R}_i}$), between R_i and D ($h_{\mathsf{R}_i,\mathsf{D}}$) and between S and D ($h_{\mathsf{S},\mathsf{D}}$) are assumed to be flat Rayleigh fading gains. In addition, $h_{\mathsf{S},\mathsf{R}_i}$, $h_{\mathsf{R}_i,\mathsf{D}}$, and $h_{\mathsf{S},\mathsf{D}}$ are mutually-independent and non-identical. We also assume here, without any loss of generality that the additive white Gaussian noise (AWGN) terms of all links have zero means and equal variance $N_0/2$.

Communications occur in two phases. In phase 1, the source transmits the modulated signal x with unit energy to the destination and the M relays. The received signals at the destination and the i^{th} relay can be respectively expressed as

$$y_{\mathsf{S},\mathsf{D}} = h_{\mathsf{S},\mathsf{D}}\sqrt{E_s}x + n_{\mathsf{S},\mathsf{D}}, \tag{2.1}$$

$$y_{\mathsf{S},\mathsf{R}_i} = h_{\mathsf{S},\mathsf{R}_i}\sqrt{E_s}x + n_{\mathsf{S},\mathsf{R}_i}, \tag{2.2}$$

where E_s is the average received symbol energy, $n_{\mathsf{S},\mathsf{D}}$ and $n_{\mathsf{S},\mathsf{R}_i}$ are the AWGN between S and D and S and R_i, respectively. The chosen relay by the SEC scheme amplifies the received signal and transmits it to the destination in the second phase of communication. During this phase, the received signal at the destination from the selected relay can be expressed as

$$y_{\mathsf{R}_{\text{sel}},\mathsf{D}} = \mathsf{G}h_{\mathsf{R}_{\text{sel}},\mathsf{D}}\sqrt{E_s}x + n_{\mathsf{R}_{\text{sel}},\mathsf{D}}, \tag{2.3}$$

where G is the active relay amplifying gain, chosen as $\mathsf{G}^2 = E_s/(E_s h^2_{\mathsf{S},\mathsf{R}_{\text{sel}}} + N_0)$

[34]. The composite SNR of the relay link can be written as [6]

$$\gamma_{\mathsf{S},\mathsf{R}_i,\mathsf{D}} = \frac{\gamma_{\mathsf{S},\mathsf{R}_i}\gamma_{\mathsf{R}_i,\mathsf{D}}}{\gamma_{\mathsf{S},\mathsf{R}_i} + \gamma_{\mathsf{R}_i,\mathsf{D}} + 1}, \tag{2.4}$$

where $\gamma_{\mathsf{S},\mathsf{R}_i} = h^2_{\mathsf{S},\mathsf{R}_i} E_s/N_0$ is the instantaneous SNR of the source signal at R_i and $\gamma_{\mathsf{R}_i,\mathsf{D}} = h^2_{\mathsf{R}_i,\mathsf{D}} E_s/N_0$ is the instantaneous SNR of the relay signal (by R_i) at D. By using MRC at the destination node, the total SNR at the combiner output is simply the addition of the two random variables at its inputs as follows

$$\gamma_{\mathsf{tot}} = \gamma_{\mathsf{S},\mathsf{D}} + \gamma_{\mathrm{SEC}}, \tag{2.5}$$

where $\gamma_{\mathsf{S},\mathsf{D}} = h^2_{\mathsf{S},\mathsf{D}} E_s/N_0$ is the instantaneous SNR between S and D, and γ_{SEC} is the SNR at the output of the SEC selection scheme. To simplify the ensuing derivations, (2.4) should be expressed in a more mathematically tractable form. A tight upper bound for $\gamma_{\mathsf{S},\mathsf{R}_i,\mathsf{D}}$ is given in [35] by

$$\gamma_{\mathsf{S},\mathsf{R}_i,\mathsf{D}} \leq \gamma_i = \min(\gamma_{\mathsf{S},\mathsf{R}_i}, \gamma_{\mathsf{R}_i,\mathsf{D}}). \tag{2.6}$$

Assuming Rayleigh fading channels between source, relays, and destination, the distribution of γ_i in (2.6) is exponential and hence, its PDF can be expressed in terms of the average SNR $\bar{\gamma}_{\mathsf{S},\mathsf{R}_i} = \mathbb{E}[h^2_{\mathsf{S},\mathsf{R}_i}]E_s/N_0$ and $\bar{\gamma}_{\mathsf{R}_i,\mathsf{D}} = \mathbb{E}[h^2_{\mathsf{R}_i,\mathsf{D}}]E_s/N_0$ (where $\mathbb{E}[\cdot]$ is the expectation operator) as

$$f_{\gamma_i}(\gamma) = \frac{1}{\bar{\gamma}_i} \exp\left(-\frac{\gamma}{\bar{\gamma}_i}\right), \tag{2.7}$$

where $\bar{\gamma}_i = \bar{\gamma}_{\mathsf{S},\mathsf{R}_i}\bar{\gamma}_{\mathsf{R}_i,\mathsf{D}}/(\bar{\gamma}_{\mathsf{S},\mathsf{R}_i} + \bar{\gamma}_{\mathsf{R}_i,\mathsf{D}})$.

2.4 SEC-Based Relay Selection

In this section, we derive the performance of the proposed SEC relay selection scheme. In the following, we present closed-from expressions for both the e2e outage probability and SEP.

2.4.1 Performance Analysis

Our results on the outage probability are summarized in Lemma 2.1 and Corollary 2.1 as follows.

Lemma 2.1 *The outage probability of the SEC-based relaying scheme for the case of i.n.d. relay paths* $\{\bar{\gamma}_i\}_{i=1}^{M}$ *is given in a closed-form expression as*

$$P_{\mathsf{out}} = \sum_{i=0}^{M-1} \pi_i \prod_{\substack{k=0 \\ k\neq i}}^{M-1} \left(1 - \exp\left(-\frac{\gamma_{\mathsf{T}}}{\bar{\gamma}_k}\right)\right) \left[\frac{\left(1 - \exp\left(-\frac{\gamma_{\mathsf{out}}}{\bar{\gamma}_{\mathsf{S},\mathsf{D}}}\right)\right)}{\left(1 - \frac{\bar{\gamma}_i}{\bar{\gamma}_{\mathsf{S},\mathsf{D}}}\right)} + \frac{\left(1 - \exp\left(-\frac{\gamma_{\mathsf{out}}}{\bar{\gamma}_i}\right)\right)}{\left(1 - \frac{\bar{\gamma}_{\mathsf{S},\mathsf{D}}}{\bar{\gamma}_i}\right)}\right.$$
$$- \exp\left(-\frac{\gamma_{\mathsf{T}}}{\bar{\gamma}_i}\right) \times \left\{\frac{\exp\left(\frac{\gamma_{\mathsf{T}}}{\bar{\gamma}_{\mathsf{S},\mathsf{D}}}\right)}{\left(1 - \frac{\bar{\gamma}_i}{\bar{\gamma}_{\mathsf{S},\mathsf{D}}}\right)} \left(\exp\left(-\frac{\gamma_{\mathsf{T}}}{\bar{\gamma}_{\mathsf{S},\mathsf{D}}}\right) - \exp\left(-\frac{\gamma_{\mathsf{out}}}{\bar{\gamma}_{\mathsf{S},\mathsf{D}}}\right)\right) + \frac{\exp\left(\frac{\gamma_{\mathsf{T}}}{\bar{\gamma}_i}\right)}{\left(1 - \frac{\bar{\gamma}_{\mathsf{S},\mathsf{D}}}{\bar{\gamma}_i}\right)}\right.$$
$$\left.\left.\times \left(\exp\left(-\frac{\gamma_{\mathsf{T}}}{\bar{\gamma}_i}\right) - \exp\left(-\frac{\gamma_{\mathsf{out}}}{\bar{\gamma}_i}\right)\right)\right\}\right] + \sum_{j=0}^{M-1} \pi_{((i-j))_M} \prod_{k=0}^{j-1} \left(1 - \exp\left(-\frac{\gamma_{\mathsf{T}}}{\bar{\gamma}_{((i-j+k))_M}}\right)\right)$$
$$\times \left[\exp\left(-\frac{\gamma_{\mathsf{T}}}{\bar{\gamma}_i}\right) \left\{\frac{\exp\left(\frac{\gamma_{\mathsf{T}}}{\bar{\gamma}_{\mathsf{S},\mathsf{D}}}\right)}{\left(1 - \frac{\bar{\gamma}_i}{\bar{\gamma}_{\mathsf{S},\mathsf{D}}}\right)} \left(1 - \exp\left(-\frac{\gamma_{\mathsf{out}}}{\bar{\gamma}_{\mathsf{S},\mathsf{D}}}\right)\right) + \frac{\exp\left(\frac{\gamma_{\mathsf{T}}}{\bar{\gamma}_i}\right)}{\left(1 - \frac{\bar{\gamma}_{\mathsf{S},\mathsf{D}}}{\bar{\gamma}_i}\right)} \left(1 - \exp\left(-\frac{\gamma_{\mathsf{out}}}{\bar{\gamma}_i}\right)\right)\right\}\right]. \tag{2.8}$$

Proof. See Appendix A.1. ∎

Corollary 2.1 *The outage probability of the SEC-based relaying scheme for the case of i.i.d. relay paths ($\bar{\gamma}_1 = \ldots = \bar{\gamma}_M = \bar{\gamma}_{\text{path}}$) is given in a closed-form expression as*

$$\begin{aligned} P_{\mathsf{out}} =& \frac{1}{\left(\frac{\bar{\gamma}}{2} - \bar{\gamma}_{\mathsf{S,D}}\right)} \Bigg\{ \left(1 - \exp\left(-\frac{2\gamma_{\mathsf{T}}}{\bar{\gamma}}\right)\right)^{M-1} \left[\frac{\bar{\gamma}}{2}\left(1 - \exp\left(-\frac{2\gamma_{\mathsf{out}}}{\bar{\gamma}}\right)\right)\right. \\ & \left. - \bar{\gamma}_{\mathsf{S,D}}\left(1 - \exp\left(-\frac{\gamma_{\mathsf{out}}}{\bar{\gamma}_{\mathsf{S,D}}}\right)\right)\right] + \sum_{j=0}^{M-2}\left(1 - \exp\left(-\frac{2\gamma_{\mathsf{T}}}{\bar{\gamma}}\right)\right)^{j} \\ & \times \left[\frac{\bar{\gamma}}{2}\left\{\exp\left(-\frac{2\gamma_{\mathsf{T}}}{\bar{\gamma}}\right) - \exp\left(-\frac{2\gamma_{\mathsf{out}}}{\bar{\gamma}}\right)\right\} - \bar{\gamma}_{\mathsf{S,D}} \exp\left(\left(-\frac{2}{\bar{\gamma}} + \frac{1}{\bar{\gamma}_{\mathsf{S,D}}}\right)\gamma_{\mathsf{T}}\right)\right. \\ & \left. \times \left\{\exp\left(-\frac{\gamma_{\mathsf{T}}}{\bar{\gamma}_{\mathsf{S,D}}}\right) - \exp\left(-\frac{\gamma_{\mathsf{out}}}{\bar{\gamma}_{\mathsf{S,D}}}\right)\right\}\right]\Bigg\}. \end{aligned} \tag{2.9}$$

Proof. The CDF of γ_{SEC} for i.i.d. relay paths can be written as [22]

$$F_{\gamma_{\text{SEC}}}(\gamma) = \begin{cases} \left[F_\gamma(\gamma_{\mathsf{T}})\right]^{M-1} F_\gamma(\gamma), & \gamma < \gamma_{\mathsf{T}}; \\ \sum_{j=0}^{M-1}\left[F_\gamma(\gamma) - F_\gamma(\gamma_{\mathsf{T}})\right] & \\ \left[F_\gamma(\gamma_{\mathsf{T}})\right]^{j} + \left[F_\gamma(\gamma_{\mathsf{T}})\right]^{M}, & \gamma \geq \gamma_{\mathsf{T}}. \end{cases} \tag{2.10}$$

Using the CDF in (2.10) and following the same procedure as in Appendix A.1, the outage probability for the case of i.i.d. relay paths can be obtained in a closed-form expression as in (2.9), where i.i.d. symmetrical hops, i.e. $\bar{\gamma}_{\mathsf{S,R}_i} = \bar{\gamma}_{\mathsf{R}_i,\mathsf{D}} = \bar{\gamma}$ $\forall i$, $i \in \{1, \ldots, M\}$ have been assumed in obtaining this result. ∎

Our results on the SEP are summarized in Lemma 2.2 and Corollary 2.2 as follows.

Lemma 2.2 *The SEP of the SEC-based relaying scheme for the case of i.n.d. relay paths is given in a closed-form expression as*

$$\begin{aligned}
\mathsf{SEP} = &\sum_{i=0}^{M-1} \pi_i \prod_{\substack{k=0 \\ k\neq i}}^{M-1} \left(1 - \exp\left(-\frac{\gamma_{\mathsf{T}}}{\bar{\gamma}_k}\right)\right) \left[\frac{\left(1 - \sqrt{\frac{\bar{\gamma}_{\mathsf{S,D}}}{1+\bar{\gamma}_{\mathsf{S,D}}}}\right)}{2\left(1 - \frac{\bar{\gamma}_i}{\bar{\gamma}_{\mathsf{S,D}}}\right)} + \frac{\left(1 - \sqrt{\frac{\bar{\gamma}_i}{1+\bar{\gamma}_i}}\right)}{2\left(1 - \frac{\bar{\gamma}_{\mathsf{S,D}}}{\bar{\gamma}_i}\right)} \right. \\
&- \frac{\exp\left(-\frac{\gamma_{\mathsf{T}}}{\bar{\gamma}_i}\right)}{\left(1 - \frac{\bar{\gamma}_i}{\bar{\gamma}_{\mathsf{S,D}}}\right)} \left\{ Q\left(\sqrt{2\gamma_{\mathsf{T}}}\right) - \frac{\exp\left(\frac{\gamma_{\mathsf{T}}}{\bar{\gamma}_{\mathsf{S,D}}}\right) Q\left(\sqrt{2\left(\gamma_{\mathsf{T}} + \frac{\gamma_{\mathsf{T}}}{\bar{\gamma}_{\mathsf{S,D}}}\right)}\right)}{\sqrt{1 + \frac{1}{\bar{\gamma}_{\mathsf{S,D}}}}} \right\} \\
&\left. - \frac{\exp\left(-\frac{\gamma_{\mathsf{T}}}{\bar{\gamma}_i}\right)}{\left(1 - \frac{\bar{\gamma}_{\mathsf{S,D}}}{\bar{\gamma}_i}\right)} \left\{ Q\left(\sqrt{2\gamma_{\mathsf{T}}}\right) - \frac{\exp\left(\frac{\gamma_{\mathsf{T}}}{\bar{\gamma}_i}\right) Q\left(\sqrt{2\left(\gamma_{\mathsf{T}} + \frac{\gamma_{\mathsf{T}}}{\bar{\gamma}_i}\right)}\right)}{\sqrt{1 + \frac{1}{\bar{\gamma}_i}}} \right\} \right] \\
&+ \sum_{i=0}^{M-1} \sum_{j=0}^{M-1} \pi_{((i-j))_M} \prod_{k=0}^{j-1} \left(1 - \exp\left(-\frac{\gamma_{\mathsf{T}}}{\bar{\gamma}_{((i-j+k))_M}}\right)\right) \\
&\times \left[\frac{\exp\left(-\frac{\gamma_{\mathsf{T}}}{\bar{\gamma}_i}\right)}{\left(1 - \frac{\bar{\gamma}_i}{\bar{\gamma}_{\mathsf{S,D}}}\right)} \left\{ Q\left(\sqrt{2\gamma_{\mathsf{T}}}\right) - \frac{\exp\left(\frac{\gamma_{\mathsf{T}}}{\bar{\gamma}_{\mathsf{S,D}}}\right)}{\sqrt{1 + \frac{1}{\bar{\gamma}_{\mathsf{S,D}}}}} Q\left(\sqrt{2\left(\gamma_{\mathsf{T}} + \frac{\gamma_{\mathsf{T}}}{\bar{\gamma}_{\mathsf{S,D}}}\right)}\right) \right\} \right. \\
&\left. + \frac{\exp\left(-\frac{\gamma_{\mathsf{T}}}{\bar{\gamma}_i}\right)}{\left(1 - \frac{\bar{\gamma}_{\mathsf{S,D}}}{\bar{\gamma}_i}\right)} \left\{ Q\left(\sqrt{2\gamma_{\mathsf{T}}}\right) - \frac{\exp\left(\frac{\gamma_{\mathsf{T}}}{\bar{\gamma}_i}\right) Q\left(\sqrt{2\left(\gamma_{\mathsf{T}} + \frac{\gamma_{\mathsf{T}}}{\bar{\gamma}_i}\right)}\right)}{\sqrt{1 + \frac{1}{\bar{\gamma}_i}}} \right\} \right], \quad (2.11)
\end{aligned}$$

where $Q(\cdot)$ is the Gaussian Q-function defined in [22, Eq. 4.1].

Proof. See Appendix A.2. ∎

Corollary 2.2 *The SEP of the SEC-based relaying scheme for the case of i.i.d.*

relay paths is given in a closed-form expression as

$$\begin{aligned}\mathsf{SEP} =& \frac{\left(1-\exp\left(-\frac{2\gamma_{\mathsf{T}}}{\bar{\gamma}}\right)\right)^{M-1}}{2}\left[\frac{\left(1-\sqrt{\frac{\bar{\gamma}_{\mathsf{S,D}}}{1+\bar{\gamma}_{\mathsf{S,D}}}}\right)}{\left(1-\frac{\bar{\gamma}}{2\bar{\gamma}_{\mathsf{S,D}}}\right)}+\frac{\left(1-\sqrt{\frac{\frac{\bar{\gamma}}{2}}{1+\frac{\bar{\gamma}}{2}}}\right)}{\left(1-\frac{\bar{\gamma}_{\mathsf{S,D}}}{\bar{\gamma}}\right)}\right] \\ &+\exp\left(-\frac{2\gamma_{\mathsf{T}}}{\bar{\gamma}}\right)\sum_{j=0}^{M-2}\left(1-\exp\left(-\frac{2\gamma_{\mathsf{T}}}{\bar{\gamma}}\right)\right)^{j} \\ &\times\left\{\frac{1}{\left(1-\frac{\bar{\gamma}}{2\bar{\gamma}_{\mathsf{S,D}}}\right)}\left[Q\left(\sqrt{2\gamma_{\mathsf{T}}}\right)-\frac{\exp\left(\frac{\gamma_{\mathsf{T}}}{\bar{\gamma}_{\mathsf{S,D}}}\right)Q\left(\sqrt{2\left(\gamma_{\mathsf{T}}+\frac{\gamma_{\mathsf{T}}}{\bar{\gamma}_{\mathsf{S,D}}}\right)}\right)}{\sqrt{1+\frac{1}{\bar{\gamma}_{\mathsf{S,D}}}}}\right]\right. \\ &\left.+\frac{1}{\left(1-\frac{2\bar{\gamma}_{\mathsf{S,D}}}{\bar{\gamma}}\right)}\left[Q\left(\sqrt{2\gamma_{\mathsf{T}}}\right)-\frac{\exp\left(\frac{2\gamma_{\mathsf{T}}}{\bar{\gamma}}\right)Q\left(\sqrt{2\left(\gamma_{\mathsf{T}}+\frac{2\gamma_{\mathsf{T}}}{\bar{\gamma}}\right)}\right)}{\sqrt{1+\frac{2}{\bar{\gamma}}}}\right]\right\}, \quad (2.12)\end{aligned}$$

Proof. To derive (2.12), the MGF $\mathcal{M}_{\gamma_{\mathrm{SEC}}}(s)$ needs to be derived first using $f_{\gamma_{\mathrm{SEC}}}(\gamma)$ of the i.i.d. relay paths case. Then, following the same procedure as in Appendix A.2, a closed-form expression for the SEP of the i.i.d. case of relay paths can be obtained as in (2.12), where i.i.d. symmetrical hops, i.e. $\bar{\gamma}_{\mathsf{S,R}_i} = \bar{\gamma}_{\mathsf{R}_i,\mathsf{D}} = \bar{\gamma}$ $\forall i$, $i \in \{1, \ldots, M\}$ have been assumed in obtaining this result. ∎

2.4.2 Asymptotic Analysis

In this section, we derive the outage performance of the SEC proposed relay selection scheme at high SNR regime. At high SNR values, the outage probability can be expressed as $P_{\mathsf{out}} \approx (G_{\mathsf{c}}\mathrm{SNR})^{-G_{\mathsf{d}}}$, where G_{c} and G_{d} are respectively the coding gain and the diversity order of the system.

At high SNR regime, the exponential CDF and PDF can be respectively ap-

proximated by $F_\gamma(\gamma) \approx \frac{\gamma}{\bar{\gamma}}$ and $f_\gamma(\gamma) \approx \frac{1}{\bar{\gamma}}$. Upon using these statistics and following the same procedure as in Appendix A.1, the outage probability for the SEC selection scheme can be obtained at high SNR as

$$P_{\mathsf{out}} \approx \frac{1}{\bar{\gamma}\bar{\gamma}_{\mathsf{S,D}}} \left\{ \left(\frac{2\gamma_{\mathsf{T}}}{\bar{\gamma}} \right)^{M-1} \left[2\gamma_{\mathsf{T}}\gamma_{\mathsf{out}} - (\gamma_{\mathsf{T}})^2 \right] + \sum_{j=0}^{M-1} \left(\frac{2\gamma_{\mathsf{T}}}{\bar{\gamma}} \right)^{j} \left[(\gamma_{\mathsf{out}})^2 + (\gamma_{\mathsf{T}})^2 - 2\gamma_{\mathsf{T}}\gamma_{\mathsf{out}} \right] \right\}. \tag{2.13}$$

This expression can be further simplified due to the fact that it is still dominant when $j = 0$. In addition, upon evaluating (3.23) in MAPLE software, we have noticed that the first part of the expression has a negligible effect on the performance, especially, when we further increase the value of SNR. Therefore, the result in (3.23) can be simplified as

$$P_{\mathsf{out}} \approx \frac{1}{\bar{\gamma}\bar{\gamma}_{\mathsf{S,D}}} \left[(\gamma_{\mathsf{out}})^2 + (\gamma_{\mathsf{T}})^2 - 2\gamma_{\mathsf{T}}\gamma_{\mathsf{out}} \right]. \tag{2.14}$$

By noticing that $\bar{\gamma} = \bar{\gamma}_{\mathsf{S,D}} = \mathrm{SNR}$, the result in (3.25) can be rewritten as

$$P_{\mathsf{out}} \approx \left(\left[(\gamma_{\mathsf{out}})^2 + (\gamma_{\mathsf{T}})^2 - 2\gamma_{\mathsf{T}}\gamma_{\mathsf{out}} \right]^2 \mathrm{SNR} \right)^{-2}. \tag{2.15}$$

As can be noticed from the last result, the coding gain of the system is $\left[(\gamma_{\mathsf{out}})^2 + (\gamma_{\mathsf{T}})^2 - 2\gamma_{\mathsf{T}}\gamma_{\mathsf{out}} \right]^2$; while the diversity order is 2. This is clear in figure 2.4 where all the curves of different M asymptotically converge to the same behavior and result in a diversity order of 2 (relay path + direct link). Also, it is shown in figure 2.4 that the system performance is affected by several param-

eters as γ_{T} and γ_{out} which are only affecting the coding gain of the system. It is expected from results to have the maximum gain in system performance due to increasing M to happen at the values of SNR that are comparable to γ_{T}. As in this case, the switching rate will increase and the probability to have better relays increases also. At the same time, as the asymptotic analysis is done at high SNR values and with constant γ_{T} and γ_{out}, it is expected to have most of the relays to be acceptable the whole time and thus, the first checked relay is being selected in both selection schemes. This means all curves of different M asymptotically converge to the same behavior and hence, the same diversity order and coding gain are achieved for the different curves. Also, this explains why the system with the SEC and SECps selection schemes achieves the same diversity order and coding gain.

2.5 SECps-Based Relay Selection

In this section, we derive the performance of the proposed SECps relay selection scheme. In the following, we present closed-from expressions for both the e2e outage probability and SEP.

2.5.1 Performance Analysis

Our results on the outage probability and the SEP are respectively summarized in Corollary 2.3 and Corollary 2.4 as follows.

Corollary 2.3 *The outage probability of the SECps-based relaying scheme for*

the case of i.i.d. relay paths ($\bar{\gamma}_1 = \ldots = \bar{\gamma}_M = \bar{\gamma}_{\text{path}}$) is given in a closed-form expression as

$$P_{\mathsf{out}} = \frac{\left(1 - \left(1 - \exp\left(-\frac{2\gamma_{\mathsf{T}}}{\bar{\gamma}}\right)\right)^M\right)}{\left(\frac{\bar{\gamma}}{2} - \bar{\gamma}_{\mathsf{S,D}}\right)} \Bigg[\frac{\bar{\gamma}}{2} \exp\left(\frac{2\gamma_{\mathsf{T}}}{\bar{\gamma}}\right) \left(\exp\left(-\frac{2\gamma_{\mathsf{T}}}{\bar{\gamma}}\right) - \exp\left(-\frac{2\gamma_{\mathsf{out}}}{\bar{\gamma}}\right)\right)$$

$$- \bar{\gamma}_{\mathsf{S,D}} \exp\left(\frac{\gamma_{\mathsf{T}}}{\bar{\gamma}_{\mathsf{S,D}}}\right) \left(\exp\left(-\frac{\gamma_{\mathsf{T}}}{\bar{\gamma}_{\mathsf{S,D}}}\right) - \exp\left(-\frac{\gamma_{\mathsf{out}}}{\bar{\gamma}_{\mathsf{S,D}}}\right)\right) \Bigg] + M \sum_{j=0}^{M-1} \binom{M-1}{j} (-1)^j$$

$$\times \frac{1}{\left(\frac{\bar{\gamma}}{2} - (j+1)\bar{\gamma}_{\mathsf{S,D}}\right)} \Bigg[\frac{\bar{\gamma}}{2(j+1)} \left(1 - \exp\left(-\frac{2(j+1)\gamma_{\mathsf{out}}}{\bar{\gamma}}\right)\right) - \bar{\gamma}_{\mathsf{S,D}} \left(1 - \exp\left(-\frac{\gamma_{\mathsf{out}}}{\bar{\gamma}_{\mathsf{S,D}}}\right)\right)$$

$$- \exp\left(\frac{-2(j+1)\gamma_{\mathsf{T}}}{\bar{\gamma}}\right) \Bigg\{ \frac{\bar{\gamma} \exp\left(\frac{2(j+1)\gamma_{\mathsf{T}}}{\bar{\gamma}}\right)}{2(j+1)} \left(\exp\left(-\frac{2(j+1)\gamma_{\mathsf{T}}}{\bar{\gamma}}\right) - \exp\left(-\frac{2(j+1)\gamma_{\mathsf{out}}}{\bar{\gamma}}\right)\right)$$

$$- \bar{\gamma}_{\mathsf{S,D}} \exp\left(\frac{\gamma_{\mathsf{T}}}{\bar{\gamma}_{\mathsf{S,D}}}\right) \left(\exp\left(-\frac{\gamma_{\mathsf{T}}}{\bar{\gamma}_{\mathsf{S,D}}}\right) - \exp\left(-\frac{\gamma_{\mathsf{out}}}{\bar{\gamma}_{\mathsf{S,D}}}\right)\right) \Bigg\} \Bigg]. \tag{2.16}$$

Proof. The CDF of γ_{SECps} for i.i.d. relay paths can be written as [22]

$$F_{\gamma_{\text{SECps}}}(\gamma) = \begin{cases} 1 - \sum_{j=0}^{M-1} \left[F_\gamma(\gamma_{\mathsf{T}})\right]^j \left[1 - F_\gamma(\gamma)\right], & \gamma \geq \gamma_{\mathsf{T}}; \\ \left[F_\gamma(\gamma)\right]^M, & \gamma < \gamma_{\mathsf{T}}. \end{cases} \tag{2.17}$$

Using the CDF in (2.17) and following the same procedure as in Appendix A.1, the outage probability for the SECps-based relaying scheme can be obtained in a closed-form expression as in (2.16), where i.i.d. symmetrical hops, i.e. $\bar{\gamma}_{\mathsf{S,R}_i} = \bar{\gamma}_{\mathsf{R}_i,\mathsf{D}} = \bar{\gamma}\ \forall i,\ i \in \{1, \ldots, M\}$ have been assumed in obtaining this result. ∎

Corollary 2.4 *The SEP of the SECps-based relaying scheme for the case of i.i.d.*

relay paths is given in a closed-form expression as

$$
\begin{aligned}
\mathsf{SEP} &= \left[1-\left(1-\exp\left(-\frac{2\gamma_{\mathsf{T}}}{\bar{\gamma}}\right)\right)^{M}\right] \\
&\times\left\{\frac{1}{\left(1-\frac{\bar{\gamma}}{2\bar{\gamma}_{\mathsf{S,D}}}\right)}\left(Q\left(\sqrt{2\gamma_{\mathsf{T}}}\right)-\frac{\exp\left(\frac{\gamma_{\mathsf{T}}}{\bar{\gamma}_{\mathsf{S,D}}}\right)Q\left(\sqrt{2\left(\gamma_{\mathsf{T}}+\frac{\gamma_{\mathsf{T}}}{\bar{\gamma}_{\mathsf{S,D}}}\right)}\right)}{\sqrt{1+\frac{1}{\bar{\gamma}_{\mathsf{S,D}}}}}\right)+\frac{1}{\left(1-\frac{2\bar{\gamma}_{\mathsf{S,D}}}{\bar{\gamma}}\right)}\right. \\
&\left.\times\left(Q\left(\sqrt{2\gamma_{\mathsf{T}}}\right)-\frac{\exp\left(\frac{2\gamma_{\mathsf{T}}}{\bar{\gamma}}\right)Q\left(\sqrt{2\left(\gamma_{\mathsf{T}}+\frac{2\gamma_{\mathsf{T}}}{\bar{\gamma}}\right)}\right)}{\sqrt{1+\frac{2}{\bar{\gamma}}}}\right)\right\}+M\sum_{j=0}^{M-1}\binom{M-1}{j}(-1)^{j} \\
&\times\left[\frac{\left(1-\sqrt{\frac{\bar{\gamma}_{\mathsf{S,D}}}{1+\bar{\gamma}_{\mathsf{S,D}}}}\right)}{2\left(j+1-\frac{\bar{\gamma}}{2\bar{\gamma}_{\mathsf{S,D}}}\right)}+\frac{\left(1-\sqrt{\frac{\bar{\gamma}}{2\left(j+1+\frac{\bar{\gamma}}{2}\right)}}\right)}{2(j+1)\left(1-(j+1)\frac{2\bar{\gamma}_{\mathsf{S,D}}}{\bar{\gamma}}\right)}-\exp\left(\frac{-2(j+1)\gamma_{\mathsf{T}}}{\bar{\gamma}}\right)\right. \\
&\times\left\{\frac{1}{\left(j+1-\frac{\bar{\gamma}}{2\bar{\gamma}_{\mathsf{S,D}}}\right)}\left(Q\left(\sqrt{2\gamma_{\mathsf{T}}}\right)-\frac{\exp\left(\frac{\gamma_{\mathsf{T}}}{\bar{\gamma}_{\mathsf{S,D}}}\right)Q\left(\sqrt{2\left(\gamma_{\mathsf{T}}+\frac{\gamma_{\mathsf{T}}}{\bar{\gamma}_{\mathsf{S,D}}}\right)}\right)}{\sqrt{1+\frac{1}{\bar{\gamma}_{\mathsf{S,D}}}}}\right)\right. \\
&\left.\left.+\frac{1}{(j+1)\left(1-(j+1)\frac{2\bar{\gamma}_{\mathsf{S,D}}}{\bar{\gamma}}\right)}\left(Q\left(\sqrt{2\gamma_{\mathsf{T}}}\right)-\frac{\exp\left(\frac{2(j+1)\gamma_{\mathsf{T}}}{\bar{\gamma}}\right)Q\left(\sqrt{2\left(\gamma_{\mathsf{T}}+\frac{2(j+1)\gamma_{\mathsf{T}}}{\bar{\gamma}}\right)}\right)}{\sqrt{1+\frac{2(j+1)}{\bar{\gamma}}}}\right)\right\}\right].
\end{aligned}
\tag{2.18}
$$

Proof. To derive (2.18), the MGF $\mathcal{M}_{\gamma_{\mathrm{SECps}}}(s)$ needs to be derived first using $f_{\gamma_{\mathrm{SECps}}}(\gamma)$ of the i.i.d. relay paths case. Then, following the same procedure as in Appendix A.2, a closed-form expression for the SEP of the i.i.d. case of relay paths can be obtained as in (2.18), where again i.i.d. symmetrical hops, i.e. $\bar{\gamma}_{\mathsf{S,R}_i}=\bar{\gamma}_{\mathsf{R}_i,\mathsf{D}}=\bar{\gamma}\ \forall i,\ i\in\{1,\ldots,M\}$ have been assumed in obtaining this result. ∎

2.5.2 Asymptotic Analysis

Upon using the approximate expressions of the exponential statistics and following the same procedure as in Appendix A.1, the outage probability for the SECps selection scheme can be obtained at high SNR as

$$P_{\mathsf{out}} \approx \frac{1}{\bar{\gamma}\bar{\gamma}_{\mathsf{S,D}}} \Bigg\{ \frac{2M!}{\left(\frac{\bar{\gamma}}{2}\right)^{M-1}} \Bigg[\frac{(\gamma_{\mathsf{out}})^{M+1}}{M!\,(M+1)} - \sum_{k=0}^{M-1} \frac{(-1)^{-k}}{(M-k)!\,k!} \sum_{i=0}^{M-k} \binom{M-k}{i} \frac{(-\gamma_{\mathsf{T}})^{M-i}}{(i+1)} \times \left[(\gamma_{\mathsf{out}})^{i+1} - (\gamma_{\mathsf{T}})^{i+1} \right] \Bigg] + \sum_{j=0}^{M-1} \left(\frac{2\gamma_{\mathsf{T}}}{\bar{\gamma}} \right)^{j} \left[(\gamma_{\mathsf{out}})^2 + (\gamma_{\mathsf{T}})^2 - 2\gamma_{\mathsf{T}}\gamma_{\mathsf{out}} \right] \Bigg\}. \quad (2.19)$$

This expression can be further simplified due to the fact that it is still dominant when $k = 0$, $i = 0$, and $j = 0$. In addition, upon evaluating (2.19) in MAPLE software, we have noticed that the first part of the expression has a negligible effect on the performance, especially, when we go further in increasing the value of SNR. Therefore, the result in (2.19) can be simplified as

$$P_{\mathsf{out}} \approx \frac{1}{\bar{\gamma}\bar{\gamma}_{\mathsf{S,D}}} \left[(\gamma_{\mathsf{out}})^2 + (\gamma_{\mathsf{T}})^2 - 2\gamma_{\mathsf{T}}\gamma_{\mathsf{out}} \right]. \quad (2.20)$$

As can be seen, the asymptotic outage probability in (2.20) which corresponds to the SECps selection scheme is exactly the same as that in (3.25) for the SEC scheme. Hence, it can be easily concluded that both selection schemes have the same coding gain and the same diversity order as derived before for the SEC relaying scheme. This is clear from the numerical examples where the SECps selection scheme behaves similar to the SEC scheme, especially, at high SNR values. This is expected as at high SNR values, most of the relays will be acceptable the whole

time and hence, the first checked relay will be suitable and thus selected in both schemes. Again, as the asymptotic analysis is conducted at high SNR values, this explains why the system with the two selection schemes achieves the same diversity order and coding gain.

2.6 Simple Design for Calculating Optimum Switching Threshold

From the design point of view, calculating an optimum switching threshold using the achieved expressions of the SEP would be highly complicated due to complexity of those expressions. For engineers, it would be more convenient if other practical approaches can be suggested. In this section, we present a simple way by which the optimum switching threshold can be calculated for the SEC relaying scheme. In particular, the switching threshold can be calculated to maximize the average SNR at the output of the relaying scheme which is given by

$$\bar{\gamma}_{\mathrm{SEC}} = \int_0^\infty x f_{\gamma_{\mathrm{SEC}}}(x) dx. \tag{2.21}$$

Upon differentiating the CDF in (2.10) with respect to γ, the PDF $f_{\gamma_{\mathrm{SEC}}}$ can be obtained. Substituting the derived PDF in (2.21), we get

$$\bar{\gamma}_{\mathrm{SEC}} = \sum_{j=0}^{M-2} [F_\gamma(\gamma_{\mathsf{T}})]^j \int_{\gamma_{\mathsf{T}}}^\infty x f_\gamma(x) dx + [F_\gamma(\gamma_{\mathsf{T}})]^{M-1} \int_0^\infty x f_\gamma(x) dx. \tag{2.22}$$

Using Leibnitz's rule, the derivative of (2.22) with respect to γ_{T} is set to zero $\frac{d\bar{\gamma}_{\mathrm{SEC}}}{d\gamma_{\mathsf{T}}} = 0$, which can be written under the assumption of Rayleigh fading channels as

$$\sum_{j=0}^{M-2} \left[1 - \exp\left(-\frac{2\gamma_{\mathsf{T}}}{\bar{\gamma}}\right)\right]^{j-1} \left\{ j \exp\left(-\frac{2\gamma_{\mathsf{T}}}{\bar{\gamma}}\right) - \frac{2\gamma_{\mathsf{T}}}{\bar{\gamma}} + 2(j+1)\frac{\gamma_{\mathsf{T}}}{\bar{\gamma}} \exp\left(-\frac{2\gamma_{\mathsf{T}}}{\bar{\gamma}}\right) \right\}$$
$$+ (M-1)\left[1 - \exp\left(-\frac{2\gamma_{\mathsf{T}}}{\bar{\gamma}}\right)\right]^{M-2} = 0, \tag{2.23}$$

where finding γ_{T} as a function of $\bar{\gamma}$ and M is now our goal. Unfortunately, the solution of (2.23) can not be obtained as a closed-form, but it has only a single root and a simple numerical search is possible to find the root. With representing γ_{T} as $\frac{\alpha\bar{\gamma}}{2}$, the goal now can be rephrased as finding α as a function of $\bar{\gamma}$ and M. Substituting $\gamma_{\mathsf{T}} = \frac{\alpha\bar{\gamma}}{2}$ into (2.22), the average output SNR based on the switching threshold maximizing the output SNR can be given in a simple closed-form as

$$\bar{\gamma}_{\mathrm{SEC}} = \frac{\bar{\gamma}}{2}\left\{\alpha + 1 - \alpha\left(1 - \exp(-\alpha)\right)^{M-1}\right\}. \tag{2.24}$$

Now, dealing with the result in (2.24) is very simple. For any values of $\bar{\gamma}$ and M, the value of α and hence, γ_{T} that maximizes $\bar{\gamma}_{\mathrm{SEC}}$ can be easily obtained. The same approach can be followed in the case of SECps relaying scheme.

2.7 Numerical Results

In this section, we illustrate the validity of the achieved analytical expressions and the tightness of the used SNR bound via a comparison with Monte-Carlo simulations. We also provide some numerical examples to prove the effectiveness of the proposed relay selection schemes in reducing the system complexity and to show the effect of some system parameters like number of relays, switching threshold, outage threshold, and the location of relays on the system performance.

Figure 2.3 portrays the system outage probability vs SNR for the SEC and SECps relaying schemes for different values of outage threshold γ_{out}. It is clear from this figure that as γ_{out} increases, the system performance is more degraded, as expected. Also, the enhancement achieved in system performance when the SECps is used is obvious in this figure compared to the SEC relaying scheme. This gain is more noticeable in the range where the value of γ_{T} is comparable to the average SNR. For the case where γ_{T} is much larger than the average SNR, the probability that all relays are unacceptable is high and thus the two selection schemes almost behave the same. As the average SNR increases and becomes close to γ_{T}, more relays become acceptable and hence, the SECps scheme behaves better than the SEC scheme. In the region where γ_{T} is much smaller than the average SNR, the probability that all the relays will be acceptable is very high and thus the two schemes give the same behavior. In addition, the perfect match between the analytical results and the asymptotic curves is obvious in this figure for both the SEC and the SECps selection schemes. Finally, this figure shows that

increasing γ_{out} degrades the system performance of both schemes via affecting the coding gain while the diversity order is remained constant at 2.

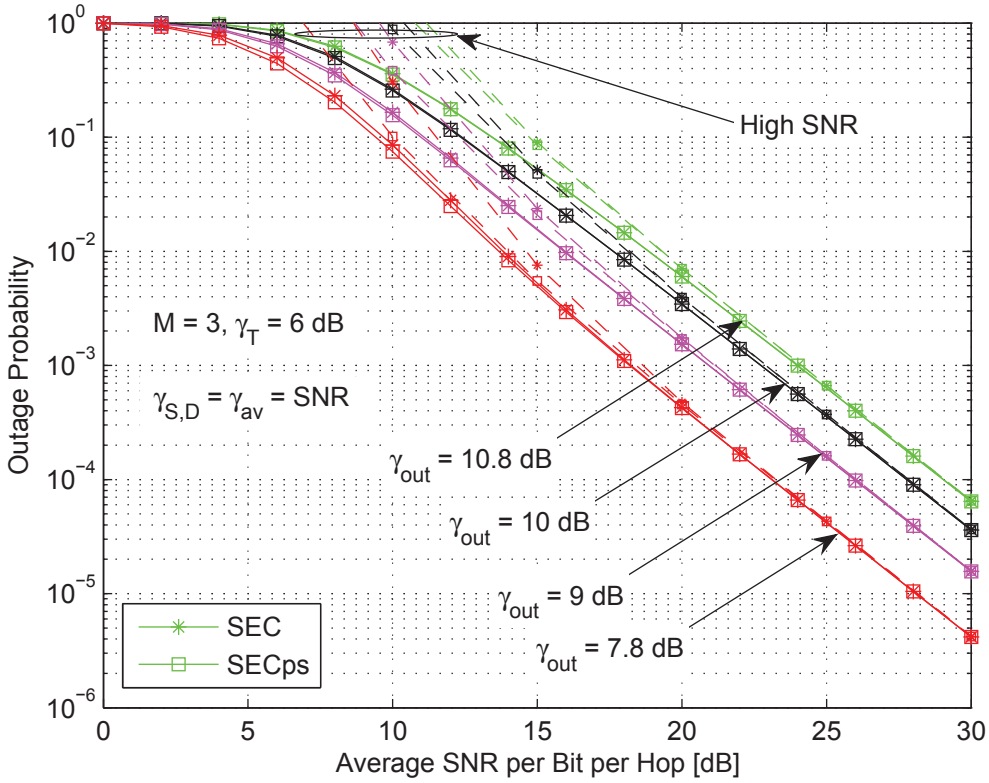

Figure 2.3: Outage probability vs average SNR for AF relay system with SEC and SECps relaying schemes and MRC at destination for different values of outage threshold γ_{out}.

Figure 2.4 shows the system outage probability vs SNR for the SEC and SECps relaying schemes for different numbers of relays M. We can see that at the medium values of SNR, as M increases, the better the achieved behavior. Also, one can notice that as M continues increasing in this region, the gain in system performance becomes smaller. More importantly, it is obvious in this figure that at both low and high SNR values, all curves asymptotically converge to the same behavior and no gain is achieved in system performance with adding more relays.

This is expected since when the switching threshold γ_T takes values much smaller or larger than the average SNR, the system asymptotically converges to the case of two relays and hence, adding more relays will not help in enhancing the system performance. Finally, it is clear from this figure that the curves asymptotically behave similar, especially, at high SNR values and this leads to the same diversity order. In other words, this figure shows that M has no effect on the diversity order of the system which remains constant at 2 in all cases of this figure.

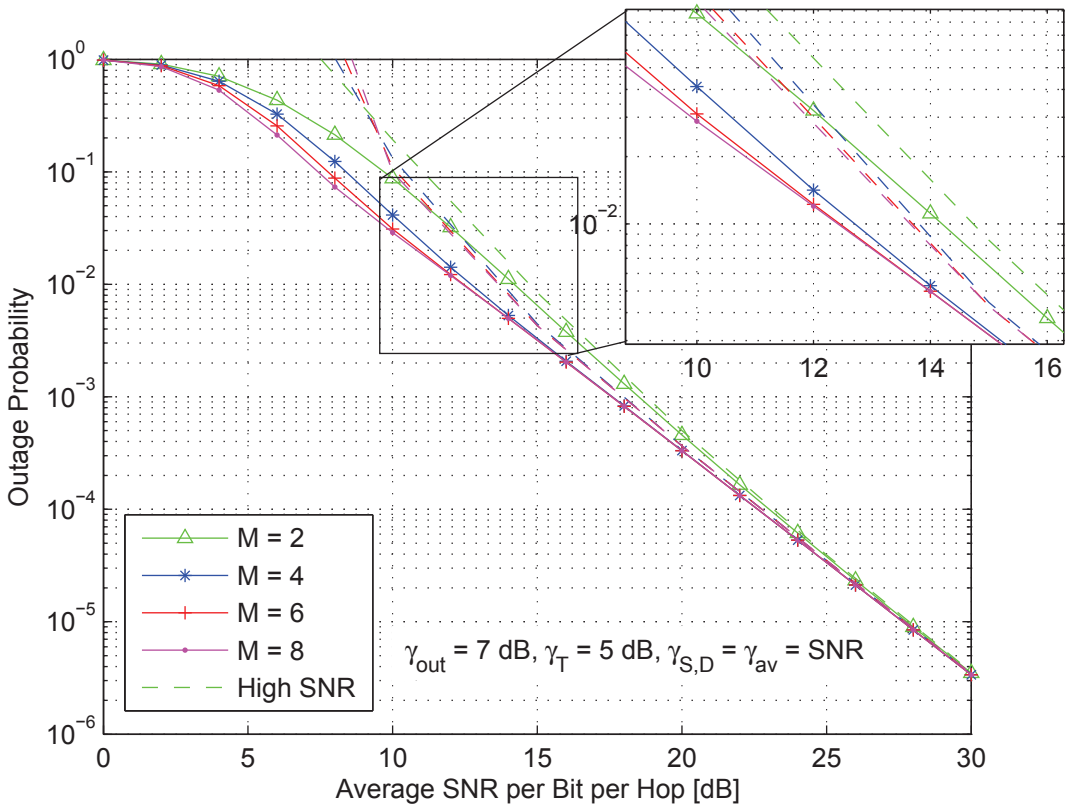

Figure 2.4: Outage probability vs average SNR for AF relay system with SEC relaying scheme and MRC at destination for different numbers of relays M.

Figure 2.5 illustrates the system outage probability vs outage threshold γ_{out} for the proposed SEC relaying scheme for different values of SNR. As expected, as the value of SNR increases and hence, enhancing the direct link and relay paths

channels, the better the achieved performance. In addition, the gain achieved in system performance when the SECps scheme is used is clear in this figure compared to the case where the SEC is used. This gain is more noticeable for the case where the SNR value is comparable to γ_T. As the value of the average SNR becomes much larger than the switching threshold, the gain in system behavior becomes smaller.

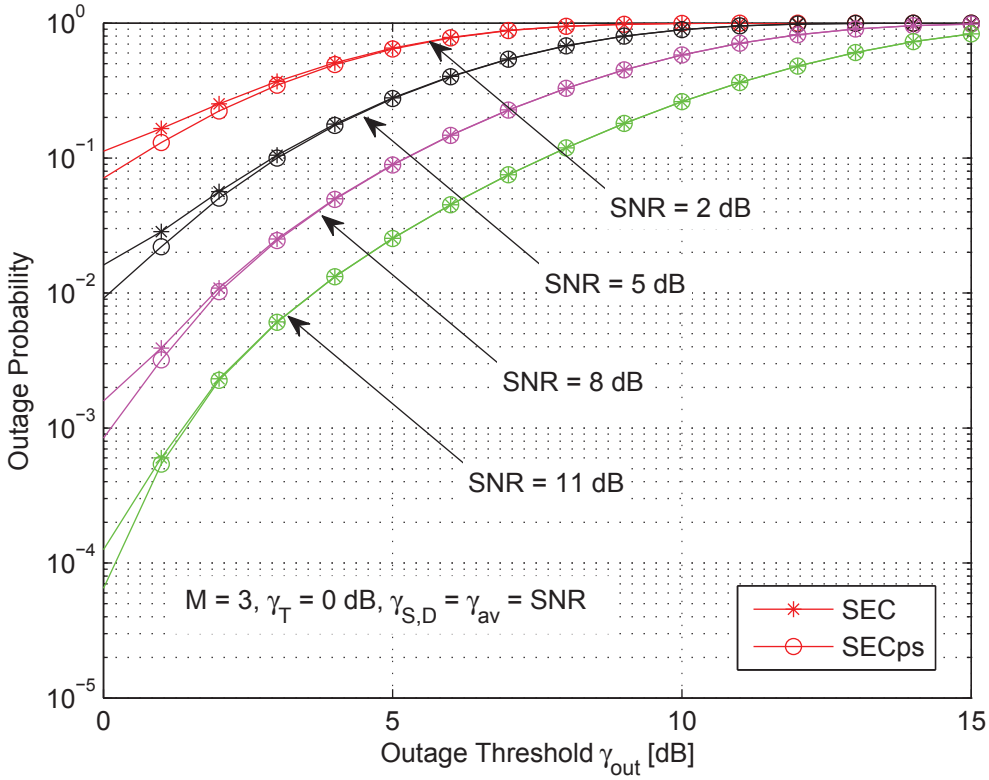

Figure 2.5: Outage probability vs outage threshold for AF relay system with SEC and SECps relaying schemes and MRC at destination for different values of SNR.

Figure 2.6 studies the system SEP vs SNR for various relay selection schemes; SEC, SECps, and best relay selection. In this figure, the switching threshold was assumed to fixed $\gamma_T = 6$ dB and $\bar{\gamma}_{S,D} = \bar{\gamma} =$ SNR. It is clear to notice from this figure that the SECps has nearly the same performance as the best relay

selection for low SNR region. When the SNR increases, the error performance of the SECps scheme degrades and eventually becomes the same as that of SEC. This is expected since when γ_{T} is large in comparison with the average SNR, no relay will be acceptable and the SECps selection scheme will always select the best relay, just as in best relay selection scheme; whereas, when γ_{T} is small compared to the average SNR, the SECps selection scheme works more like conventional SEC scheme.

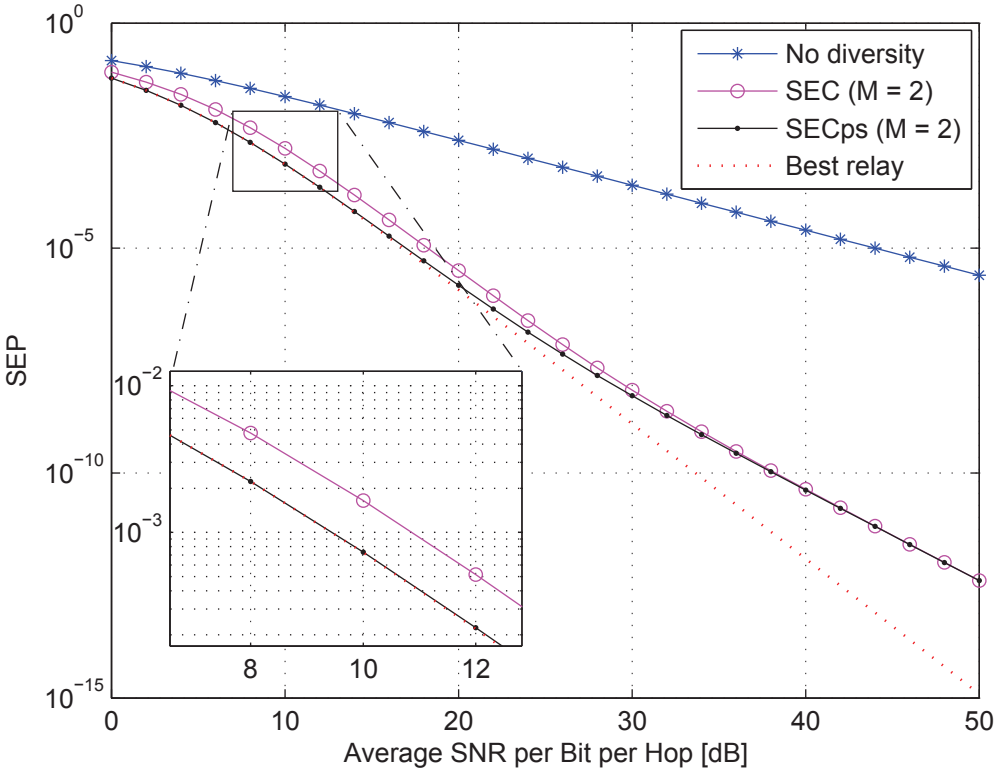

Figure 2.6: Average SEP vs average SNR for AF relay system with SEC relaying scheme and MRC at destination in comparison with SECps relaying scheme and MRC at destination, and best relay selection scheme and MRC at destination for $\bar{\gamma}_{\mathsf{S,D}} = \bar{\gamma} = \text{SNR}$.

Figure 2.7 shows the SEP vs SNR for no diversity, SEC, and SEC+MRC cases with optimal switching threshold $\gamma_{\mathsf{T-Opt}}$ being used. It can be noticed from

this figure that the derived upper bound of the total SNR (lower bound of SEP) is tight enough, especially, at medium and high SNR values. For example, the exact average SEP (simulation) for the SEC+MRC case at SNR = 15 dB equals $1 \times 10^{-4.7}$, while the analytical average SEP is $1 \times 10^{-4.8}$. This trend is valid for both the SEC and the SEC+MRC cases. This bound on the SNR is also used in the case of SECps relaying scheme. The gain that the SEC and the SEC+MRC cases add to system performance compared to the no diversity case is obvious in this figure. In addition, the enhancement the direct link adds to the system behavior via the SEC+MRC case compared to the case of no direct link through the SEC alone is also clear in this figure.

Figure 2.8 illustrates the system SEP vs SNR for the SEC and SECps relaying schemes for different numbers of relays M. As we can see, increasing M leads to a significant gain in system performance for both schemes, especially, in the region where the average SNR value is comparable to γ_{T}. Also, the enhancement the SECps scheme adds to system performance compared to the SEC scheme is clear in this figure. Finally, the achievement in system performance due to the relay cooperative diversity is obvious in this figure when compared to the no diversity case.

Figure 2.9 studies the effect of the switching threshold γ_{T} and the number of relays M on the error performance of the proposed relaying schemes. For the case of SEC relaying scheme, increasing M leads to a significant gain in system performance, especially, in the medium region of SNR values. On the other hand,

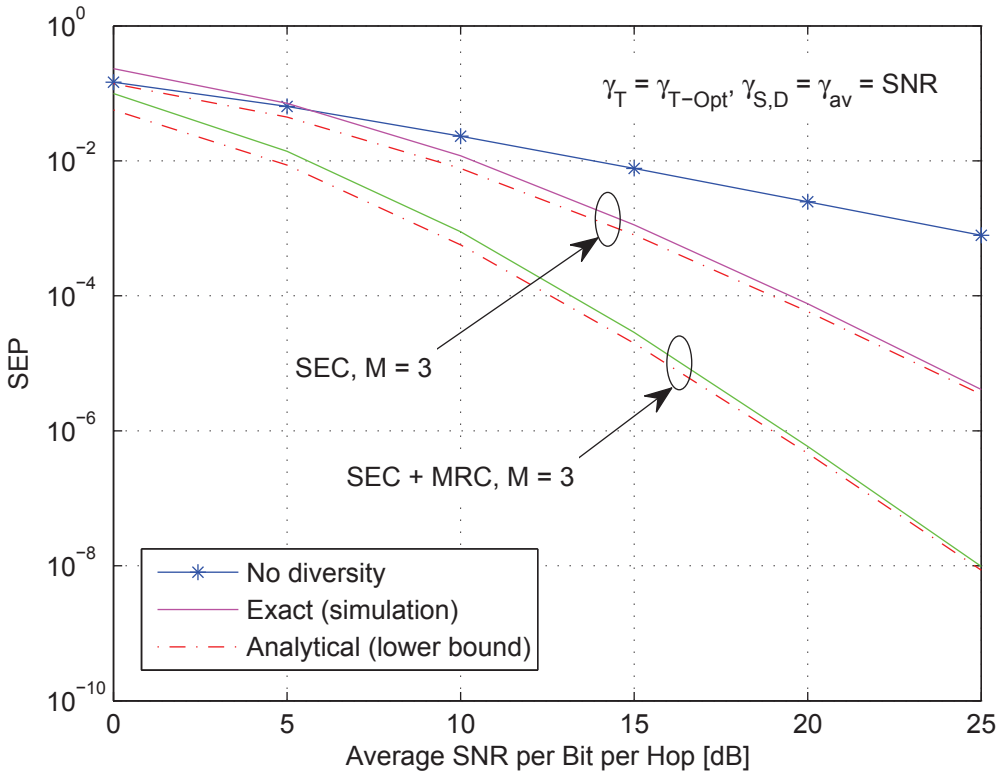

Figure 2.7: Average SEP vs average SNR for AF relay system with SEC relaying scheme and MRC at destination for cases of no relaying, SEC relaying only, and SEC relaying with MRC at destination.

as γ_T becomes much smaller or much larger than the average SNR, the SEP improvement decreases, as all curves asymptotically converge to the case of two relays. This is due to the fact that, if the average SNR is very small compared to γ_T, all the relays will be unacceptable most of the time. On the other hand, if the average SNR is very high in compared to γ_T, all the relays will be acceptable and one relay will be used most of the time. Thus, in both cases, the additional relays will not lead to any gain in system behavior. On the other hand, the SECps relaying scheme gives the same performance as the SEC scheme in the region where γ_T is much smaller than the average SNR, as expected; whereas, in the

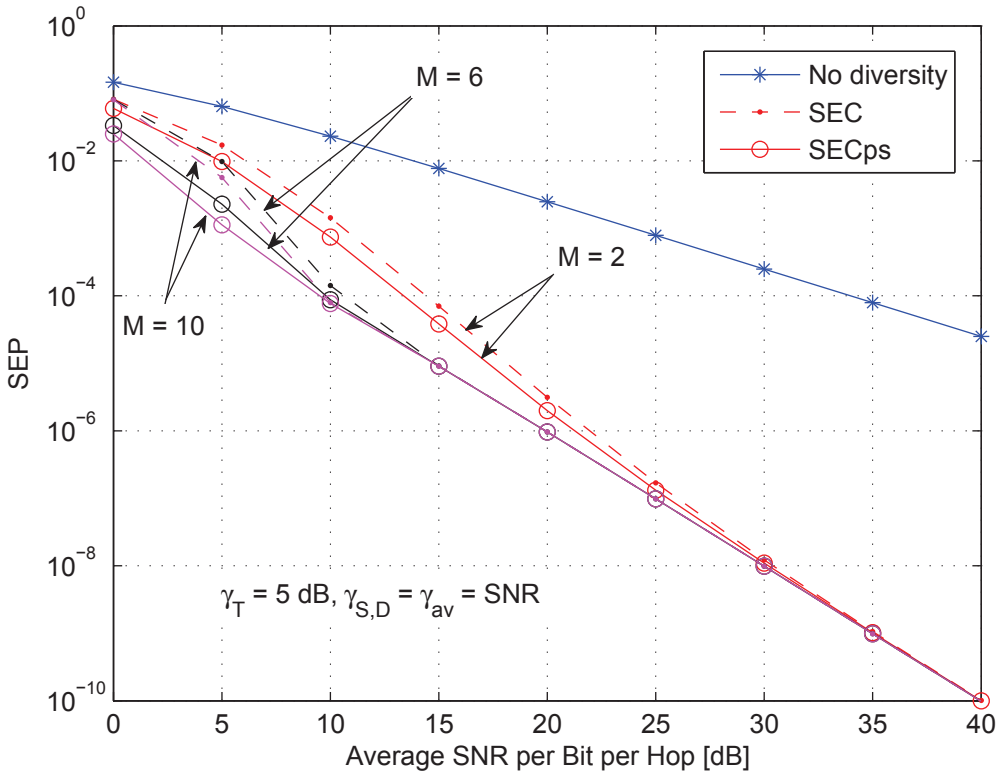

Figure 2.8: Average SEP vs average SNR for AF relay system with SEC and SECps relaying schemes and MRC at destination for different numbers of relays M.

region where γ_T is much larger than the average SNR, the SECps gives better performance compared to the SEC scheme. This is because in the SECps scheme, when the last relay is reached and found unacceptable, the scheme selects the best relay among all relays in contrast to the SEC scheme which in this case sticks to that last relay. This explains the gap in system performance between the two schemes in this region of γ_T.

Figure 2.10 illustrates the system SEP vs SNR for the proposed SEC relaying scheme for different values of switching threshold γ_T. It is clear from this figure that the best performance is achieved when the optimum switching threshold

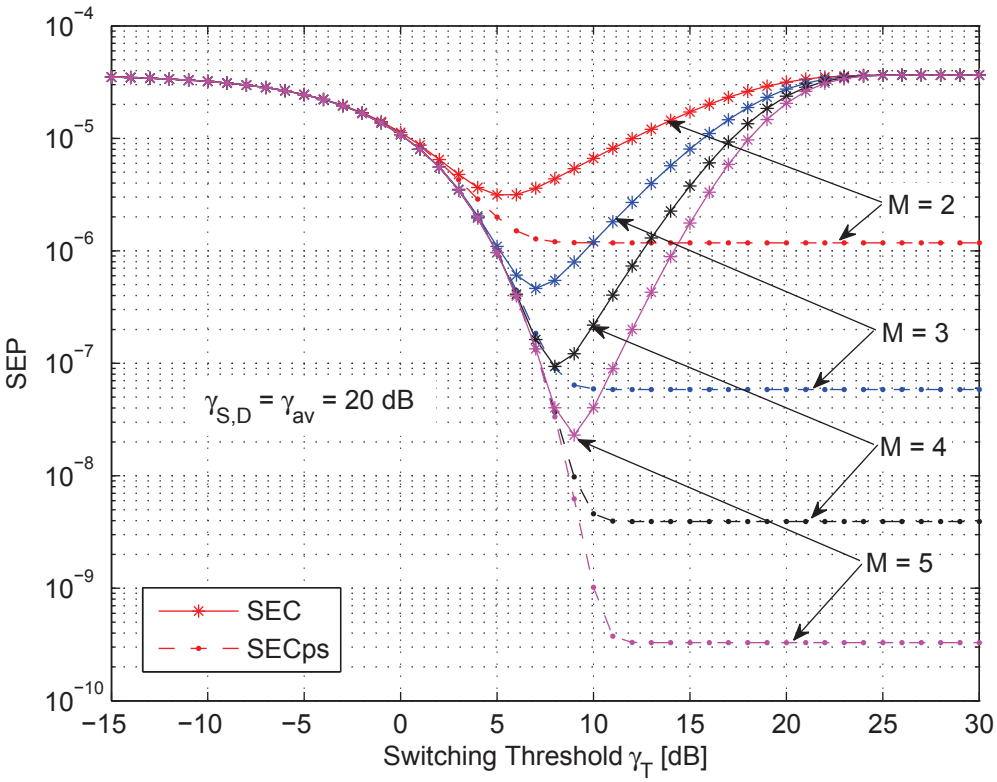

Figure 2.9: Average SEP vs switching threshold for AF relay system with SEC and SECps relaying schemes and MRC at destination for different numbers of relays M.

$\gamma_{\mathsf{T-Opt}}$ is used, as expected.

Figure 2.11 demonstrates the SEP performance vs SNR for the SEC relaying scheme for different numbers of relays M. As expected, as M increases, the better the achieved performance, especially, in the region where the average SNR values are comparable to γ_{T}. The figure also shows that this behavior extends to the case of i.n.d. relay hops.

Figure 2.12 demonstrates the effectiveness of the proposed selection schemes compared to some popular schemes. As an example, for the case of 4 relays, the number of active relays in the best relay and partial relay selection schemes is 4

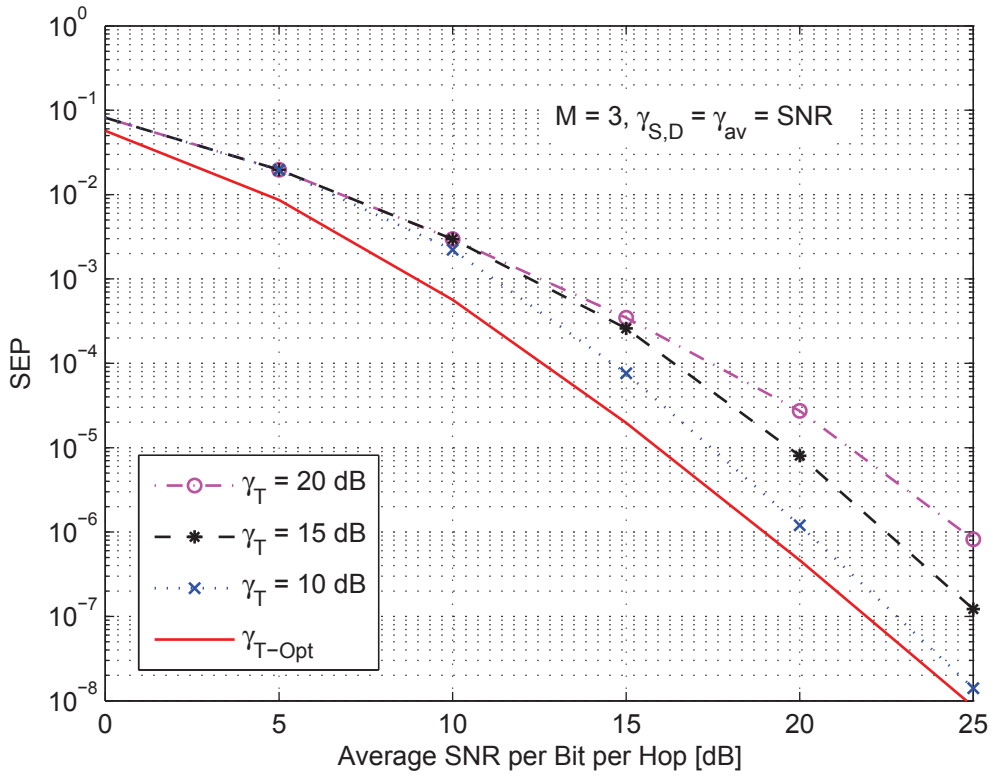

Figure 2.10: Average SEP vs average SNR for AF relay system with SEC relaying scheme and MRC at destination for different values of switching threshold γ_T.

all the time; whereas, it is smaller in the case of the SEC proposed scheme and depends on γ_T. In the worst case, it reaches 3. For channel estimations, in the case of the best and partial relay selection schemes, 4 and 8 channels are required to be estimated, respectively; whereas, it is lower in the proposed SEC protocol which reaches 6 at the worst case. This shows the significant reduction in system complexity the proposed schemes achieve.

Figure 2.13 shows a 3-dimensional portray for the system SEP versus the distances from the source to relays for the case of two relays of the proposed SEC relaying scheme. This is equivalent to the case where the relays have i.n.d. hops. The curve studies the effect of the relays position on the average SEP performance

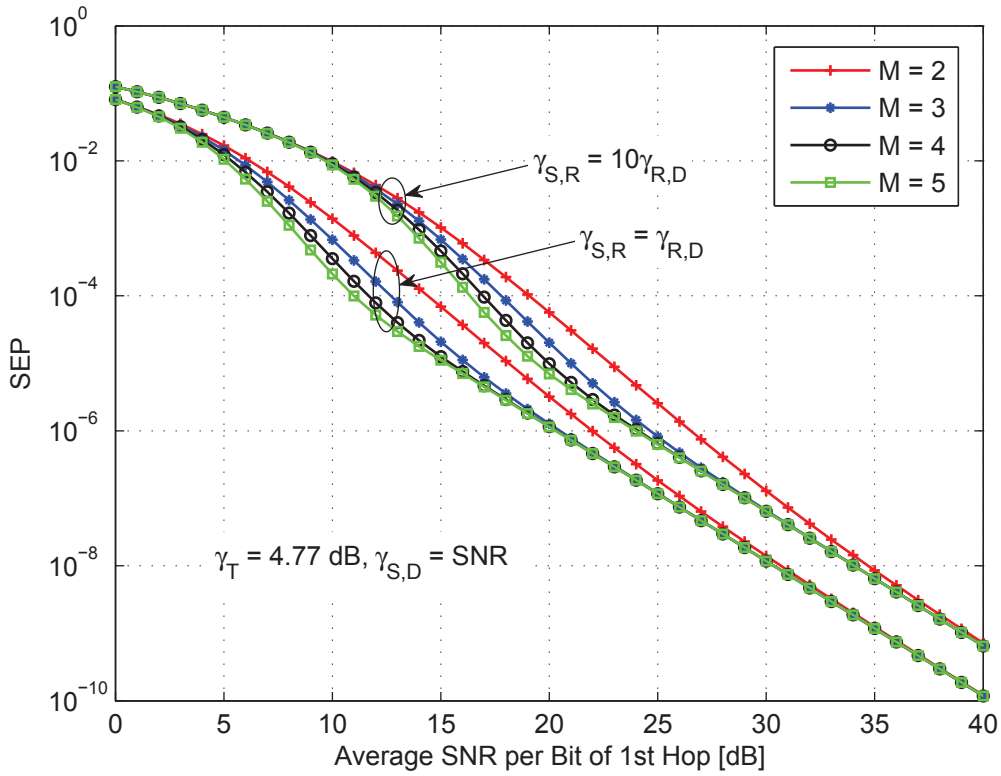

Figure 2.11: Average SEP vs average SNR for AF relay system with SEC relaying scheme and MRC at destination for i.n.d. hops and different numbers of relays M.

for different values of SNR. It is clear that in order to have best performance for this AF relay system, the two relays must be located in the midway between the source and the destination. In addition, it can be seen that as the value of SNR increases, the system performance is more enhanced.

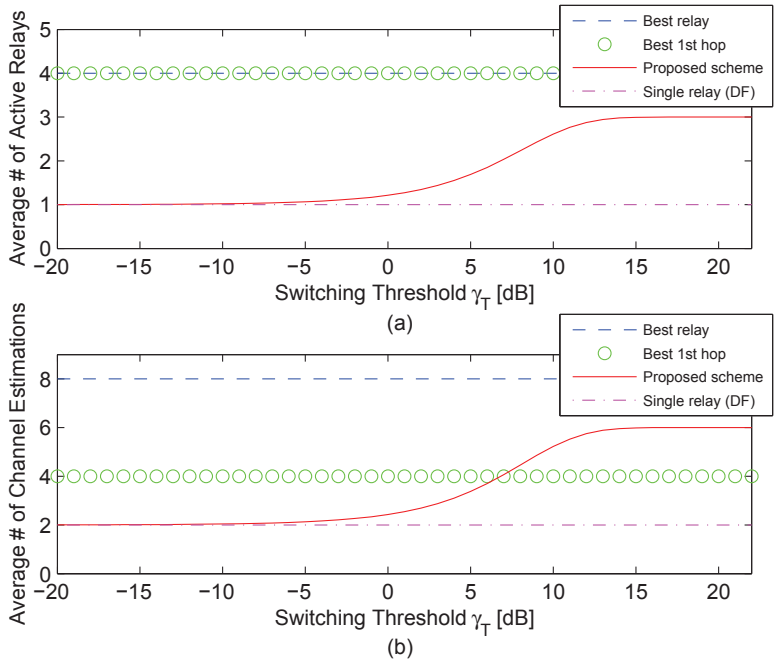

Figure 2.12: Complexity-performance tradeoff of the proposed SEC relaying scheme for AF relay system with $M = 4$ and $\bar{\gamma} = 7$ dB, (a) Average number of active relays, (b) Average number of channel estimations.

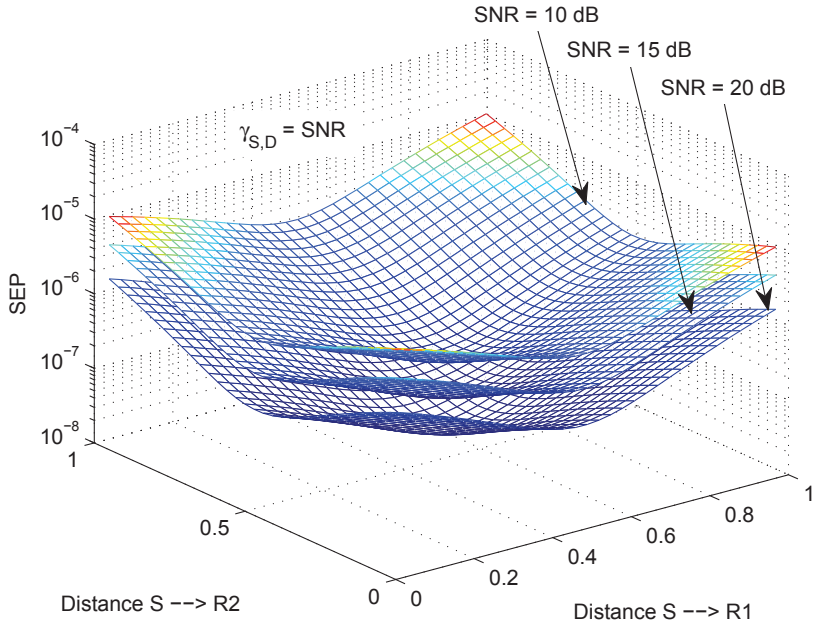

Figure 2.13: Average SEP vs $D_{\mathsf{S}\to\mathsf{R}_1}$ and $D_{\mathsf{S}\to\mathsf{R}_2}$ for AF relay system with SEC relaying scheme for different values of SNR.

2.8 Conclusions

In this chapter, we proposed a low-complexity SEC-based relay selection scheme for AF relay systems. This scheme is based on the well known SEC and SECps diversity combining techniques. Using an upper bound on the SNR of the relay paths, the probability density and the cumulative distribution functions of the SNR at output of the SEC combiner were first derived. Then, the e2e outage probability and bit error probability were derived for i.n.d. and i.i.d. relay channels. Monte-Carlo simulations proved the accuracy of the analytical results and the tightness of the used bound, especially, at medium to high SNR values. Asymptotic high SNR results showed that the system with the SEC and SECps relaying schemes has the same diversity order of 2 and the same coding gain which is affected by the switching and outage thresholds. Furthermore, findings illustrated the effectiveness of the proposed relay selection schemes in reducing the system complexity compared to the existing relay selection schemes. Also, results showed that the gain achieved in system performance due to increasing the number of relays happens in the range of SNR values that are comparable to the switching threshold. Finally, findings illustrated the gain achieved in system performance by the SECps relaying scheme over the conventional SEC relaying, especially, at low to medium SNR values.

CHAPTER 3

DF RELAY SELECTION USING SWITCH-AND-EXAMINE

3.1 Introduction

In chapter 2, the low complexity SEC and SECps relaying schemes were proposed for AF relay systems. Noise-limited environment was assumed in the analysis of that chapter without considering the interference. As known, the co-channel interference (CCI) is inherently existed in relay networks and hence, studying its effect on system performance is of a great importance. Due to the difficulty of mathematical manipulations, studying the performance of AF SEC and SECps relay systems with interference at the relays and destination is highly complicated. Alternatively, we study the effect of interference on such relaying schemes but with DF relaying, especially, the DF and AF relaying schemes approximately have the same performance at low and medium SNR values and the same performance at

high SNR values.

In this chapter, we propose and evaluate the outage performance of a new low-complexity relay selection scheme for dual-hop DF relay systems in the presence of CCI at the relay and destination nodes. The scheme is mainly based on the SEC and SECps diversity combining techniques in which a relay out of multiple relays is selected to forward the source message to destination. The selection process is performed such that the SNR of the second hop of the selected relay satisfies a predetermined switching threshold. Such a relay that satisfies this threshold is chosen instead of the best relay to forward the source message to destination. In the analysis, we first derive the PDF of the SNR of the relay selection scheme and the conditional CDF of the e2e signal-to-interference plus noise ratio (SINR) assuming Rayleigh fading channels. The derived statistics along with the statistics of the first hop channels of the relays and the direct link are then used to derive a closed-form expression for the outage probability of the system. We assume that MRC is used at the destination to combine the signal from the selected relay with that on the direct link. Furthermore, to get more about system insights, the outage performance is studied at high SNR regime where approximate expressions for the outage probability, diversity order, and coding gain are derived and analyzed. Monte-Carlo simulations and some numerical results are provided to illustrate the validity of the derived analytical results and to show the effect of interference and other parameters on the system performance. Main results illustrate the significant reduction in the required number of channel estimations and hence,

the system complexity our proposed relay selection scheme can cause compared to the existed schemes. Findings illustrate that when the interference power does not scale with SNR, the system can still achieve diversity gain; especially, at SNR values that are comparable to the switching threshold. Asymptotic results show that at high SNR values, the system with the SEC and SECps relaying schemes achieve a diversity order of 2 and approximately the same coding gain. Finally, results show the severe effect of interference in reducing the gain achieved in system performance when the SECps scheme is used compared to the conventional SEC scheme.

The rest of this chapter is organized as follows. In Section 3.2, we review the related literature. Section 3.3 explains the system model. The performance analysis is conducted in Section 3.4. Section 3.5 presents the asymptotic system analysis. Section 3.6 gives the special case of noise-limited system. Some numerical results are discussed in Section 3.7. Finally, some conclusions are provided in Section 3.8.

3.2 Literature Review

Cooperative or relay networks have generally been studied with respect to the relay selection schemes, coding, multi-user communication, multi-antenna and beamforming, channel estimation errors, and power allocation, mostly, under conditions of AWGN [36]-[38]. However, the CCI dominates AWGN in such wireless systems due to the extensive re-use of frequency bands by system users. Moreover,

the effect of interference can be more severe on the relay systems where all relays may use the same frequency band and hence, CCI may exist in every link in the relay network. This shows the need for new studies that address the impact of this channel impairment on the performance of such cooperative networks.

Recently, more attention has been given to evaluate the interference effect on the performance of cooperative networks [39]-[41]. A study on the performance of multi-relay DF cooperative systems in the presence of interference at the relay and destination nodes assuming Nakagami-m fading channels was evaluated in [16]. Conventional relaying was assumed in the analysis where all successful relays participate in forwarding the source message to destination along with the direct link. Some key papers on cooperative systems with multiple relays and opportunistic relaying are the ones presented in [17], [18]. Particularly, in [17], Kim *et al.* evaluated the outage performance of an opportunistic DF cooperative system with interference at the relays and destination nodes. All channels were assumed to follow Rayleigh distribution with the existence of arbitrary number of unequal power interferers. The lack of comprehensive studies that evaluate the performance of multi-relay cooperative systems with interference at the relay and destination nodes and the importance of such cooperative systems motivate us to contribute in this area of research.

Several relay selection schemes were proposed for cooperative networks with multiple relays, among which is the best relay or opportunistic relaying [34]. In this scheme, only the best relay is always selected among all other relays to for-

ward the source message to destination which makes it an optimum relay selection scheme in this sense. Compared to the conventional relaying schemes where all relays participate in the cooperation process, the opportunistic relaying enhances the system spectral efficiency and eliminates the inefficient use of channel resources. Another relay selection scheme is the partial relaying [11]. In such a scheme, the relay with the first hop SNR greater than a predetermined SNR threshold and being the maximum among other relays is chosen to be the best. This is useful for certain practical situations in ad-hoc networks where only the first hop channels of the relays are available to the source. As can be seen, in order for these relay selection schemes to be able to select the best relay, a large number of channels need to be estimated each transmission time. This increases the power consumption, reduces the relay battery life, and increases the system complexity.

Motivated by the above, we propose the low-complexity SEC-based relaying schemes for dual-hop DF relay systems and evaluate the performance of such systems in the presence of interference at the relays and destination over Rayleigh fading channels. Our contributions in this area over the existing studies can be summarized in the following points: *i*) we propose a new low-complexity SEC-based and SECps relay selection schemes for dual-hop DF relay systems with interference at the relays and destination; *ii*) in contrast to the relay selection schemes presented in [16], [17] for DF relay systems, in our proposed schemes, only the first checked relay whose second hop channel SNR exceeds a predeter-

mined switching threshold is selected to forward the source message to destination. Thus, in contrast to the aforementioned relay selection schemes, the channels of only an arbitrary relay are required to be estimated each time of data transmission. In this case, the other relays remain silent and do not need to operate as channel estimators. This results in a noticeable reduction in the required number of channel estimations and saves the power of the relays and hence, reducing the system complexity; *iii*) we present a full evaluation for the system outage performance where the effectiveness of the proposed relay selection scheme in reducing the complexity of the considered system is illustrated and the effect of interference and some system parameters on the system performance is provided; *iv*) furthermore, in order to get more about system insights, we study the outage performance at high SNR regime where approximate expressions for the outage probability, diversity order, and coding gain are derived and analyzed. In the analysis, we derive exact closed-form expressions for the outage probability for the generic i.n.d. case of relay second hop channels for the SEC-based selection scheme and for the i.i.d. case for the SECps-based relay selection scheme. Firstly, the PDF of the SNR at the selection scheme output, the CDF of the e2e SINR, the CDF of the SINR of the relays first hop channels, and the CDF of the direct link are derived. Then, these statistics are used to derive a closed-form expression for the system outage probability. Further analysis is conducted following the same procedure to evaluate the asymptotic system behavior. The switching threshold is selected to optimize the e2e outage probability. Due to its inherent effect on

system behavior, the direct link is considered in all derivations in this chapter. The situation where the direct link is not existed becomes a special case of the considered system.

3.3 System Model

Figure 3.1 shows the relay system under consideration. It consists of one source, one destination, K relay nodes, and arbitrary number of interferers at both the relays and the destination.

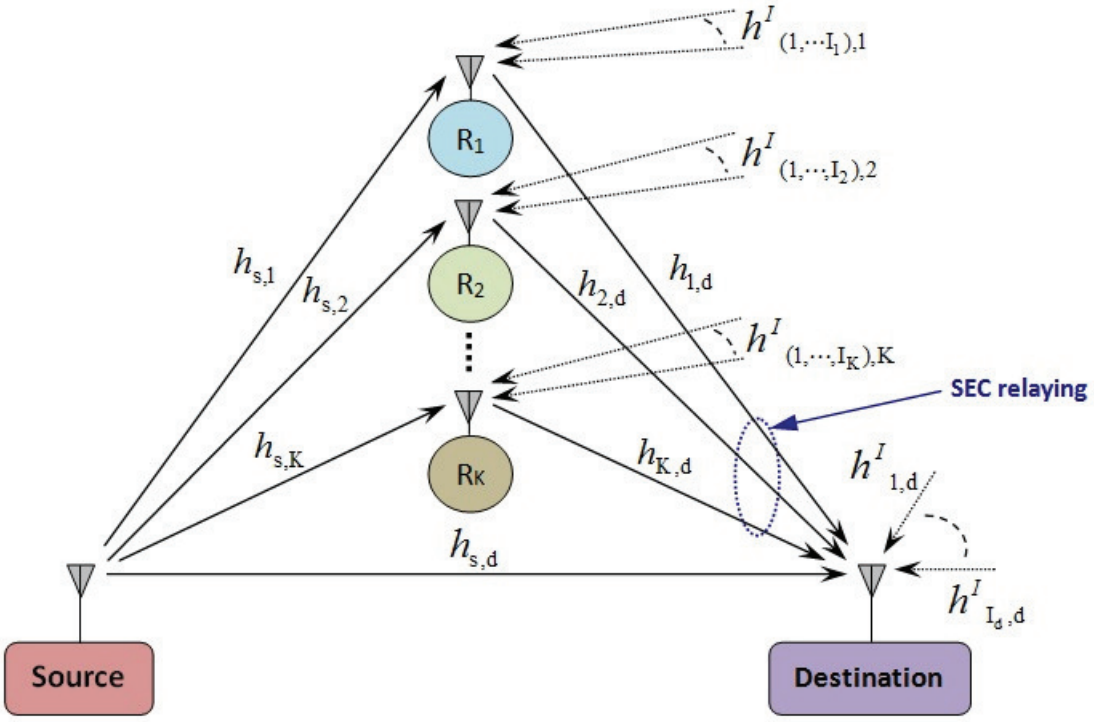

Figure 3.1: A schematic diagram for dual-hop DF relay system with SEC relay selection scheme and interference at the relays and destination.

The entire communication takes place in two phases. In the first phase, the source S transmits its message to the destination D and the K relays. In the

second phase, the relay which satisfies a predetermined switching threshold among all other relays who succeeded to decode the source message in the first phase is selected to forward it to D. The SEC-based relay selection scheme works as follows: at the guard period of each transmission time, the source sends a RTS packet to relays and destination. This packet allows each relay to estimate its first hop channel. To reduce the overall overhead in communication, a method based on time is selected: as soon as the RTS packet is received, each relay who successfully received the source message starts a timer based on its first hop instantaneous channel estimation. The relay whose timer is expired first sends a RTS packet to destination through which the destination estimates its second hop channel. Then, this channel is compared with the switching threshold. If it is larger, the destination +ve acknowledges this relay and asks it to start transmitting through a one bit feedback. This suitable relay sends a flag to other relays signaling its presence. All relays, while waiting for their timer to reduce to zero, are in listening mode. As soon as they hear another relay to flag its presence or forward information, they back off. If this relay is found unacceptable, it will be -ve acknowledged by the destination where it will keep silent. In this case, the timer of other relay expires and the same process is repeated. This process continues till the last relay is reached. If this relay is found acceptable, it will be +ve acknowledged by the destination to start its transmission. If not, the destination will -ve acknowledge it and wait for a certain time Δ. If it does not receive other RTS packet from other active relay. It will ask the last checked relay to start its

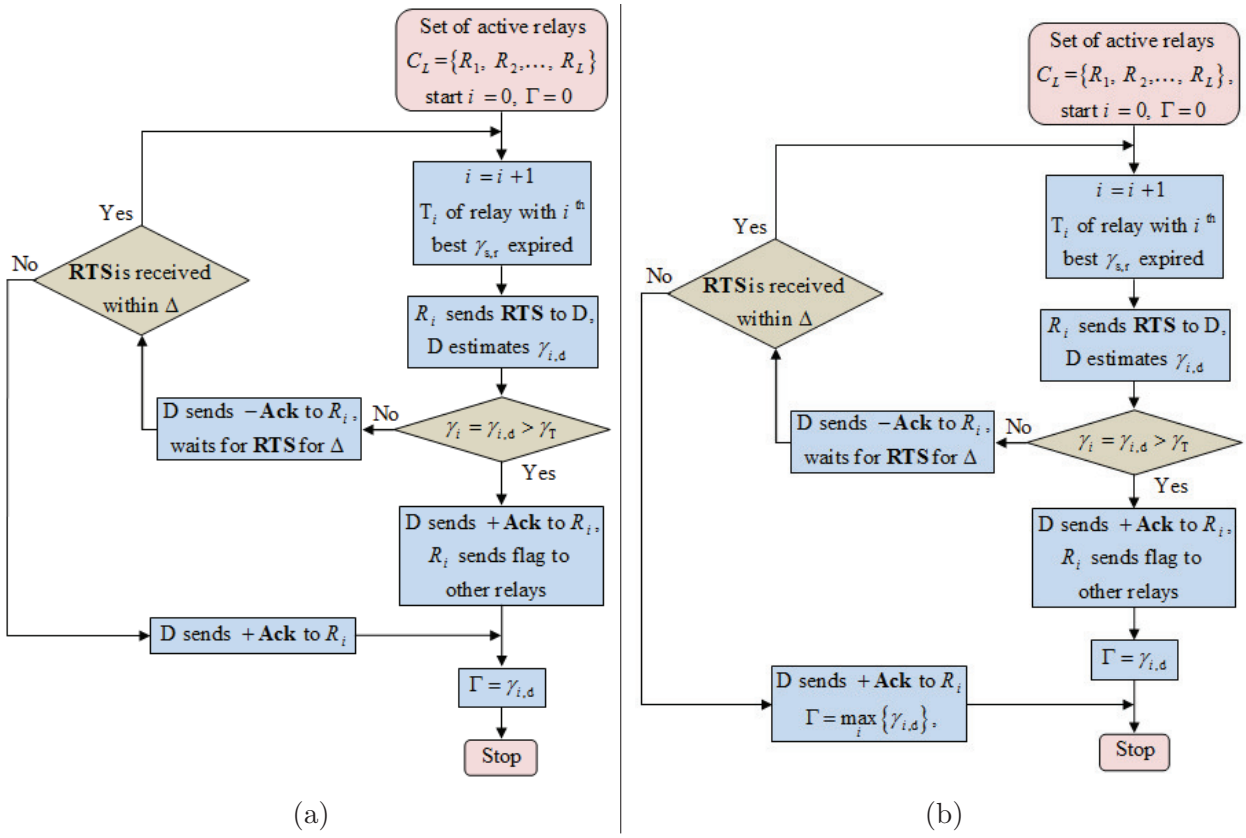

Figure 3.2: Flowcharts for the proposed relaying schemes, (a) SEC relaying, (b) SECps relaying.

transmission. In the case of SECps, the destination will ask the best relay among all checked relays to conduct its transmission.

We assume that the signal at the k^{th} relay is corrupted by interfering signals from I_k co-channel interferers $\{x_i\}_{i=1}^{I_k}$. The received signal at the k^{th} relay can be expressed as

$$y_{\mathsf{r}_k} = h_{\mathsf{s},k} x_0 + \sum_{i_k=1}^{I_k} h^I_{i_k,k} x^I_{i_k,k} + n_{\mathsf{s},k}, \tag{3.1}$$

where $h_{\mathsf{s},k}$ is the channel coefficient between S and the k^{th} relay, x_0 is the transmitted symbol with $\mathbb{E}\{|x_0|^2\} = P_0$, $h^I_{i_k,k}$ is the channel coefficient between the i_k^{th} interferer and k^{th} relay, $x^I_{i_k,k}$ is the transmitted symbol from the i_k^{th} interferer with

$\mathbb{E}\{|x^I_{i_k,k}|^2\} = P^I_{i_k,k}$, and $n_{\mathsf{s},k} \sim \mathcal{CN}(0, N_0)$ is an AWGN. Let us define $h_{\mathsf{s},\mathsf{d}}$, $h_{k,\mathsf{d}}$, and $h^I_{i_d,\mathsf{d}}$ as the channel coefficients between S and D, the k^{th} relay and D, the i_d^{th} interferer and D, respectively. All the channel gains are assumed to follow Rayleigh distribution. That is, the channel powers denoted by $|h_{\mathsf{s},\mathsf{d}}|^2$, $|h_{\mathsf{s},k}|^2$, $|h_{k,\mathsf{d}}|^2$, $|h^I_{i_k,k}|^2$, and $|h^I_{i_d,\mathsf{d}}|^2$ are exponential distributed random variables (RVs) with parameters $\sigma^2_{\mathsf{s},\mathsf{d}}$, $\sigma^2_{\mathsf{s},k}$, $\sigma^2_{k,\mathsf{d}}$, $\sigma^2_{I,i_k,k}$, and $\sigma^2_{I,i_d,\mathsf{d}}$, respectively. Using (3.1), the SINR at the k^{th} relay can be written as

$$\gamma_{\mathsf{s},k} = \frac{\frac{P_0}{N_0}|h_{\mathsf{s},k}|^2}{\sum_{i_k=1}^{I_k} \frac{P^I_{i_k,k}}{N_0}|h^I_{i_k,k}|^2 + 1}. \tag{3.2}$$

Let C_L denote a decoding set defined by the set of active relays that could have correctly decoded the message sent from the source in the first phase. It is defined as [17]

$$\begin{aligned} C_L &\triangleq \left\{ k \in \mathcal{S}_r : \frac{1}{2}\log_2\left(1+\gamma_{\mathsf{s},k}\right) \geq R \right\} \\ &= \left\{ k \in \mathcal{S}_r : \gamma_{\mathsf{s},k} \geq 2^{2R} - 1 \right\}, \end{aligned} \tag{3.3}$$

where $\mathcal{S}_r$ is a set of L relays and R denotes a fixed spectral efficiency threshold.

In the second phase after decoding the received signal, the first checked relay in C_L whose second hop channel SNR is greater than the predetermined switching threshold forwards the re-encoded signal to the destination. The selected relay is chosen according to the SEC selection scheme and it is the first checked relay in C_L whose $\gamma_{l,\mathsf{d}}$ is greater than a predetermined switching threshold. It can be

written as

$$\gamma_{l,\mathsf{d}} = \frac{\frac{P_l}{N_0}|h_{l,\mathsf{d}}|^2}{\sum_{i_d=1}^{I_d} \frac{P^I_{i_d,\mathsf{d}}}{N_0}\left|h^I_{i_d,\mathsf{d}}\right|^2 + 1}, \tag{3.4}$$

where P_l, $P^I_{i_d,\mathsf{d}}$, and N_0 are the transmit power of the l^{th} active relay, the transmit power of the i_d^{th} interferer, and the AWGN power at the destination, respectively, and I_d is the number of interferers at the destination node. Equivalently, the relay with the second hop channel SNR $\left\{\frac{P_l}{N_0}|h_{l,\mathsf{d}}|^2\right\}$ greater than a predetermined switching threshold is selected to forward the source message to destination since the denominator is common to the SINRs from all relays belonging to C_L.

In the analysis of the considered system, the destination is assumed to be located at the same point during the two phases. This means the same interference is affecting the destination node in both phases. The destination finally combines the signals from the source and the selected relay using MRC. The e2e SINR at the destination output can be written as

$$\gamma_{\mathsf{d}} \triangleq \gamma_{\mathsf{s},\mathsf{d}} + \gamma_{\text{SEC},\mathsf{d}} = \frac{\frac{P_0}{N_0}|h_{\mathsf{s},\mathsf{d}}|^2 + \frac{P_0}{N_0}|h_{\text{SEC},\mathsf{d}}|^2}{\sum_{i_d=1}^{I_d} \frac{P^I_{i_d,\mathsf{d}}}{N_0}\left|h^I_{i_d,\mathsf{d}}\right|^2 + 1}. \tag{3.5}$$

3.4 Performance Analysis

In this section, we evaluate exact closed-form expressions for the outage probability of the studied system with the proposed SEC and SECps relay selection schemes.

Let C_L be a decoding subset with a number of L active relays (i.e., cardinality $|C_L| = L$), then the distribution of this decoding set is given by

$$\mathrm{P_r}\left[C_L\right] = \prod_{l \in C_L} \mathrm{P_r}\left[\gamma_{\mathsf{s},l} \geq u\right] \prod_{m \notin C_L} \mathrm{P_r}\left[\gamma_{\mathsf{s},m} < u\right], \tag{3.6}$$

where $u = \left(2^{2R} - 1\right)$. The outage probability for the studied system is given by [17]

$$\begin{aligned} P_{\mathsf{out}} &\triangleq \mathrm{P_r}\left[\frac{1}{2}\log_2\left(1+\gamma_{\mathsf{d}}\right) < R\right] \\ &= \sum_{L=0}^{K} \sum_{C_L} \mathrm{P_r}\left[\gamma_{\mathsf{d}} < u | C_L\right] \mathrm{P_r}\left[C_L\right], \end{aligned} \tag{3.7}$$

where the internal summation is taken over all of $\binom{K}{L}$ possible subsets of size L from the set with the K relays. In order to evaluate (3.7), we need first to derive $\mathrm{P_r}\left[\gamma_{\mathsf{d}} < u | C_L\right]$ and $\mathrm{P_r}\left[C_L\right]$.

3.4.1 SEC-Based Relay Selection

In this section, we evaluate the outage probability of the studied system with the SEC relaying when the CDFs of second hops of relays are non-identical and the interferers at the relays and destination have unequal average powers.

Let $\rho \triangleq P_0/N_0 = P_l/N_0$ and $\rho_{I_k} \triangleq P^I_{i_k,k}/N_0 = P^I_{i_d,\mathsf{d}}/N_0 = \rho_I$. Then, $\rho|h_{\mathsf{s},\mathsf{d}}|^2$, $\rho|h_{\mathsf{s},k}|^2$, $\rho_I|h^I_{i_k,k}|^2$, $\rho|h_{l,\mathsf{d}}|^2$, and $\rho_I|h^I_{i_d,\mathsf{d}}|^2$ are exponential distributed with parameters $\lambda_{\mathsf{s},\mathsf{d}} = 1/\rho\sigma^2_{\mathsf{s},\mathsf{d}}$, $\lambda_{\mathsf{s},k} = 1/\rho\sigma^2_{\mathsf{s},k}$, $\lambda^I_{i_k,k} = 1/\rho_I\sigma^2_{I,i_k,k}$, $\lambda_{l,\mathsf{d}} = 1/\rho\sigma^2_{l,\mathsf{d}}$, and $\lambda^I_{i_d,\mathsf{d}} = 1/\rho_I\sigma^2_{I,i_d,\mathsf{d}}$. For the case of unequal power interferers, we have $\alpha^I_{i_n,n} \neq \alpha^I_{j_n,n}$,

when $i_n \neq j_n$, $n \in \mathcal{S}_r \bigcup \{d\}$.

The results of the terms $\mathrm{P_r}\left[\gamma_{\mathsf{d}} < u | C_L\right]$ and $\mathrm{P_r}\left[C_L\right]$ for the case of i.n.d. second hops $\{\lambda_{i,\mathsf{d}}\}_{i=1}^{L}$ and unequal power interferers $\{\lambda_{i_n,n}^{I}\}_{i_n=1}^{I_n}$ are summarized in the following two Lemmas, respectively.

Lemma 3.1 *The term* $\mathrm{P_r}\left[\gamma_{\mathsf{d}} < u | C_L\right]$ *in (3.7) is given for* $L \geq 1$ *by*

$$\begin{aligned}
\mathrm{P_r}\left[\gamma_{\mathsf{d}} < u | C_L\right] &= \prod_{i_d=1}^{I_d} \lambda_{i_d,\mathsf{d}}^{I} \exp\left(\lambda_{i_d,\mathsf{d}}^{I}\right) \sum_{g=1}^{I_d} \frac{1}{\prod_{\substack{m=1 \\ m\neq g}}^{I_d} \left(\lambda_{m,\mathsf{d}}^{I} - \lambda_{g,\mathsf{d}}^{I}\right)} \\
&\times \Bigg\{ \sum_{i=0}^{L-1} \pi_i \prod_{\substack{k=0 \\ k\neq i}}^{L-1} \left(1 - \exp\left(-\frac{\gamma_{\mathsf{T}}}{\bar{\gamma}_{k,\mathsf{d}}}\right)\right) \Bigg[\frac{\left(\Xi_1 - \Xi_2\right)}{\left(1 - \frac{\lambda_{\mathsf{s},\mathsf{d}}}{\lambda_{i,\mathsf{d}}}\right)} + \frac{\left(\Xi_1 - \Xi_3\right)}{\left(1 - \frac{\lambda_{i,\mathsf{d}}}{\lambda_{\mathsf{s},\mathsf{d}}}\right)} \\
&+ \exp\left(-\lambda_{i,\mathsf{d}}\gamma_{\mathsf{T}}\right) \left(\frac{\left(\Xi_1 - \exp\left(\lambda_{\mathsf{s},\mathsf{d}}\gamma_{\mathsf{T}}\right)\Xi_2\right)}{\left(1 - \frac{\lambda_{\mathsf{s},\mathsf{d}}}{\lambda_{i,\mathsf{d}}}\right)} + \frac{\left(\Xi_1 - \exp\left(\lambda_{i,\mathsf{d}}\gamma_{\mathsf{T}}\right)\Xi_3\right)}{\left(1 - \frac{\lambda_{i,\mathsf{d}}}{\lambda_{\mathsf{s},\mathsf{d}}}\right)} \right) \Bigg] \\
&+ \sum_{i=0}^{L-1} \sum_{j=0}^{L-1} \pi_{((i-j))_L} \left(1 - \exp\left(-\lambda_{((i-j+k))_L,\mathsf{d}}\gamma_{\mathsf{T}}\right)\right) \\
&\times \left(\frac{\exp\left(-\left(\lambda_{i,\mathsf{d}} - \lambda_{\mathsf{s},\mathsf{d}}\right)\gamma_{\mathsf{T}}\right)\left(\Xi_1 - \Xi_2\right)}{\left(1 - \frac{\lambda_{\mathsf{s},\mathsf{d}}}{\lambda_{i,\mathsf{d}}}\right)} + \frac{\left(\Xi_1 - \Xi_3\right)}{\left(1 - \frac{\lambda_{i,\mathsf{d}}}{\lambda_{\mathsf{s},\mathsf{d}}}\right)} \right) \Bigg\},
\end{aligned} \tag{3.8}$$

where $\Xi_1 = \Gamma\left(1, \lambda_{i_d,\mathsf{d}}^{I}\right) / \lambda_{i_d,\mathsf{d}}^{I}$, $\Xi_2 = \Gamma\left(1, \lambda_{\mathsf{s},\mathsf{d}}u + \lambda_{i_d,\mathsf{d}}^{I}\right) / \left(\lambda_{\mathsf{s},\mathsf{d}}u + \lambda_{i_d,\mathsf{d}}^{I}\right)$, *and* $\Xi_3 = \Gamma\left(1, \lambda_{i,\mathsf{d}}u + \lambda_{i_d,\mathsf{d}}^{I}\right) / \left(\lambda_{i,\mathsf{d}}u + \lambda_{i_d,\mathsf{d}}^{I}\right)$, *where* $\Gamma(.,.)$ *denotes the incomplete gamma function [42, Eq. (8.352.2)].*

Proof. See Appendix B.1. ∎

Lemma 3.2 *The CDF* $\mathrm{P_r}\left[\gamma_{\mathsf{s},k} < u\right]$ *which is a part of the term* $\Pr\left[C_L\right]$ *in (3.6)*

is given by

$$\mathrm{P_r}\left[\gamma_{\mathsf{s},k} < u\right] = \prod_{i_k=1}^{I_k} \lambda_{i_k,k}^{I} \exp\left(\lambda_{i_k,k}^{I}\right) \sum_{g=1}^{I_k} \frac{\left(\Xi_1^{'} - \Xi_2^{'}\right)}{\prod_{\substack{m=1 \\ m\neq g}}^{I_k} \left(\lambda_{m,k}^{I} - \lambda_{g,k}^{I}\right)}, \tag{3.9}$$

where $\Xi_1^{'} = \Xi_1$ *and* $\Xi_2^{'} = \Xi_2$ *with replacing* i_d *by* i_k *and* d *by* k.

Proof. See Appendix B.2. ∎

Having the terms $\mathrm{P_r}\left[\gamma_{\mathsf{d}} < u|C_L\right]$ and $\mathrm{P_r}\left[C_L\right]$ being evaluated, a closed-form expression for the outage probability in (3.7) can be obtained.

For the case of non-identical second hops and identical interferers at the relays and destination ($\lambda_{i_k,k}^{I} = \cdots = \lambda_{k}^{I}$), ($\lambda_{i_d,\mathsf{d}}^{I} = \cdots = \lambda_{\mathsf{d}}^{I}$), the results of the terms $\mathrm{P_r}\left[\gamma_{\mathsf{d}} < u|C_L\right]$ and $\mathrm{P_r}\left[C_L\right]$ are summarized in the following two Corollaries, respectively.

Corollary 3.1 *The term* $\mathrm{P_r}\left[\gamma_{\mathsf{d}} < u|C_L\right]$ *in (3.7) is given for* $L \geq 1$ *by*

$$\begin{aligned}
\mathrm{P_r}\left[\gamma_{\mathsf{d}} < u|C_L\right] &= -\frac{\left(\lambda_{\mathsf{d}}^{I}\right)^{I_d}}{(I_d-1)!} \exp\left(\lambda_{\mathsf{d}}^{I}\right) (-1)^{I_d} \sum_{g=0}^{I_d-1} \binom{I_d-1}{g} (-1)^{g} \\
&\times \Bigg\{ \sum_{i=0}^{L-1} \pi_i \prod_{\substack{k=0 \\ k\neq i}}^{L-1} \left(1 - \exp\left(-\frac{\gamma_{\mathsf{T}}}{\bar{\gamma}_{k,\mathsf{d}}}\right)\right) \Bigg[\frac{(\Lambda_1 - \Lambda_2)}{\left(1 - \frac{\lambda_{\mathsf{s},\mathsf{d}}}{\lambda_{i,\mathsf{d}}}\right)} + \frac{(\Lambda_1 - \Lambda_3)}{\left(1 - \frac{\lambda_{i,\mathsf{d}}}{\lambda_{\mathsf{s},\mathsf{d}}}\right)} \\
&+ \exp\left(-\lambda_{i,\mathsf{d}}\gamma_{\mathsf{T}}\right) \left(\frac{\left(\Lambda_1 - \exp\left(\lambda_{\mathsf{s},\mathsf{d}}\gamma_{\mathsf{T}}\right)\Lambda_2\right)}{\left(1 - \frac{\lambda_{\mathsf{s},\mathsf{d}}}{\lambda_{i,\mathsf{d}}}\right)} + \frac{\left(\Lambda_1 - \exp\left(\lambda_{i,\mathsf{d}}\gamma_{\mathsf{T}}\right)\Lambda_3\right)}{\left(1 - \frac{\lambda_{i,\mathsf{d}}}{\lambda_{\mathsf{s},\mathsf{d}}}\right)} \right) \Bigg] \\
&+ \sum_{i=0}^{L-1} \sum_{j=0}^{L-1} \pi_{((i-j))_L} \left(1 - \exp\left(-\lambda_{((i-j+k))_L,\mathsf{d}}\gamma_{\mathsf{T}}\right)\right) \\
&\times \left(\frac{\exp\left(-\left(\lambda_{i,\mathsf{d}} - \lambda_{\mathsf{s},\mathsf{d}}\right)\gamma_{\mathsf{T}}\right)(\Lambda_1 - \Lambda_2)}{\left(1 - \frac{\lambda_{\mathsf{s},\mathsf{d}}}{\lambda_{i,\mathsf{d}}}\right)} + \frac{(\Lambda_1 - \Lambda_3)}{\left(1 - \frac{\lambda_{i,\mathsf{d}}}{\lambda_{\mathsf{s},\mathsf{d}}}\right)} \right) \Bigg\},
\end{aligned} \tag{3.10}$$

where $\Lambda_1 = \Gamma\left(g+1, \lambda_{\mathsf{d}}^I\right) / \left(\lambda_{\mathsf{d}}^I\right)^{g+1}$, $\Lambda_2 = \Gamma\left(g+1, \lambda_{\mathsf{s,d}} u + \lambda_{\mathsf{d}}^I\right) / \left(\lambda_{\mathsf{s,d}} u + \lambda_{\mathsf{d}}^I\right)^{g+1}$, *and* $\Lambda_3 = \Gamma\left(g+1, \lambda_{i,\mathsf{d}} u + \lambda_{\mathsf{d}}^I\right) / \left(\lambda_{i,\mathsf{d}} u + \lambda_{\mathsf{d}}^I\right)^{g+1}$.

In evaluating this term, the e2e SINR γ_{d} can be written as Y_1/Z_2, where Y_1 as defined in Appendix B.1 with a PDF as derived in (B.4) and Z_2 is now constituting of a summation of i.i.d. RVs $Z_2 = \sum_{i_d=1}^{I_d} \rho_I |h_{i_d,\mathsf{d}}^I|^2 + 1 = X_2 + 1$.

The PDF of X_2 is given by

$$f_{X_2}(x) = \frac{(\lambda_{\mathsf{d}}^I)^{I_d}}{(I_d-1)!}\, x^{I_d-1} \exp\left(-\lambda_{\mathsf{d}}^I x\right). \tag{3.11}$$

Using the transformation of RVs for $Z_2 = X_2 + 1$, we get

$$f_{Z_2}(z) = \frac{(\lambda_{\mathsf{d}}^I)^{I_d}}{(I_d-1)!}\, (z-1)^{I_d-1} \exp\left(-\lambda_{\mathsf{d}}^I (z-1)\right). \tag{3.12}$$

Now, using the Binomial rule, the PDF of Z_2 can be obtained as

$$f_{Z_2}(z) = -\frac{(\lambda_{\mathsf{d}}^I)^{I_d}}{(I_d-1)!} \exp\left(\lambda_{\mathsf{d}}^I\right) (-1)^{I_d} \sum_{g=0}^{I_d-1} \binom{I_d-1}{g} (-1)^g z^g \exp\left(-\lambda_{\mathsf{d}}^I z\right). \tag{3.13}$$

Upon substituting (B.4) and (3.13) in (B.7), and with the help of [42, Eq. (3.351.2)] and after some algebraic manipulations, we obtain the result in (3.10).

Corollary 3.2 *The CDF* $\mathrm{P_r}\left[\gamma_{\mathsf{s},k} < u\right]$ *which is a part of the term* $\Pr\left[C_L\right]$ *in (3.6)*

is given by

$$\mathrm{P_r}\left[\gamma_{\mathsf{s},k} < u\right] = -\frac{(\lambda_k^I)^{I_k}}{(I_k-1)!}\exp\left(\lambda_k^I\right)(-1)^{I_k}\sum_{g=0}^{I_k-1}\binom{I_k-1}{g}(-1)^g\left(\Lambda_1^{'}-\Lambda_2^{'}\right), \tag{3.14}$$

where $\Lambda_1^{'} = \Lambda_1$ *and* $\Lambda_2^{'} = \Lambda_2$ *with replacing* d *by* k.

In evaluating this CDF, the SINR $\gamma_{\mathsf{s},k}$ can be written as Y_a/Z_b, where Y_a has an exponential distribution as given in Appendix B.1 and the PDF of Z_b is as derived in (3.13) with replacing i_d by i_k and d by k.

Upon substituting the PDF of Y_a and that of Z_b in (B.7), and with the help of [42, Eq. (3.351.2)] and after some algebraic manipulations, we obtain the result in (3.14). Having the terms $\mathrm{P_r}\left[\gamma_{\mathsf{d}} < u|C_L\right]$ and $\mathrm{P_r}\left[C_L\right]$ being evaluated, a closed-form expression for the outage probability in (3.7) can be obtained.

For the case where the CDFs of second hops of relays are identical ($\lambda_{1,\mathsf{d}} = \lambda_{2,\mathsf{d}} = \ldots = \lambda_{K,\mathsf{d}} = \lambda_{R,\mathsf{d}}$) and the interferers at the relays and destination have unequal average powers $\{\lambda_{i_n,n}^I\}_{i_n=1}^{I_n}$, the term $\mathrm{P_r}\left[C_L\right]$ is as derived in Lemma 3.2 and the term $\mathrm{P_r}\left[\gamma_{\mathsf{d}} < u|C_L\right]$ is given in the following Lemma.

Lemma 3.3 *The term* $\mathrm{P_r}\left[\gamma_{\mathsf{d}} < u | C_L\right]$ *in (3.7) is given for* $L \geq 1$ *by*

$$\mathrm{P_r}\left[\gamma_{\mathsf{d}} < u | C_L\right] = \prod_{i_d=1}^{I_d} \lambda_{i_d,\mathsf{d}}^{I} \exp\left(\lambda_{i_d,\mathsf{d}}^{I}\right) \sum_{g=1}^{I_d} \frac{\left(\frac{1}{\lambda_{R,\mathsf{d}}} - \frac{1}{\lambda_{\mathsf{s},\mathsf{d}}}\right)^{-1}}{\prod_{\substack{m=1 \\ m \neq g}}^{I_d} \left(\lambda_{m,\mathsf{d}}^{I} - \lambda_{g,\mathsf{d}}^{I}\right)}$$
$$\times \left\{ \left(1 - \exp\left(-\lambda_{R,\mathsf{d}} \gamma_{\mathsf{T}}\right)\right)^{L-1} \left[\frac{\left(\Xi_1 - \Xi_3^{'}\right)}{\lambda_{R,\mathsf{d}}} - \frac{\left(\Xi_1 - \Xi_2\right)}{\lambda_{\mathsf{s},\mathsf{d}}} \right] + \sum_{i=0}^{L-2} \left(1 - \exp\left(-\lambda_{R,\mathsf{d}} \gamma_{\mathsf{T}}\right)\right)^{i} \right.$$
$$\left. \times \left[\frac{\left(\exp\left(-\lambda_{R,\mathsf{d}} \gamma_{\mathsf{T}}\right) \Xi_1 - \Xi_3^{'}\right)}{\lambda_{R,\mathsf{d}}} - \exp\left(\left(\lambda_{\mathsf{s},\mathsf{d}} - \lambda_{R,\mathsf{d}}\right) \gamma_{\mathsf{T}}\right) \frac{\left(\exp\left(-\lambda_{\mathsf{s},\mathsf{d}} \gamma_{\mathsf{T}}\right) \Xi_1 - \Xi_2\right)}{\lambda_{\mathsf{s},\mathsf{d}}} \right] \right\}, \tag{3.15}$$

where Ξ_1, Ξ_2 *are as defined before, and* $\Xi_3^{'} = \Xi_3$ *with replacing* i *by* R.

Proof. In evaluating this term, the e2e SINR can be written as Y_2/Z_1, where Z_1 is as defined in Appendix B.1 with a PDF as derived in (B.1). The CDF of $\rho|h_{\mathrm{SEC},\mathsf{d}}|^2$ which is a part of Y_2 can be written for the i.i.d. second hops as [22]

$$F_{\rho|h_{\mathrm{SEC},\mathsf{d}}|^2}(\gamma) = \begin{cases} \left[F_{\rho|h_{R,\mathsf{d}}|^2}(\gamma_{\mathsf{T}})\right]^{L-1} F_{\rho|h_{R,\mathsf{d}}|^2}(\gamma), & \gamma < \gamma_{\mathsf{T}}; \\ \sum_{j=0}^{L-1} \left[F_{\rho|h_{R,\mathsf{d}}|^2}(\gamma) - F_{\rho|h_{R,\mathsf{d}}|^2}(\gamma_{\mathsf{T}})\right] & \\ \left[F_{\rho|h_{R,\mathsf{d}}|^2}(\gamma_{\mathsf{T}})\right]^{j} + \left[F_{\rho|h_{R,\mathsf{d}}|^2}(\gamma_{\mathsf{T}})\right]^{L}, & \gamma \geq \gamma_{\mathsf{T}}. \end{cases} \tag{3.16}$$

Using the CDF in (3.16) and following the same procedure as in Proposition B.2,

the PDF of Y_2 can be obtained as

$$f_{Y_2}(\gamma) = \left(\frac{1}{\lambda_{R,\mathsf{d}}} - \frac{1}{\lambda_{\mathsf{s},\mathsf{d}}}\right)^{-1} \Bigg\{ \left(1 - \exp\left(-\lambda_{R,\mathsf{d}}\gamma_{\mathsf{T}}\right)\right)^{L-1} \Big[\exp\left(-\lambda_{R,\mathsf{d}}\gamma\right) - \exp\left(-\lambda_{\mathsf{s},\mathsf{d}}\gamma\right) \Big]$$
$$+ \sum_{i=0}^{L-2} \left(1 - \exp\left(-\lambda_{R,\mathsf{d}}\gamma_{\mathsf{T}}\right)\right)^{i} \Big[\exp\left(-\lambda_{R,}\gamma\right) - \exp\left(\left(\lambda_{\mathsf{s},\mathsf{d}} - \lambda_{R,\mathsf{d}}\right)\gamma_{\mathsf{T}}\right) \exp\left(-\lambda_{\mathsf{s},\mathsf{d}}\gamma\right) \Big] U\left(\gamma - \gamma_{\mathsf{T}}\right) \Bigg\}. \tag{3.17}$$

Upon substituting (3.17) and (B.1) in (B.7), and with the help of [42, Eq. (3.351.2)] and after some algebraic manipulations, we obtain the result in (3.15).∎

For the case of identical second hops and identical interferers at the relays and destination ($\lambda^I_{i_k,k} = \cdots = \lambda^I_k$), ($\lambda^I_{i_d,\mathsf{d}} = \cdots = \lambda^I_{\mathsf{d}}$), the term $\mathrm{P_r}\left[C_L\right]$ is as derived in Corollary 3.2 and the term $\mathrm{P_r}\left[\gamma_{\mathsf{d}} < u | C_L\right]$ is given in the following Corollary.

Corollary 3.3 *The term* $\mathrm{P_r}\left[\gamma_{\mathsf{d}} < u | C_L\right]$ *in (3.7) is given for* $L \geq 1$ *by*

$$\mathrm{P_r}\left[\gamma_{\mathsf{d}} < u | C_L\right] = -\frac{\left(\lambda^I_{\mathsf{d}}\right)^{I_d}}{(I_d - 1)!} \exp\left(\lambda^I_{\mathsf{d}}\right) (-1)^{I_d} \sum_{g=0}^{I_d - 1} \binom{I_d - 1}{g} (-1)^g \left(\frac{1}{\lambda_{R,\mathsf{d}}} - \frac{1}{\lambda_{\mathsf{s},\mathsf{d}}}\right)^{-1}$$
$$\times \Bigg\{ \left(1 - \exp\left(-\lambda_{R,\mathsf{d}}\gamma_{\mathsf{T}}\right)\right)^{L-1} \left[\frac{\left(\Lambda_1 - \Lambda_3^{'}\right)}{\lambda_{R,\mathsf{d}}} - \frac{\left(\Lambda_1 - \Lambda_2\right)}{\lambda_{\mathsf{s},\mathsf{d}}} \right] + \sum_{i=0}^{L-2} \left(1 - \exp\left(-\lambda_{R,\mathsf{d}}\gamma_{\mathsf{T}}\right)\right)^{i}$$
$$\times \left[\frac{\left(\exp\left(-\lambda_{R,\mathsf{d}}\gamma_{\mathsf{T}}\right)\Lambda_1 - \Lambda_3^{'}\right)}{\lambda_{R,\mathsf{d}}} - \exp\left(\left(\lambda_{\mathsf{s},\mathsf{d}} - \lambda_{R,\mathsf{d}}\right)\gamma_{\mathsf{T}}\right) \frac{\left(\exp\left(-\lambda_{\mathsf{s},\mathsf{d}}\gamma_{\mathsf{T}}\right)\Lambda_1 - \Lambda_2\right)}{\lambda_{\mathsf{s},\mathsf{d}}} \right] \Bigg\}, \tag{3.18}$$

where Λ_1 *and* Λ_2 *are as defined before and* $\Lambda_3^{'} = \Lambda_3$ *with replacing* i *by* R.

Upon substituting (3.13) and (3.17) in (B.7), and with the help of [42, Eq. (3.351.2)] and after some algebraic manipulations, we obtain the result in (3.18).

3.4.2 SECps-Based Relay Selection

In this section, we evaluate the outage probability of the studied system with the SECps relaying when the CDFs of second hops of relays are identical ($\lambda_{1,\mathsf{d}} = \lambda_{2,\mathsf{d}} = \ldots = \lambda_{K,\mathsf{d}} = \lambda_{R,\mathsf{d}}$) and the interferers at both the relays and destination have unequal average powers $\{\lambda^I_{i_n,n}\}_{i_n=1}^{I_n}$. For this case, the term $\mathrm{P_r}[C_L]$ is as found in Lemma 2 and the term $\mathrm{P_r}[\gamma_{\mathsf{d}} < u|C_L]$ is given in the following Lemma.

Lemma 3.4 *The term* $\mathrm{P_r}[\gamma_{\mathsf{d}} < u|C_L]$ *in (3.7) is given for* $L \geq 1$ *by*

$$\begin{aligned}
\mathrm{P_r}[\gamma_{\mathsf{d}} < u|C_L] &= \prod_{i_d=1}^{I_d} \lambda^I_{i_d,\mathsf{d}} \exp\left(\lambda^I_{i_d,\mathsf{d}}\right) \sum_{g=1}^{I_d} \frac{1}{\prod_{\substack{m=1\\m\neq g}}^{I_d} \left(\lambda^I_{m,\mathsf{d}} - \lambda^I_{g,\mathsf{d}}\right)} \\
&\times \left\{ \frac{\left(1-\left(1-\exp\left(-\lambda_{R,\mathsf{d}}\gamma_{\mathsf{T}}\right)\right)^L\right)}{\left(\frac{1}{\lambda_{R,\mathsf{d}}} - \frac{1}{\lambda_{\mathsf{s},\mathsf{d}}}\right)} \left[\exp\left(\lambda_{R,\mathsf{d}}\gamma_{\mathsf{T}}\right) \frac{\left(\exp\left(-\lambda_{R,\mathsf{d}}\gamma_{\mathsf{T}}\right)\Xi_1 - \Xi_3\right)}{\lambda_{R,\mathsf{d}}} \right.\right. \\
&\left. - \exp\left(\lambda_{\mathsf{s},\mathsf{d}}\gamma_{\mathsf{T}}\right) \frac{\left(\exp\left(-\lambda_{\mathsf{s},\mathsf{d}}\gamma_{\mathsf{T}}\right)\Xi_1 - \Xi_2\right)}{\lambda_{\mathsf{s},\mathsf{d}}} \right] + L \sum_{i=0}^{L-1} \binom{L-1}{i} \frac{(-1)^i}{\left(\frac{1}{\lambda_{R,\mathsf{d}}} - \frac{(i+1)}{\lambda_{\mathsf{s},\mathsf{d}}}\right)} \\
&\times \left[\frac{(\Xi_1 - \Xi_3)}{(i+1)\lambda_{R,\mathsf{d}}} - \frac{(\Xi_1 - \Xi_2)}{\lambda_{\mathsf{s},\mathsf{d}}} - \exp\left(-(i+1)\lambda_{R,\mathsf{d}}\gamma_{\mathsf{T}}\right) \left\{ \exp\left((i+1)\lambda_{R,\mathsf{d}}\gamma_{\mathsf{T}}\right) \right.\right. \\
&\left.\left. \times \frac{\left(\exp\left(-(i+1)\lambda_{R,\mathsf{d}}\gamma_{\mathsf{T}}\right)\Xi_1 - \Xi_4\right)}{(i+1)\lambda_{R,\mathsf{d}}} - \exp\left(\lambda_{\mathsf{s},\mathsf{d}}\gamma_{\mathsf{T}}\right) \frac{\left(\exp\left(-\lambda_{\mathsf{s},\mathsf{d}}\gamma_{\mathsf{T}}\right)\Xi_1 - \Xi_2\right)}{\lambda_{\mathsf{s},\mathsf{d}}} \right\} \right] \Bigg\},
\end{aligned} \tag{3.19}$$

where Ξ_1, Ξ_2, Ξ_3 *are as defined before, and* $\Xi_4 = \Gamma(1, (i+1)\lambda_{R,\mathsf{d}}u + \lambda^I_{i_d,\mathsf{d}})/((i+1)\lambda_{R,\mathsf{d}}u + \lambda^I_{i_d,\mathsf{d}})$.

Proof. In evaluating this term, the e2e SINR can be written as Y_3/Z_1, where Z_1 is as defined in Appendix B.1 with a PDF as derived in (B.1). The CDF of

$\rho|h_{\mathrm{SECps,d}}|^2$ which is a part of Y_3 can be written as [22]

$$F_{\rho|h_{\mathrm{SECps,d}}|^2}(\gamma) = \begin{cases} 1 - \sum_{j=0}^{L-1} \left[F_{\rho|h_{R,\mathsf{d}}|^2}(\gamma_\mathsf{T})\right]^j \left[1 - F_{\rho|h_{R,\mathsf{d}}|^2}(\gamma)\right], & \gamma \geq \gamma_\mathsf{T}; \\ \left[F_{\rho|h_{R,\mathsf{d}}|^2}(\gamma)\right]^L, & \gamma < \gamma_\mathsf{T}. \end{cases} \tag{3.20}$$

Using the CDF in (3.20) and following the same procedure as in Appendix B.1, the PDF of Y_3 can be obtained as

$$\begin{aligned} f_{Y_3}(\gamma) &= \left[1 - \left(1 - \exp\left(-\lambda_{R,\mathsf{d}}\gamma_\mathsf{T}\right)\right)^L\right] \\ &\times \left\{ \left(\frac{\exp\left(-\lambda_{\mathsf{s,d}}\left(\gamma - \gamma_\mathsf{T}\right)\right)}{\left(\frac{1}{\lambda_{\mathsf{s,d}}} - \frac{1}{\lambda_{R,\mathsf{d}}}\right)} + \frac{\exp\left(-\lambda_{R,\mathsf{d}}\left(\gamma - \gamma_\mathsf{T}\right)\right)}{\left(\frac{1}{\lambda_{R,\mathsf{d}}} - \frac{1}{\lambda_{\mathsf{s,d}}}\right)} \right) U\left(\gamma - \gamma_\mathsf{T}\right) \right\} + L \sum_{i=0}^{L-1} \binom{L-1}{i} \\ &\times (-1)^i \left[\frac{\exp\left(-\lambda_{\mathsf{s,d}}\left(\gamma - \gamma_\mathsf{T}\right)\right)}{\left(\frac{(i+1)}{\lambda_{\mathsf{s,d}}} - \frac{1}{\lambda_{R,\mathsf{d}}}\right)} + \frac{\exp\left(-(i+1)\lambda_{R,\mathsf{d}}\gamma\right)}{\left(\frac{1}{\lambda_{R,\mathsf{d}}} - \frac{(i+1)}{\lambda_{\mathsf{s,d}}}\right)} - \exp\left(-(i+1)\lambda_{R,\mathsf{d}}\gamma\right) \right. \\ &\times \left. \left(\frac{\exp\left(-\lambda_{\mathsf{s,d}}\left(\gamma - \gamma_\mathsf{T}\right)\right)}{\left(\frac{(i+1)}{\lambda_{\mathsf{s,d}}} - \frac{1}{\lambda_{R,\mathsf{d}}}\right)} + \frac{\exp\left(-(i+1)\lambda_{R,\mathsf{d}}\gamma\right)}{\left(\frac{1}{\lambda_{R,\mathsf{d}}} - \frac{(i+1)}{\lambda_{\mathsf{s,d}}}\right)} \right) U\left(\gamma - \gamma_\mathsf{T}\right) \right]. \end{aligned} \tag{3.21}$$

Upon substituting (B.1) and (3.21) in (B.7), and with the help of [42, Eq. (3.351.2)] and after some algebraic manipulations, we obtain the result in (3.19).∎

For the case of identical second hops and identical interferers at the relays and destination ($\lambda^I_{i_k,k} = \cdots = \lambda^I_k$), ($\lambda^I_{i_d,\mathsf{d}} = \cdots = \lambda^I_\mathsf{d}$), the term $\mathrm{P_r}\left[C_L\right]$ is as derived in Corollary 3.2 and the term $\mathrm{P_r}\left[\gamma_\mathsf{d} < u | C_L\right]$ is given in the following Corollary.

Corollary 3.4 *The term* $\mathrm{P_r}\left[\gamma_{\mathsf{d}} < u | C_L\right]$ *in (3.7) is given for* $L \geq 1$ *by*

$$\mathrm{P_r}\left[\gamma_{\mathsf{d}} < u | C_L\right] = -\frac{(\lambda_{\mathsf{d}}^I)^{I_d}}{(I_d-1)!}\exp\left(\lambda_{\mathsf{d}}^I\right)(-1)^{I_d}\sum_{g=0}^{I_d-1}\binom{I_d-1}{g}(-1)^g$$
$$\times\left\{\frac{\left(1-(1-\exp\left(-\lambda_{R,\mathsf{d}}\gamma_{\mathsf{T}}\right)\right)^L\right)}{\left(\frac{1}{\lambda_{R,\mathsf{d}}}-\frac{1}{\lambda_{\mathsf{s},\mathsf{d}}}\right)}\left[\exp\left(\lambda_{R,\mathsf{d}}\gamma_{\mathsf{T}}\right)\frac{\left(\exp\left(-\lambda_{R,\mathsf{d}}\gamma_{\mathsf{T}}\right)\Lambda_1-\Lambda_3\right)}{\lambda_{R,\mathsf{d}}}\right.\right.$$
$$\left.-\exp\left(\lambda_{\mathsf{s},\mathsf{d}}\gamma_{\mathsf{T}}\right)\frac{\left(\exp\left(-\lambda_{\mathsf{s},\mathsf{d}}\gamma_{\mathsf{T}}\right)\Lambda_1-\Lambda_2\right)}{\lambda_{\mathsf{s},\mathsf{d}}}\right]+L\sum_{i=0}^{L-1}\binom{L-1}{i}\frac{(-1)^i}{\left(\frac{1}{\lambda_{R,\mathsf{d}}}-\frac{(i+1)}{\lambda_{\mathsf{s},\mathsf{d}}}\right)}$$
$$\times\left[\frac{(\Lambda_1-\Lambda_3)}{(i+1)\lambda_{R,\mathsf{d}}}-\frac{(\Lambda_1-\Lambda_2)}{\lambda_{\mathsf{s},\mathsf{d}}}-\exp\left(-(i+1)\lambda_{R,\mathsf{d}}\gamma_{\mathsf{T}}\right)\left\{\exp\left((i+1)\lambda_{R,\mathsf{d}}\gamma_{\mathsf{T}}\right)\right.\right.$$
$$\left.\left.\times\frac{\left(\exp\left(-(i+1)\lambda_{R,\mathsf{d}}\gamma_{\mathsf{T}}\right)\Lambda_1-\Lambda_4\right)}{(i+1)\lambda_{R,\mathsf{d}}}-\exp\left(\lambda_{\mathsf{s},\mathsf{d}}\gamma_{\mathsf{T}}\right)\frac{\left(\exp\left(-\lambda_{\mathsf{s},\mathsf{d}}\gamma_{\mathsf{T}}\right)\Lambda_1-\Lambda_2\right)}{\lambda_{\mathsf{s},\mathsf{d}}}\right\}\right]\Bigg\}, \tag{3.22}$$

where Λ_1*,* Λ_2*,* Λ_3 *are as defined before, and* $\Lambda_4 = \Gamma(g+1,(i+1)\lambda_{R,\mathsf{d}}u+\lambda_{\mathsf{d}}^I)\big/((i+1)\lambda_{R,\mathsf{d}}u+\lambda_{i_d,\mathsf{d}}^I)^{g+1}$.

Upon substituting (3.13) and (3.21) in (B.7), and with the help of [42, Eq. (3.351.2)] and after some algebraic manipulations, we obtain the result in (3.22).

3.5 Asymptotic Analysis

In this section, we evaluate the outage probability of the studied system at high SNR regime with the proposed SEC and SECps relay selection schemes.

Due to complexity of the achieved expressions in previous sections, it is hard to get more insights about system performance. Therefore, we see it is important

to derive simple expressions where more about system behavior can be achieved. In this section, we evaluate asymptotic outage performance of the studied system with the proposed SEC and SECps relay selection schemes. At high SNR, the outage probability can be expressed as $P_{\mathsf{out}} \approx (G_{\mathsf{c}}\mathrm{SNR})^{-G_{\mathsf{d}}}$, where G_{c} denotes the coding gain of the system and G_{d} is the diversity order of the system. In the upcoming analysis, the I_d and ρ_I are assumed to be constant. Also, the second hops of relays are assumed to be identical and the interferers at the relays and destination are assumed to have equal powers.

3.5.1 SEC-Based Relay Selection

In this section, we derive the asymptotic outage probability for the studied system with the SEC relaying scheme. At high SNR regime, the exponential CDF and PDF can be respectively approximated by $F_\gamma(\gamma) \approx \frac{\gamma}{\bar{\gamma}}$ and $f_\gamma(\gamma) \approx \frac{1}{\bar{\gamma}}$. Upon substituting these statistics in (3.16) and following the same procedure as in Appendix B.1, the term $\mathrm{P_r}\left[\gamma_{\mathsf{d}} < u | C_L\right]$ in (3.7) can be obtained at high SNR for $L \geq 1$ as

$$\mathrm{P_r}\left[\gamma_{\mathsf{d}} < u | C_L\right] \approx -\frac{\left(\lambda_{\mathsf{d}}^I\right)^{I_d}}{(I_d-1)!} \exp\left(\lambda_{\mathsf{d}}^I\right) (-1)^{I_d} \sum_{g=0}^{I_d-1} \binom{I_d-1}{g} (-1)^g \lambda_{R,\mathsf{d}} \lambda_{\mathsf{s},\mathsf{d}}$$
$$\times \left\{ \left(\lambda_{R,\mathsf{d}}\gamma_{\mathsf{T}}\right)^{L-1} \left[\gamma_{\mathsf{T}}\chi_1 u - \frac{(\gamma_{\mathsf{T}})^2 \chi_2}{2}\right] + \sum_{j=0}^{L-1} \left(\lambda_{R,\mathsf{d}}\gamma_{\mathsf{T}}\right)^j \left[\frac{\chi_3}{2}u^2 - \frac{\gamma_{\mathsf{T}}\chi_1}{2}u + (\gamma_{\mathsf{T}})^2\chi_2\right] \right\}, \tag{3.23}$$

where $\chi_1 = \Gamma\left(g+2, \lambda_{\mathsf{d}}^I\right) / \left(\lambda_{\mathsf{d}}^I\right)^{g+2}$, $\chi_2 = \Gamma\left(g+1, \lambda_{\mathsf{d}}^I\right) / \left(\lambda_{\mathsf{d}}^I\right)^{g+1}$, and $\chi_3 = \Gamma\left(g+3, \lambda_{\mathsf{d}}^I\right) / \left(\lambda_{\mathsf{d}}^I\right)^{g+3}$.

Now, the CDF $\mathrm{P_r}\left[\gamma_{\mathsf{s},k} < u\right]$ which is a part of the term $\Pr\left[C_L\right]$ in (3.6) can be obtained at high SNR as

$$\mathrm{P_r}\left[\gamma_{\mathsf{s},k} < u\right] \approx -\frac{(\lambda_k^I)^{I_k}}{(I_k-1)!}(-1)^{I_k}\lambda_{\mathsf{s},k}\exp\left(\lambda_k^I\right)\sum_{g=0}^{I_k-1}\binom{I_k-1}{g}(-1)^g\chi_1^{'}u, \qquad (3.24)$$

where $\chi_1^{'} = \chi_1$ with replacing d by k.

Upon substituting (3.24) in (3.6) and then substituting (3.6) and (3.23) in (3.7), the asymptotic outage probability can be evaluated. While evaluating the outage probability in some common mathematical tools like Maple, it was noticed that the term $\mathrm{P_r}\left[\gamma_{\mathsf{d}} < u|C_L\right]$ in (3.23) is the one who dominates the final result when compared with the term $\mathrm{P_r}\left[\gamma_{\mathsf{s},k} < u\right]$ in (3.24). Also, it was noticed that the first part in (3.23) is dominated by the second part. Furthermore, this term can be further simplified due to the fact that it is still dominant when $j = 0$. Therefore, the result in (3.23) can be simplified as

$$\begin{aligned}\mathrm{P_r}\left[\gamma_{\mathsf{d}} < u|C_L\right] \approx &-\frac{(\lambda_{\mathsf{d}}^I)^{I_d}}{(I_d-1)!}\exp\left(\lambda_{\mathsf{d}}^I\right)(-1)^{I_d}\sum_{g=0}^{I_d-1}\binom{I_d-1}{g}(-1)^g \\ &\times\left\{\lambda_{R,\mathsf{d}}\lambda_{\mathsf{s},\mathsf{d}}\left[\frac{\chi_3}{2}u^2 - \frac{\gamma_{\mathsf{T}}\chi_1}{2}u + (\gamma_{\mathsf{T}})^2\chi_2\right]\right\}. \qquad (3.25)\end{aligned}$$

By noticing that $\lambda_{R,\mathsf{d}} = \lambda_{\mathsf{s},\mathsf{d}} = (\mathrm{SNR})^{-1}$, the result in (3.25) can be rewritten at $u = \gamma_{\mathsf{out}}$ as

$$P_{\mathsf{out}} \approx \Bigg(\Bigg\{ - \frac{(\lambda_{\mathsf{d}}^I)^{I_d}}{(I_d-1)!} \exp\left(\lambda_{\mathsf{d}}^I\right) (-1)^{I_d} \sum_{g=0}^{I_d-1} \binom{I_d-1}{g} (-1)^g \times \left[\frac{\chi_3}{2} (\gamma_{\mathsf{out}})^2 - \frac{\gamma_{\mathsf{T}} \chi_1}{2} \gamma_{\mathsf{out}} + (\gamma_{\mathsf{T}})^2 \chi_2 \right] \Bigg\}^2 \mathrm{SNR} \Bigg)^{-2}. \tag{3.26}$$

3.5.2 SECps-Based Relay Selection

In this section, we derive the asymptotic outage probability for the studied system with the SECps relaying scheme. Upon substituting the approximate statistics of the exponential distribution in (3.20) and following the same procedure as in Appendix B.1, the term $\mathrm{P_r}\left[\gamma_{\mathsf{d}} < u | C_L\right]$ in (3.7) can be obtained at high SNR for $L \geq 1$ as

$$\mathrm{P_r}\left[\gamma_{\mathsf{d}} < u | C_L\right] \approx - \frac{(\lambda_{\mathsf{d}}^I)^{I_d}}{(I_d-1)!} \exp\left(\lambda_{\mathsf{d}}^I\right) (-1)^{I_d} \sum_{g=0}^{I_d-1} \binom{I_d-1}{g} (-1)^g \Bigg\{ \sum_{i=0}^{L-1} \left(\lambda_{R,\mathsf{d}} \gamma_{\mathsf{T}}\right)^i \times \lambda_{R,\mathsf{d}} \lambda_{\mathsf{s},\mathsf{d}} \left(\frac{\chi_3}{2} u^2 - \gamma_{\mathsf{T}} \chi_1 u + \frac{(\gamma_{\mathsf{T}})^2 \chi_2}{2} \right) + L! (\lambda_{R,\mathsf{d}})^L \lambda_{\mathsf{s},\mathsf{d}} \Bigg[\frac{\Gamma\left(g+L+2, \lambda_{\mathsf{d}}^I\right)}{(L+1)! (\lambda_{\mathsf{d}}^I)^{g+L+2}} u^{L+1} - \sum_{k=0}^{L-1} \frac{(\gamma_{\mathsf{T}})^k}{k!(L-k)!} \sum_{j=0}^{L-k} \binom{L-k}{j} \frac{(-\gamma_{\mathsf{T}})^{L-k-j}}{(j+1)} \left(\frac{\Gamma\left(g+j+2, \lambda_{\mathsf{d}}^I\right)}{(\lambda_{\mathsf{d}}^I)^{g+j+2}} u^{j+1} - (\gamma_{\mathsf{T}})^{j+1} \chi_2 \right) \Bigg] \Bigg\}, \tag{3.27}$$

where χ_2 as defined before.

The CDF $\mathrm{P_r}\left[\gamma_{\mathsf{s},k} < u\right]$ which is a part of the term $\Pr\left[C_L\right]$ in (3.6) is similar to that obtained in (3.24). Upon substituting (3.24) in (3.6) and then substituting

(3.6) and (3.27) in (3.7), the asymptotic outage probability can be evaluated. While evaluating the outage probability in Maple, it was noticed that the term $\mathrm{P_r}\left[\gamma_{\mathsf{d}} < u | C_L\right]$ in (3.27) is the one who dominates the final result when compared with the term $\mathrm{P_r}\left[\gamma_{\mathsf{s},k} < u\right]$ in (3.24). Also, it was noticed that the second part in (3.27) is dominated by the first part. Furthermore, this term can be further simplified due to the fact that it is still dominant when $i = 0$. Therefore, the result in (3.27) can be simplified as

$$\mathrm{P_r}\left[\gamma_{\mathsf{d}} < u | C_L\right] \approx - \frac{(\lambda_{\mathsf{d}}^I)^{I_d}}{(I_d-1)!} \exp\left(\lambda_{\mathsf{d}}^I\right) (-1)^{I_d} \sum_{g=0}^{I_d-1} \binom{I_d-1}{g} (-1)^g \times \left\{ \lambda_{R,\mathsf{d}} \lambda_{\mathsf{s},\mathsf{d}} \left(\frac{\chi_3}{2} u^2 - \gamma_{\mathsf{T}} \chi_1 u + \frac{(\gamma_{\mathsf{T}})^2 \chi_2}{2} \right) \right\}. \tag{3.28}$$

Again, by noticing that $\lambda_{R,\mathsf{d}} = \lambda_{\mathsf{s},\mathsf{d}} = 1/\mathrm{SNR}$, the result in (3.28) can be rewritten at $u = \gamma_{\mathsf{out}}$ as

$$P_{\mathsf{out}} \approx \left(\left\{ - \frac{(\lambda_{\mathsf{d}}^I)^{I_d}}{(I_d-1)!} \exp\left(\lambda_{\mathsf{d}}^I\right) (-1)^{I_d} \sum_{g=0}^{I_d-1} \binom{I_d-1}{g} (-1)^g \times \left(\frac{\chi_3}{2} (\gamma_{\mathsf{out}})^2 - \gamma_{\mathsf{T}} \chi_1 \gamma_{\mathsf{out}} + \frac{(\gamma_{\mathsf{T}})^2 \chi_2}{2} \right) \right\}^2 \mathrm{SNR} \right)^{-2}. \tag{3.29}$$

As can be seen from the results in (3.25) and (3.29), the coding gain of the system with the SEC and SECps relaying schemes is affected by several parameters as λ_{d}^I, I_d, γ_{T}, and γ_{out}; while the diversity order is constant at 2. This is clear in the numerical examples where all curves of different K asymptotically converge to the same behavior and result in a diversity order of 2 (the relay path + direct

link). It is expected from results to have the achieved gain in system performance due to increasing K to happen at the values of SNR that are comparable to γ_{T}. As in this case, the switching rate will increase and the probability to have better relays increases also. At the same time, as the asymptotic analysis is done at high SNR values, it is expected to have most of the relays being acceptable the whole time and thus, the first checked relay is being selected in the two relaying schemes. This means all curves of different K asymptotically converge to same behavior which explains why the system with the two relaying schemes has the same diversity order and approximately the same coding gain as will be shown in the coming section.

3.6 Special Case of Noise-Limited System

For the case of no interference, the received signal at the k^{th} relay can be expressed as

$$y_{\mathsf{r}_k} = h_{\mathsf{s},k} x_0 + n_{\mathsf{s},k}, \tag{3.30}$$

where $h_{\mathsf{s},k}$ is the channel coefficient between S and the k^{th} relay, x_0 is the transmitted symbol with $\mathbb{E}\{|x_0|^2\} = P_0$, and $n_{\mathsf{s},k} \sim \mathcal{CN}(0, N_0)$ is an AWGN. Let us define $h_{\mathsf{s},\mathsf{d}}$ and $h_{k,\mathsf{d}}$ as the channel coefficients between S and D and the k^{th} relay and D, respectively. All the channel gains are assumed to follow Rayleigh distribution. That is, the channel powers denoted by $|h_{\mathsf{s},\mathsf{d}}|^2$, $|h_{\mathsf{s},k}|^2$, and $|h_{k,\mathsf{d}}|^2$ are exponential distributed RVs with parameters $\sigma^2_{\mathsf{s},\mathsf{d}}$, $\sigma^2_{\mathsf{s},k}$, and $\sigma^2_{k,\mathsf{d}}$, respectively. Using (3.30), the SNR at the k^{th} relay can be written as $\gamma_{\mathsf{s},k} = \frac{P_0}{N_0}|h_{\mathsf{s},k}|^2$.

In the second phase after decoding the received signal, the first checked relay in C_L whose second hop channel SNR is greater than the predetermined switching threshold forwards the re-encoded signal to the destination. The selected relay is chosen according to the SEC selection scheme and it is the first checked relay in C_L whose $\gamma_{l,\mathsf{d}}$ is greater than a predetermined switching threshold. It can be written as $\gamma_{l,\mathsf{d}} = \frac{P_l}{N_0}|h_{l,\mathsf{d}}|^2$, where P_l and N_0 are the transmit power of the l^{th} active relay and the AWGN power at the destination, respectively.

The destination finally combines the signals from the source and the selected relay using MRC. The e2e SNR at the destination output can be written as

$$\gamma_{\mathsf{d}} \triangleq \gamma_{\mathsf{s},\mathsf{d}} + \gamma_{\text{SEC},\mathsf{d}} = \frac{P_0}{N_0}|h_{\mathsf{s},\mathsf{d}}|^2 + \frac{P_0}{N_0}|h_{\text{SEC},\mathsf{d}}|^2. \tag{3.31}$$

3.6.1 SEC-Based Relay Selection

In this section, we evaluate the outage probability of the studied system with the SEC relaying when the CDFs of second hops of relays are non-identical.

Let $\rho \triangleq P_0/N_0 = P_l/N_0$. Then, $\rho|h_{\mathsf{s},\mathsf{d}}|^2$, $\rho|h_{\mathsf{s},k}|^2$, and $\rho|h_{l,\mathsf{d}}|^2$ are exponential distributed with parameters $\lambda_{\mathsf{s},\mathsf{d}} = 1/\rho\sigma^2_{\mathsf{s},\mathsf{d}}$, $\lambda_{\mathsf{s},k} = 1/\rho\sigma^2_{\mathsf{s},k}$, and $\lambda_{l,\mathsf{d}} = 1/\rho\sigma^2_{l,\mathsf{d}}$. The result of the term $\mathrm{P_r}\left[\gamma_{\mathsf{d}} < u|C_L\right]$ for the case of i.n.d. second hops $\{\lambda_{i,\mathsf{d}}\}_{i=1}^{L}$ is given in the following Lemma.

Lemma 3.5 *The term* $\mathrm{P_r}\left[\gamma_{\mathsf{d}} < u | C_L\right]$ *in (3.7) is given for* $L \geq 1$ *by*

$$\mathrm{P_r}\left[\gamma_{\mathsf{d}} < u | C_L\right] = \sum_{i=0}^{L-1} \pi_i \prod_{\substack{k=0 \\ k\neq i}}^{L-1} \left(1 - \exp\left(-\lambda_{k,\mathsf{d}}\gamma_{\mathsf{T}}\right)\right) \Bigg[\Xi_1 + \Xi_2 - \exp\left(-\lambda_{i,\mathsf{d}}\gamma_{\mathsf{T}}\right)$$
$$\times \left\{ \Xi_3\Big(\exp\left(-\lambda_{\mathsf{s},\mathsf{d}}\gamma_{\mathsf{T}}\right) - \exp\left(-\lambda_{\mathsf{s},\mathsf{d}}u\right) \Big) + \Xi_4\Big(\exp\left(-\lambda_{i,\mathsf{d}}\gamma_{\mathsf{T}}\right) - \exp\left(-\lambda_{i,\mathsf{d}}u\right) \Big) \right\} \Bigg]$$
$$+ \sum_{j=0}^{L-1} \pi_{((i-j))_L} \prod_{k=0}^{j-1} \left(1 - \exp\left(-\lambda_{((i-j+k))_L,\mathsf{d}}\gamma_{\mathsf{T}}\right)\right)$$
$$\times \left[\exp\left(-\lambda_{i,\mathsf{d}}\gamma_{\mathsf{T}}\right) \left\{ \Xi_3\left(1 - \exp\left(-\lambda_{\mathsf{s},\mathsf{d}}u\right)\right) + \Xi_4\left(1 - \exp\left(-\lambda_{i,\mathsf{d}}u\right)\right) \right\} \right], \qquad (3.32)$$

where $\Xi_1 = \left(1 - \exp\left(-\lambda_{\mathsf{s},\mathsf{d}}u\right)\right) \Big/ \left(1 - \frac{\lambda_{\mathsf{s},\mathsf{d}}}{\lambda_{i,\mathsf{d}}}\right)$, $\Xi_2 = \left(1 - \exp\left(-\lambda_{i,\mathsf{d}}u\right)\right) \Big/ \left(1 - \frac{\lambda_{i,\mathsf{d}}}{\lambda_{\mathsf{s},\mathsf{d}}}\right)$, $\Xi_3 = \exp\left(\lambda_{\mathsf{s},\mathsf{d}}\gamma_{\mathsf{T}}\right) \Big/ \left(1 - \frac{\lambda_{\mathsf{s},\mathsf{d}}}{\lambda_{i,\mathsf{d}}}\right)$, *and* $\Xi_4 = \exp\left(\lambda_{i,\mathsf{d}}\gamma_{\mathsf{T}}\right) \Big/ \left(1 - \frac{\lambda_{i,\mathsf{d}}}{\lambda_{\mathsf{s},\mathsf{d}}}\right)$.

Proof. For the case of no interference, the SINR at the MRC combiner output at the destination γ_{d} is exactly as Y_1 in Appendix B.1 with a PDF as derived in (B.4). Upon, integrating this PDF using $\int_{-\infty}^{u} f_{\gamma_{\mathsf{d}}}(\gamma) d\gamma$, we obtain the result in (3.32). ∎

The second term $\mathrm{P_r}\left[C_L\right]$ in (3.7) can be obtained by using the CDF $\mathrm{P_r}\left[\gamma_{\mathsf{s},l} \leq u\right]$ which is an exponential distribution given by $\mathrm{P_r}\left[\gamma_{\mathsf{s},l} \leq u\right] = 1 - \exp\left(-\lambda_{\mathsf{s},l}u\right)$, where $\lambda_{\mathsf{s},l}$ is the rate of this distribution as defined before. Having the terms $\mathrm{P_r}\left[\gamma_{\mathsf{d}} < u | C_L\right]$ and $\mathrm{P_r}\left[C_L\right]$ being evaluated, a closed-form expression for the outage probability in (3.7) can be obtained.

For the case where the CDFs of second hops of relays are identical ($\lambda_{1,\mathsf{d}} =$

$\lambda_{2,\mathsf{d}} = \ldots = \lambda_{K,\mathsf{d}} = \lambda_{R,\mathsf{d}}$), the term $\mathrm{P_r}\left[C_L\right]$ is as derived in Lemma 3.5 and the term $\mathrm{P_r}\left[\gamma_{\mathsf{d}} < u | C_L\right]$ is given in the following Lemma.

Lemma 3.6 *The term* $\mathrm{P_r}\left[\gamma_{\mathsf{d}} < u | C_L\right]$ *in (3.7) is given for* $L \geq 1$ *by*

$$\mathrm{P_r}\left[\gamma_{\mathsf{d}} < u | C_L\right] = \frac{1}{\left(\frac{1}{\lambda_{R,\mathsf{d}}} - \frac{1}{\lambda_{\mathsf{s},\mathsf{d}}}\right)} \Bigg\{ \left(1 - \exp\left(-\lambda_{R,\mathsf{d}}\gamma_{\mathsf{T}}\right)\right)^{L-1} \Bigg[\frac{\left(1 - \exp\left(-\lambda_{R,\mathsf{d}}u\right)\right)}{\lambda_{R,\mathsf{d}}} - \frac{\left(1 - \exp\left(-\lambda_{\mathsf{s},\mathsf{d}}u\right)\right)}{\lambda_{\mathsf{s},\mathsf{d}}} \Bigg] + \sum_{j=0}^{L-2} \left(1 - \exp\left(-\lambda_{R,\mathsf{d}}\gamma_{\mathsf{T}}\right)\right)^{j} \Bigg[\frac{\left\{\exp\left(-\lambda_{R,\mathsf{d}}\gamma_{\mathsf{T}}\right) - \exp\left(-\lambda_{R,\mathsf{d}}u\right)\right\}}{\lambda_{R,\mathsf{d}}} - \exp\left(\left(-\lambda_{R,\mathsf{d}} + \lambda_{\mathsf{s},\mathsf{d}}\right)\gamma_{\mathsf{T}}\right) \frac{\left\{\exp\left(-\lambda_{\mathsf{s},\mathsf{d}}\gamma_{\mathsf{T}}\right) - \exp\left(-\lambda_{\mathsf{s},\mathsf{d}}u\right)\right\}}{\lambda_{\mathsf{s},\mathsf{d}}} \Bigg] \Bigg\}. \tag{3.33}$$

Proof. For the case of no interference, the SINR at the MRC combiner output at the destination γ_{d} is exactly as Y_2 in Lemma 3.3 with a PDF as derived in (3.17). Upon integrating this PDF using $\int_{-\infty}^{u} f_{\gamma_{\mathsf{d}}}(\gamma) d\gamma$, we obtain the result in (3.33). ∎

3.6.2 SECps-Based Relay Selection

In this section, we evaluate the outage probability of the studied system with the SECps relaying when the CDFs of second hops of relays are identical ($\lambda_{1,\mathsf{d}} = \lambda_{2,\mathsf{d}} = \ldots = \lambda_{K,\mathsf{d}} = \lambda_{R,\mathsf{d}}$). For this case the term $\mathrm{P_r}\left[\gamma_{\mathsf{d}} < u | C_L\right]$ is given in the following Lemma.

Lemma 3.7 *The term* $\mathrm{P_r}\left[\gamma_{\mathsf{d}} < u | C_L\right]$ *in (3.7) is given for* $L \geq 1$ *by*

$$\mathrm{P_r}\left[\gamma_{\mathsf{d}} < u | C_L\right] = \frac{\left(1-\left(1-\exp\left(-\lambda_{R,\mathsf{d}}\gamma_{\mathsf{T}}\right)\right)^{L}\right)}{\left(\frac{1}{\lambda_{R,\mathsf{d}}}-\frac{1}{\lambda_{\mathsf{s},\mathsf{d}}}\right)}\Bigg[\frac{\exp\left(\lambda_{R,\mathsf{d}}\gamma_{\mathsf{T}}\right)\left(\exp\left(-\lambda_{R,\mathsf{d}}\gamma_{\mathsf{T}}\right)-\exp\left(-\lambda_{R,\mathsf{d}}u\right)\right)}{\lambda_{R,\mathsf{d}}}$$

$$-\frac{\exp\left(\lambda_{\mathsf{s},\mathsf{d}}\gamma_{\mathsf{T}}\right)\left(\exp\left(-\lambda_{\mathsf{s},\mathsf{d}}\gamma_{\mathsf{T}}\right)-\exp\left(-\lambda_{\mathsf{s},\mathsf{d}}u\right)\right)}{\lambda_{\mathsf{s},\mathsf{d}}}\Bigg] + L\sum_{j=0}^{L-1}\binom{L-1}{j}\frac{(-1)^j}{\left(\frac{1}{\lambda_{R,\mathsf{d}}}-\frac{(j+1)}{\lambda_{\mathsf{s},\mathsf{d}}}\right)}$$

$$\times\Bigg[\frac{\left(1-\exp\left(-(j+1)\lambda_{R,\mathsf{d}}u\right)\right)}{(j+1)\lambda_{R,\mathsf{d}}}-\frac{\left(1-\exp\left(-\lambda_{\mathsf{s},\mathsf{d}}u\right)\right)}{\lambda_{\mathsf{s},\mathsf{d}}}-\exp\left(-(j+1)\lambda_{R,\mathsf{d}}\gamma_{\mathsf{T}}\right)$$

$$\times\Bigg\{\frac{\exp\left((j+1)\lambda_{R,\mathsf{d}}\gamma_{\mathsf{T}}\right)}{(j+1)\lambda_{R,\mathsf{d}}}\left(\exp\left(-(j+1)\lambda_{R,\mathsf{d}}\gamma_{\mathsf{T}}\right)-\exp\left(-(j+1)\lambda_{R,\mathsf{d}}u\right)\right)$$

$$-\frac{\exp\left(\lambda_{\mathsf{s},\mathsf{d}}\gamma_{\mathsf{T}}\right)\left(\exp\left(-\lambda_{\mathsf{s},\mathsf{d}}\gamma_{\mathsf{T}}\right)-\exp\left(-\lambda_{\mathsf{s},\mathsf{d}}u\right)\right)}{\lambda_{\mathsf{s},\mathsf{d}}}\Bigg\}\Bigg]. \tag{3.34}$$

Proof. For the case of no interference, the SINR at the MRC combiner output at the destination γ_{d} is exactly as Y_3 in Lemma 3.4 with a PDF as derived in (3.21). Upon, integrating this PDF, we obtain the result in (3.34). ∎

Again, the second term $\mathrm{P_r}\left[C_L\right]$ in (3.7) can be obtained by using the CDF $\mathrm{P_r}\left[\gamma_{\mathsf{s},l} \leq u\right]$ which is an exponential distribution given by $\mathrm{P_r}\left[\gamma_{\mathsf{s},l} \leq u\right] = 1 - \exp\left(-\lambda_{\mathsf{s},l}u\right)$, where $\lambda_{\mathsf{s},l}$ is the rate of this distribution as defined before. Having the terms $\mathrm{P_r}\left[\gamma_{\mathsf{d}} < u | C_L\right]$ and $\mathrm{P_r}\left[C_L\right]$ being evaluated, a closed-form expression for the outage probability in (3.7) can be obtained.

Due to complexity of the achieved analytical results, it would be hard to calculate the switching threshold in such a way optimizing the e2e outage probability. Alternatively, the same method presented in Section 2.6.

3.7 Numerical Results

In this section, we illustrate the validity of the achieved analytical expressions via a comparison with Monte-Carlo simulations. We also provide some numerical examples to prove the effectiveness of the proposed relay selection schemes in reducing the system complexity and to show the effect of the interference and some system parameters like number of relays, switching threshold, and outage threshold on the system performance.

Figure 3.3 portrays the system outage probability vs SNR for the SEC-based relaying scheme for different numbers of relays K. It is clear from this figure that the achieved analytical and asymptotic results perfectly fit with Monte-Carlo simulations. Also, it can be seen from this figure that the SEC relaying scheme has nearly the same performance as the best relay selection for very low SNR region; whereas, as we go further in increasing the SNR, the best relay selection scheme is clearly outperforming the SEC relaying, as expected. In addition, we can see from this figure that for the SEC relaying as K increases, the system performance becomes more enhanced, especially, at the range of SNR values that is comparable to the switching threshold γ_{T}. More importantly, for $K = 2$, 3, and 4, it is obvious in this figure that at both low and high SNR values, all curves asymptotically converge to the same behavior and no gain is achieved in system performance with adding more relays. This is expected since when γ_{T} takes values much smaller or larger than the average SNR, the system asymptotically converges to the case of two relays and hence, adding more relays will not help in

enhancing the system performance. The curves in this figure greatly match the results achieved from the asymptotic or high SNR analysis where the diversity order was shown to be constat and equal 2. Another important result in this figure is that as the interference power is assumed not scaling with SNR, the system still can achieve more diversity gain due to adding more relays and this is clear in the range of SNR values that are comparable to the value of γ_T.

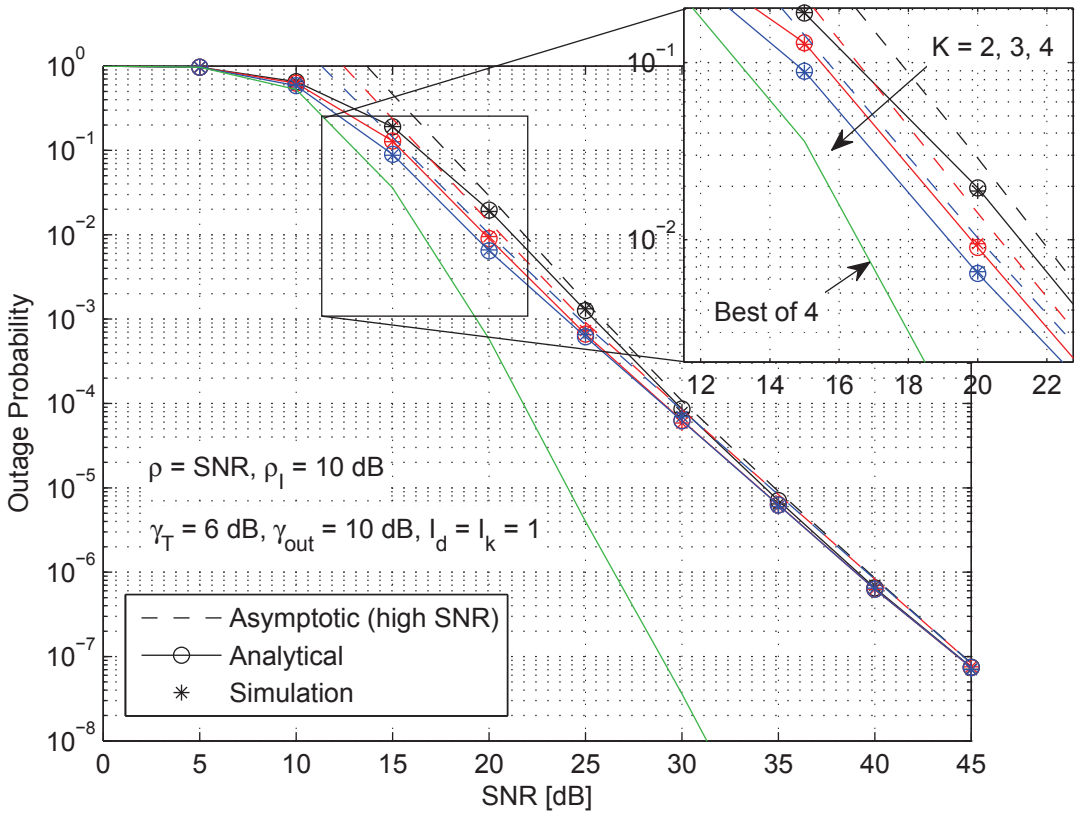

Figure 3.3: Outage probability vs average SNR for DF relay system with SEC relaying and interference at the relays and destination for different values of K and $\sigma^2_{\mathsf{s,d}} = 1$, $\sigma^2_{\mathsf{s},1} = 0.2$, $\sigma^2_{\mathsf{s},2} = 0.4$, $\sigma^2_{\mathsf{s},3} = 0.6$, $\sigma^2_{\mathsf{s},4} = 0.8$, $\sigma^2_{k,\mathsf{d}} = 0.4$ and $(\sigma^I_k)^2 = 0.01$ for $k = 1, \ldots, 4$, and $(\sigma^I_{\mathsf{d}})^2 = 0.01$.

Figure 3.4 illustrates the system outage performance vs SNR for the SECps-based relaying scheme for different values of $\sigma^2_{\mathsf{s,d}}$ for the cases of interference and

no interference. As expected, as $\sigma^2_{s,d}$ increases and hence, the quality of direct link channel the better the achieved performance. This is valid for both cases; the system with and without interference. Also, one can notice from this figure that for the case where the interference power scales with SNR, a noise floor appears and a zero diversity gain is achieved in all curves of this case due to the effect of interference on the system performance. On the other hand, for the case where the interference power does not scale with SNR, the system can still achieve full diversity and the system outage performance enhances as we increase the SNR.

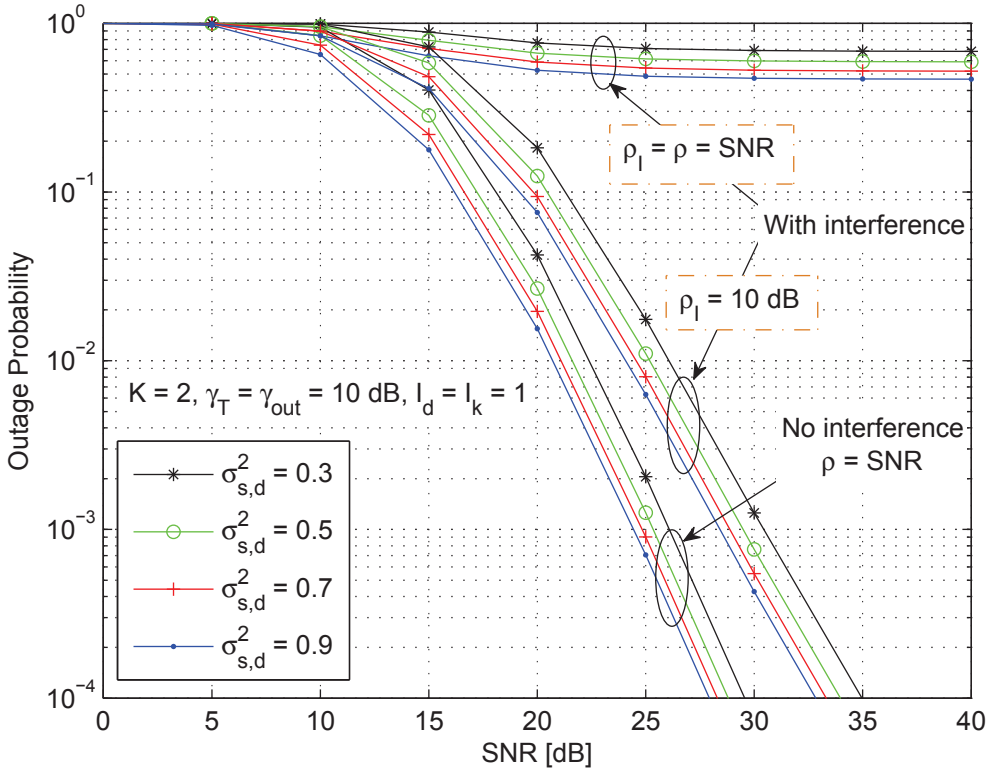

Figure 3.4: Outage probability vs average SNR for DF relay system with SECps relaying and interference at the relays and destination for different values of $\rho^2_{s,d}$ and $\sigma^2_{s,k} = 0.2$, $\sigma^2_{k,d} = 0.4$, $(\sigma^I_k)^2 = 0.1$ for $k = 1, 2$, and $(\sigma^I_d)^2 = 0.1$.

Figure 3.5 studies the system outage performance vs SNR for the SEC-based

relaying scheme for different numbers of relays K for the i.i.d. and i.n.d. cases of relay hops. As expected, as K increases, the better the achieved performance, especially, in the region where the average SNR values are comparable to γ_{T}. The figure also shows that this behavior extends to the case of i.n.d. relay hops. Furthermore, we can see from this figure that the gain achieved in system performance becomes smaller as we go further in increasing K.

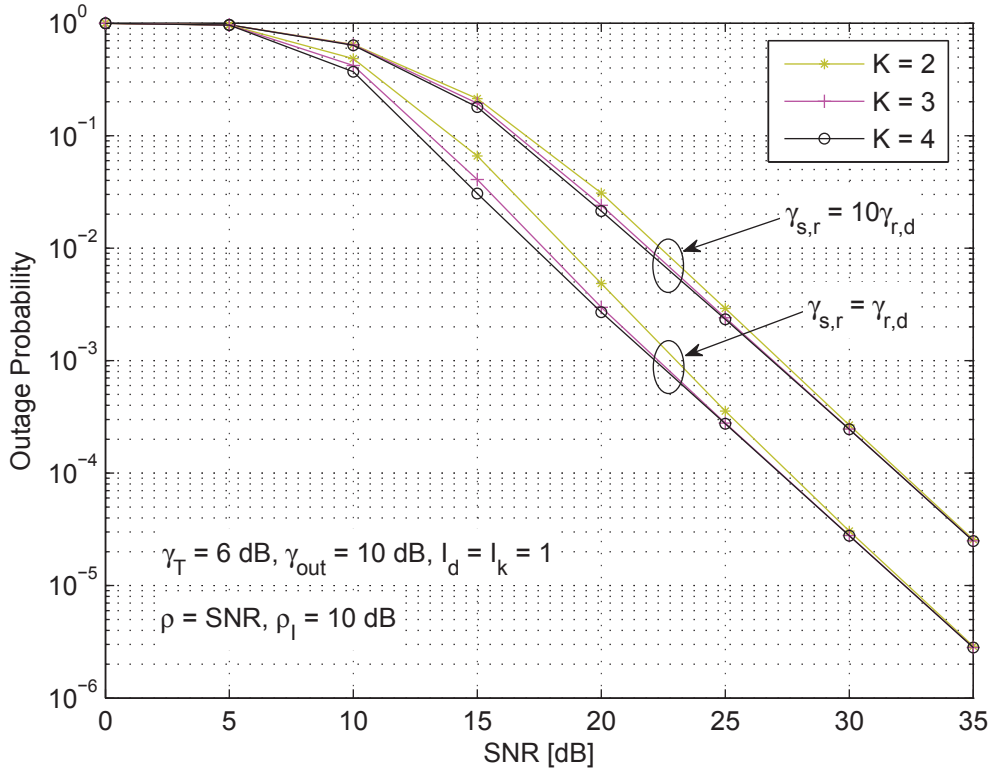

Figure 3.5: Outage probability vs average SNR for DF relay system with SEC relaying and interference at the relays and destination for different values of K for i.n.d. hops and $\sigma^2_{\mathsf{s,d}} = 1$, $(\sigma^I_k)^2 = 0.01$ for $k = 1, \ldots, 4$, and $(\sigma^I_{\mathsf{d}})^2 = 0.01$.

Figure 3.6 illustrates the system outage probability vs SNR for the SEC-based relaying scheme for different numbers of relays K for the cases with and without direct link. The important role of direct link in relay systems is clear in this figure

where better performance is achieved when the direct link is existed compared to the case of no direct link. Also, a noise floor is noticeable in all cases of this figure due to the effect of interference on the system performance. This is expected as the interference power is assumed to scale with SNR and thus, a zero diversity gain is achieved. Finally, it is clear from this figure that the cases of $K = 2, 3,$ and 4 almost behave the same at high SNR values, as expected.

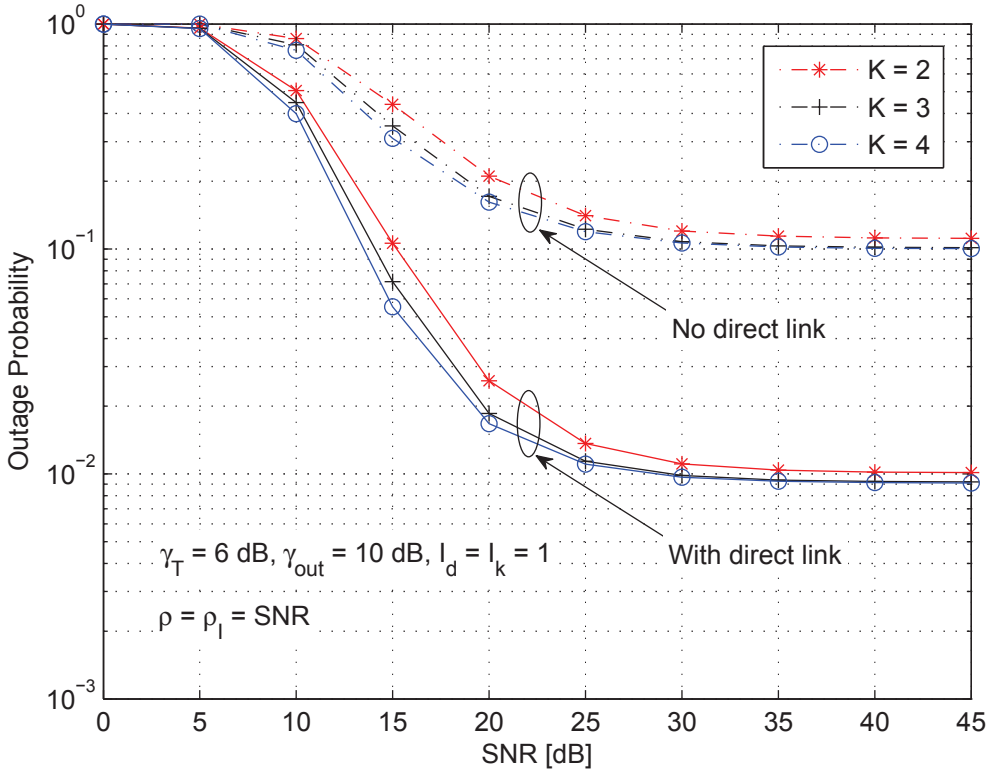

Figure 3.6: Outage probability vs average SNR for DF relay system with SEC relaying and interference at the relays and destination for different values of K with and without direct link and $\sigma^2_{\mathsf{s,d}} = 1$, $\sigma^2_{\mathsf{s},k} = 0.8$, $\sigma^2_{k,\mathsf{d}} = 0.9$ and $(\sigma^I_k)^2 = 0.01$ for $k = 1, \ldots, 4$, and $(\sigma^I_{\mathsf{d}})^2 = 0.01$.

Figure 3.7 portrays the system outage performance vs outage threshold γ_{out} for the SEC and SECps-based relaying schemes for different values of SNR. As

expected, as the average SNR takes larger values and hence, enhancing the direct link and relay paths channels, the better the achieved performance. In addition, the gain achieved in system performance when the SECps relaying scheme is used is clear in this figure compared to the case where the SEC scheme is used. This gain is more noticeable in the case where the SNR value is comparable to γ_{T}.

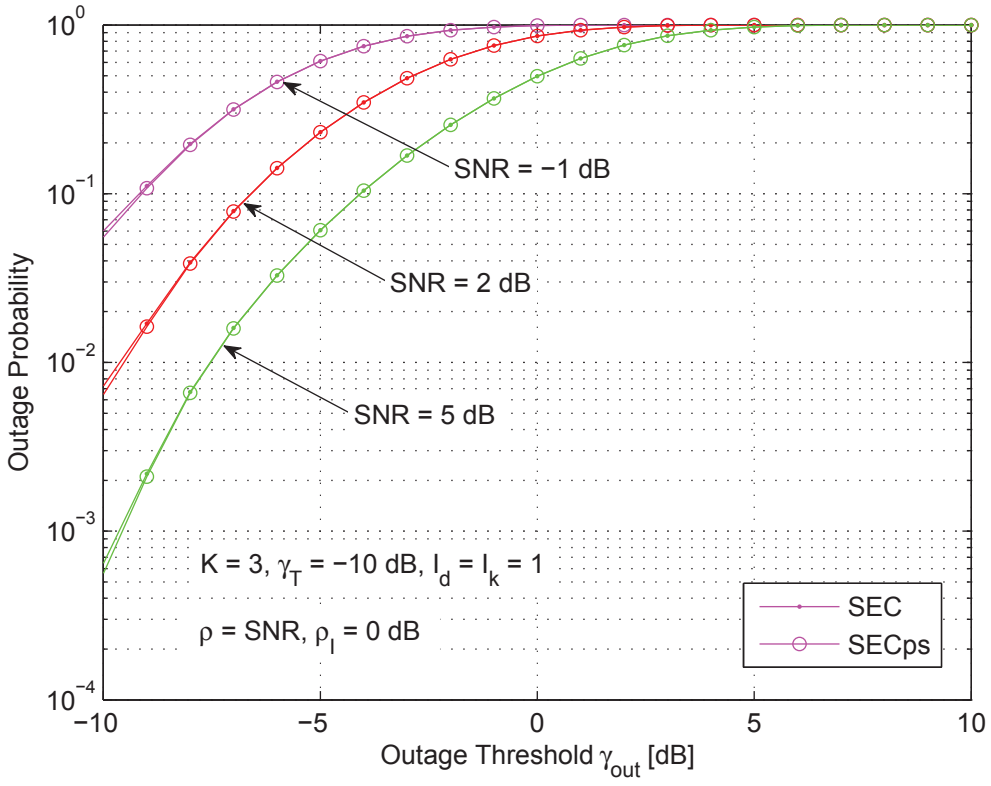

Figure 3.7: Outage probability vs outage threshold for DF relay system with SEC and SECps relaying schemes and interference at the relays and destination for different values of SNR and $\sigma^2_{\mathsf{s,d}} = 0.1$, $\sigma^2_{\mathsf{s},1} = 0.2$, $\sigma^2_{\mathsf{s},2} = 0.4$, $\sigma^2_{\mathsf{s},3} = 0.6$, and $\sigma^2_{k,\mathsf{d}} = 0.4$, $(\sigma^I_k)^2 = 0.01$ for $k = 1, \ldots, 3$, and $(\sigma^I_{\mathsf{d}})^2 = 0.01$.

Figure 3.8 studies the system outage performance vs SNR for the SEC and SECps-based relaying schemes for different values of $\sigma^2_{\mathsf{s,d}}$. As can be seen from this figure, the gain achieved in system performance in the case of SECps relaying

is clear compared to the case where the SEC scheme is used. This gain is more noticeable in the range of SNR values that are close to γ_T. As the value of the average SNR becomes much larger or smaller than the average SNR, the gain in system behavior becomes smaller and both scheme behave the same. Clearly, the amount of this gain is highly reduced due to the effect of interference on the system performance.

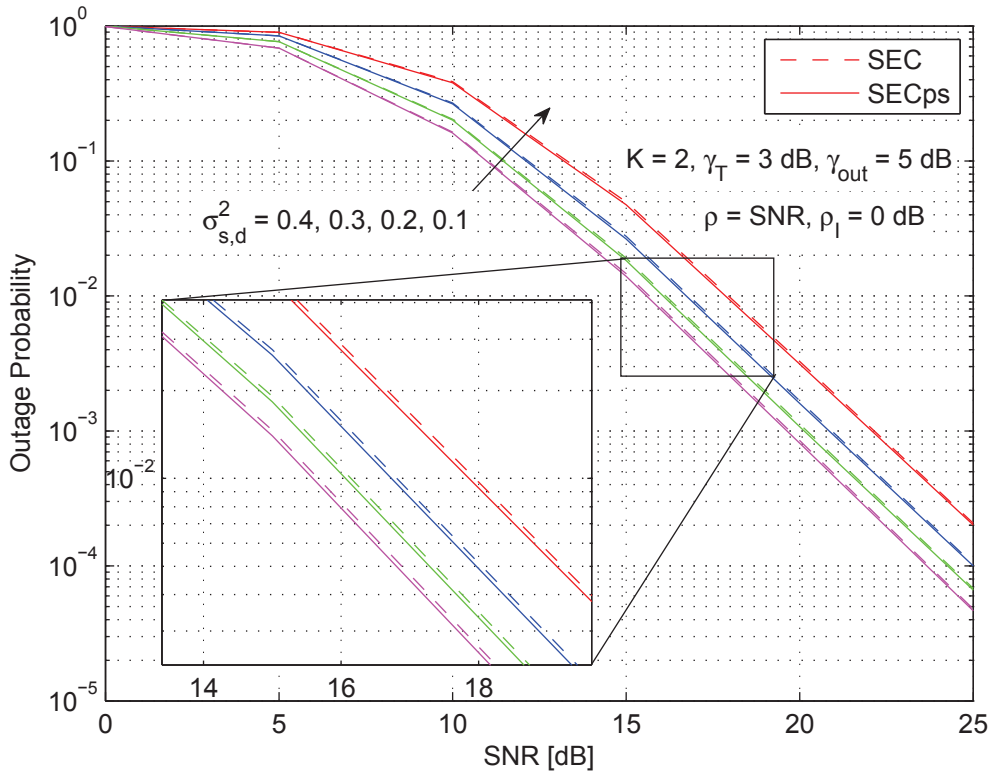

Figure 3.8: Outage probability vs average SNR for DF relay system with SEC and SECps relaying schemes and interference at the relays and destination for different values of $\sigma^2_{s,d}$ and $\sigma^2_{s,1} = 0.1$, $\sigma^2_{s,2} = 0.5$, $\sigma^2_{1,d} = 0.1$, $\sigma^2_{2,d} = 0.5$, and $(\sigma^I_k)^2 = 0.001$, $I_k = 1$ for $k = 1, 2$, $(\sigma^I_d)^2 = 0.001$, and $I_d = 1$.

Figure 3.9 shows the outage performance versus average SNR for the studied system with the SECps-based relaying scheme for different values of interference

power ρ_I. A perfect fitting between the analytical and the asymptotic results is obvious in this figure. Also, the effect of interference power on the system performance is clear in this figure where as ρ_I increases, the system behavior becomes more degraded, as expected. This degradation in system performance is due to the reduction in coding gain caused by the interference.

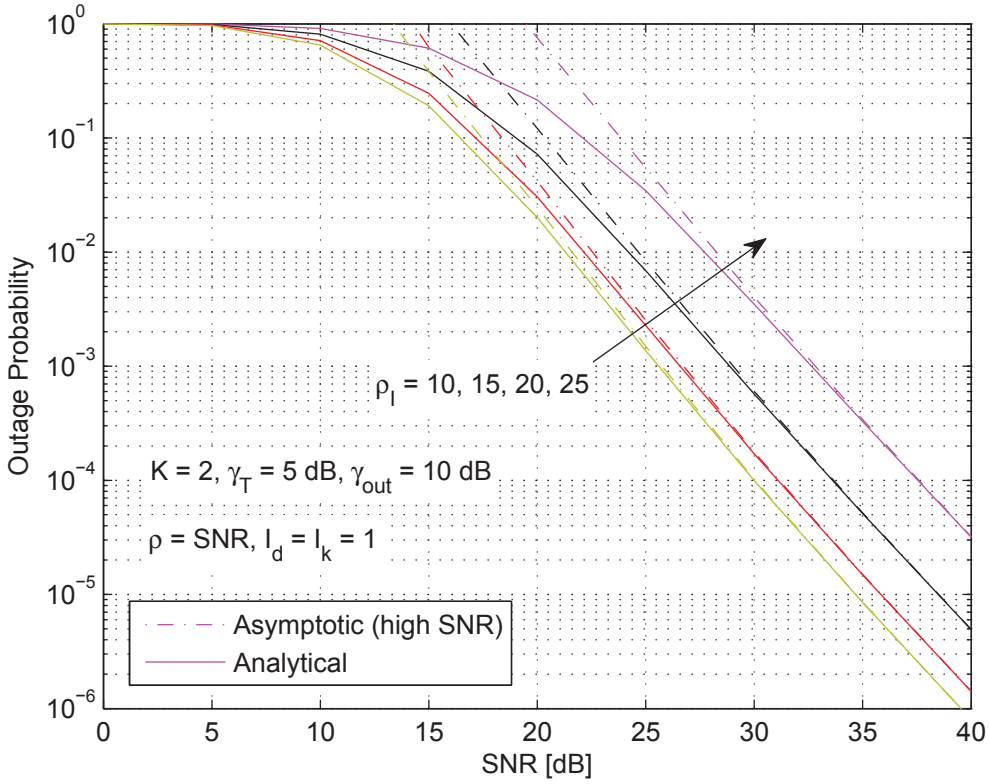

Figure 3.9: Outage probability vs average SNR for DF relay system with SECps relaying scheme and interference at the relays and destination for different values of ρ_I and $\sigma^2_{\mathsf{s,d}} = 1$, $\sigma^2_{\mathsf{s},1} = 0.2$, $\sigma^2_{\mathsf{s},2} = 0.4$, $\sigma^2_{k,\mathsf{d}} = 0.4$, $(\sigma^I_k)^2 = 0.01$, and $I_k = 1$ for $k = 1, 2$, $(\sigma^I_{\mathsf{d}})^2 = 0.01$, and $I_d = 1$.

Figure 3.10 illustrates the system outage probability vs SNR for the SEC-based relaying scheme for different values of switching threshold γ_{T}. It is clear from this figure that the best performance is achieved when the optimum switching

threshold $\gamma_{\mathsf{T-Opt}}$ is used, as expected.

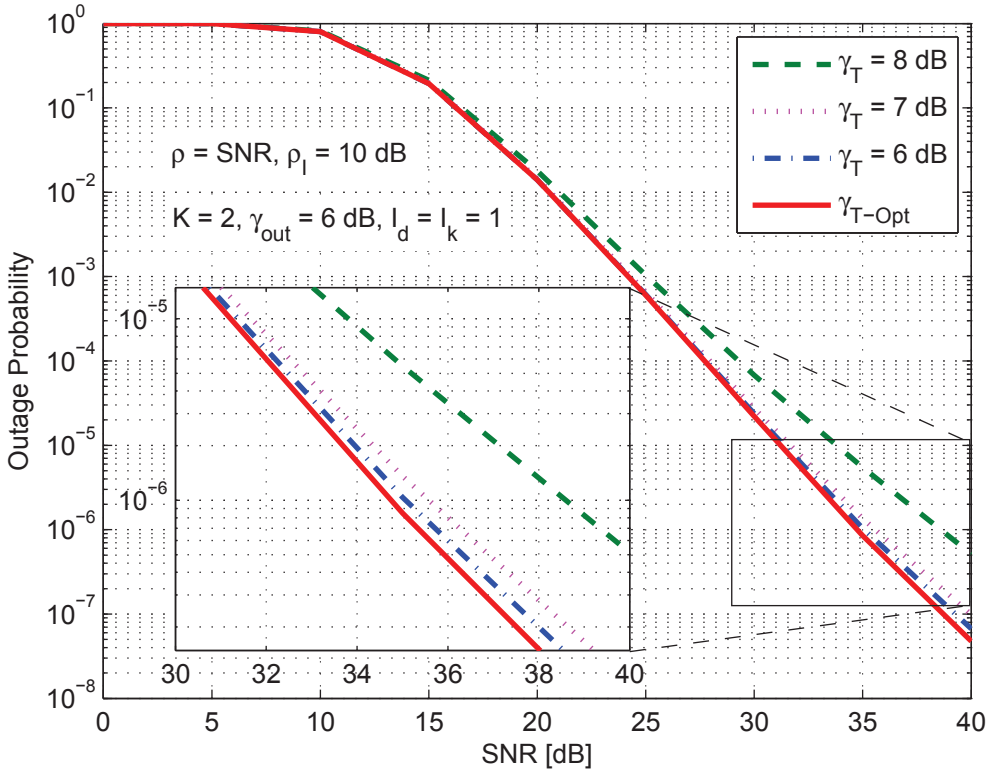

Figure 3.10: Outage probability vs average SNR for DF relay system with SEC relaying and interference at the relays and destination for different values of γ_{T} and $\sigma^2_{\mathsf{s,d}} = 0.1$, $\sigma^2_{\mathsf{s},1} = 0.2$, $\sigma^2_{\mathsf{s},2} = 0.4$, and $\sigma^2_{k,\mathsf{d}} = 0.4$, $(\sigma^I_k)^2 = 0.01$ for $k = 1, 2$, and $(\sigma^I_{\mathsf{d}})^2 = 0.01$.

Figure 3.11 shows the system outage performance vs SNR for the SEC-based relaying scheme for different values of outage threshold γ_{out}. As expected, as γ_{out} increases and hence, the probability of outage, the worse the achieved performance. Also, the case where there is no interference is clear in this figure. In contrast to the case where the interference is existed, no noise floor appears in this case.

Figure 3.12 portrays the system outage performance vs number of interferers I_k

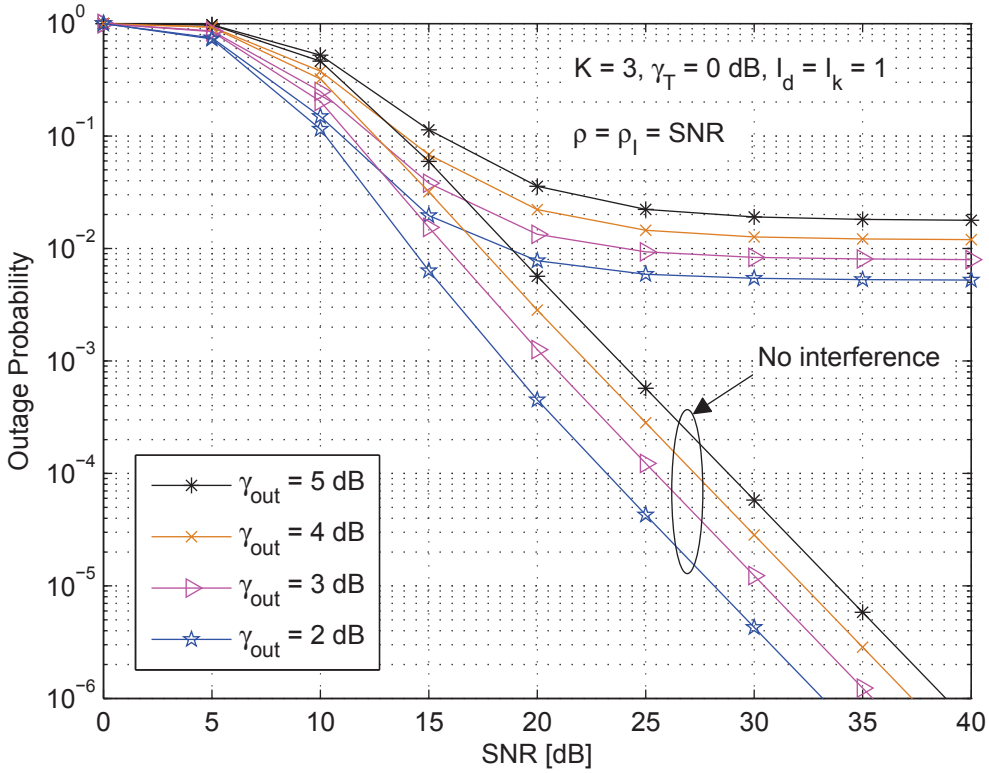

Figure 3.11: Outage probability vs average SNR for DF relay system with SEC relaying and interference at the relays and destination for different values of γ_{out} and $\sigma^2_{\text{s,d}} = 0.1$, $\sigma^2_{\text{s},1} = 0.2$, $\sigma^2_{\text{s},2} = 0.4$, $\sigma^2_{\text{s},3} = 0.6$, and $\sigma^2_{k,\text{d}} = 0.4$, $(\sigma^I_k)^2 = 0.01$ for $k = 1, \ldots, 3$, and $(\sigma^I_{\text{d}})^2 = 0.01$.

and I_d for the SEC-based relaying scheme for different values of SNR. As expected, as SNR increases and hence, the better the desired user channels, the better the achieved performance. Also, as I_k and I_d increase, the probability of system to be in outage increases.

Figure 3.13 illustrates the system outage probability vs SNR for the SEC-based relaying scheme for different values of I_d and I_k when they are equal. It can be seen from this figure that as $I_d = I_k$ increases, the worse the achieved performance, as expected.

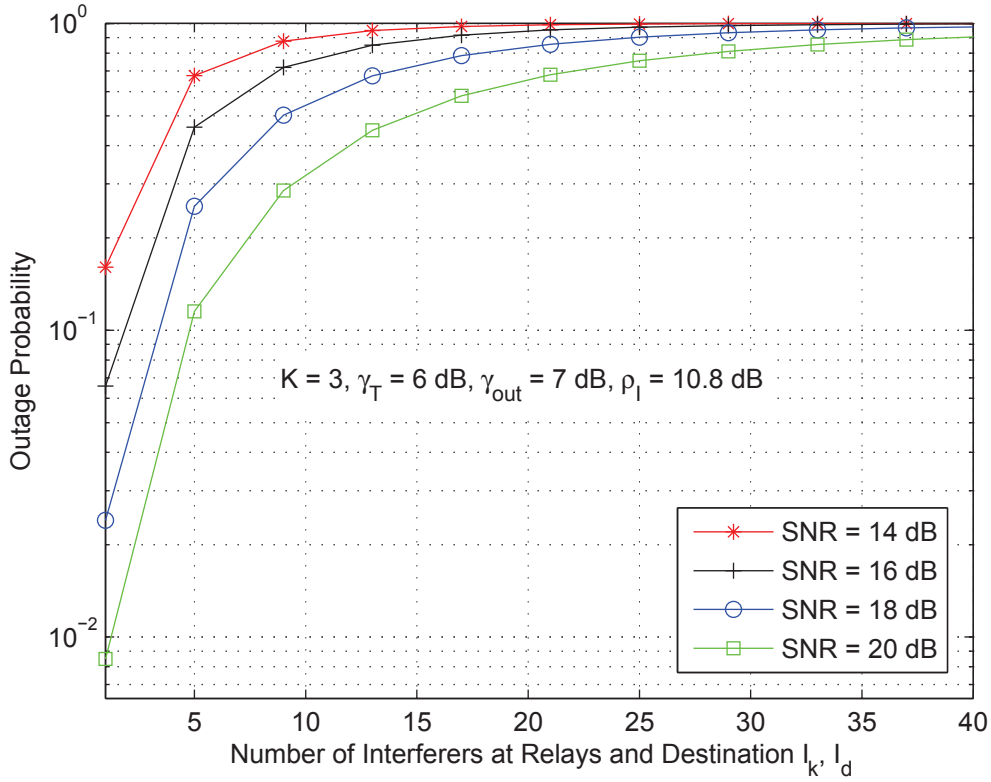

Figure 3.12: Outage probability vs number of interferers at relays and destination for DF relay system with SEC relaying and interference at the relays and destination for different values of SNR and $\sigma^2_{s,d} = 1$, $\sigma^2_{s,1} = 0.2$, $\sigma^2_{s,2} = 0.4$, $\sigma^2_{s,3} = 0.6$, and $\sigma^2_{k,d} = 0.6$, $(\sigma^I_k)^2 = 0.1$ for $k = 1, \ldots, 3$, and $(\sigma^I_d)^2 = 0.1$.

Figure 3.14 studies the system outage performance vs SNR for the SEC-based relaying scheme for different values of I_d and I_k when they are unequal. As can be seen, the interference at the destination node affects the system performance more severely than the interference at the relay. This is because the impact of the interference at the relay node is reduced by the decoding process performed by the relay itself. Furthermore, this result is expected as the interference at the destination affects the signals on the direct link and that through the relay. Finally, the worst performance is achieved when the interference simultaneously

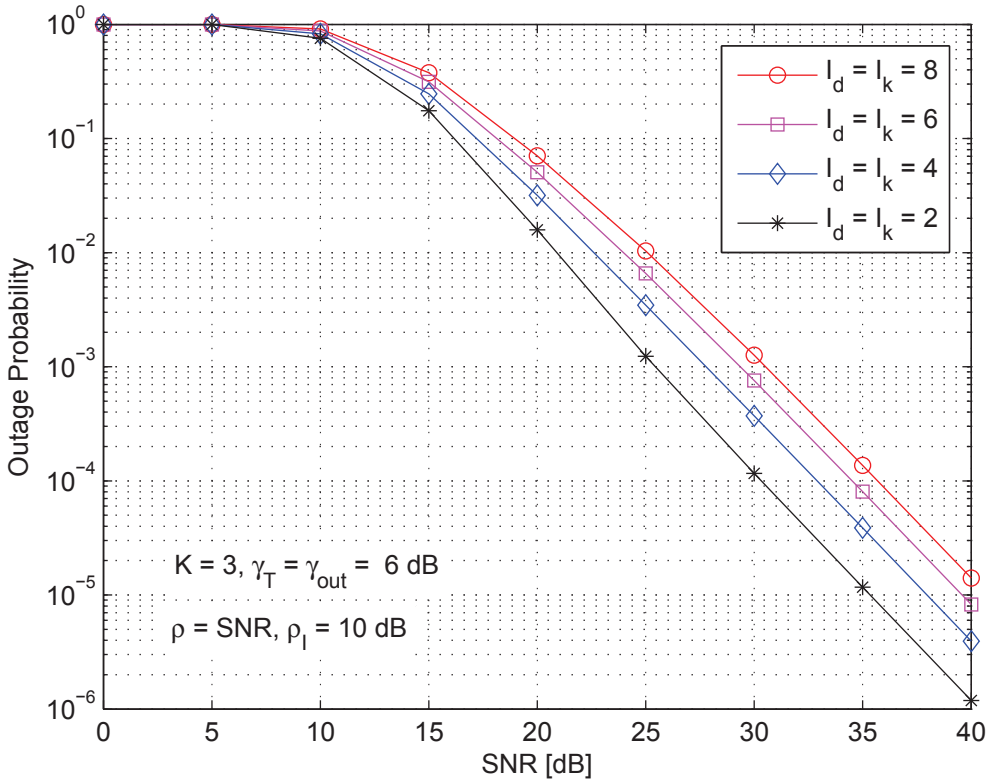

Figure 3.13: Outage probability vs average SNR for DF relay system with SEC relaying and interference at the relays and destination for different values of I_d and I_k when they are equal and $\sigma^2_{\mathrm{s,d}} = 0.01$, $\sigma^2_{\mathrm{s},1} = 0.2$, $\sigma^2_{\mathrm{s},2} = 0.4$, $\sigma^2_{\mathrm{s},3} = 0.6$, and $\sigma^2_{k,\mathrm{d}} = 0.4$, $(\sigma^I_k)^2 = 0.01$ for $k = 1, \ldots, 3$, and $(\sigma^I_{\mathrm{d}})^2 = 0.01$.

increases at the relay and the destination nodes, as expected.

Figure 3.15 shows the system outage performance vs number of relays K for the SEC-based relaying scheme for different values of SNR. It can be seen from this figure that the considered relay system still achieves performance gain and the outage probability decreases when the number of relays K increases, but the slope depends on the SNR values. Also, the achieved gain in system performance due to the existence of the direct link is clear in the figure.

Figure 3.16 illustrates the average number of channel estimations versus the

switching threshold γ_T for the SEC and SECps-based relaying schemes in comparison with the opportunistic relaying scheme. We can see from this figure that as the quality of all relay second hop channels are required for its operation, opportunistic relaying always needs 4 channel estimations. On the other hand, the SEC relaying needs to estimate at most 3 relay second hop channels because when the second hop channels of the first 3 relays are found unacceptable, the last checked relay will be used at the destination. Therefore, the SEC relaying scheme requires less path estimations than the SECps relaying. Also, we can notice from this figure that as γ_T increases, the average number of channel estimations of relays increases since it is more difficult to find a suitable relay.

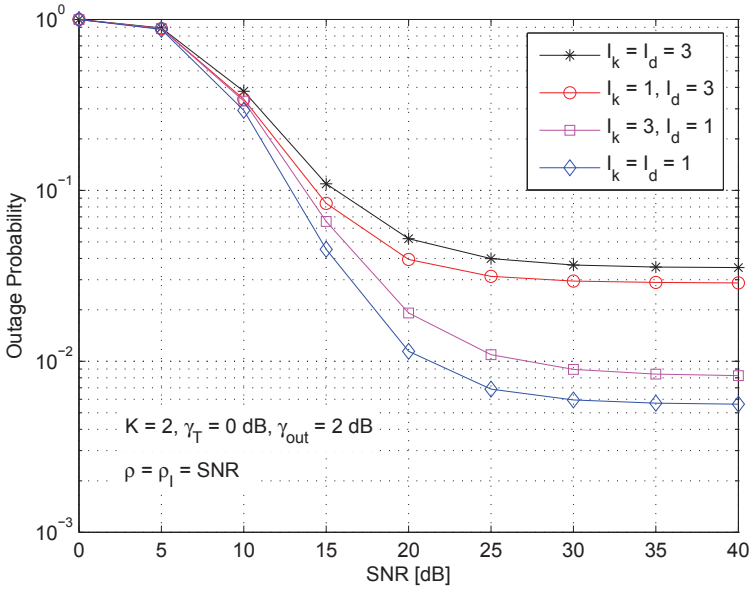

Figure 3.14: Outage probability vs average SNR for DF relay system with SEC relaying and interference at the relays and destination for different values of I_d and I_k when they are unequal and $\sigma^2_{s,d} = 0.1$, $\sigma^2_{s,1} = 0.2$, $\sigma^2_{s,2} = 0.4$, and $\sigma^2_{k,d} = 0.4$, $(\sigma^I_k)^2 = 0.01$ for $k = 1, 2$, and $(\sigma^I_d)^2 = 0.01$.

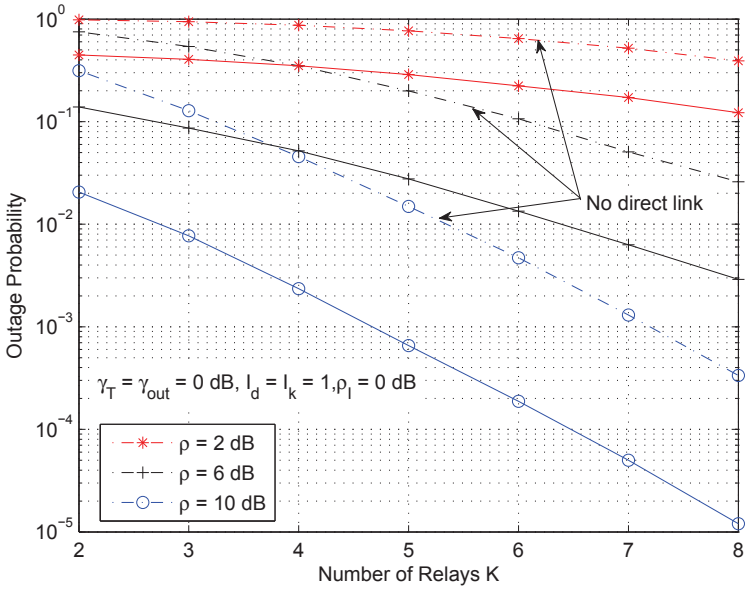

Figure 3.15: Outage probability vs number of relays for DF relay system with SEC relaying and interference at the relays and destination for different values of SNR and $\sigma^2_{\mathrm{s},k} = 1$, and $\sigma^2_{\mathrm{s},k} = \sigma^2_{k,\mathrm{d}} = (k+1)/10$, $(\sigma^I_k)^2 = 0.01$ for $k = 1, \ldots, 8$, and $(\sigma^I_{\mathrm{d}})^2 = 0.01$.

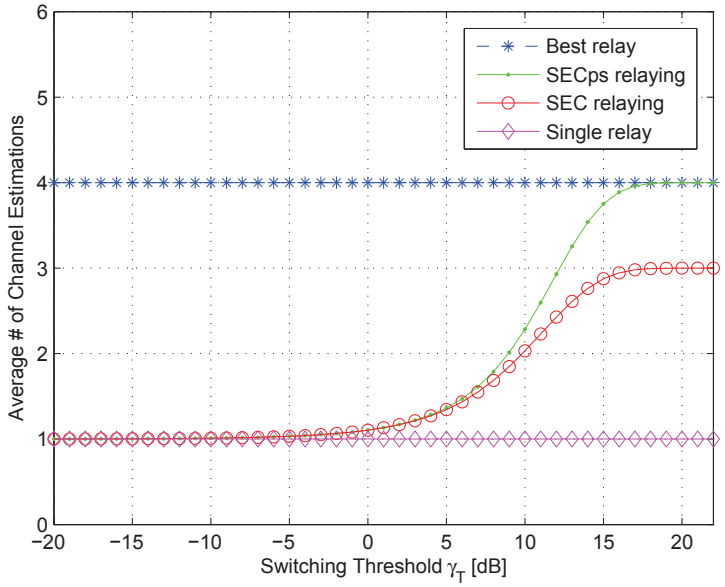

Figure 3.16: Average number of channel estimations of the proposed SEC relaying schemes for DF relay systems in comparison with the best relay selection scheme with $L = 4$ and $\bar{\gamma}_{R,\mathrm{d}} = 10$ dB.

3.8 Conclusions

In this chapter, we proposed and evaluated the performance of new low-complexity relay selection schemes for dual-hop DF relay systems with interference at the relays and destination nodes. These schemes are based on the well known switch-and-examine and switch-and-examine post-selection diversity combining techniques. The e2e outage probability was derived for the generic i.n.d. case of second hops of the SEC relaying scheme and for the i.i.d. case for the SECps scheme. Furthermore, the system outage performance was evaluated at high SNR values where simple expressions for the outage probability, diversity order, and coding gain were derived and analyzed. Monte-Carlo simulations proved the accuracy of the achieved analytical and asymptotic results. Findings illustrated that for fixed number of interferers of fixed power or equivalently, when the interference power does not scale with SNR, the system can still achieve diversity gain; especially, in the range of SNR that is comparable to the switching threshold. Also, asymptotic results showed that the system achieves the same diversity order which is 2 and approximately the same coding gain for the cases of SEC and SECps relaying schemes. Finally, findings illustrated the severe effect of interference on the gain achieved by the SECps relaying scheme compared to the conventional SEC scheme.

CHAPTER 4

OPPORTUNISTIC DF RELAYING USING BEST RELAY

4.1 Introduction

In chapters 2 and 3, the SEC and SECps low-complexity relaying schemes were proposed for AF and DF relaying systems to achieve the lowest system complexity with satisfying an adequate system performance. In some systems, the performance has the highest priority if compared with the system complexity. An excellent relaying scheme for such systems is the opportunistic relaying. It gives the optimum system performance compared to its counterparts. Also, due to the lack in number of papers that address the interference effect on the performance of DF relay systems assuming the very general Nakagami-m fading environment,

it would be highly motivating to present such a study.

In this chapter, we investigate the outage behavior of a dual-hop opportunistic DF relay system with CCI at both the relay and the destination. The source-relay and relay-destination channels as well as the interferers' channels at both the relay and the destination nodes are assumed to follow Nakagami-m distribution. Exact closed-form expressions for the outage probability for both i.n.d. and i.i.d. cases of interferers' channels are derived. Furthermore, the system behavior at high SNR values is studied via deriving the asymptotic outage probability and hence, the diversity order and the coding gain are characterized. Our results show that the co-channel interferers do not reduce the diversity gain of the system, instead, they degrade the outage performance by affecting the coding gain of the system. The accuracy of the analytical results are supported by Monte-Carlo simulations.

The rest of this chapter is organized as follows. Section 4.2 provides a literature review on the most related studies. Section 4.3 explains the system model. The exact performance analysis is conducted in Section 4.4. Section 4.5 presents the asymptotic system analysis. In Section 4.6, some numerical results are discussed. Finally, some conclusions are provided in Section 4.7.

4.2 Literature Review

As mentioned in the previous chapter, most of the work on relay systems has focused on noise-limited environments and ignored the interference effect on system performance. Some key papers on relay systems with multiple relays are the ones

presented in [16]-[18]. The work that includes the impact of CCI looks important as the interference can be one of the major limiting-factors of the cooperative performance. Most of the existing papers on relay networks considered the effect of CCI assuming single relay with interference at the relay, the destination, or at both. Other studies considered the interference impact in multi-relay systems with single interferer at the relay or the destination node. The lack of strong studies that evaluate the performance of multi-relay cooperative systems with interference at both the relay and the destination nodes motivates us to contribute in this area of research. Another contribution of our work in this chapter is that it is a development to the work presented in [16] where the conventional DF relaying is extended to an opportunistic DF relaying by using different approach than the MGF one. Using the best relay scheme reduces the amount of cooperation overheads and enhances the system spectral efficiency. Also, an important contribution is the studying of system performance at high SNR values.

To the best of our knowledge, the interference effect at both the relay and the destination nodes in opportunistic DF relay systems over Nakagami-m fading channels has not been studied yet. In this chapter, we consider the system of [17] where the best DF relay is selected to forward the source message to destination with interference at the relays and destination. We derive exact closed-form expressions for the outage probability for both i.n.d. and i.i.d. cases of interferers' channels. Furthermore, we evaluate the system performance at high SNR regime where an asymptotic expression for the outage probability is derived and analyzed

and the diversity order and coding gain are provided. Due to its inherent effect on system behavior, the direct link is considered in all derivations in this chapter.

4.3 System Model

The system under consideration is as shown in Figure 3.1 with the best relay among all active relays forwarding the source message to destination. All the channel gains are assumed to follow Nakagami-m distribution. That is, the channel powers denoted by $|h_{\mathsf{s},\mathsf{d}}|^2$, $|h_{\mathsf{s},k}|^2$, $|h_{k,\mathsf{d}}|^2$, $|h^I_{i_k,k}|^2$, and $|h^I_{i_d,\mathsf{d}}|^2$ are gamma distributed RVs with parameters $\left(m_{\mathsf{s},\mathsf{d}}, \sigma^2_{\mathsf{s},\mathsf{d}}/m_{\mathsf{s},\mathsf{d}}\right)$, $\left(m_{\mathsf{s},k}, \sigma^2_{\mathsf{s},k}/m_{\mathsf{s},k}\right)$, $\left(m_{k,\mathsf{d}}, \sigma^2_{k,\mathsf{d}}/m_{k,\mathsf{d}}\right)$, $\left(m^I_{i_k,k}, \sigma^2_{I,i_k,k}/m^I_{i_k,k}\right)$, and $\left(m^I_{i_d,\mathsf{d}}, \sigma^2_{I,i_d,\mathsf{d}}/m^I_{i_d,\mathsf{d}}\right)$, respectively. Using (3.1), the SINR at the k^{th} relay can be written as in (3.2).

The decoding set C_L of active relays that could have correctly decoded the message sent from the source in the first phase is as defined by (3.3). In the second phase after decoding the received signal, only the best relay in C_L forwards the re-encoded message to the destination. The best relay is selected such that

$$b = \arg\, \max_{l \in C_L} \left\{\gamma_{l,\mathsf{d}}\right\}, \tag{4.1}$$

where $\gamma_{l,\mathsf{d}}$ is the SINR at the destination resulting from the l^{th} relay being the relay which forwarded the source information as given by (3.4). Equivalently,

$$b = \arg\, \max_{l \in C_L} \left\{ \frac{P_l}{N_0} |h_{l,\mathsf{d}}|^2 \right\}, \tag{4.2}$$

since the denominator is common to the SINRs from all relays belonging to C_L.

In the analysis of the considered system, the destination is assumed to be located at the same point during the two phases. This means the same interference is affecting the destination node in both phases. The destination finally combines the signals from the source and the best relay using MRC. The e2e SINR at the destination output can be written as

$$\gamma_{\mathsf{d}} \triangleq \gamma_{\mathsf{s},\mathsf{d}} + \gamma_{b,\mathsf{d}} = \frac{\frac{P_0}{N_0}|h_{\mathsf{s},\mathsf{d}}|^2 + \frac{P_b}{N_0}|h_{b,\mathsf{d}}|^2}{\sum_{i_d=1}^{I_d} \frac{P^I_{i_d,\mathsf{d}}}{N_0}\left|h^I_{i_d,\mathsf{d}}\right|^2 + 1}. \tag{4.3}$$

4.4 Performance Analysis

In this section, we evaluate the system outage probability for both i.n.d. and i.i.d. interferers' fading channels. The distribution of the decoding set defined by (3.3) is as given by (3.6) and the outage probability for the considered system can be achieved by averaging over all possible decoding sets as given by (3.7). In order to evaluate (3.7), we first need to derive $\mathrm{P_r}\left[\gamma_{\mathsf{d}} < u | C_L\right]$ and then $\mathrm{P_r}\left[C_L\right]$ as follows.

4.4.1 Non-Identical Interferers

Let $\rho \triangleq P_0/N_0 = P_l/N_0$ and $\rho_{I_k} \triangleq P^I_{i_k,k}/N_0 = P^I_{i_d,\mathsf{d}}/N_0 = \rho_I$. Then, $\rho|h_{\mathsf{s},\mathsf{d}}|^2$, $\rho|h_{\mathsf{s},k}|^2$, $\rho_I|h^I_{i_k,k}|^2$, $\rho|h_{l,\mathsf{d}}|^2$, and $\rho_I|h^I_{i_d,\mathsf{d}}|^2$ are gamma distributed with parameters $\left(m_{\mathsf{s},\mathsf{d}},\ \rho\sigma^2_{\mathsf{s},\mathsf{d}}/m_{\mathsf{s},\mathsf{d}} = 1/\alpha_{\mathsf{s},\mathsf{d}}m_{\mathsf{s},\mathsf{d}}\right)$, $\left(m_{\mathsf{s},k},\ \rho\sigma^2_{\mathsf{s},k}/m_{\mathsf{s},k} = 1/\alpha_{\mathsf{s},k}m_{\mathsf{s},k}\right)$, $\left(m^I_{i_k,k},\ \rho_I\sigma^2_{I,i_k,k}/m^I_{i_k,k} = 1/\alpha^I_{i_k,k}m^I_{i_k,k}\right)$, $\left(m_{l,\mathsf{d}},\ \rho\sigma^2_{l,\mathsf{d}}/m_{l,\mathsf{d}} = 1/\alpha_{l,\mathsf{d}}m_{l,\mathsf{d}}\right)$, and $\left(m^I_{i_k,k},\ \rho_I\sigma^2_{I,i_d,\mathsf{d}}/m^I_{i_k,k} = 1/\alpha^I_{i_d,\mathsf{d}}m^I_{i_k,k}\right)$, respectively. For the case of unequal power inter-

ferers, we have $\alpha^I_{i_n,n} \neq \alpha^I_{j_n,n}$, when $i_n \neq j_n$, $n \in \mathcal{S}_r \bigcup \{d\}$. We can then calculate P_{out} in (3.7) using the following results.

Lemma 4.1 *The term* $\mathrm{P_r}\left[\gamma_{\mathsf{d}} < u | C_L\right]$ *for* $L \geq 1$ *is given by*

$$\mathrm{P_r}\left[\gamma_{\mathsf{d}} < u | C_L\right]_{\mathrm{NI}} = -\sum_{i_d=1}^{I_d}(-1)^{m^I_{i_d,\mathsf{d}}} \exp\left(\alpha^I_{i_d,\mathsf{d}}\right) \sum_{i=1}^{m^I_{i_d,\mathsf{d}}} \frac{\beta^{i-1}_{i_d}}{(i-1)!} \sum_{g=0}^{m^I_{i_d,\mathsf{d}}-1} \binom{m^I_{i_d,\mathsf{d}}-1}{g}(-1)^g$$
$$\times C_a \sum_{r=0}^{m_{\mathsf{s},\mathsf{d}}-1} \binom{m_{\mathsf{s},\mathsf{d}}-1}{r}(-1)^r \sum_{l=1}^{L} C_b(l) \Bigg[\frac{C_1(r,l)!}{C_2(l)^{m_{l,\mathsf{d}}+r}} \Bigg(\frac{C_3(r)!C_4(i_d,g)}{\left(\frac{m_{\mathsf{s},\mathsf{d}}}{\Omega_{\mathsf{s},\mathsf{d}}}\right)^{m_{\mathsf{s},\mathsf{d}}-r}} - \sum_{k_3=0}^{C_3(r)} C_3(r)!$$
$$\times \frac{\Lambda_1(i_d,u)^{-g-k_3-1}u^{k_3}}{k_3!\left(\frac{m_{\mathsf{s},\mathsf{d}}}{\Omega_{\mathsf{s},\mathsf{d}}}\right)^{m_{\mathsf{s},\mathsf{d}}-r-k_3}} \Gamma\left(g+k_3+1, \Lambda_1(i_d,u)\right) \Bigg) - \sum_{k_1=0}^{C_1(r,l)} \frac{1}{k_1!} \frac{C_1(r,l)!}{C_2(l)^{m_{l,\mathsf{d}}+r-k_1}}$$
$$\times \left(\frac{C_5(r,k_1)!C_4(i_d,g)}{\left(\frac{m_{l,\mathsf{d}}}{\Omega_{l,\mathsf{d}}}\right)^{m_{\mathsf{s},\mathsf{d}}-r+k_1}} - \sum_{k_4=0}^{C_5(r,k_1)} \frac{C_5(r,k_1)!\Lambda_2(i_d,l,u)^{-g-k_4-1}u^{k_4}}{k_4!\left(\frac{m_{l,\mathsf{d}}}{\Omega_{l,\mathsf{d}}}\right)^{m_{\mathsf{s},\mathsf{d}}-r+k_1-k_4}} \Gamma\left(g+k_4+1, \Lambda_2(i_d,l,u)\right) \right)$$
$$+ \sum_{n=1}^{L}(-1)^n \sum_{j_1<\cdots<j_n, j_{(.)}\neq l} \sum_{q_1=\cdots=q_n=0} \frac{\prod_{w=1}^{n}\left(\frac{m_{j_w,\mathsf{d}}}{\Omega_{j_w,\mathsf{d}}}\right)^{q_w}}{\prod_{p=1}^{n} q_p!} \Bigg\{ \frac{C_6(r,l,q_i)!}{C_7(l,j_s)^{\sum_{i=1}^{n} q_i + m_{l,\mathsf{d}}+r}}$$
$$\times \left(\frac{C_3(r)!C_4(i_d,g)}{\left(\frac{m_{\mathsf{s},\mathsf{d}}}{\Omega_{\mathsf{s},\mathsf{d}}}\right)^{m_{\mathsf{s},\mathsf{d}}-r}} - \sum_{k_5=0}^{C_3(r)} \frac{C_3(r)!}{k_5!} \frac{\Lambda_1(i_d,u)^{-g-k_5-1}u^{k_5}}{\left(\frac{m_{\mathsf{s},\mathsf{d}}}{\Omega_{\mathsf{s},\mathsf{d}}}\right)^{m_{\mathsf{s},\mathsf{d}}-r-k_5}} \Gamma\left(g+k_5+1, \Lambda_1(i_d,u)\right) \right)$$
$$- \sum_{k_2=0}^{C_6(r,l,q_i)} \frac{C_6(r,l,q_i)!}{k_2!C_7(l,j_s)^{\sum_{i=1}^{n} q_i + m_{l,\mathsf{d}}+r-k_2}} \Bigg(\frac{C_8(r,k_2)!C_4(i_d,g)}{C_9(l,j_s)^{m_{\mathsf{s},\mathsf{d}}-r+k_2}} - \sum_{k_6=0}^{C_8(r,k_2)} \frac{C_8(r,k_2)!u^{k_6}}{k_6!}$$
$$\times \frac{\Lambda_3(i_d,l,j_s,u)^{-g-k_6-1}}{C_9(l,j_s)^{m_{\mathsf{s},\mathsf{d}}-r+k_2-k_6}} \Gamma\left(g+k_6+1, \Lambda_3(i_d,l,j_s,u)\right) \Bigg) \Bigg\} \Bigg], \tag{4.4}$$

where $C_3(r) = m_{\mathsf{s},\mathsf{d}} - r - 1, C_4(i_d,g) = \frac{\Gamma\left(g+1,\alpha^I_{i_d,\mathsf{d}}\right)}{\left(\alpha^I_{i_d,\mathsf{d}}\right)^{g+1}}, C_5(r,k_1) = m_{\mathsf{s},\mathsf{d}} - r + k_1 - 1, C_8(r,k_2) = m_{\mathsf{s},\mathsf{d}} - r + k_2 - 1, C_9(l,j_s) = \sum_{s=1}^{n} \frac{m_{j_s,\mathsf{d}}}{\Omega_{j_s,\mathsf{d}}} + \frac{m_{l,\mathsf{d}}}{\Omega_{l,\mathsf{d}}}, \Lambda_1(i_d,u) = \frac{m_{\mathsf{s},\mathsf{d}}}{\Omega_{\mathsf{s},\mathsf{d}}}u + \alpha^I_{i_d,\mathsf{d}}, \Lambda_2(i_d,l,u) = \frac{m_{l,\mathsf{d}}}{\Omega_{l,\mathsf{d}}}u + \alpha^I_{i_d,\mathsf{d}},$ *and* $\Lambda_3(i_d,l,j_s,u) = \left(\sum_{s=1}^{n} \frac{m_{j_s,\mathsf{d}}}{\Omega_{j_s,\mathsf{d}}} + \frac{m_{l,\mathsf{d}}}{\Omega_{l,\mathsf{d}}}\right)u + \alpha^I_{i_d,\mathsf{d}}.$

Proof. See Appendix C.1. ∎

For $L = 0$, the term $\mathrm{P_r}\left[\gamma_{\mathsf{d}} < u | C_L\right]$ can be simply obtained by replacing k for relay by d for destination and i_k by i_d in the CDF of $\gamma_{\mathsf{s},k}$ in Lemma 4.2.

Now, we find the second term in (3.7) $\Pr\left[C_L\right]$.

Lemma 4.2 *The CDF* $\mathrm{P_r}\left[\gamma_{\mathsf{s},k} < u\right]$ *which is a part of the term* $\Pr\left[C_L\right]$ *in (3.6) is given by*

$$\mathrm{P_r}\left[\gamma_{\mathsf{s},k} < u\right]_{\mathrm{NI}} = -\sum_{i_k=1}^{I_k}\sum_{i=1}^{m_{i_k,k}^I} \frac{(-1)^{m_{i_k,k}^I}\beta_{i_k}^{i-1}\exp\left(\alpha_{i_k,k}^I\right)}{(i-1)!} \sum_{g=0}^{m_{i_k,k}^I-1}\binom{m_{i_k,k}^I-1}{g}\frac{(-1)^g m_{\mathsf{s},k}^{m_{\mathsf{s},k}}}{\Omega_{\mathsf{s},k}^{m_{\mathsf{s},k}}\Gamma(m_{\mathsf{s},k})}$$
$$\times\left(\frac{(m_{\mathsf{s},k}-1)!}{\left(\frac{m_{\mathsf{s},k}}{\Omega_{\mathsf{s},k}}\right)^{m_{\mathsf{s},k}}}\frac{\Gamma\left(g+1,\alpha_{i_k,k}^I\right)}{\left(\alpha_{i_k,k}^I\right)^{g+1}} - \sum_{j=0}^{m_{\mathsf{s},k}-1}\frac{(m_{\mathsf{s},k}-1)!u^j}{j!\left(\frac{m_{\mathsf{s},k}}{\Omega_{\mathsf{s},k}}\right)^{m_{\mathsf{s},k}-j}}\frac{\Gamma\left(g+j+1,\frac{m_{\mathsf{s},k}}{\Omega_{\mathsf{s},k}}u+\alpha_{i_k,k}^I\right)}{\left(\frac{m_{\mathsf{s},k}}{\Omega_{\mathsf{s},k}}u+\alpha_{i_k,k}^I\right)^{g+j+1}}\right). \tag{4.5}$$

Proof. See Appendix C.2. ∎

Having the terms $\mathrm{P_r}\left[\gamma_{\mathsf{d}} < u | C_L\right]$ and $\mathrm{P_r}\left[C_L\right]$ being evaluated, a closed-form expression for the outage probability in (3.7) can be obtained.

4.4.2 Identical Interferers

This section considers the case where the interferers have identical powers, i.e. $\left(m_{i_k,k}^I = \cdots = m_k^I,\ \alpha_{i_k,k}^I = \cdots = \alpha_k^I\right)$, $\left(m_{i_d,\mathsf{d}}^I = \cdots = m_{\mathsf{d}}^I,\ \alpha_{i_d,\mathsf{d}}^I = \cdots = \alpha_{\mathsf{d}}^I\right)$. Now, the denominator of γ_{d} becomes $Z_2 = \sum_{i_d=1}^{I_d}\rho_I|h_{i_d,\mathsf{d}}^I|^2 + 1 = X_2 + 1$, where X_2 is a summation of gamma distributed RVs with the same parameter and the same average power with a PDF given by $f_{X_2}(x) = \frac{(\alpha_{\mathsf{d}}^I)^{I_d m_{\mathsf{d}}^I}}{\Gamma\left(I_d m_{\mathsf{d}}^I\right)}\ x^{I_d m_{\mathsf{d}}^I - 1}\exp\left(-\alpha_{\mathsf{d}}^I x\right)$. Using

the transformation of RVs, we get

$$f_{Z_2}(z) = \frac{(\alpha_{\mathsf{d}}^I)^{I_d m_{\mathsf{d}}^I}}{\Gamma\left(I_d m_{\mathsf{d}}^I\right)} \left(z-1\right)^{I_d m_{\mathsf{d}}^I - 1} \exp\left(-\alpha_{\mathsf{d}}^I (z-1)\right). \tag{4.6}$$

Now, using the Binomial formula, we get

$$f_{Z_2}(z) = - \frac{(\alpha_{\mathsf{d}}^I)^{I_d m_{\mathsf{d}}^I} (-1)^{I_d m_{\mathsf{d}}^I} \exp\left(\alpha_{\mathsf{d}}^I\right)}{\Gamma\left(I_d m_{\mathsf{d}}^I\right)} \sum_{g=0}^{I_d m_{\mathsf{d}}^I - 1} \binom{I_d m_{\mathsf{d}}^I - 1}{g} (-1)^g z^g \exp\left(-\alpha_{\mathsf{d}}^I z\right). \tag{4.7}$$

Following the same procedure as in Appendix C.1, the term $\mathrm{P_r}\left[\gamma_{\mathsf{d}} < u | C_L\right]$ in (3.7) can be obtained as

$$\begin{aligned}
\mathrm{P_r}\left[\gamma_{\mathsf{d}} < u | C_L\right]_{\mathrm{I}} = & - \sum_{i_d=1}^{I_d} (-1)^{m_{i_d,\mathsf{d}}^I} \exp\left(\alpha_{i_d,\mathsf{d}}^I\right) \sum_{i=1}^{m_{i_d,\mathsf{d}}^I} \frac{\beta_{i_d}^{i-1}}{(i-1)!} \sum_{g=0}^{m_{i_d,\mathsf{d}}^I - 1} \binom{m_{i_d,\mathsf{d}}^I - 1}{g} (-1)^g \sum_{l=1}^{L} C_b(l) \\
& \times \Bigg[\frac{(m_{l,\mathsf{d}}-1)! C_4(i_d, g)}{\left(\frac{m_{l,\mathsf{d}}}{\Omega_{l,\mathsf{d}}}\right)^{m_{l,\mathsf{d}}}} - \sum_{k_1=0}^{m_{l,\mathsf{d}}-1} \frac{(m_{l,\mathsf{d}}-1)! \Lambda_2(i_d, l, u)^{-g-k_1-1} u^{k_1}}{k_1! \left(\frac{m_{l,\mathsf{d}}}{\Omega_{l,\mathsf{d}}}\right)^{m_{l,\mathsf{d}}-k_1}} \Gamma\left(g+k_1+1, \Lambda_2(i_d, l, u)\right) \\
& + \sum_{n=1}^{L} (-1)^n \sum_{j_1 < \cdots < j_n, j_{(.)} \neq l} \sum_{q_1 = \cdots = q_n = 0} \frac{\prod_{w=1}^{n} \left(\frac{m_{j_w,\mathsf{d}}}{\Omega_{j_w,\mathsf{d}}}\right)^{q_w}}{\prod_{p=1}^{n} q_p!} \Bigg\{ \frac{(C_6(r,l,q_i)-r)! C_4(i_d, g)}{\left(C_9(l, j_s)\right)^{\sum_{i=1}^{n} q_i + m_{l,\mathsf{d}}}} \\
& - \sum_{k_2=0}^{C_6(r,l,q_i)-r} \frac{(C_6(r,l,q_i)-r)! \Lambda_3(i_d, l, j_s, u)^{-g-k_2-1} u^{k_2}}{k_2! \left(C_9(l, j_s)\right)^{\sum_{i=1}^{n} q_i + m_{l,\mathsf{d}} - k_2}} \Gamma\left(g+k_2+1, \Lambda_3(i_d, l, j_s, u)\right) \Bigg\} \Bigg],
\end{aligned} \tag{4.8}$$

where $C_b(l), C_4(i_d, g), \Lambda_2(i_d, l, u), C_6(r, l, q_i), C_9(l, j_s)$, and $\Lambda_3(i_d, l, j_s, u)$ are as defined before.

In evaluating the term $\mathrm{P_r}\left[C_L\right]$ for the this case, the SINR $\gamma_{\mathsf{s},k}$ can be written as

$\gamma_{\mathsf{s},k} = Y_1/Z_3$, where Y_1 is similar to $f_{\rho|h_{l,\mathsf{d}}|^2}(\tau)$ in Appendix C.1 with replacing l by s and d by k and Z_3 with a PDF similar to that derived in (4.7) with replacing d by k. Now, following the same procedure as in Appendix C.2, the CDF $\mathrm{P_r}\left[\gamma_{\mathsf{s},k} < u\right]$ can be obtained as

$$\mathrm{P_r}\left[\gamma_{\mathsf{s},k} < u\right]_{\mathrm{I}} = -\frac{(\alpha_k^I)^{I_k m_k^I}(-1)^{I_k m_k^I}\exp\left(\alpha_k^I\right)}{\Gamma\left(I_k m_k^I\right)} \sum_{g=0}^{I_k m_k^I - 1} \binom{I_k m_k^I - 1}{g} \frac{(-1)^g m_{\mathsf{s},k}^{m_{\mathsf{s},k}}}{\Omega_{\mathsf{s},k}^{m_{\mathsf{s},k}}\Gamma(m_{\mathsf{s},k})}$$
$$\times \left(\frac{(m_{\mathsf{s},k}-1)!}{\left(\frac{m_{\mathsf{s},k}}{\Omega_{\mathsf{s},k}}\right)^{m_{\mathsf{s},k}}} \frac{\Gamma\left(g+1,\alpha_k^I\right)}{\left(\alpha_k^I\right)^{g+1}} - \sum_{j=0}^{m_{\mathsf{s},k}-1} \frac{(m_{\mathsf{s},k}-1)! u^j}{j!\left(\frac{m_{\mathsf{s},k}}{\Omega_{\mathsf{s},k}}\right)^{m_{\mathsf{s},k}-j}} \frac{\Gamma\left(g+j+1,\frac{m_{\mathsf{s},k}}{\Omega_{\mathsf{s},k}}u+\alpha_k^I\right)}{\left(\frac{m_{\mathsf{s},k}}{\Omega_{\mathsf{s},k}}u+\alpha_k^I\right)^{g+j+1}} \right). \tag{4.9}$$

Having $\mathrm{P_r}\left[\gamma_{\mathsf{d}} < u|C_L\right]$ and $\mathrm{P_r}\left[C_L\right]$ being evaluated, the outage probability in (3.7) can be obtained.

4.5 Asymptotic Analysis

Since the achieved results are too complex to give any insight about the key performance measures. It is of great interest to look into the high SNR regime, where simple expressions can be obtained. Note, at high SNR values, the outage probability can be expressed as $P_{\mathsf{out}} \approx (G_{\mathsf{c}}\rho)^{-G_{\mathsf{d}}}$, where G_{d} is the achieved diversity order of the system and G_{c} is the coding gain. When $\rho \to \infty$ with finite values of ρ_I, I_k, and I_d, the outage probability is approximated as follows

$$P_{\mathsf{out}} \approx \begin{cases} \mathbb{L}_1 \frac{\left(\frac{m_{\mathsf{s},k}}{\alpha_k^I}\right)^{m_{\mathsf{s},k}}}{\Gamma(m_{\mathsf{s},k}+1)} \left(\frac{u}{\rho}\right)^{m_{\mathsf{s},k}}, & m_{\mathsf{s},k} < m_{l,\mathsf{d}}; \\ \mathbb{L}_2 \frac{\left(\frac{m_{\mathsf{s},k}}{\alpha_k^I}\right)\left(\frac{m_{l,\mathsf{d}}}{\alpha_k^I}\right)^{\sum_{l=1}^{L} m_{l,\mathsf{d}}}}{\Gamma(\sum_{l=1}^{L} m_{\mathsf{s},k}+1)\Gamma(m_{\mathsf{s},\mathsf{d}})} \left(\frac{u}{\rho}\right)^{\sum_{l=1}^{L} m_{l,\mathsf{d}}+m_{\mathsf{s},\mathsf{d}}}, & m_{\mathsf{s},k} > m_{l,\mathsf{d}}, \end{cases} \tag{4.10}$$

where $\mathbb{L}_1$ and $\mathbb{L}_2$ are constants given by $\mathbb{L}_1 = \frac{(-1)^{I_k m_k^I} \exp\left(\alpha_k^I\right)}{m_{\mathsf{s},k}\left(\alpha_k^I\right)^{-1}\Gamma\left(I_k m_k^I\right)} \sum_{g=0}^{I_k m_k^I - 1} \binom{I_k m_k^I - 1}{g}$ $\Gamma\left(m_{\mathsf{s},k}+g+1, \alpha_k^I\right)(-1)^g \left(\alpha_k^I\right)^{-g}$, $\mathbb{L}_2 = \frac{(-1)^{I_d m_{\mathsf{d}}^I} B\left(a_1, m_{\mathsf{s},\mathsf{d}}\right)\left(\alpha_{\mathsf{d}}^I\right)^{-I_d m_{\mathsf{d}}^I + 1} \exp\left(\alpha_{\mathsf{d}}^I\right)}{\Gamma\left(I_d m_{\mathsf{d}}^I\right)} \sum_{g=0}^{I_d m_{\mathsf{d}}^I - 1}$ $\binom{I_d m_{\mathsf{d}}^I - 1}{g}(-1)^g \left(\alpha_{\mathsf{d}}^I\right)^{-g} \Gamma\left(a_2, \alpha_{\mathsf{d}}^I\right)$, $B(\lambda, \mu)$ is the beta function defined as $B(\lambda, \mu) = \Gamma(\lambda)\Gamma(\mu)/\Gamma(\lambda+\mu)$ [42, Eq. (8.38)], $a_1 = \sum_{l=1}^{L} m_{l,\mathsf{d}} + 1$, and $a_2 = \sum_{l=1}^{L} m_{l,\mathsf{d}} + m_{\mathsf{s},\mathsf{d}} + g + 1$. We observe that the diversity order of the system is given by $\min(m_{\mathsf{s},k}, m_{l,\mathsf{d}})L + m_{\mathsf{s},\mathsf{d}}$, while the coding gain of the system is given by

$$G_{\mathsf{c}} = \begin{cases} \left(\mathbb{L}_1 \frac{\left(\frac{m_{\mathsf{s},k}}{\alpha_k^I}\right)^{m_{\mathsf{s},k}}}{\Gamma(m_{\mathsf{s},k}+1)}\right)^{-\frac{1}{m_{\mathsf{s},k}}}, & m_{\mathsf{s},k} < m_{l,\mathsf{d}}; \\ \left(\mathbb{L}_2 \frac{\left(m_{\mathsf{s},k}\right)\left(\frac{m_{l,\mathsf{d}}}{\alpha_k^I}\right)^{\sum_{l=1}^{L} m_{\mathsf{s},k}}}{\Gamma(\sum_{l=1}^{L} m_{l,\mathsf{d}}+1)\Gamma(m_{\mathsf{s},\mathsf{d}})}\right)^{-\frac{1}{\sum_{l=1}^{L} m_{l,\mathsf{d}}+m_{\mathsf{s},\mathsf{d}}}}, & m_{\mathsf{s},k} > m_{l,\mathsf{d}}. \end{cases} \tag{4.11}$$

We assume that the fading parameters over all links are equal, i.e., ($m_{\mathsf{s},r} = m_{l,k} = m_{\mathsf{s},\mathsf{d}} = m$). Therefore, it is clear that this system model achieves a full diversity order equal to $m(L+1)$, despite the presence of the interference. This is expected since the interferers' powers α_k^I and α_{d}^I are assumed to be finite while deriving the diversity order of the system. In addition, we can observe that the coding gain is affected by the interferers' powers. More importantly, our findings show that the diversity order is determined by the most severely faded link while

the coding gain is affected by the total interferers' powers.

In evaluating the asymptotic outage behavior, the gamma density and distribution functions can be respectively approximated by $f_{\rho|h_{l,\mathrm{d}}|^2}(\tau) \approx \left(\frac{m_{l,\mathrm{d}}}{\Omega_{l,\mathrm{d}}}\right)^{m_{l,\mathrm{d}}} \frac{\tau^{m_{l,\mathrm{d}}-1}}{\Gamma(m_{l,\mathrm{d}})}$, $F_{\rho|h_{l,\mathrm{d}}|^2}(\tau) \approx \left(\frac{m_{l,\mathrm{d}}}{\Omega_{l,\mathrm{d}}}\right)^{m_{l,\mathrm{d}}} \frac{\tau^{m_{l,\mathrm{d}}}}{\Gamma(m_{l,\mathrm{d}}+1)}$. Based on that, the PDF of the best relay can be written as $f_{\rho|h_{l,\mathrm{d}}|^2}(\tau) \approx \prod_{l=1}^{L} \left(\frac{m_{l,\mathrm{d}}}{\Omega_{l,\mathrm{d}}}\right)^{m_{l,\mathrm{d}}} \frac{\tau^{m_{l,\mathrm{d}}-1}}{\Gamma(m_{l,\mathrm{d}})}$. Following the same procedure as in Appendix C.1, the PDF $f_Y(y)$ can be obtained. Upon substituting $f_{Z_2}(z)$ given by (4.7) and $f_Y(y)$ in (B.7), the first term in (3.7) can be obtained. Following the same procedure as in Appendix C.2, the second term in (3.7) can be obtained. After some mathematical manipulations, we obtain the result in (4.10).

4.6 Numerical Results

In this section, we illustrate the validity of the derived analytical results. We also provide some numerical examples to demonstrate the effect of fading parameter and the interference on the system performance.

Figure 4.1 illustrates the system outage performance vs SNR for different number of relays K. It can be seen from this figure that the analytical results as well as the asymptotic curves perfectly fit with Monte-Carlo simulations. Moreover, the enhancement on system performance due to use of more relays is obvious in this figure. It is also clear that the system can still achieve full diversity gain in the presence of finite number of interferers with finite powers.

Figure 4.2 shows the system outage probability vs SNR for different values of I_d and I_k when they are equal. It is clear to see that as $I_d = I_k$ increases, hence the

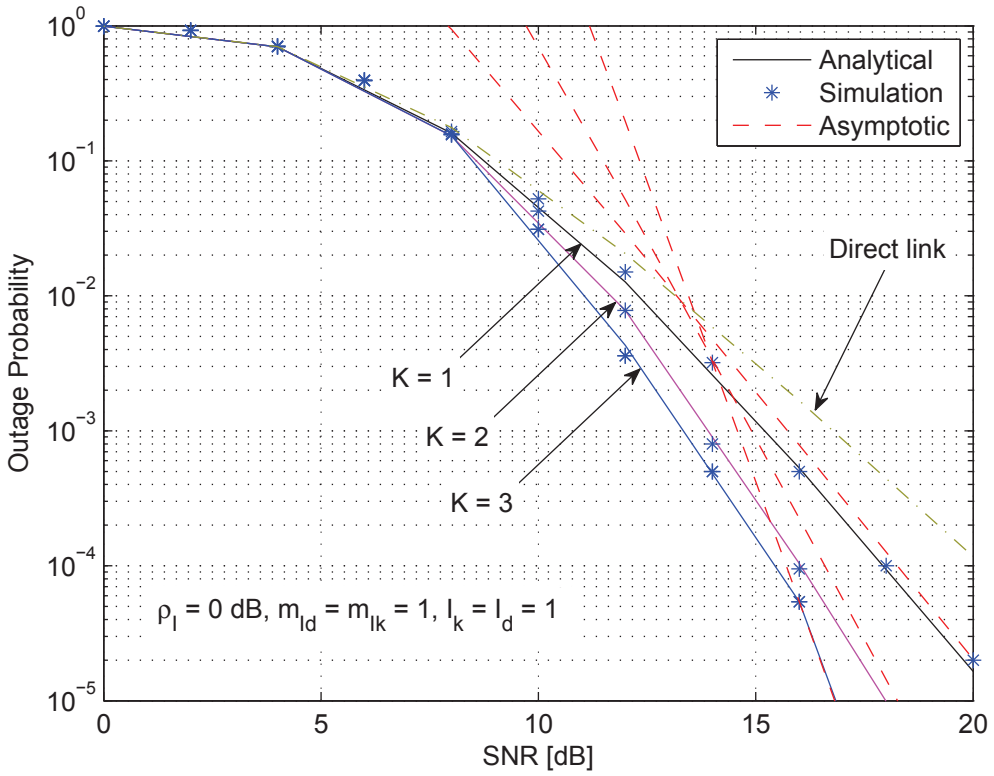

Figure 4.1: Outage probability vs average SNR for opportunistic DF relaying system with interference at the relays and destination for different values of K and $\gamma_{\text{out}} = 4.77$ dB, $m_{\text{s,d}} = 3$, $\sigma^2_{\text{s,d}} = 1$, $m_{\text{s},1} = m_{1,\text{d}} = 1$, $\sigma^2_{\text{s},1} = 0.2$, $\sigma^2_{1,\text{d}} = 0.4$, $m_{\text{s},2} = m_{2,\text{d}} = 2$, $\sigma^2_{\text{s},2} = 0.2$, $\sigma^2_{2,\text{d}} = 0.6$, $m_{\text{s},3} = m_{3,\text{d}} = 3$, $\sigma^2_{\text{s},3} = 0.2$, $\sigma^2_{3,\text{d}} = 0.8$, and $(\sigma^I_k)^2 = (\sigma^I_{\text{d}})^2 = 0.01$.

total interference power, the outage probability performance deteriorated further, as expected. Also, the improvement achieved in the system performance due to the direct link is obvious in this figure.

Figure 4.3 provides the system outage performance vs SNR for different values of I_d and I_k when they unequal. The figure provides a comparison between the interference effect at the relay node and that at the destination on the system behavior. As can be seen, the interference at the destination node affects the system performance more severely than the interference at the relay. This is

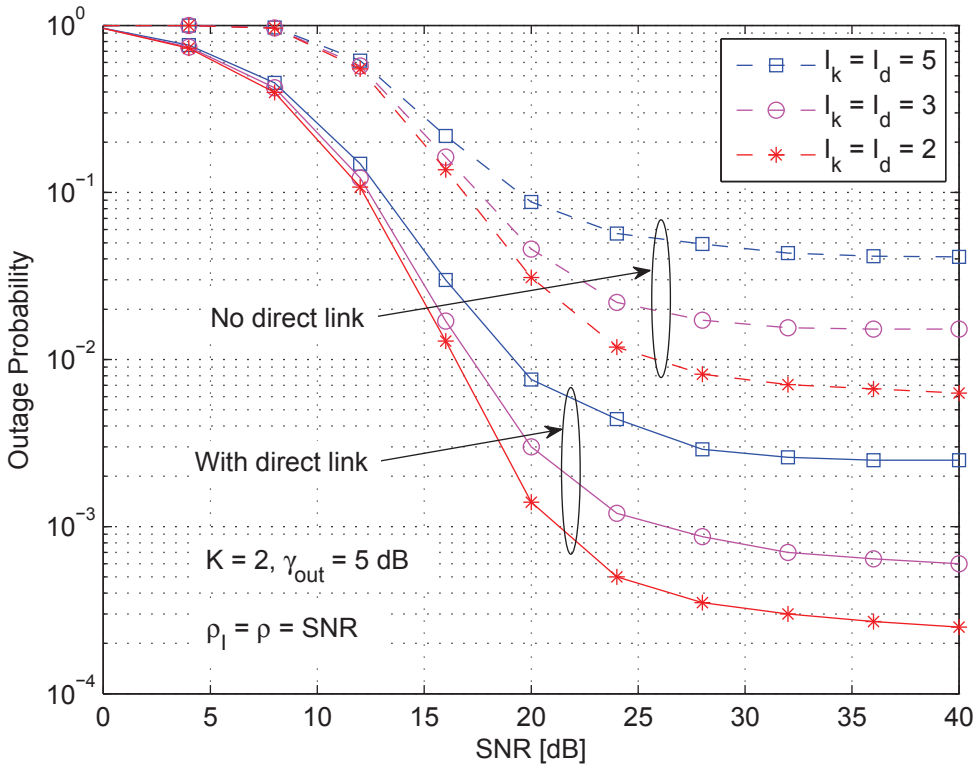

Figure 4.2: Outage probability vs average SNR for opportunistic DF relaying system with two relays for different values of I_d and I_k when they are equal and $m_{\mathrm{s,d}} = 1$, $\sigma^2_{\mathrm{s,d}} = 1$, $m_{\mathrm{s},k}$, $m_{k,\mathrm{d}} = k$, and $(\sigma^I_k)^2$ for $k = 1, 2$, $\sigma^2_{\mathrm{s},1} = \sigma^2_{\mathrm{s},2} = 0.2$, $\sigma^2_{1,\mathrm{d}} = 0.4$, $\sigma^2_{2,\mathrm{d}} = 0.6$, $m^I_1 = m^I_2 = 1$, $(\sigma^I_{\mathrm{d}})^2 = 0.01$, and $m^I_{\mathrm{d}} = 1$.

because, the impact of the interference at the relay node is reduced by the decoding process performed by the relay itself. Also, this is expected as the interference at the destination affects the signals at both the relay path and that on the direct link; whereas, the interference at the relay affects only the signal on the first hop only. Finally, a floor appears in these two figures due to the effect of interference on the system performance. This is expected since the transmit SNR of both the desired user ρ and the interferers ρ_I and thus their powers are assumed to be increasing. This explains why the diversity gain of this case reaches zero.

Figure 4.4 illustrates the system outage probability vs number of interferers

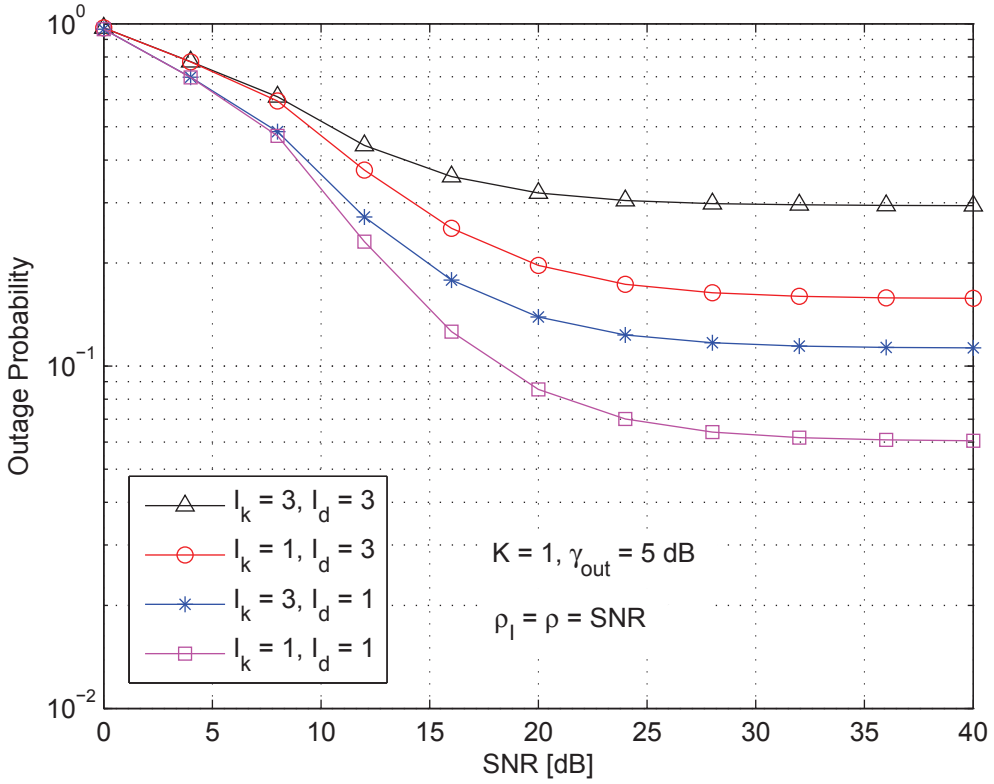

Figure 4.3: Outage probability vs average SNR for opportunistic DF relaying system with one relay for different values of I_d and I_k when they are unequal and $m_{\mathsf{s,d}} = 1$, $\sigma^2_{\mathsf{s,d}} = 1$, $m_{\mathsf{s},1} = 1$, $m_{1,\mathsf{d}} = 2$, $\sigma^2_{\mathsf{s},1} = 0.2$, $\sigma^2_{1,\mathsf{d}} = 0.4$, $m^I_1 = 1$, $(\sigma^I_1)^2 = (\sigma^I_{\mathsf{d}})^2 = 0.05$, and $m^I_{\mathsf{d}} = 1$.

I_k and I_d for different values of SNR. In this figure, the number of interferers at both the relays and the destination is assumed to be equal. It is clear that as the number of interferers increases, the system behavior becomes more degraded, as expected. Also, one can notice that as the SNR increases, better the performance can be achieved.

Fig. 4.5 shows the system outage performance vs outage threshold γ_{out} for different values of fading parameters m_1, m_2. In the figure, we use m_1 and m_2 to represent the fading parameters of the first hop and second hop of both relays, respectively. It can be seen from this figure that the worst behavior is achieved

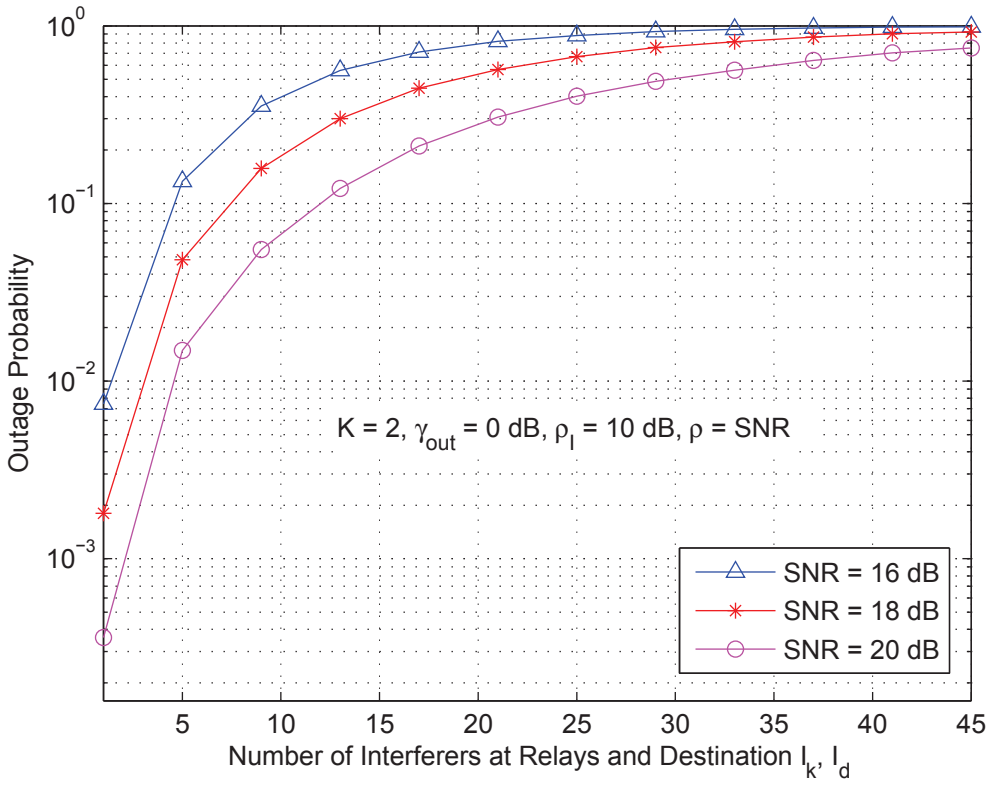

Figure 4.4: Outage probability vs number of interferers at relays and destination for opportunistic DF relaying system for different values of SNR and $m_{\mathsf{s},\mathsf{d}} = 1$, $\sigma^2_{\mathsf{s},\mathsf{d}} = 1$, $m_{\mathsf{s},k} = m_{k,\mathsf{d}} = k$, $m^I_k = 1$ and $(\sigma^I_k)^2 = 0.5$ for $k = 1, 2$, $\sigma^2_{\mathsf{s},1} = \sigma^2_{\mathsf{s},2} = 0.2$, $\sigma^2_{1,\mathsf{d}} = 0.4$, $\sigma^2_{2,\mathsf{d}} = 0.6$, $m^I_{\mathsf{d}} = 1$, and $(\sigma^I_{\mathsf{d}})^2 = 0.5$.

when the fading parameters of the two hops of both relays equal unity which is the Rayleigh case, as expected. Also, we can see that having m_1 larger than m_2 gives better performance compared to the case where m_2 is larger than m_1. This is because having m_1 being smaller may cause the relays unable to decode the source message which will affect the transmission on the second hop and thus the over all system behavior. Finally, the best behavior can be achieved by enhancing the channels of both hops at the same time, as expected.

Figure 4.6 illustrates the system outage probability vs number of relays K for different values of SNR. It is clear from this figure that the considered relay

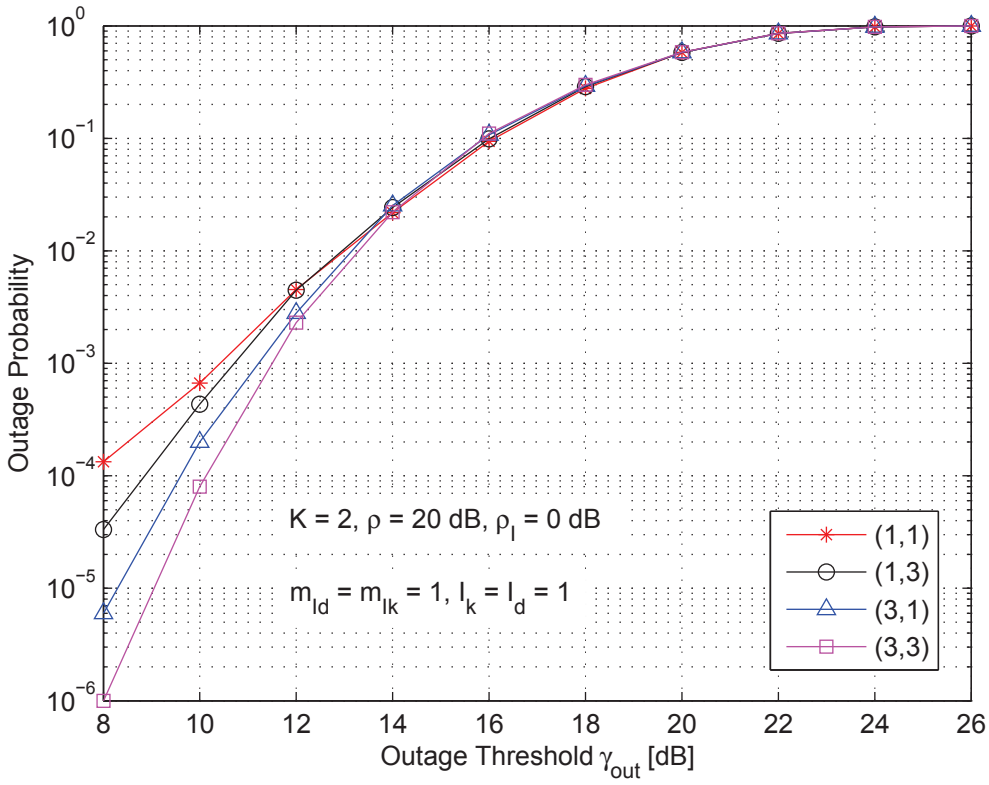

Figure 4.5: Outage probability vs outage threshold for opportunistic DF relaying system for different values of $(m_{\mathsf{s},k},\ m_{k,\mathsf{d}})$ and $m_{\mathsf{s},\mathsf{d}} = 3$, $\sigma^2_{\mathsf{s},\mathsf{d}} = 1$, $\sigma^2_{\mathsf{s},1} = 0.2$, $\sigma^2_{1,\mathsf{d}} = 0.4$, $\sigma^2_{\mathsf{s},2} = 0.2$, $\sigma^2_{2,\mathsf{d}} = 0.6$, and $(\sigma^I_k)^2 = (\sigma^I_{\mathsf{d}})^2 = 0.01$.

system still achieves performance gain and the outage probability decreases when the number of relays K increases, but the slope depends on the SNR values. Also, the achieved gain in system behavior due to the existence of direct link is clear in the figure.

Figure 4.7 shows the system outage performance vs SNR for different values of outage threshold γ_{out}. As can be seen from this figure, as γ_{out} increases, the worse the achieved behavior, as expected.

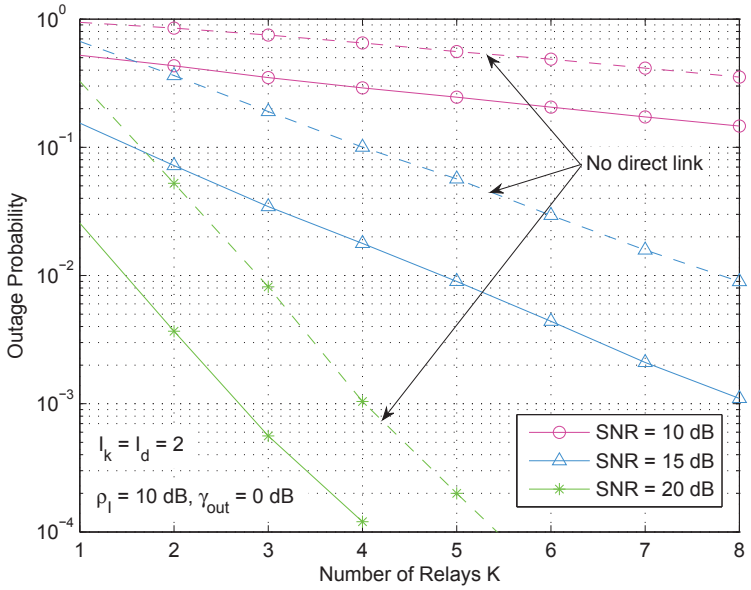

Figure 4.6: Outage probability vs number of relays for opportunistic DF relaying system for different values of SNR and $m_{\mathsf{s,d}} = 1$, $\sigma^2_{\mathsf{s,d}} = 1$, $\sigma^2_{\mathsf{s},1} = \ldots = \sigma^2_{\mathsf{s},8} = 0.2$, $m_{\mathsf{s},k} = m_{k,\mathsf{d}} = k$, $\sigma^2_{k,\mathsf{d}} = (k+2)/10$, $m^I_k = 1$, and $(\sigma^I_k)^2 = 0.5$ for $k = 1, \ldots, 8$, $m^I_{\mathsf{d}} = 1$, and $(\sigma^I_{\mathsf{d}})^2 = 0.5$.

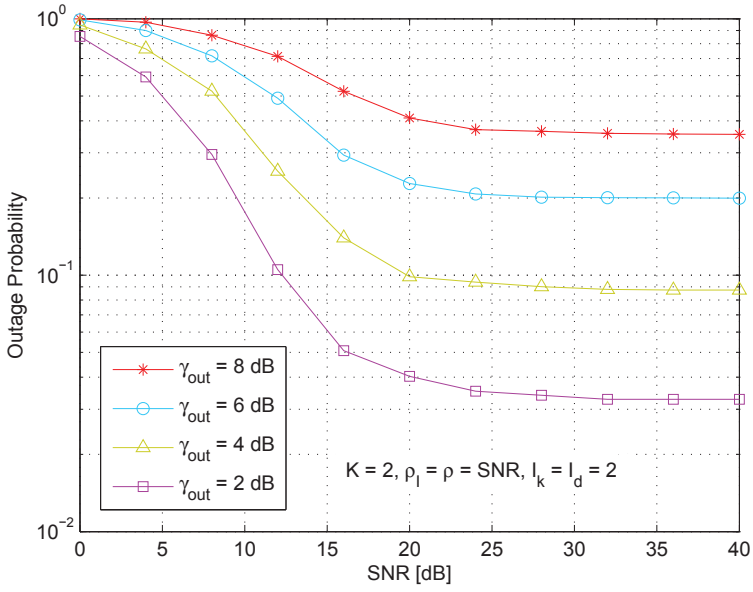

Figure 4.7: Outage probability vs average SNR for opportunistic DF relaying system for different values of γ_{out} and $m_{\mathsf{s,d}} = 1$, $\sigma^2_{\mathsf{s,d}} = 1$, $m_{\mathsf{s},k} = m_{k,\mathsf{d}} = k$, and $(\sigma^I_k)^2 = 0.1$ for $k = 1, 2$, $\sigma^2_{\mathsf{s},1} = \sigma^2_{\mathsf{s},2} = 0.2$, $\sigma^2_{1,\mathsf{d}} = 0.4$, $\sigma^2_{2,\mathsf{d}} = 0.6$, $m^I_1 = m^I_2 = 2$, $(\sigma^I_{\mathsf{d}})^2 = 0.1$, and $m^I_{\mathsf{d}} = 1$.

4.7 Conclusions

In this chapter, we evaluated the outage performance of a dual-hop opportunistic DF relay system in the presence of interference at the relays and destination. We derived exact closed-form expressions for the outage probability with the desired user channels and the interferers' channels being Nakagami-m distributed. Furthermore, the outage performance of the proposed system is studied at high SNR regime via deriving the asymptotic outage probability. The achieved results were validated via Monte-Carlo simulations which showed an accurate fitting with the analytical and asymptotic results. Also, findings revealed that for the case where the interference power does not scale with SNR, the presence of interference does not reduce the diversity order of the system, however it affects the system performance through the coding gain. On the other hand, having the interference power scales with SNR results in a noise floor in the outage performance and hence a zero diversity gain. Finally, the results illustrated that having the fading parameter of the first hop better than that of the second hop, gives better performance compared to the case of vise versa.

CHAPTER 5

OPPORTUNISTIC DF RELAYING USING N^{th}-BEST RELAY

5.1 Introduction

In chapter 4, the opportunistic relaying was used in DF relay systems with interference at the relays and destination. Again, this relaying scheme gives the optimum performance in the sense that it selects the best relay among all relays each time of transmission. Sometimes, the source or the destination makes an error in selecting the best relay and instead the second or even the N^{th} best relay is selected. In addition, there are some situations as in ad-hoc networks where the best relay could be busy in load balancing and scheduling duties. In such cases, the decision could be made to select the second or even the N^{th} best relay

to forward the source message to destination.

In this chapter, we investigate the outage behavior of a dual-hop N^{th}-best DF relay system in which the relay and the destination undergo independent sources of CCI. The fading envelopes associated with the desired and interfering users are assumed to follow i.n.d. Rayleigh fading models. Through the analysis, exact and approximate expressions for the outage probability are derived based on which the diversity order and coding gain are obtained. Our findings suggest that the diversity order linearly increases with the number of relays and decreases with the order of the relay. Furthermore, results reveal that the system is still able to achieve full diversity gain in the presence of finite number of interferers with finite powers. The analytical results are supported and validated by Monte-Carlo simulations.

The rest of this chapter is organized as follows. In Section 5.2, we provide a literature review on the analyzed system. Section 5.3 explains the system model. The exact performance analysis is conducted in Section 5.4. Section 5.5 presents the asymptotic analysis. Some numerical results are discussed in Section 5.6. Finally, some conclusions are provided in Section 5.7.

5.2 Literature Review

As mentioned in Section 2.2, an efficient relay selection scheme used in relay networks is the N^{th}-best relaying. This scheme is efficient is situations where the best relay may not be available due to some scheduling or load balancing

conditions. In this case, the decision may be made to use the second best relay or more generally the N^{th} best relay to cooperate. The performance of dual-hop AF and DF relay systems with such efficient relaying scheme was studied in [12] assuming Rayleigh fading channels.

In this chapter, we evaluate the outage performance of a dual-hop DF relay system with interference at the relays and destination with the N^{th}-best relay selection scheme being used. In the analysis, we derive an exact closed-form expression for the system outage probability for the generic i.n.d. case of interferers' channels assuming Rayleigh fading channels. We also evaluate the system performance at high SNR regime where an asymptotic expression for the outage probability is derived and analyzed in addition to deriving the diversity order and the coding gain. Due to its inherent effect on system behavior, the direct link is considered in all derivations in this chapter.

5.3 System Model

The system under consideration is as shown in Figure 3.1 with the N^{th} best relay among all active relays forwarding the source message to destination. All the channel gains are assumed to follow Rayleigh distribution. That is, the channel powers are exponential distributed RVs as explained in Section 3.3.

The decoding set C_L of active relays that could have correctly decoded the message sent from the source in the first phase is as defined by (3.3). In the second phase and after decoding the received signal, only the N^{th} best relay in C_L

forwards the re-encoded signal to the destination. The N^{th} best relay is the relay with the N^{th} maximum $\gamma_{l,\mathsf{d}}$, where $\gamma_{l,\mathsf{d}}$ is the SINR at the destination resulting from the l^{th} relay being the relay which forwarded the source information as given by (3.4). Since the denominator is common to the SINRs from all relays belonging to C_L, the N^{th} best relay is the relay with the N^{th} maximum $\left\{\frac{P_l}{N_0}|h_{l,\mathsf{d}}|^2\right\}$.

In the analysis of the considered system, the destination is assumed to be located at the same point during the two phases. This means the same interference is affecting the destination node in both phases. As the MRC is being used at the destination, the signals on the direct link and the N^{th} best relay are added. The e2e SINR at the destination output can be written as

$$\gamma_{\mathsf{d}} \triangleq \gamma_{\mathsf{s},\mathsf{d}} + \gamma_{N_b^{\text{th}},\mathsf{d}} = \frac{\frac{P_0}{N_0}|h_{\mathsf{s},\mathsf{d}}|^2 + \frac{P_{N_b^{\text{th}}}}{N_0}|h_{N_b^{\text{th}},\mathsf{d}}|^2}{\sum_{i_d=1}^{I_d}\frac{P^I_{i_d,\mathsf{d}}}{N_0}\left|h^I_{i_d,\mathsf{d}}\right|^2 + 1}. \tag{5.1}$$

5.4 Performance Analysis

In this section, we derive a closed-from expression for the system outage probability. The distribution of the decoding set defined by (3.3) is as given by (3.6) and the outage probability for the considered system can be achieved by averaging over all possible decoding sets as as given by (3.7). In order to evaluate (3.7), we first need to derive $\mathrm{P_r}\left[\gamma_{\mathsf{d}} < u|C_L\right]$ and then $\mathrm{P_r}\left[C_L\right]$ need to be obtained first. The results on the outage probability for the cases of non-identical and identical second hops are summarized in the following Theorem and Lemma, respectively.

Theorem 5.1 *The outage probability of the N^{th}-best DF relay systems for i.n.d.*

second hops $\{\lambda_{i,\mathsf{d}}\}_{i=1}^{L}$ *and non-identical interferers* $\{\lambda_{i_n,n}^{I}\}_{i_n=1}^{I_n}$ *can be obtained in a closed-form expression by using* (3.7)*, after evaluating the term* $\mathrm{P_r}\left[\gamma_{\mathsf{d}} < u|C_L\right]$ *and the CDF* $\mathrm{P_r}\left[\gamma_{\mathsf{s},k} < u\right]$ *which is a part of the term* $\mathrm{P_r}\left[C_L\right]$ *as follows*

$$\mathrm{P_r}\left[\gamma_{\mathsf{d}} < u|C_L\right] = \prod_{i_d=1}^{I_d} \lambda_{i_d,\mathsf{d}}^{I} \exp\left(\lambda_{i_d,\mathsf{d}}^{I}\right) \sum_{g=1}^{I_d} \frac{\sum_{l=1}^{L} \lambda_{l,\mathsf{d}} \lambda_{\mathsf{s},\mathsf{d}}}{\prod_{\substack{m=1 \\ m\neq g}}^{I_d} \left(\lambda_{m,\mathsf{d}}^{I} - \lambda_{g,\mathsf{d}}^{I}\right)} \times \sum_{\mathcal{P}} \left[\frac{\left(\frac{\Xi_1}{\lambda_{\mathsf{s},\mathsf{d}}} - \frac{\Xi_2}{C_a}\right)}{C_a - \lambda_{\mathsf{s},\mathsf{d}}} + \sum_{q=1}^{L-N} (-1)^q \sum_{s_1<\ldots<s_q} \frac{\left(\frac{\Xi_1}{\lambda_{\mathsf{s},\mathsf{d}}} - \frac{\Xi_2}{C_c}\right)}{C_c - \lambda_{\mathsf{s},\mathsf{d}}} \right], \quad (5.2)$$

where $C_c = \sum_{w=L-N+1}^{L-1} \lambda_{i_w,\mathsf{d}} + \sum_{n=1}^{q} \lambda_{s_n,\mathsf{d}} + \lambda_{l,\mathsf{d}}$, $\Xi_1 = \Gamma(1, \lambda_{i_d,\mathsf{d}}^{I})/\lambda_{i_d,\mathsf{d}}^{I} - \Gamma(1, \lambda_{i_d,\mathsf{d}}^{I} + \lambda_{\mathsf{s},\mathsf{d}} u)/(\lambda_{i_d,\mathsf{d}}^{I} + \lambda_{\mathsf{s},\mathsf{d}} u)$, $\Xi_2 = \Gamma(1, \lambda_{i_d,\mathsf{d}}^{I})/\lambda_{i_d,\mathsf{d}}^{I} - \Gamma(1, \lambda_{i_d,\mathsf{d}}^{I} + C_a u)/(\lambda_{i_d,\mathsf{d}}^{I} + C_a u)$.

$$\mathrm{P_r}\left[\gamma_{\mathsf{s},k} < u\right] = \prod_{i_k=1}^{I_k} \lambda_{i_k,k}^{I} \exp\left(\lambda_{i_k,k}^{I}\right) \sum_{g=1}^{I_k} \frac{\Xi_3}{\prod_{\substack{m=1 \\ m\neq g}}^{I_k} \left(\lambda_{m,k}^{I} - \lambda_{g,k}^{I}\right)}, \quad (5.3)$$

where $\Xi_3 = \Gamma(1, \lambda_{i_k,k}^{I})/\lambda_{i_k,k}^{I} - \Gamma(1, \lambda_{i_k,k}^{I} + \lambda_{\mathsf{s},k} u)/(\lambda_{i_k,k}^{I} + \lambda_{\mathsf{s},k} u)$*. This CDF is then used in (3.6) to evaluate the second term in (3.7)* $\mathrm{P_r}\left[C_L\right]$.

Proof. See Appendix C.3. ∎

For the case of identical interferers ($\lambda_{i_k,k}^{I} = \cdots = \lambda_{k}^{I}$), ($\lambda_{i_d,\mathsf{d}}^{I} = \cdots = \lambda_{\mathsf{d}}^{I}$), the results of the term $\mathrm{P_r}\left[\gamma_{\mathsf{d}} < u|C_L\right]$ and the CDF $\mathrm{P_r}\left[\gamma_{\mathsf{s},k} < u\right]$ which is a part of the term $\mathrm{P_r}\left[C_L\right]$ are given in the following Corollary.

Corollary 5.2 *The term* $\mathrm{P_r}\left[\gamma_{\mathsf{d}} < u | C_L\right]$ *for* $L \geq 1$ *is given by*

$$\mathrm{P_r}\left[\gamma_{\mathsf{d}} < u | C_L\right] = -\frac{(\lambda_{\mathsf{d}}^I)^{I_d}}{(I_d-1)!}\exp\left(\lambda_{\mathsf{d}}^I\right)(-1)^{I_d}\sum_{g=0}^{I_d-1}\binom{I_d-1}{g}(-1)^g\sum_{l=1}^{L}\lambda_{l,\mathsf{d}}\lambda_{\mathsf{s},\mathsf{d}} \times\sum_{\mathcal{P}}\left[\frac{\left(\frac{\Lambda_1}{\lambda_{\mathsf{s},\mathsf{d}}}-\frac{\Lambda_2}{C_a}\right)}{C_a-\lambda_{\mathsf{s},\mathsf{d}}}+\sum_{q=1}^{L-N}(-1)^q\sum_{s_1<\ldots<s_q}\frac{\left(\frac{\Lambda_1}{\lambda_{\mathsf{s},\mathsf{d}}}-\frac{\Lambda_3}{C_c}\right)}{C_c-\lambda_{\mathsf{s},\mathsf{d}}}\right], \quad (5.4)$$

where $\Lambda_1 = \Gamma(g+1,\lambda_{\mathsf{d}}^I)/(\lambda_{\mathsf{d}}^I)^{g+1} - \Gamma(g+1,\lambda_{\mathsf{d}}^I+\lambda_{\mathsf{s},\mathsf{d}}u)/(\lambda_{\mathsf{d}}^I+\lambda_{\mathsf{s},\mathsf{d}}u)^{g+1}$, $\Lambda_2 = \Gamma(g+1,\lambda_{\mathsf{d}}^I)/(\lambda_{\mathsf{d}}^I)^{g+1} - \Gamma(g+1,\lambda_{\mathsf{d}}^I+C_au)/(\lambda_{\mathsf{d}}^I+C_au)^{g+1}$, *and* $\Lambda_3 = \Gamma(g+1,\lambda_{\mathsf{d}}^I)/(\lambda_{\mathsf{d}}^I)^{g+1} - \Gamma(g+1,\lambda_{\mathsf{d}}^I+C_cu)/(\lambda_{\mathsf{d}}^I+C_cu)^{g+1}$.

The CDF $\mathrm{P_r}\left[\gamma_{\mathsf{s},k} < u\right]$ *which is a part of the term* $\mathrm{P_r}\left[C_L\right]$ *is given by*

$$\mathrm{P_r}\left[\gamma_{\mathsf{s},k} < u\right] = -\frac{(\lambda_k^I)^{I_k}}{(I_k-1)!}\exp\left(\lambda_k^I\right)(-1)^{I_k}\sum_{g=0}^{I_k-1}\binom{I_k-1}{g}(-1)^g\Lambda_3, \quad (5.5)$$

where $\Lambda_4 = \Gamma(g+1,\lambda_k^I)/(\lambda_k^I)^{g+1} - \Gamma(g+1,\lambda_k^I+\lambda_{\mathsf{s},k}u)/(\lambda_k^I+\lambda_{\mathsf{s},k}u)^{g+1}$.

In evaluating the term $\mathrm{P_r}\left[\gamma_{\mathsf{d}} < u | C_L\right]$, the PDF of X_2 in Appendix C.3 is now given by $f_{X_2}(x) = \frac{(\lambda_{\mathsf{d}}^I)^{I_d}}{(I_d-1)!}x^{I_d-1}\exp\left(-\lambda_{\mathsf{d}}^I x\right)$. Following the same procedure as in Appendix C.3, we obtain the results in (5.4) and (5.5).

Lemma 5.1 *The outage probability of the* N^{th}*-best DF relay systems for i.i.d. second hops* ($\lambda_{1,\mathsf{d}} = \lambda_{2,\mathsf{d}} = \ldots = \lambda_{K,\mathsf{d}} = \lambda_{R,\mathsf{d}}$) *and non-identical interferers* $\{\lambda_{i_n,n}^I\}_{i_n=1}^{I_n}$ *can be obtained in a closed-form expression by using* (3.7)*, after evaluating the term* $\mathrm{P_r}\left[\gamma_{\mathsf{d}} < u | C_L\right]$ *and the CDF* $\mathrm{P_r}\left[\gamma_{\mathsf{s},k} < u\right]$ *which is a part of the*

term $\mathrm{P_r}\left[C_L\right]$ *as follows*

$$\mathrm{P_r}\left[\gamma_{\mathsf{d}} < u|C_L\right] = L\binom{L-1}{N-1}\lambda_{\mathsf{s,d}}\lambda_{R,\mathsf{d}}\prod_{i_d=1}^{I_d}\lambda^I_{i_d,\mathsf{d}}\exp\left(\lambda^I_{i_d,\mathsf{d}}\right)\sum_{g=1}^{I_d}\frac{1}{\prod_{\substack{m=1\\m\neq g}}^{I_d}\left(\lambda^I_{m,\mathsf{d}}-\lambda^I_{g,\mathsf{d}}\right)}$$
$$\times\sum_{k=0}^{L-N}\binom{L-N}{k}(-1)^k\left[\frac{\left(\frac{\Xi_1}{\lambda_{\mathsf{s,d}}}-\frac{\Xi_4}{C_d}\right)}{C_d-\lambda_{\mathsf{s,d}}}\right], \tag{5.6}$$

where $C_d = (k+N)\lambda_{R,\mathsf{d}}$ *and* $\Xi_4 = \Gamma(1,\lambda^I_{i_d,\mathsf{d}})/\lambda^I_{i_d,\mathsf{d}} - \Gamma(1,\lambda^I_{i_d,\mathsf{d}}+C_du)/(\lambda^I_{i_d,\mathsf{d}}+C_du)$.

The CDF $\mathrm{P_r}\left[\gamma_{\mathsf{s},k} < u\right]$ *is as derived in Theorem 5.1 and hence, the same* $\mathrm{P_r}\left[C_L\right]$.

Proof. In evaluating the term $\mathrm{P_r}\left[\gamma_{\mathsf{d}} < u|C_L\right]$, the PDF of the N^{th} best relay can be written as

$$f_{\rho|h_{N_b^{\text{th}},\mathsf{d}}|^2}(\tau) = \binom{L-1}{N-1}Lf_{\rho|h_{R,\mathsf{d}}|^2}(\tau)\left(F_{\rho|h_{R,\mathsf{d}}|^2}(\tau)\right)^{L-N}\left(1-F_{\rho|h_{R,\mathsf{d}}|^2}(\tau)\right)^{N-1}. \tag{5.7}$$

Using the PDF in (5.7) and following the same procedure as in Appendix C.3, we obtain the result in (5.6). ∎

For the case of identical interferers ($\lambda^I_{i_k,k} = \cdots = \lambda^I_k$), ($\lambda^I_{i_d,\mathsf{d}} = \cdots = \lambda^I_{\mathsf{d}}$), the results of the term $\mathrm{P_r}\left[\gamma_{\mathsf{d}} < u|C_L\right]$ and the CDF $\mathrm{P_r}\left[\gamma_{\mathsf{s},k} < u\right]$ which is a part of the term $\mathrm{P_r}\left[C_L\right]$ are given in the following Corollary.

Corollary 5.3 *The term* $\mathrm{P_r}\left[\gamma_{\mathsf{d}} < u | C_L\right]$ *for* $L \geq 1$ *is given by*

$$\mathrm{P_r}\left[\gamma_{\mathsf{d}} < u | C_L\right] = -L\binom{L-1}{N-1}\lambda_{\mathsf{s,d}}\lambda_{R,\mathsf{d}}\frac{(\lambda_{\mathsf{d}}^I)^{I_{\mathsf{d}}}}{(I_d-1)!}\exp\left(\lambda_{\mathsf{d}}^I\right)(-1)^{I_d}\sum_{g=0}^{I_d-1}\binom{I_d-1}{g}$$
$$\times(-1)^g\sum_{k=0}^{L-N}\binom{L-N}{k}(-1)^k\left[\frac{\left(\frac{\Lambda_1}{\lambda_{\mathsf{s,d}}}-\frac{\Lambda_5}{C_d}\right)}{C_d-\lambda_{\mathsf{s,d}}}\right], \tag{5.8}$$

where $\Lambda_5 = \Gamma(g+1,\lambda_{\mathsf{d}}^I)/(\lambda_{\mathsf{d}}^I)^{g+1} - \Gamma(g+1,\lambda_{\mathsf{d}}^I + C_d u)/(\lambda_{\mathsf{d}}^I + C_d u)^{g+1}$.

The CDF $\mathrm{P_r}\left[\gamma_{\mathsf{s},k} < u\right]$ *is as derived in Corollary 5.2 and hence, the same* $\mathrm{P_r}\left[C_L\right]$.

In evaluating the term $\mathrm{P_r}\left[\gamma_{\mathsf{d}} < u | C_L\right]$, the PDF of X_2 in Appendix C.3 is as given in Corollary 5.2 and with the PDF in (5.7) and following the same procedure as in Appendix C.3, we obtain the result in (5.8).

5.5 Asymptotic Analysis

In this section, we evaluate the system performance at high SNR values in which the outage probability can be expressed as $P_{\mathsf{out}} \approx (G_{\mathsf{c}}\rho)^{-G_{\mathsf{d}}}$, where G_{d} is referred to as the achieved diversity order of the system while G_{c} is referred to as the coding gain of the system.

Theorem 5.4 *At high SNR regime and with finite number of interferers of finite powers, the outage probability of the* N^{th}*-best DF relay systems with interference*

under Rayleigh fading channels can be approximated as

$$P_{\mathsf{out}} \approx -L\binom{L-1}{N-1}\frac{\Gamma\left(L-N+3,\lambda_{\mathsf{d}}^{I}\right)\left(\lambda_{\mathsf{d}}^{I}\right)^{-(L-N-I_d+3)}(-1)^{I_d}}{(L-N+1)(L-N+2)\left(I_d-1\right)!}\exp\left(\lambda_{\mathsf{d}}^{I}\right)$$
$$\times\left(1+\frac{L}{\lambda_{\mathsf{d}}^{I}}\right)\rho^{-(L-N+2)}(\gamma_{\mathsf{out}})^{L-N+3}. \tag{5.9}$$

Proof. See Appendix C.4. ∎

Based on (5.9), the diversity order G_{d} and coding gain G_{c} can be characterized as follows.

Corollary 5.5 *The diversity order of the system is given by* $G_{\mathsf{d}} = L - N + 2$*; while the coding gain is given by*

$$G_{\mathsf{c}} = \Bigg\{ -L\binom{L-1}{N-1}\frac{\Gamma\left(L-N+3,\lambda_{\mathsf{d}}^{I}\right)\left(\lambda_{\mathsf{d}}^{I}\right)^{-(L-N-I_d+3)}(-1)^{I_d}}{(L-N+1)(L-N+2)\left(I_d-1\right)!}\exp\left(\lambda_{\mathsf{d}}^{I}\right)$$
$$\times\left(1+\frac{L}{\lambda_{\mathsf{d}}^{I}}\right)(\gamma_{\mathsf{out}})^{L-N+3}\Bigg\}^{L-N+2}. \tag{5.10}$$

Note that increasing the number of relays provides extra diversity order. Also, it helps to reduce the outage probability via improving the coding gain achieved by the system.

5.6 Numerical Results

In this section, we illustrate the validity of the achieved analytical expressions via a comparison with Monte-Carlo simulations. We also provide some numerical examples to show the effect of the interference and some system parameters like

number of relays and the outage threshold on the system performance.

Figure 5.1 portrays the outage probability vs SNR for different values of N. This figure validates the achieved analytical results via a comparison with Monte-Carlo simulations and the asymptotic curves. It can be seen that the analytical expressions as well as the asymptotic curves perfectly fit with the simulation ones. We can also notice that the outage probability increases as N increases. Furthermore, it is obvious from this figure that the diversity order linearly increases with the number of active relays L although one relay is being used only. Also, it is clear that the diversity order linearly decreases as we move from the best relay ($N = 1$) to the second best relay and generally the N^{th} best relay case. This figure also shows that for the case when the interference power does not scale with SNR, the system can still achieve full diversity gain.

Figure 5.2 shows the outage probability vs SNR for different number of interferers I_d and I_k when they are equal. It is obvious from this figure that when $I_{\mathtt{d}}$ and I_k increase and hence, the total interference power, the outage performance deteriorated further, as expected. In addition, as the number of interferers decreases, the amount of achievement in system performance increases. Furthermore, the gain achieved in system performance in the case where $K = 3$ compared to the case where $K = 2$ is obvious in this figure. Finally, as the interference power is assumed to scale with SNR in this figure, the system diversity gain reaches zero and due to the effect of interference on the system performance, a noise floor appears in all cases in the figure.

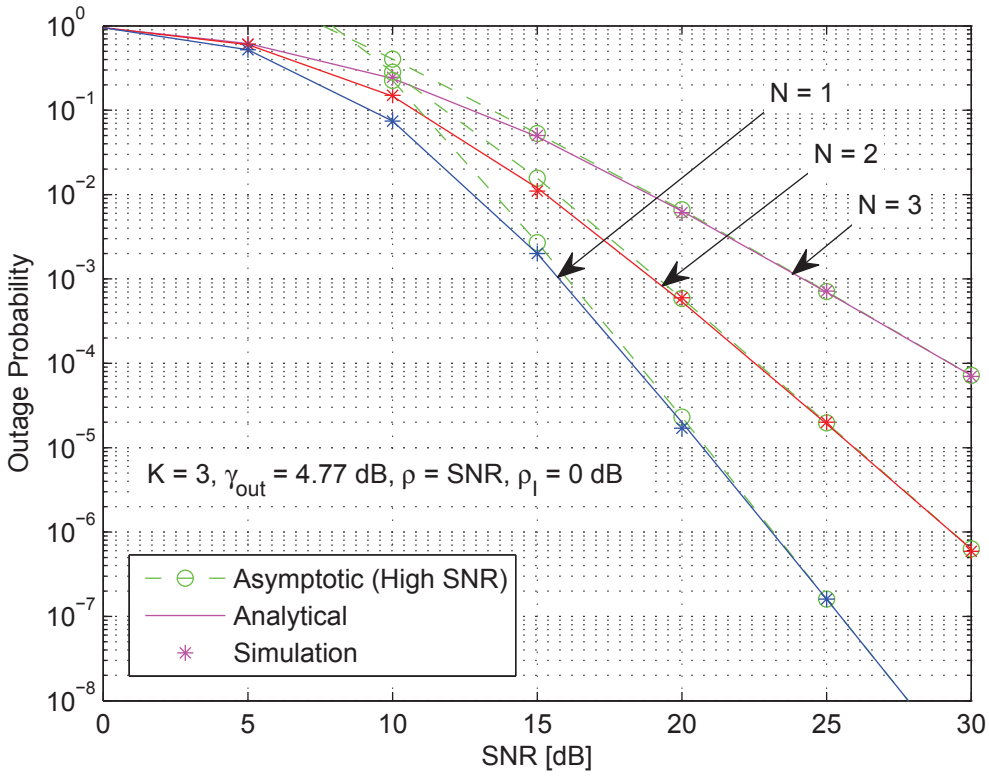

Figure 5.1: Outage probability vs average SNR for N^{th}-best DF relay system with interference at the relays and destination for different values of N and $\sigma^2_{\text{s,d}} = 1$, $\sigma^2_{\text{s},1} = 0.2$, $\sigma^2_{\text{s},2} = 0.6$, $\sigma^2_{\text{s},3} = 0.8$, $\sigma^2_{k,\text{d}} = 0.4$, $(\sigma^I_k)^2 = 0.01$ and $I_k = 1$ for $k = 1, \ldots, 3$, $(\sigma^I_{\text{d}})^2 = 0.01$, and $I_d = 1$.

Figure 5.3 illustrates the outage probability vs outage threshold γ_{out} for different numbers of interferers I_d and I_k when they are unequal. This figure compares the interference severity at the relay compared to that at the destination and demonstrates their effect on the system performance. As can be seen, the interference at the destination node affects the system performance more severely than the interference at the relay. This is expected as the interference at the relay node only affects the signal on the first hop of the relay path; whereas, the interference at the destination node affects both the signal on the relay path and that on the direct link.

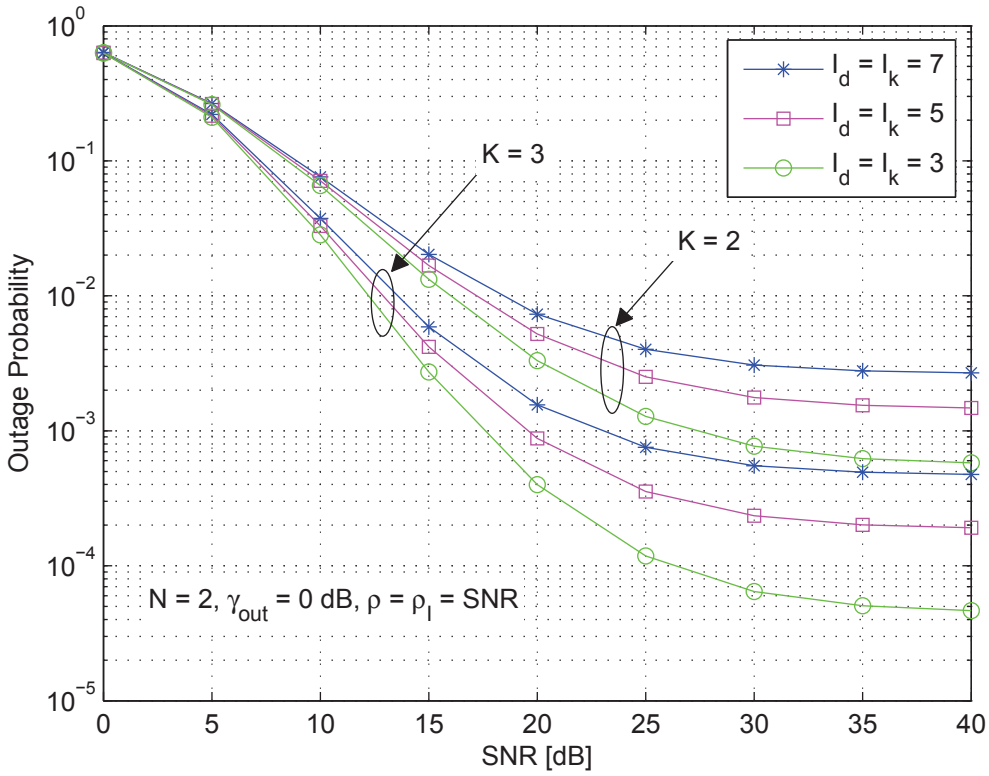

Figure 5.2: Outage probability vs average SNR for N^{th}-best DF relay system with interference at the relays and destination for different values of I_{d} and I_k when they are equal and $\sigma^2_{\text{s,d}} = 1$, $\sigma^2_{\text{s},1} = 0.2$, $\sigma^2_{\text{s},2} = 0.6$, $\sigma^2_{k,\text{d}} = 0.4$ and $(\sigma^I_k)^2 = 0.01$ for $k = 1, 2$, and $(\sigma^I_{\text{d}})^2 = 0.001$.

Figure 5.4 provides the outage probability vs number of interferers I_k and I_d for different values of SNR. In this figure, the number of interferers at both the relays and the destination is assumed to be equal. It is clear from this figure that as the number of interferers increases, the system behavior becomes more degraded, as expected. Also, one can notice that as the SNR increases, better the performance can be achieved.

Figure 5.5 shows the outage probability vs SNR for different values of outage threshold γ_{out}. Clearly and as expected, as the value of the outage threshold increases, the worse the achieved performance.

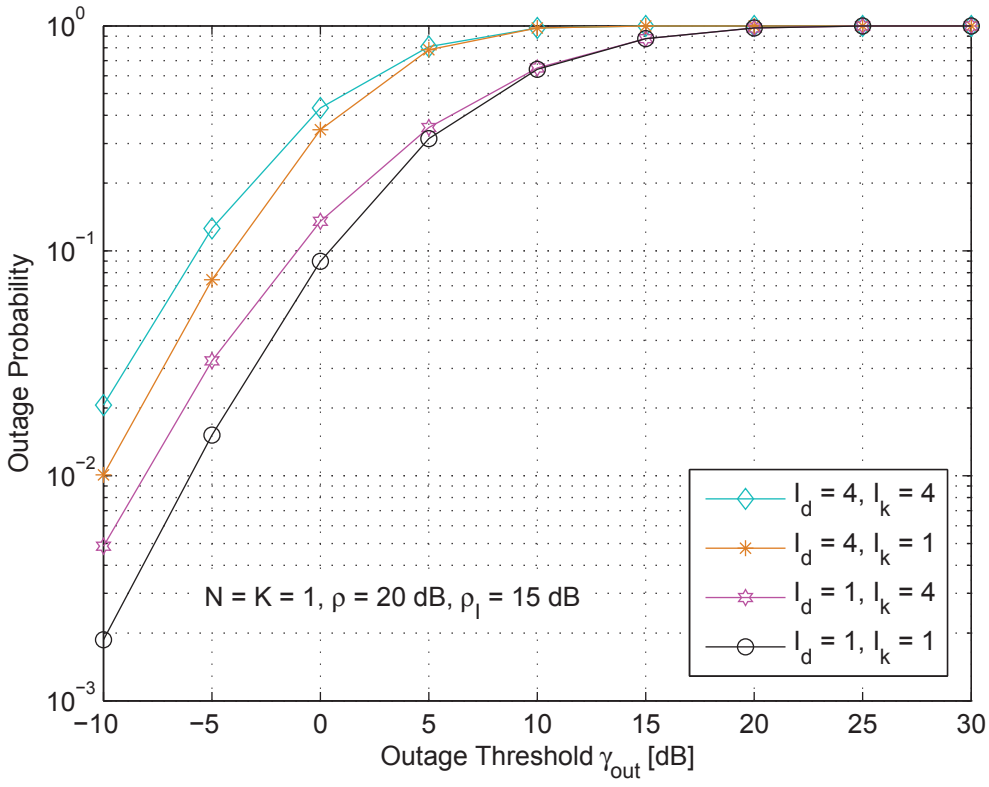

Figure 5.3: Outage probability vs outage threshold for N^{th}-best DF relay system with interference at the relays and destination for different values of I_{d} and I_k when they are unequal and $\sigma^2_{\mathsf{s},1} = 1$, $\sigma^2_{\mathsf{s},1} = 0.2$, $\sigma^2_{1,\mathsf{d}} = 0.4$, $(\sigma^I_1)^2 = 0.5$, and $(\sigma^I_{\mathsf{d}})^2 = 0.5$.

Figure 5.6 illustrates the outage probability vs outage threshold γ_{out} for different values of SNR. As can be seen, as γ_{out} increases, the larger the probability the system falling in outage. Also, one can notice that the best performance can be achieved at the highest value of SNR, as expected.

Figure 5.7 portrays the outage probability vs number of relays K for different values of SNR and $\sigma^2_{\mathsf{s},\mathsf{d}}$. It can be seen that the considered relay system still can achieve performance gain and the outage probability decreases when K increases, but the slope depends on the SNR values. The figure also shows that enhancing the quality of the direct link via increasing $\sigma^2_{\mathsf{s},\mathsf{d}}$ is noticeably improving the system

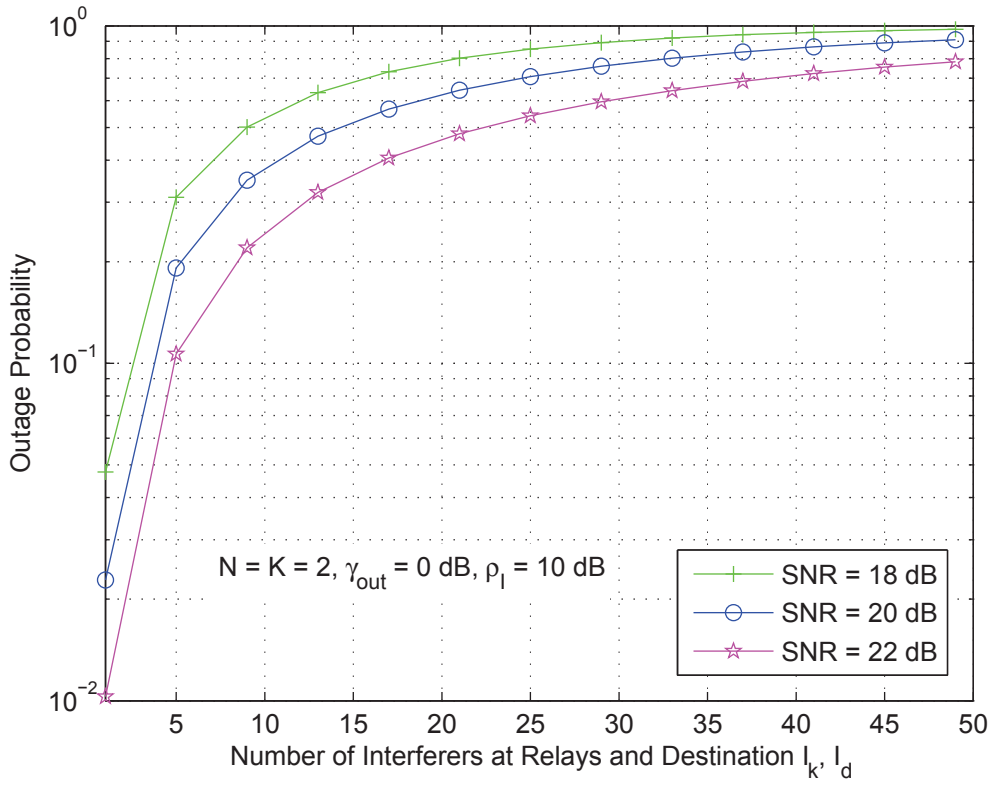

Figure 5.4: Outage probability vs number of interferers at relays and destination for N^{th}-best DF relay system with interference at the relays and destination for different values of SNR and $\sigma^2_{\text{s,d}} = 1$, $\sigma^2_{\text{s,1}} = 0.2$, $\sigma^2_{\text{s,2}} = 0.4$, $\sigma^2_{\text{1,d}} = 0.4$, $\sigma^2_{\text{2,d}} = 0.6$, $(\sigma^I_k)^2 = 0.4$ for $k = 1, 2$, and $(\sigma^I_{\text{d}})^2 = 0.5$.

performance, as expected.

5.7 Conclusions

In this chapter, the outage performance of a dual-hop N^{th}-best DF relay system was evaluated in the presence of interference at the relays and the destination. We derived exact closed-form expression for the outage probability with all system channels assumed to be Rayleigh distributed. Furthermore, the asymptotic outage performance of the considered system was studied via deriving the asymptotic

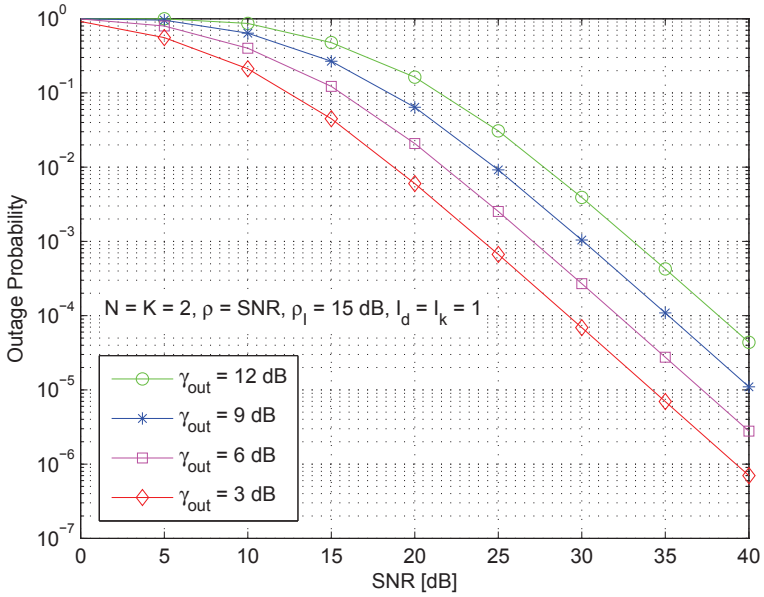

Figure 5.5: Outage probability vs average SNR for N^{th}-best DF relay system with interference at the relays and destination for different values of γ_{out} and $\sigma^2_{\text{s,d}} = 1$, $\sigma^2_{\text{s},1} = 0.2$, $\sigma^2_{\text{s},2} = 0.4$, $\sigma^2_{k,\text{d}} = 0.4$ and $(\sigma^I_k)^2 = 0.01$ for $k = 1, \ldots, 3$, and $(\sigma^I_{\text{d}})^2 = 0.01$.

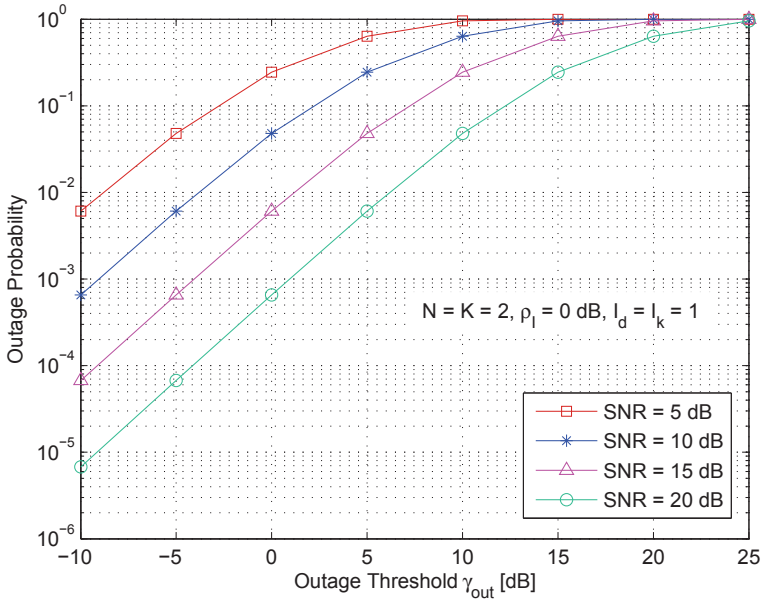

Figure 5.6: Outage probability vs outage threshold for N^{th}-best DF relay system with interference at relays and the destination for different values of SNR and $\sigma^2_{\text{s,d}} = 1$, $\sigma^2_{\text{s},1} = 0.2$, $\sigma^2_{\text{s},2} = 0.6$, $\sigma^2_{k,\text{d}} = 0.4$ and $(\sigma^I_k)^2 = 0.01$ for $k = 1, 2$, and $(\sigma^I_{\text{d}})^2 = 0.01$.

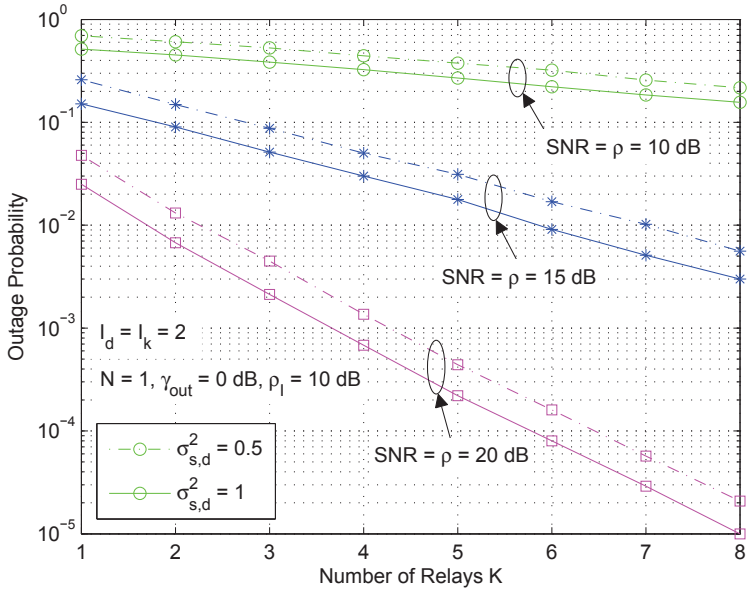

Figure 5.7: Outage probability vs number of relays for N^{th}-best DF relay system with interference at relays and the destination for different values of SNR and $\sigma^2_{\text{s,d}}$ and $\sigma^2_{\text{s,d}} = 1$, $\sigma^2_{\text{s},1} = \ldots = \sigma^2_{\text{s},8} = 0.2$, $\sigma^2_{k,\text{d}} = (k+2)/10$ and $(\sigma^I_k)^2 = 0.5$ for $k = 1, \ldots, 8$, and $(\sigma^I_{\text{d}})^2 = 0.5$.

outage probability. Compared with Monte-Carlo simulations, perfect fitting was noticed between all curves. Findings showed that the outage probability increases as the order of relay increases. Furthermore, results illustrated that the diversity order linearly increases with the number of active relays although one relay is being used only. Furthermore, results showed that the diversity order linearly increases with the number of relays and linearly decreases with the order of the relay. Finally, asymptotic results illustrated that the system is still able to achieve full diversity gain in the presence of finite number of interferers.

CHAPTER 6

SINGLE-RELAY AF IN RICIAN ENVIRONMENTS

6.1 Introduction

For cases where LOS components exist between communicating nodes, other fading models like Rician distribution could be more efficient in studying the performance o such systems. Assuming the Rician fading model for multi-relay networks as the ones studied in previous chapters may result in a highly complicated analysis. To simplify the analysis, relay network with a single relay can be considered.

In this chapter, we investigate the performance of a dual-hop fixed-gain AF relay system in the presence of CCI at the destination node. Different fading scenarios for the desired user and interferers' channels are studied. We consider the Rician/Nakagami-m, the Rician/Rician, and the Nakagami-m/Rician fading environments. In our analysis, we derive accurate approximations for the outage

probability and SEP of the considered scenarios. The generic i.n.d. case of interferers' channels is considered for the Rician/Nakagami-m scenario; whereas, the i.i.d. case is studied for the Rician/Rician and the Nakagami-m/Rician environments. Furthermore, to get more insights on the considered systems, high SNR asymptotic analysis of the outage probability, SEP, diversity order, and coding gain are derived for special cases. Monte-Carlo simulations and numerical examples are presented in order to validate the analytical and asymptotic results and to illustrate the effect of interference and other system parameters on the system performance. Results show that the different fading models of interferers' channels have the same diversity order and that the interference degrades the system performance by only reducing the coding gain. Furthermore, findings show that the case where the fading parameter of the desired user first hop channel is better than that of the second hop gives better performance compared to the vise versa case, especially, at low SNR values; whereas, both cases almost behave the same at high SNR values where the performance of the system is dominated by the interference affecting the worst link. Finally, results show the big gap in system performance due to approximating the Rician fading distribution with the Nakagami-m distribution which is an indication on the inaccuracy of making such approximations in systems like the considered.

The rest of this chapter is organized as follows. Section 6.2 gives a literature review on the most related studies. Section 6.3 explains the system model. The system performance of the Rician/Nakagami-m, Rician/Rician, and Nakagami-

m/Rician fading scenarios is analyzed in Sections 6.4, 6.5, 6.6, respectively. In Section 6.7, some numerical results are discussed. Finally, some conclusions are provided in Section 6.8.

6.2 Literature Review

In general, the AF systems are classified into two subcategories, the CSI-assisted gain relays, which use the instantaneous CSI from the previous hop, and the fixed-gain relays, which introduce a fixed gain in forwarding the source signals. The CSI-assisted AF relay systems require continuous estimation of the fading channel in order to produce their gain and to limit the relay output power. In contrast, fixed-gain relay systems introduce a fixed scale to the received signal regardless of the fading amplitudes which leads to a variable signal power at the relay output.

Despite of the inherent effect of interference in wireless systems, most of the conducted research on the AF and DF relay systems assume noise-limited environments; whereas, few papers study this effect on the performance of such cooperative systems. In general, the interference effect on system performance can be considered at the relay, at the destination, or at both. A situation where the interference may exist only at the relay node is in the frequency-division relay systems where the relay and destination terminals experience different interference patterns [43]. In [43], an approximate expression for the outage probability of a DF relay system with arbitrary number of interferers was derived assuming Nakagami-m fading channels. In [40], a closed-from expression for the outage

probability and an approximate expression for the bit error probability were derived for a CSI-assisted AF relay system assuming Nakagami-m fading channels and an interferer at the relay. In [41], Al-Qahtani *et al.* studied the impact of arbitrary number of interferers at the relay node on the performance of a CSI-assisted AF relay system where closed-form expressions for the outage probability and SEP were derived assuming Nakagami-m fading channels. Furthermore, the authors evaluated those measures at the high SNR regime. The assumption of Rayleigh or Nakagami-m fading in such systems may not be accurate for situations where LOS components exist between the interferers and the relay in the desired cell. Such a situation can be seen in pico-cell relay systems where the interferers' channels are Rician distributed [44].

In relay systems, considering the interference at the destination node is particularly relevant to TDMA systems in which a single time-slot is shared by many relays [19]. This greatly motivates the model where a destination is corrupted by many interferers. In [20], the authors evaluated closed-form expressions for both the outage and asymptotic outage probability of fixed-gain AF and DF relay systems in Rayleigh fading environments. A key result of this study is that the worst behavior happens when the interference power is equally distributed between the interferers. In [21], exact expressions for both the outage and asymptotic outage probability and SEP were derived with all links assumed to follow the Nakagami-m distribution. Again, in situations where LOS components exist between the interferers and the desired destination, the Rayleigh and Nakagami-m

assumptions may not reflect the accurate behavior of the studied systems.

A more general scenario in relay networks is to consider the interference impact at both the relay and destination nodes. An early study that considered the interference at the relay and destination in relay systems was appeared in [45], in which the authors evaluated the performance of a dual-hop CSI-assisted AF relay system with an arbitrary number of interferers of i.i.d. fading channels. The outage probability was numerically evaluated assuming Nakagami-m fading channels. The outage probability of a fixed-gain AF relay system with interference at the relay and destination over Rayleigh and Nakagami-m fading channels was derived in closed-form expression in [46] and [47], respectively. In [48], the authors evaluated the outage performance of a CSI-assisted AF relay system when the desired user channels are Rician distributed and the interferers' channels follow Rayleigh distribution. In [49], the authors derived both the outage probability and SEP of a CSI-assisted AF relay system over Rayleigh fading channels. They further evaluated the asymptotic outage probability and SEP assuming i.n.d. and i.i.d. interferers' fading channels. More on the interference at the relay and destination nodes in relay systems can be found in [50], [51]. Again, the situation where LOS components may exist between the interferers and the desired relay and destination are not widely studied.

Despite of the importance of Rician fading, only few studies considered such a channel model in literature. It is known that the Rician distribution models wireless propagation comprising a LOS component in addition to other scattered

components. The presence of LOS has been confirmed through physical measurement for a number of applications, such as micro-cellular mobile and indoor radio. LOS arises in ad-hoc network applications (especially for dense networks), which are currently receiving considerable interest. In such networks, due to the presence of a LOS propagation between the base station (BS) and users in the desired cell, it is acceptable to assume Rician fading for the desired user channels and Nakagami-m or Rayleigh fading for the interferers' channels. Another fading model that can be considered for interferers' channels is the Rician distribution as in micro-cell and pico-cell networks (radii in the range of 10-100 m) where the size cell is small as in buildings, markets, and industrial compounds [44]. We would like to note that approximating the Rician fading with other distributions such as the Nakagami-m as an example, may not give accurate results in some situations as will be shown in our findings. Also, it may not reflect the actual behavior of the system currently under consideration. Other important fading models that can be considered in relay networks is to assume Nakagami-m fading for the desired user channels and Rician fading for the interferers' channels. The importance of these models is that they are very general and accurately reflect the impact of the interference and other parameters on the behavior of studied systems. Such fading models were used in [52] in which Suraweera *et al.* considered two scenarios; noisy relay and destination with interference at the relay, and noisy relay with interference and an interference-limited destination. The desired user channels were assumed to be Rayleigh faded while the single interferer was assumed to

follow Rician distribution. A key result of this study is that the overall system performance is hardly affected by the Rician-K factor of the interfering signal.

As can be seen, none of the literature studies considered the performance of fixed-gain AF relay systems with the desired user and interferers' channels being Rician/Nakagami-m, Rician/Rician, and Nakagami-m/Rician, respectively. As mentioned before, considering the interference at the destination node is particularly relevant to TDMA systems in which a single time-slot is shared by many relays. Furthermore, the assumption of Rician fading is motivated by the fact that it is used to model wireless propagation comprising a LOS component and a scattered component which is most likely to be existed in micro-cellular mobile and indoor radio. Also, the proposed fading models find their practicality in pico-cells as the dense ad-hoc networks. In the analysis of this chapter, we derive accurate approximations for the outage probability and SEP for the Rician/Nakagmi-m fading scenario for i.n.d. and i.i.d. interferers' channels. In addition, we derive accurate approximate expressions for the outage probability and SEP for both the Rician/Rician and the Nakagami-m/Rician fading scenarios for i.i.d. interferers' channels. The derived analytical expressions quantify the impact of interference on the performance of relay networks for a large set of fading environments. Further, the analysis of Rician channels is generally more difficult and as a special case, includes the commonly assumed Rayleigh fading. Finally, in order to get more about the system insights, we evaluate the asymptotic system performance at high SNR values for special cases of the proposed fading environments. The

asymptotic outage probability and SEP in addition to the diversity order and coding gain are derived and compared.

6.3 System Model

Consider a dual-hop relay where a source node S transmits to a destination node D with the assistance of a relay node R. The entire communication takes place in two separate phases. In the first phase, S transmits the signal to R and then in the second phase the received signal at R is amplified with a gain and then forwarded to D. We consider that the signal at D is corrupted by interfering signals from N co-channel interferers $\{x_i\}_{i=1}^{N}$, each with an average power of P_i.

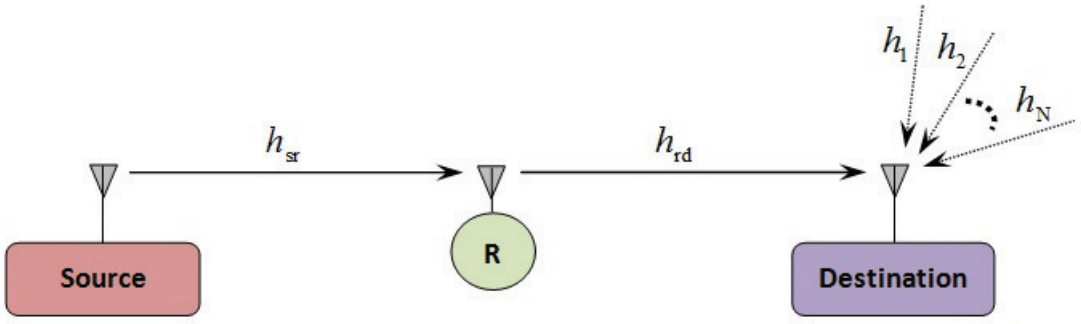

Figure 6.1: A schematic diagram for dual-hop fixed-gain AF relay system with interference-limited destination.

The received signal at R can be expressed as

$$y_{\mathsf{r}} = h_{\mathsf{sr}} x_0 + n_{\mathsf{sr}}, \tag{6.1}$$

where h_{sr} is the channel coefficient for S-R link, x_0 is the transmitted symbol with $\mathbb{E}\{|x_0|^2\} = P_0$, and $n_{sr} \sim \mathcal{CN}(0, N_0)$ denotes the AWGN. In the second phase,

the received signal at R is first scaled with the gain $\mathsf{G} \triangleq \sqrt{\frac{P_{\mathsf{r}}}{P_0\sigma_{\mathsf{sr}}^2+N_0}}$ and forwarded to D, where P_{r} is the power at R, and $\sigma_{\mathsf{sr}}^2 = \mathbb{E}\{|h_{\mathsf{sr}}|^2\}$. In practical situations where different time-slots are used by the source and a single time-slot is shared by many relays as in TDMA systems, the interference effect appears only at the destination node [19]. Therefore, the signal at D can be expressed as

$$y_{\mathsf{d}} = \mathsf{G}h_{\mathsf{rd}}(h_{\mathsf{sr}}x_0 + n_{\mathsf{sr}}) + \sum_{i=1}^{N} h_i x_i + n_{\mathsf{rd}}, \tag{6.2}$$

where h_{rd} denotes the channel coefficient for the R-D link, $\{h_i\}_{i=1}^{N}$ are the channel coefficients from interferers to D, and $n_{\mathsf{rd}} \sim \mathcal{CN}(0, N_0)$.

From (6.2), the e2e SINR at D can be written as

$$\gamma_{\mathsf{D}} = \frac{\mathsf{G}^2|h_{\mathsf{rd}}|^2 P_0 |h_{\mathsf{sr}}|^2}{\sum_{i=1}^{N} P_i|h_i|^2 + \mathsf{G}^2 N_0 |h_{\mathsf{rd}}|^2}. \tag{6.3}$$

As the destination is interference-limited, the effect of n_{rd} has been neglected in last result. This assumption is acceptable in practical situations where the interference is a crucial factor that governs the overall system performance as compared to noise [20].

Substituting G in (3), and after some algebraic manipulations, the e2e SINR can be written as $\gamma_{\mathsf{D}} = \frac{X_1 X_2}{CY+Y+X_2}$, where $X_1 = \frac{P_0}{N_0}|h_{\mathsf{sr}}|^2$, $X_2 = P_r|h_{\mathsf{rd}}|^2$, $C = \frac{P_0\sigma_{\mathsf{sr}}^2}{N_0}$, and $Y = \sum_{i=1}^{N} Y_i$, where $Y_i = P_i|h_i|^2$.

In the rest of this chapter, the system performance is analyzed for different fading environments, Rician/ Nakagami-m, Rician/Rician, and Nakagami-m/Rician.

6.4 Rician/Nakagami-m Environment

Such fading scenario is applicable in micro-cellular mobile and indoor radio where a LOS propagation is existed between the BS and users in the desired cell.

6.4.1 Outage Probability

In this section, we derive the outage probability for the i.n.d. and i.i.d. cases of interferers' channels. For this scenario, the channel coefficients of the desired user h_{sr}, h_{rd} are Rician distributed, while the interferers' channels coefficients h_i are Nakagami-m distributed. Based on that, the channel gains $|h_{\mathsf{sr}}|^2$, $|h_{\mathsf{rd}}|^2$ are non-central chi square distributed with parameters K_1 and $\frac{1}{\eta_1}$, K_2 and $\frac{1}{\eta_2}$, respectively, and the gains $|h_i|^2$, $i = 1, \ldots, N$, are i.n.d. gamma distributed with parameters m_{I_i} and α_{I_i}.

Lemma 6.1 *The outage probability of the Rician/Nakagami-m fading scenario can be obtained for the case of i.n.d. interferers' channels as*

$$
\begin{aligned}
P_{\mathsf{out}} &= 1 - \exp\left(-\left(K_1 + K_2\right)\right) \exp\left(-\frac{1+K_1}{\eta_1}\gamma_{\mathsf{th}}\right) \sum_{k=0}^{N} \Omega_{I_k}^{m_{I_k}} \sum_{i=1}^{m_{I_k}} \frac{\beta_k^{i-1}}{(i-1)!} \\
&\times \sum_{n=0}^{M_1} K_2^n \sum_{j=0}^{M_2} K_2^j \frac{\Gamma(j+m_{I_k})}{j!\,\Gamma(n+j+1)} \left(\frac{\Omega_{I_k}(1+K_1)(1+K_2)(C+1)}{\eta_1\eta_2}\right)^{\frac{j}{2}} \gamma_{\mathsf{out}}^{\frac{j}{2}} \sum_{l=0}^{M_3} \frac{K_1^l}{(l!)^2} \\
&\times \left(\frac{1+K_1}{\eta_1}\right)^{l} \gamma_{\mathsf{out}}^{l} \sum_{q=0}^{l} \binom{l}{q} \Gamma(q+m_{I_k}+1) \left(\frac{\eta_1\Omega_{I_k}(1+K_2)(C+1)}{\eta_2(1+K_1)}\right)^{\frac{q}{2}} \gamma_{\mathsf{out}}^{-\frac{q}{2}} \\
&\times \exp\left(\frac{\Omega_{I_k}(1+K_1)(1+K_2)(C+1)}{2\eta_1\eta_2}\gamma_{\mathsf{out}}\right) W_{a,b}\left(\frac{\Omega_{I_k}(1+K_1)(1+K_2)(C+1)}{\eta_1\eta_2}\gamma_{\mathsf{out}}\right),
\end{aligned}
\tag{6.4}
$$

where $M_{(.)}$ are parameters for series convergence and take values from 1-50, $W_{.,.}(\cdot)$ is the Whittaker function defined in [42, Eq. (9.22)], $a = -\left(\frac{j}{2} + \frac{q}{2} + m_{I_k}\right)$, and $b = (-j + q + 1)/2$.

Proof. See Appendix D.1. ∎

For the special case where the interfering channels have the same fading parameter $\{m_{I_i}\}_{i=1}^{N} = m_I$ and experience the same average power $\{\Omega_{I_i}\}_{i=1}^{N} = \Omega_I$, the PDF of Y is given by

$$f_Y(y) = \frac{\alpha_I^{Nm_I}}{\Gamma(Nm_I)}\, y^{Nm_I - 1} \exp\left(-\alpha_I y\right). \tag{6.5}$$

Upon substituting (6.5) in (D.2), and after following the same procedure as in Appendix D.1, the outage probability for the i.i.d. case of this scenario can be obtained as

$$\begin{aligned} P_{\mathsf{out}} = 1 - \frac{\exp\left(-\left(K_1 + K_2\right)\right)}{\Gamma(Nm_I)} \exp\left(-\frac{1 + K_1}{\eta_1}\gamma_{\mathsf{th}}\right) \sum_{n=0}^{M_1} K_2^n \sum_{j=0}^{M_2} \frac{K_2^j\, \Gamma(j + Nm_I)}{j!\, \Gamma(n + j + 1)} \\ \times \left(\frac{(1 + K_1)(1 + K_2)\Omega_I(C + 1)}{\eta_1\eta_2}\right)^{\frac{j}{2}} \gamma_{\mathsf{out}}^{\frac{j}{2}} \sum_{l=0}^{M_3} \frac{K_1^l}{(l!)^2} \left(\frac{1 + K_1}{\eta_1}\right)^l \gamma_{\mathsf{out}}^l \sum_{q=0}^{l} \binom{l}{q} \left(\frac{\eta_1(1 + K_2)}{\eta_2(1 + K_1)}\right)^{\frac{q}{2}} \\ \times \left(\Omega_I(C + 1)\right)^{\frac{q}{2}} \gamma_{\mathsf{out}}^{-\frac{q}{2}} \Gamma(q + Nm_I + 1) \exp\left(\frac{\Omega_I(1 + K_1)(1 + K_2)(C + 1)}{2\eta_1\eta_2}\gamma_{\mathsf{out}}\right) \\ \times W_{\hat{a},\hat{b}}\left(\frac{\Omega_I(1 + K_1)(1 + K_2)(C + 1)}{\eta_1\eta_2}\gamma_{\mathsf{out}}\right), \end{aligned} \tag{6.6}$$

where $\hat{a} = -\left(\frac{j}{2} + \frac{q}{2} + Nm_I\right)$ and $\hat{b} = (-j + q + 1)/2$.

6.4.2 Symbol Error Probability

In this section, we derive the SEP for the i.n.d. and i.i.d. cases of interferers' channels. It is given by

$$\mathsf{SEP} = \int_0^\infty aQ\left(\sqrt{2b\gamma}\right) f_{\gamma_D}(\gamma)d\gamma = \frac{a\sqrt{b}}{2\sqrt{\pi}} \int_0^\infty \frac{e^{-b\gamma}}{\gamma^{1/2}} F_{\gamma_D}(\gamma)d\gamma, \tag{6.7}$$

where $Q(\cdot)$ is the Gaussian Q-function, a and b are modulation specific constants. Upon substituting the CDF $F_{\gamma_\mathsf{D}}(\gamma) = P_{\mathsf{out}}(\gamma)$ obtained in (6.4) in (6.7), and with the help of [42, Eq. (3.381.4)] and [42, Eq. (7.621.3)], and after some algebraic manipulations, the SEP for the i.n.d. case of this scenario can be obtained as

$$\begin{aligned}
\mathsf{SEP} = \frac{a\sqrt{b}}{2\sqrt{\pi}} \Bigg\{ & \Gamma\left(\frac{1}{2}\right) b^{-\frac{1}{2}} - \exp\left(-\left(K_1+K_2\right)\right) \left(\frac{1+K_1}{\eta_1}+b\right)^{-\frac{3}{2}} \left(\frac{\Omega_{I_k}(1+K_1)}{\eta_1}\right) \\
& \times \frac{(1+K_2)(C+1)}{\eta_2} \sum_{k=0}^{N} \Omega_{I_k}^{m_{I_k}} \sum_{i=1}^{m_{I_k}} \frac{\beta_k^{i-1}}{(i-1)!} \sum_{n=0}^{M_1} K_2^n \sum_{j=0}^{M_2} \frac{K_2^j}{j!} \frac{\Gamma(j+m_{I_k})}{\Gamma(n+j+1)} \sum_{l=0}^{M_3} \frac{K_1^l}{(l!)^2} \\
& \times \frac{\Gamma\left(l+\frac{3}{2}\right)\left(\frac{1+K_1}{\eta_1}\right)^l}{\Gamma\left(j+l+m_{I_k}+\frac{3}{2}\right)} \left(\frac{1+K_1}{\eta_1}+b\right)^{-l} \sum_{q=0}^{l} \binom{l}{q} \Gamma(q+m_{I_k}+1)\Gamma\left(-q+j+l+\frac{1}{2}\right) \\
& \times \left(\frac{\Omega_{I_k}(1+K_2)(C+1)}{\eta_2}\right)^q F\left(\hat{a},\hat{b};\hat{c};\frac{\frac{1+K_1}{\eta_1}+b-\frac{\Omega_{I_k}(1+K_1)(1+K_2)(C+1)}{\eta_1\eta_2}}{\frac{1+K_1}{\eta_1}+b}\right) \Bigg\},
\end{aligned} \tag{6.8}$$

where $F(.,.;.;.)$ is the Gauss hypergeometric function defined in [42, Eq. (9.100)], $\hat{a} = l+\frac{3}{2}$, $\hat{b} = q+m_{I_k}+1$, and $\hat{c} = j+l+m_{I_k}+\frac{3}{2}$.

For the special case where the interfering channels have the same fading parameter $\{m_{I_i}\}_{i=1}^N = m_I$ and experience the same average power $\{\Omega_{I_i}\}_{i=1}^N = \Omega_I$,

upon substituting the CDF $F_{\gamma_{\mathsf{D}}}(\gamma) = P_{\mathsf{out}}(\gamma)$ obtained in (6.6) in (6.7), and with the help of [42, Eq. (3.381.4)] and [42, Eq. (7.621.3)], and after some algebraic manipulations, the SEP for the i.i.d. case of this scenario can be obtained as

$$\begin{aligned}\mathsf{SEP} = \frac{a\sqrt{b}}{2\sqrt{\pi}}\Bigg\{ & \Gamma\left(\frac{1}{2}\right) b^{-\frac{1}{2}} - \frac{\exp\left(-\left(K_1+K_2\right)\right)}{\Gamma(Nm_I)} \left(\frac{1+K_1}{\eta_1}+b\right)^{-\frac{3}{2}} \left(\frac{\Omega_I(1+K_1)}{\eta_1}\right) \\ & \times \frac{(1+K_2)(C+1)}{\eta_2} \sum_{n=0}^{M_1} K_2^n \sum_{j=0}^{M_2} \frac{K_2^j}{j!} \frac{\Gamma(j+Nm_I)}{\Gamma(n+j+1)} \sum_{l=0}^{M_3} \frac{K_1^l \ \Gamma\left(l+\frac{3}{2}\right)}{(l!)^2 \ \Gamma\left(j+l+Nm_I+\frac{3}{2}\right)} \\ & \times \left(\frac{1+K_1}{\eta_1}+b\right)^{-l} \left(\frac{1+K_1}{\eta_1}\right)^{l} \sum_{q=0}^{l} \binom{l}{q} \Gamma(q+Nm_I+1) \Gamma\left(-q+j+l+\frac{1}{2}\right) \\ & \times F\left(\hat{a},\hat{b};\hat{c};\frac{\frac{1+K_1}{\eta_1}+b-\frac{\Omega_I(1+K_1)(1+K_2)(C+1)}{\eta_1\eta_2}}{\frac{1+K_1}{\eta_1}+b}\right) \left(\frac{\Omega_I(1+K_2)(C+1)}{\eta_2}\right)^{q} \Bigg\}, \quad (6.9)\end{aligned}$$

where $\hat{a} = l+\frac{3}{2}$, $\hat{b} = q+Nm_I+1$, and $\hat{c} = j+l+Nm_I+\frac{3}{2}$.

6.4.3 Asymptotic Analysis

Even thought the closed-form expressions of the outage probability and the SEP offer exact evaluation of the system performance, they are too complicated to give any insights about the system behavior. Therefore, in this section, we derive simple expressions for the outage probability and SEP at high SNR values where more information about the diversity order and coding gain of the system can be extracted. The asymptotic results will be for the Rayleigh/Nakagami-m fading environment which is a special case of the Rician/Nakagami-m fading scenario. In deriving the asymptotic expressions, finite number of interferers is assumed and finite powers. In other words, the interference power is assumed to be not scaling

with SNR. For the Rician/Nakagami-m fading scenario, by letting $K_1 = K_2 = 0$ in (6.6), we end up with the Rayleigh/Nakagami-m special case. The outage probability and SEP for the Rayleigh/Nakagami-m fading scenario at high SNR regime are summarized in the following Lemma.

Lemma 6.2 *The asymptotic outage probability and SEP for Rayleigh/Nakagami-m fading scenario can be respectively obtained as*

$$P_{\mathsf{out}}^{\infty} = \gamma_{\mathsf{out}} \left(\frac{1}{\eta_1} - \frac{N m_I \Omega_I \sigma_{\mathsf{sr}}^2}{\mu \eta_1} \left[\ln \left(\frac{\Omega_I \sigma_{\mathsf{sr}}^2}{\mu \eta_1} \gamma_{\mathsf{out}} \right) + \psi(N m_I + 1) + 2c - 1 \right] \right), \tag{6.10}$$

$$\mathsf{SEP}^{\infty} = \frac{a}{4b} \left\{ \frac{1}{\eta_1} - \frac{N m_I \Omega_I \sigma_{\mathsf{sr}}^2}{\mu \eta_1} \left[\psi\left(\frac{3}{2}\right) - \ln \left(b \frac{\Omega_I \sigma_{\mathsf{sr}}^2}{\mu \eta_1} \right) + \psi\left(N m_I + 1\right) + 2c - 1 \right] \right\}. \tag{6.11}$$

Proof. See Appendix D.2. ∎

6.5 Rician/Rician Environment

Such fading scenario is applicable in micro-cellular mobile and indoor radio where a LOS propagation is existed between the BS and users in the desired cell.

6.5.1 Outage Probability

For this scenario, the channel coefficients of both the desired user h_{sr}, h_{rd} and the interferers' h_i are Rician distributed. Based on that, the channel gains $|h_{\mathsf{sr}}|^2$, $|h_{\mathsf{rd}}|^2$ are as defined in the first scenario and the gains $|h_i|^2$, $i = 1, \ldots, N$, are now

i.i.d. non-central chi square distributed with parameters K_I and β_I. The outage probability for this scenario can obtained as

$$P_{\mathsf{out}} = 1 - \exp\left(-\left(K_1 + K_2 + NK_I\right)\right) \exp\left(-\frac{1+K_1}{\eta_1}\gamma_{\mathsf{out}}\right) \sum_{n=0}^{M_1} K_2^n \sum_{j=0}^{M_2} \frac{1}{j!}$$
$$\times \frac{K_2^j}{\Gamma(n+j+1)} \left(\frac{\eta_I(1+K_1)(1+K_2)(C+1)}{\eta_1\eta_2(1+K_I)}\right)^{\frac{j}{2}} \gamma_{\mathsf{out}}^{\frac{j}{2}} \sum_{l=0}^{M_3} \frac{K_1^l}{(l!)^2} \left(\frac{1+K_1}{\eta_1}\right)^l \gamma_{\mathsf{out}}^l$$
$$\times \sum_{k=0}^{M_4} \frac{(NK_I)^k\, \Gamma(j+k+N)}{k!\, \Gamma(k+N)} \sum_{q=0}^{l} \binom{l}{q} \Gamma(k+q+N+1) \left(\frac{\eta_1\eta_I(1+K_2)(C+1)}{\eta_2(1+K_1)(1+K_I)}\right)^{\frac{q}{2}}$$
$$\times \gamma_{\mathsf{out}}^{-\frac{q}{2}} \exp\left(\frac{\eta_I(1+K_1)(1+K_2)(C+1)}{2\eta_1\eta_2(1+K_I)}\gamma_{\mathsf{out}}\right) W_{\bar{a},\bar{b}}\left(\frac{\eta_I(1+K_1)(1+K_2)(C+1)}{\eta_1\eta_2(1+K_I)}\gamma_{\mathsf{out}}\right), \tag{6.12}$$

where $\bar{a} = -\left(\frac{j}{2} + k + \frac{q}{2} + N\right)$ and $\bar{b} = (-j+q+1)/2$.

In evaluating (6.12), the CDF of X_2 and the PDF of X_1 in γ_{D} are as given in Appendix D.1. Assuming i.i.d. interferers' channels, the PDF of Y is given by

$$f_Y(y) = \left(\frac{1+K_I}{\eta_I}\right)^{\frac{N+1}{2}} \exp\left(-\left(NK_I + \frac{1+K_I}{\eta_I}y\right)\right) \left(\frac{y}{NK_I}\right)^{\frac{N-1}{2}}$$
$$\times I_{N-1}\left(2\sqrt{\frac{N\left(1+K_I\right)K_I}{\eta_I}y}\right), \tag{6.13}$$

where $\eta_I{=}\frac{1}{\beta_I}$ is the average power of the interferers and $I_{N-1}(\cdot)$ is the modified Bessel function of the second type and order $N-1$ defined in [42, Eq. (8.445)]. Upon substituting the CCDF of X_2, the PDF of X_1, and the PDF of Y in (D.2), and using the same procedure as in Appendix D.1 with the help of [22, Eq. (4.35)], [42, Eq. (8.447.1)], and [42, Eq. (8.445)], and after some algebraic manipulations, the outage probability for this scenario can be obtained as in (6.12).

6.5.2 Symbol Error Probability

Upon substituting the CDF $F_{\gamma_{\mathsf{D}}}(\gamma) = P_{\mathsf{out}}(\gamma)$ obtained in (6.12) in (6.7), and with the help of [42, Eq. (3.381.4)] and [42, Eq. (7.621.3)], and after some algebraic manipulations, the SEP for this scenario can be obtained as

$$\begin{aligned}
\mathsf{SEP} = \frac{a\sqrt{b}}{2\sqrt{\pi}} \Bigg\{ & \Gamma\left(\frac{1}{2}\right) b^{-\frac{1}{2}} - \exp\left(-\left(K_1 + K_2 + NK_I\right)\right) \times \left(\frac{1+K_1}{\eta_1} + b\right)^{-\frac{3}{2}} \\
& \times \left(\frac{\eta_I(1+K_1)(1+K_2)(C+1)}{\eta_1\eta_2(1+K_I)}\right) \sum_{n=0}^{M_1} K_2^n \sum_{j=0}^{M_2} \frac{K_2^j}{j!\,\Gamma(n+j+1)} \sum_{l=0}^{M_3} \frac{K_1^l\,\Gamma\left(l+\frac{3}{2}\right)}{(l!)^2} \\
& \times \left(\frac{1+K_1}{\eta_1} + b\right)^{-l} \left(\frac{1+K_1}{\eta_1}\right)^{l} \sum_{k=0}^{M_4} \frac{(NK_I)^k}{k!\,\Gamma(k+N)} \frac{\Gamma(j+k+N)}{\Gamma\left(j+l+k+N+\frac{3}{2}\right)} \sum_{q=0}^{l} \binom{l}{q} \\
& \times \Gamma\left(j+l-q+\frac{1}{2}\right) \Gamma\left(k+q+N+1\right) \left(\frac{\eta_I(1+K_2)(C+1)}{\eta_2}\right)^{q} \\
& \times F\left(\hat{a}, \hat{b}; \hat{c}; \frac{\frac{1+K_1}{\eta_1} + b - \frac{\eta_I(1+K_1)(1+K_2)(C+1)}{\eta_1\eta_2(1+K_I)}}{\frac{1+K_1}{\eta_1} + b}\right) \Bigg\}, \qquad (6.14)
\end{aligned}$$

where $\hat{a} = l + \frac{3}{2}$, $\hat{b} = k + q + N + 1$, and $\hat{c} = j + l + +k + N + \frac{3}{2}$.

6.5.3 Asymptotic Analysis

For the Rician/Rician fading scenario, by letting $K_1 = K_2 = K_I = 0$ in (6.12), we end up with the Rayleigh/Rayleigh special case. Following the same procedure as in Appendix D.2, the asymptotic outage probability and SEP for this case can be

respectively obtained as

$$P_{\mathsf{out}}^{\infty} = \gamma_{\mathsf{out}} \left(\frac{1}{\eta_1} - \frac{N\eta_I \sigma_{\mathsf{sr}}^2}{\mu\eta_1} \left[\ln\left(\frac{\eta_I \sigma_{\mathsf{sr}}^2}{\mu\eta_1} \gamma_{\mathsf{out}} \right) + \psi(N+1) + 2c - 1 \right] \right), \tag{6.15}$$

$$\mathsf{SEP}^{\infty} = \frac{a}{4b} \left\{ \frac{1}{\eta_1} - \frac{N\eta_I \sigma_{\mathsf{sr}}^2}{\mu\eta_1} \left[\psi\left(\frac{3}{2}\right) - \ln\left(b \frac{\eta_I \sigma_{\mathsf{sr}}^2}{\mu\eta_1} \right) + \psi\left(N+1\right) + 2c - 1) \right] \right\}. \tag{6.16}$$

6.6 Nakagami-m/Rician Environment

Such fading scenario is applicable in micro-cellular mobile and indoor radio where a LOS propagation is existed between users in the desired cell.

6.6.1 Outage Probability

For this scenario, the channel coefficients of the desired user h_{sr}, h_{rd} are Nakagami-m distributed, while the interferers' channels coefficients h_i are Rician distributed. Based on that, the channel gains $|h_{\mathsf{sr}}|^2$, $|h_{\mathsf{rd}}|^2$ are now gamma distributed with parameters m_1 and $\frac{1}{\Omega_1}$, m_2 and $\frac{1}{\Omega_2}$, respectively, and the gains $|h_i|^2$, $i = 1, \ldots, N$, are as defined in the second scenario. The outage probability for this scenario can be obtained as

$$\begin{aligned} P_{\mathsf{out}} = 1 &- \frac{m_1^{m_1-1} \exp\left(-NK_I\right)}{\Omega_1^{m_1-1}\Gamma(m_1)} \gamma_{\mathsf{out}}^{m_1-1} \exp\left(\left(\frac{m_1 m_2 \eta_I (C+1)}{2\Omega_1\Omega_2(1+K_I)} - \frac{m_1}{\Omega_1} \right) \gamma_{\mathsf{out}} \right) \\ &\times \sum_{j=0}^{m_2-1} \frac{1}{j!} \left(\frac{m_1 m_2 \eta_I (C+1)}{\Omega_1\Omega_2(1+K_I)} \right)^{\frac{j}{2}} \gamma_{\mathsf{out}}^{\frac{j}{2}} \sum_{k=0}^{m_1-1} \binom{m_1-1}{k} \gamma_{\mathsf{out}}^{-\frac{k}{2}} \left(\frac{m_1 m_2 \eta_I (C+1)}{\Omega_1\Omega_2(1+K_I)} \right)^{\frac{k}{2}} \\ &\times \sum_{i=0}^{M} \frac{\Gamma(k+i+N+1)}{i!\ \Gamma(i+N)(NK_I)^{-i}} \Gamma(j+i+N) W_{\hat{a},\hat{b}} \left(\frac{m_1 m_2 \eta_I (C+1)}{\Omega_1\Omega_2(1+K_I)} \gamma_{\mathsf{out}} \right), \end{aligned} \tag{6.17}$$

where M is a parameter for series convergence and takes values from 1-50, $\hat{a} = -\left(\frac{j}{2} + \frac{k}{2} + i + N\right)$, and $\hat{b} = (-j + k + 1)/2$.

In evaluating (6.17), the PDF of Y is as given by (6.13) and the CDF of X_2 and the PDF of X_1 are respectively given by

$$F_{X_2}(x) = 1 - \sum_{j=0}^{m_2-1} \frac{1}{j!} \left(\frac{m_2}{\Omega_2}\right)^j x^j \exp\left(-\frac{m_2}{\Omega_2}x\right), \tag{6.18}$$

$$f_{X_1}(x) = \frac{m_1^{m_1}}{\Omega_1^{m_1}\Gamma(m_1)} x^{m_1-1} \exp\left(-\frac{m_1}{\Omega_1}x\right), \tag{6.19}$$

where $F_{X_2}(x)$ is valid for integer values of m_2.

Upon substituting the CCDF of X_2, the PDF of X_1, and the PDF of Y in (D.2) and using the Binomial formula, we get

$$F_X(x) = 1 - \underbrace{\frac{m_1^{m_1} \exp\left(-NK_I\right) \exp\left(-\frac{m_1}{\Omega_1}x\right)}{\Omega_1^{m_1}\Gamma(m_1)\left(\frac{1+K_I}{\eta_I}\right)^{-\frac{(N+1)}{2}}\left(\frac{1}{NK_I}\right)^{-\frac{(N-1)}{2}}} \sum_{j=0}^{m_2-1} \frac{\left(\frac{m_2}{\Omega_2}\right)^j (x(C+1))^j}{j!}}_{C_2}$$
$$\times \int_0^\infty y^{j+\frac{N}{2}-\frac{1}{2}} \exp\left(-\frac{1+K_I}{\eta_I}y\right) I_{N-1}\left(2\sqrt{\frac{N(1+K_I)K_I}{\eta_I}y}\right) \sum_{k=0}^{m_1-1} \binom{m_1-1}{k}$$
$$\times x^{-k+m_1-1} \underbrace{\int_0^\infty z^{-j+k} \exp\left(-\frac{m_2 x(C+1)y}{\Omega_2 z} - \frac{m_1}{\Omega_1}z\right) dz}_{I_1} dy. \tag{6.20}$$

Upon evaluating I_1 with the help of [42, Eq. (3.471.9)], we get

$$F_X(x) = 1 - 2C_2 \sum_{k=0}^{m_1-1} \binom{m_1-1}{k} x^{-k+m_1-1} \left(\frac{m_2\Omega_1 x(C+1)}{m_1\Omega_2}\right)^{\frac{-j+k+1}{2}} \int_0^\infty y^{\frac{j+k+N}{2}} \times \exp\left(-\frac{1+K_I}{\eta_I}y\right) I_{N-1}\left(2\sqrt{\frac{N(1+K_I)K_I}{\eta_I}y}\right) K_{-j+k+1}\left(2\sqrt{\frac{m_1m_2(C+1)x}{\Omega_1\Omega_2}y}\right) dy. \tag{6.21}$$

Unfortunately, a closed-form expression for the CDF in last result is very difficult, if not impossible, to be obtained. It can be evaluated in a series form by making the change of variables, $t^2 = y$, and using [42, Eq. (8.445)] and [42, Eq. (6.631.3)], and after some algebraic manipulations, the outage probability for this scenario can be obtained as in (6.17).

6.6.2 Symbol Error Probability

Upon substituting the CDF $F_{\gamma_\mathsf{D}}(\gamma) = P_{\mathsf{out}}(\gamma)$ obtained in (6.17) in (6.7), and with the help of [42, Eq. (3.381.4)] and [42, Eq. (7.621.3)], and after some algebraic

manipulations, the SEP for this scenario can be obtained as

$$\mathsf{SEP} = \frac{a\sqrt{b}}{2\sqrt{\pi}}\Bigg\{\Gamma\left(\frac{1}{2}\right)b^{-\frac{1}{2}} - \frac{m_1^{m_1}}{\Omega_1^{m_1}}\left(\frac{m_1}{\Omega_1}+b\right)^{-(m_1+\frac{1}{2})}\frac{\Gamma\left(m_1+\frac{1}{2}\right)}{\Gamma\left(m_1\right)}\left(\frac{m_2\eta_I(C+1)}{\Omega_2(1+K_I)}\right)$$
$$\times \exp\left(-NK_I\right)\sum_{j=0}^{m_2-1}\frac{1}{j!}\sum_{k=0}^{m_1-1}\binom{m_1-1}{k}\Gamma\left(j-k+m_1-\frac{1}{2}\right)\left(\frac{m_2\eta_I(C+1)}{\Omega_2(1+K_I)}\right)^k$$
$$\times \sum_{i=0}^{M}\frac{\Gamma(j+i+N)\Gamma(k+i+N+1)(NK_I)^i}{i!\,\Gamma(i+N)\Gamma\left(j+i+m_1+N+\frac{1}{2}\right)}F\left(\hat{a},\hat{b};\hat{c};\frac{\frac{m_1}{\Omega_1}+b-\frac{m_1m_2\eta_I(C+1)}{\Omega_1\Omega_2(1+K_I)}}{\frac{m_1}{\Omega_1}+b}\right)\Bigg\}, \tag{6.22}$$

where $\hat{a} = m_1 + \frac{1}{2}$, $\hat{b} = k + i + N + 1$, and $\hat{c} = j + i + m_1 + N + \frac{1}{2}$. It is worth to re-mention that the achieved results are valid for integer values of m_2.

6.6.3 Asymptotic Analysis

For the Nakagami-m/Rician fading scenario, by letting $m_1 = m_2 = 1$ in (6.17), we end up with the Rayleigh/Rician special case. Following the same procedure as in Appendix D.2, the asymptotic outage probability and SEP for this case can be respectively obtained as

$$P_{\mathsf{out}}^{\infty} = \gamma_{\mathsf{out}}\left(\frac{1}{\eta_1} - \frac{N\eta_I\sigma_{\mathsf{sr}}^2}{\mu\eta_1(1+K_I)}\left[\ln\left(\frac{\eta_I\sigma_{\mathsf{sr}}^2}{\mu\eta_1(1+K_I)}\gamma_{\mathsf{out}}\right)+\psi(N+1)+2c-1\right]\right), \tag{6.23}$$

$$\mathsf{SEP}^{\infty} = \frac{a}{4b}\left\{\frac{1}{\eta_1} - \frac{N\eta_I\sigma_{\mathsf{sr}}^2}{\mu\eta_1(1+K_I)}\left[\psi\left(\frac{3}{2}\right)-\ln\left(b\frac{\eta_I\sigma_{\mathsf{sr}}^2}{\mu\eta_1(1+K_I)}\right)+\psi\left(N+1\right)+2c-1\right]\right\}. \tag{6.24}$$

It is worth pointing out that the asymptotic expressions can be quantified in terms of diversity order and coding. The diversity order is defined as the negative slope of outage probability curves on a log-log scale, and the coding gain is defined as the shift of the curve in relative to the outage probability reference curve. At the high SNR regime, we can express the outage probability as $P_{\mathsf{out}} \approx (G_{\mathsf{c}}\eta_1)^{-G_{\mathsf{d}}}$, where G_{d} is the achieved diversity order of the system and G_{c} is the coding gain. As we can see, for the case where the interference power does not scale with SNR, all the analyzed scenarios in this section have the same diversity order. Therefore, we can notice that for these special cases of fading scenarios that the degradation in system behavior comes through the coding gain. Noticing that the number of interferers affects the coding gain for all scenarios, in addition, to the effect of fading parameters m_I and K_I for Rayleigh/Nakagami-m and, Rayleigh/Rician, respectively.

6.7 Numerical Results

In this section, we illustrate the validity of the derived analytical results. We also discuss and compare the diversity order and the coding gain of some cases of the proposed fading environments. We also provide some numerical examples to illustrate the effect of interference and some system parameters as the fading parameters on the system performance.

Figure 6.2 illustrates the outage performance vs SNR for some special cases of the proposed fading scenarios; Rayleigh/Rayleigh, Rayleigh/Nakagami-m, and

Nakagami-m/Rayleigh cases. As can be seen, both the analytical and asymptotical results fit accurately with the simulation curves. A key result of our analysis for the case where the interferers' channels possess Rician fading is that the Rician-K factor is hardly affecting the system performance which confirms the same result achieved in [52]. Also, for the case where the interference power does not scale with SNR, we can notice that the different fading scenarios of the interferers' channels have the same diversity order. This can be inferred from the results of the asymptotic outage probability of all scenarios where the power of $(\eta_1)^{-1}$ is the same. We can also notice that the interference degrades the system performance by only affecting the coding gain. Finally, it is clear to see that the coding gain of the Rayleigh/Nakagami-m, the Rayleigh/Rayleigh, and the Rayleigh/Rician fading scenarios is affected by the number, the fading parameters, and the average powers of the interferers.

The outage performance of the Rician/Nakagami-m fading scenario is studied in Figures 6.3, 6.4, and 6.5. Figure 6.3 illustrates the outage probability vs SNR for different numbers of interferers N. It is a validation to the achieved analytical results. We can notice from this figure the perfect fitting between the achieved expressions of this fading scenario and Monte-Carlo simulations. This is a strong indication on the accuracy of our derived analytical expressions. In addition, this figure shows the degradation happens in system performance due to the increase in number of interferers N.

Figure 6.4 shows the outage performance vs SNR for different values of fading

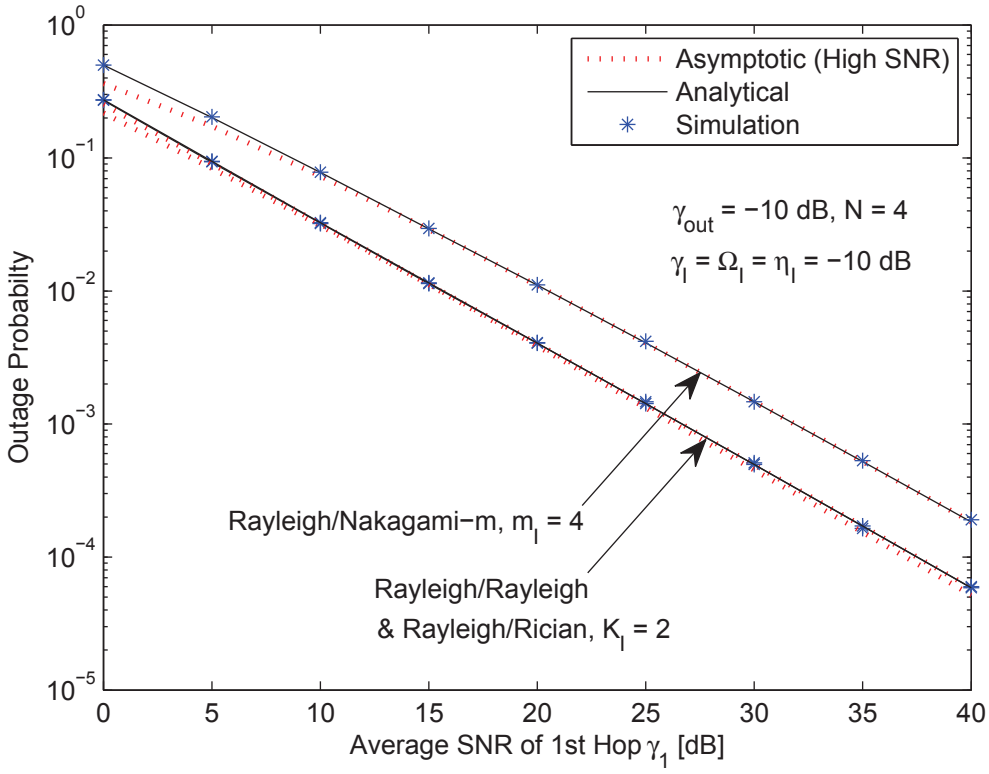

Figure 6.2: Outage probability vs average SNR for fixed-gain AF relay system with interference at destination for different fading environments.

parameter m_I. It studies the effect of the fading parameter of the interferers' channels m_I on the system behavior. As expected, as m_I increases and hence, the quality of the interferers' channels, the worse the achieved performance. It is worth to mention that increasing the fading parameter of channels is beneficial at medium and high range of SNR values. On the other hand, it could be harmful on system performance when we talk about low range of SNR values.

Figure 6.5 provides the outage probability vs outage threshold γ_{out} for different values of ρ. It illustrates the impact of the desired user channels via the power ratio ρ on the system behavior. This ratio represents the power of the second hop channel of the desired user to the power of the interferers' channels $\eta_2/N\Omega_I$,

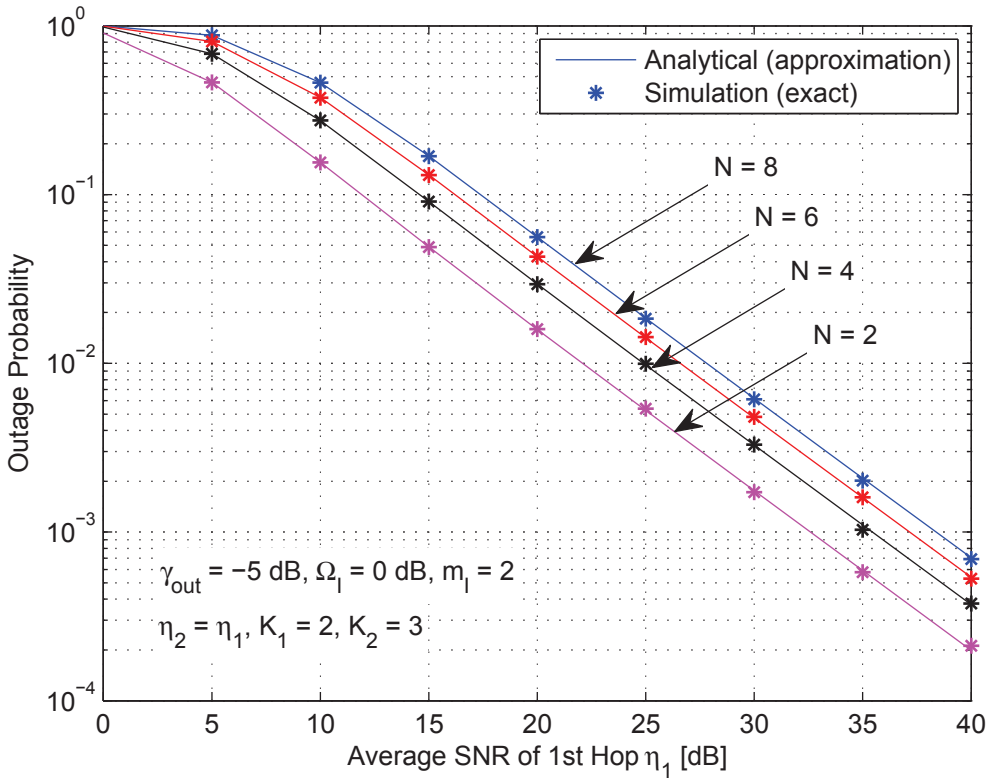

Figure 6.3: Outage probability vs average SNR for fixed-gain AF relay system with interference at destination for Rician/Nakagami-m fading scenario with different values of N.

where the interferers were assumed to be identical in this figure. As expected, as ρ increases, the system performance is more enhanced.

Figure 6.6 portrays the SEP performance vs SNR of the Rician/Nakagami-m fading scenario for different values of power ratio ρ_i and different numbers of interferers N, where ρ_i denotes a ratio of the power of the second hop channel of the desired user to that of the channel of a single interferer η_2/Ω_I, where the interferers were assumed to be identical in this figure. As expected, as ρ_i increases, the better the achieved performance. Also, we can notice that the best behavior can be achieved when N takes its minimum value. Finally, a noise floor appears in

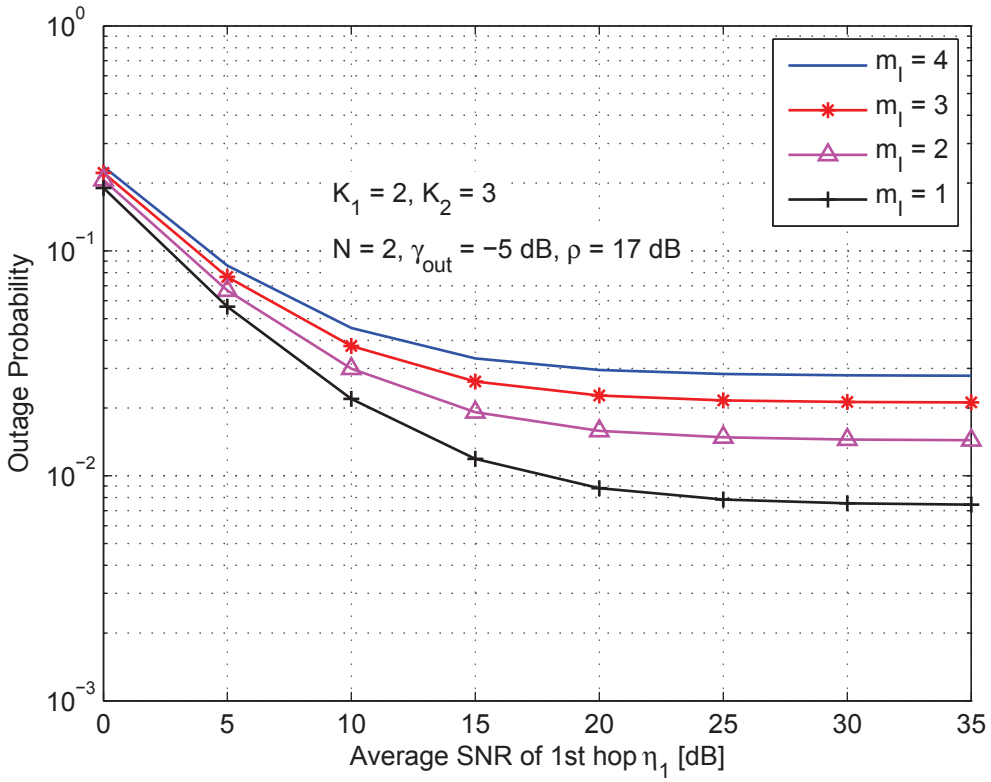

Figure 6.4: Outage probability vs average SNR for fixed-gain AF relay system with interference at destination for Rician/Nakagami-m fading scenario with different values of m_I.

all cases due to the effect of interference. Noticing that the diversity gain reaches zero as the interference power was assumed to scale with SNR in this figure.

The outage performance of the Rician/Rician fading scenario is studied in Figures 6.7 and 6.8. Figure 6.7 shows the outage performance vs SNR for different numbers of interferers N. It illustrates the validity of the derived expressions. We can notice from this figure the perfect fitting between the achieved analytical results and Monte-Carlo simulations which is a strong indication on the accuracy of our derived expressions. In addition, the figure shows the degradation happens in system performance due to the increase in number of interferers N.

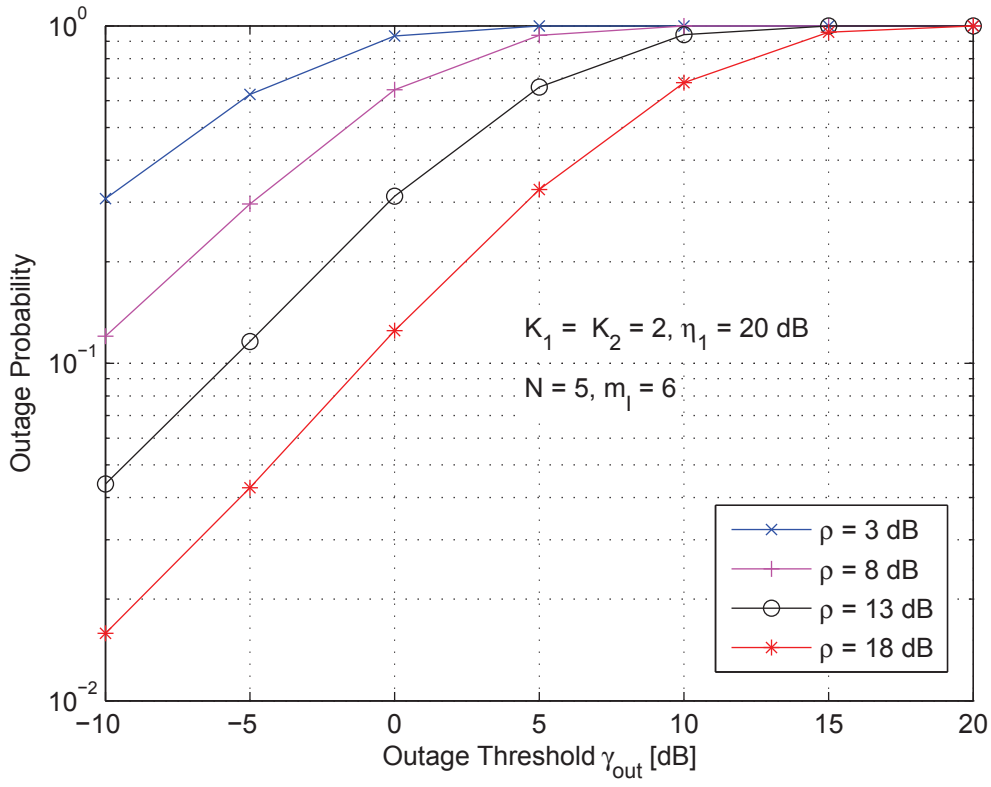

Figure 6.5: Outage probability vs outage threshold for fixed-gain AF relay system with interference at destination for Rician/Nakagami-m fading scenario with different values of ρ.

Figure 6.8 illustrates the outage performance vs outage threshold γout for different values of fading parameters K_1, K_2. It studies the effect of the fading parameters K_1 and K_2 of the desired user channel on the system performance when they possess similar values. As can be seen, as the values of this pair increase and hence, the quality of the desired user channels, the better the achieved behavior.

The SEP performance of the Rician/Rician fading scenario is studied in Figures 6.9 and 6.10. Figure 6.9 shows the SEP vs SNR for different values of fading parameters K_1, K_2. It studies the effect of fading parameters K_1 and K_2 on the system performance when they possess different values. It is clear that the worst

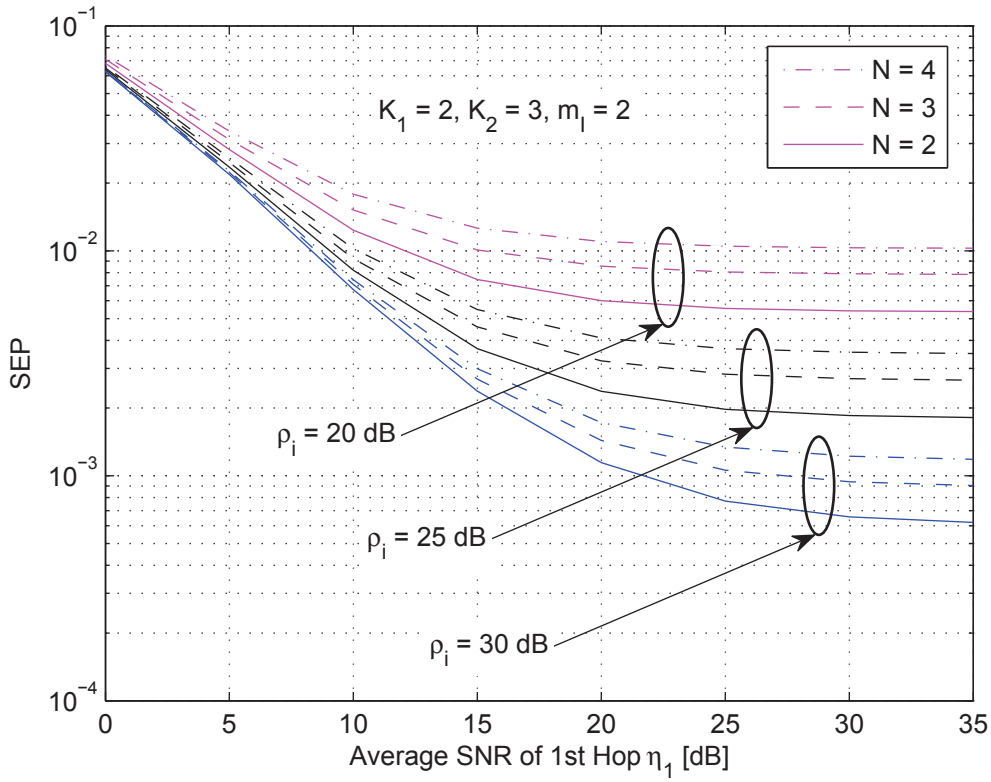

Figure 6.6: Average SEP vs average SNR for fixed-gain AF relay system with interference at destination for Rician/Nakagami-m fading scenario with different values of ρ_i and N.

behavior is achieved when K_1 and K_2 equal unity. On the other hand, when they take the values (9,1), the achieved performance is better than the case of (1,9), specially, at low values of the first hop SNR. This means that the parameter K_1 is more effective when the average SNR of the first hop is smaller than that of the second hop. At the case when these SNRs are comparable, both cases are almost behaving the same. This is because the performance of the overall system is dominated by the interference affected worst link. Finally, the best behavior is achieved when K_1 and K_2 are equal and larger than unity.

Figure 6.10 aims to show the inaccuracy in approximating the Rician fading

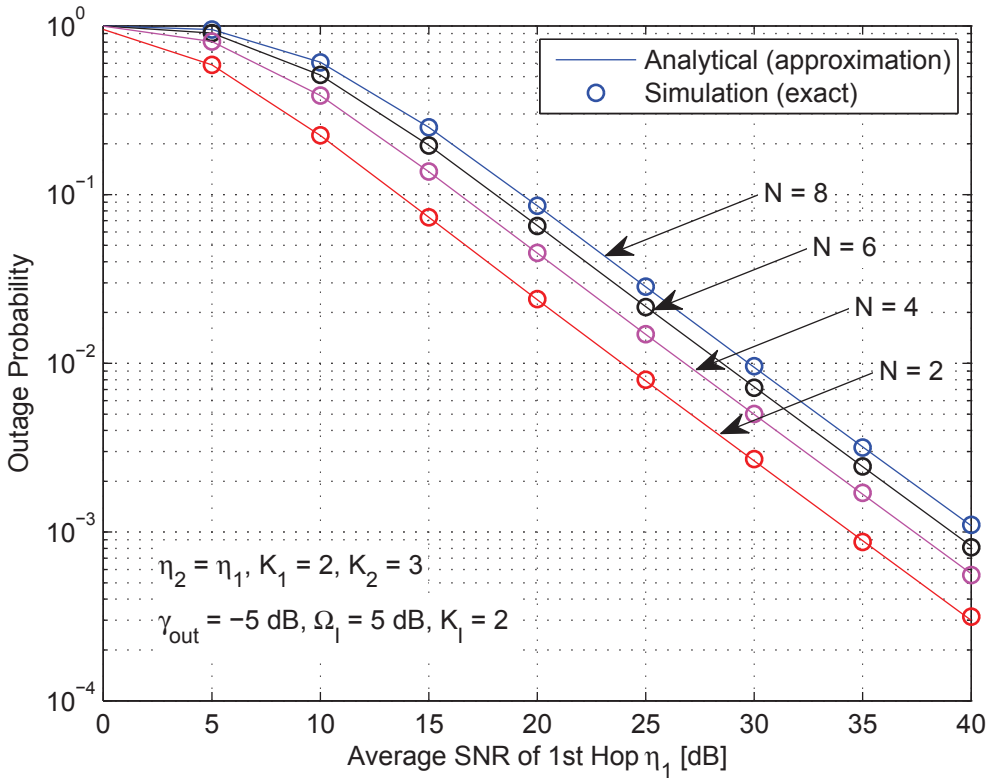

Figure 6.7: Outage probability vs average SNR for fixed-gain AF relay system with interference at destination for Rician/Rician fading scenario with different values of N.

model with the Nakagami-m model as an example. A big gap in system behavior can be seen in this figure when the the interferers' channels are approximated by Nakagami-m distribution instead of Rician distribution. In this figure, we used [22, Eq. (2.26)] to calculate the value of fading parameter m_I that approximates K_I. This result illustrates the importance of our assumption in modeling the interferers' channels to be Rician distributed and not to be approximated by any other fading models.

The outage performance of the Nakagami-m/Rician fading scenario is studied in Figures 6.11 and 6.12. Figure 6.11 provides the outage performance vs SNR

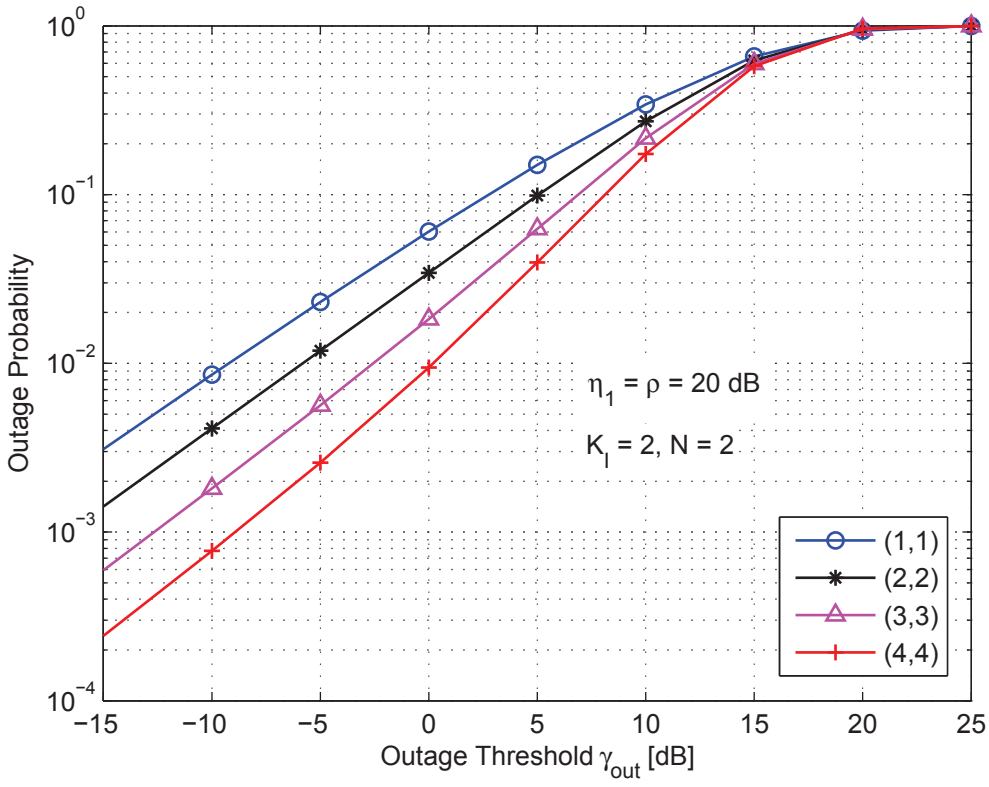

Figure 6.8: Outage probability vs outage threshold for fixed-gain AF relay system with interference at destination for Rician/Rician fading scenario with different values of (K_1, K_2).

for different numbers of interferers N. It illustrates the validity of the derived analytical expressions. A perfect fitting between the achieved analytical results and Monte-Carlo simulations can be seen in this figure. This is a clear evidence on the accuracy of our derived expressions. In addition, the figure shows the degradation happens in system performance due to the increase in number of interferers N.

Figure 6.12 illustrates the outage probability vs outage threshold γ_{out} for different values of η_I. It shows the impact of interferers' channels quality on the system behavior. As obvious, as η_I increases and hence, the quality of the interferers'

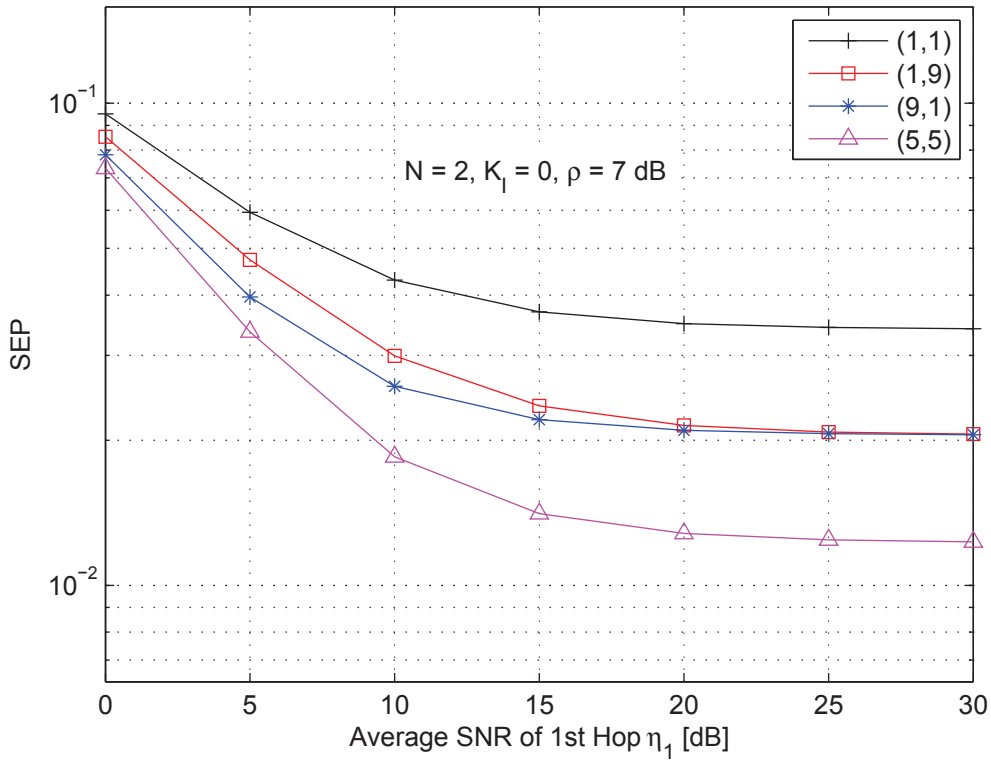

Figure 6.9: Average SEP vs average SNR for fixed-gain AF relay system with interference at destination for Rician/Rician fading scenario with different values of (K_1, K_2).

signals, the worse the achieved behavior, as expected.

Figure 6.13 shows the SEP performance vs SNR for different values of fading parameters m_1, m_2. It studies the effect of fading parameters of the desired user channels m_1 and m_2 on the SEP performance of the Nakagami-m/Rician fading scenario. As explained in the case of Rician/Rician scenario and the effect of K_1 and K_2 on its performance, the same result can be seen here. The worst behavior is achieved when m_1 and m_2 equal unity which represents the Rayleigh fading. On the other hand, the case (3,1) gives better behavior than the case (1,3), specially, at low values of the first hop SNR. This means that the parameter

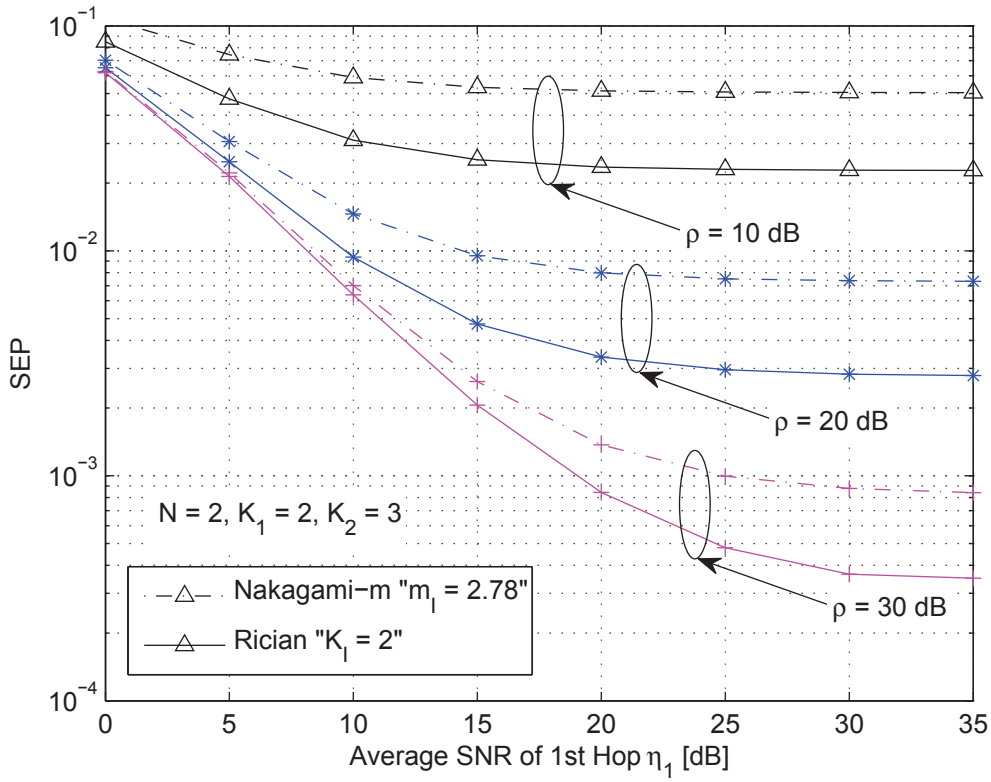

Figure 6.10: Average SEP vs average SNR for fixed-gain AF relay system with interference at destination for Rician/Rician and Rician/Nakagami-m fading scenarios with different values of ρ.

m_1 is more effective when the average SNR of the first hop is smaller than that of the second hop. At the case when these SNRs are comparable, both cases are almost behaving the same. This is because the performance of the overall system is dominated by the interference affected worst link. Finally, the best behavior is achieved when m_1 and m_2 are equal and larger than unity. Again, it is worth to mention that increasing the fading parameter of channels is beneficial at medium and high range of SNR values. On the other hand, it could be harmful on system performance when we talk about low range of SNR values.

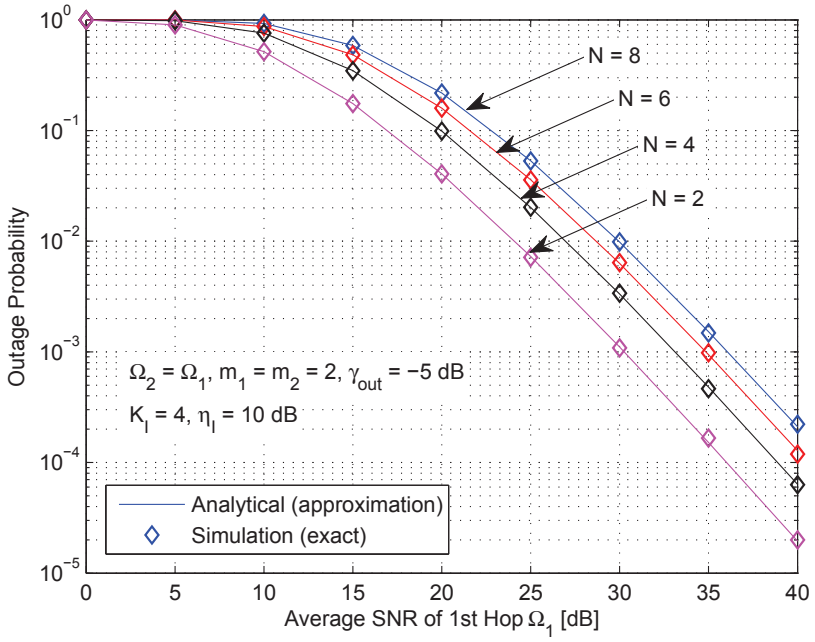

Figure 6.11: Outage probability vs average SNR for fixed-gain AF relay system with interference at destination for Nakagami-m/Rician fading scenario with different values of N.

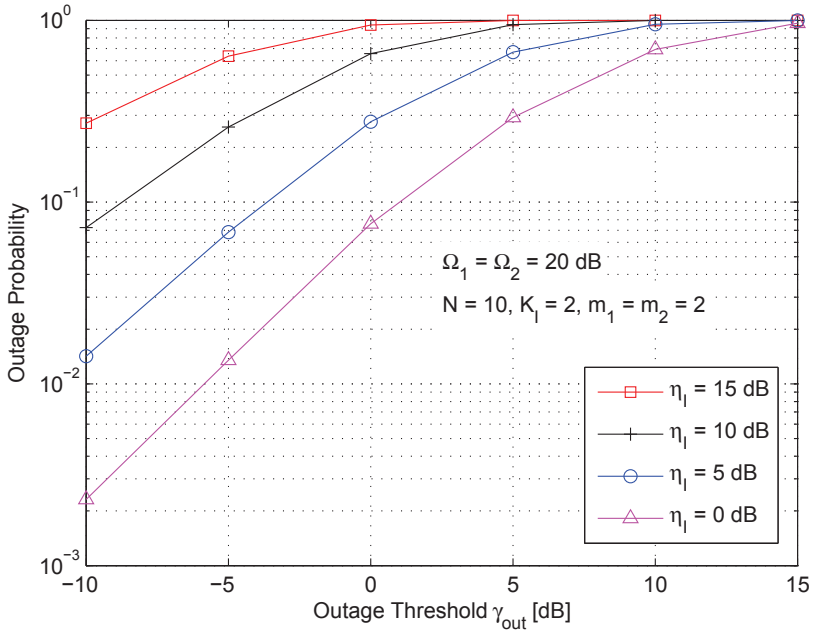

Figure 6.12: Outage probability vs outage threshold for fixed-gain AF relay system with interference at destination for Nakagami-m/Rician fading scenario with different values of η_I.

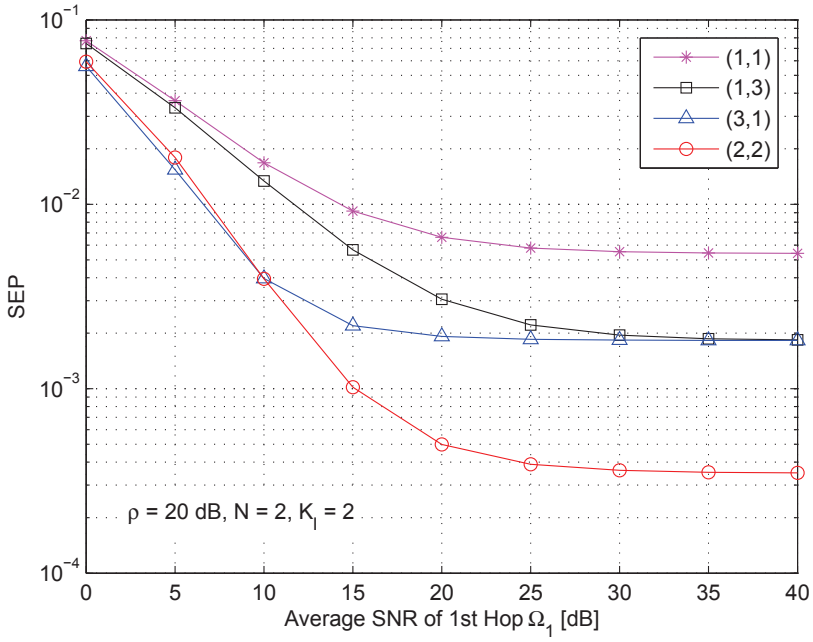

Figure 6.13: Average SEP vs average SNR for fixed-gain AF relay system with interference at destination for Nakagami-m/Rician fading scenario with different values of (m_1, m_2).

6.8 Conclusions

In this chapter, we investigated the performance of a dual-hop fixed-gain AF relay system with co-channel interference at the destination. We considered various fading scenarios; Rician/Nakagami-m, Rician/Rician, and Nakagami-m/Rician. We derived accurate approximate expressions for the outage probability and the SEP for all the proposed fading models. Furthermore, we studied the system performance of the proposed scenarios at high SNR regime. We evaluated asymptotic expressions for the outage probability and the SEP in addition to evaluating the system diversity order and coding gain. The analytical and asymptotic results were validated by Monte-Carlo simulations. A perfect fitting between both the achieved analytical results and the asymptotic results with Monte-Carlo simula-

tions was proved in some results. Also, for the case where the interference power does not scale with SNR, results showed that with different fading models for the interferers' channels, the interference is only affecting the system behavior through the coding gain without affecting the diversity order of the system. On the other hand, when the interference power scales with SNR, zero diversity gain is achieved for all fading scenarios. Other results illustrated the effect of number of interferers and the fading parameters on the system performance. Finally, results showed that approximating the Rician system model by the Nakagami-m one does not give accurate results at least in our presented study.

CHAPTER 7

CONCLUSIONS AND FUTURE RESEARCH

In this chapter, we summarize and discuss the main contributions of this dissertation and suggest some possible future research directions.

7.1 Summary of Contributions

An important contribution of this dissertation is the proposed two low-complexity SEC and SECps relay selection schemes for dual-hop CSI-assisted AF and DF relay systems. The main aim behind proposing these schemes is the critical need of relay systems for efficient relaying schemes with small number of channel estimations. In the case of CSI-assisted AF relay systems, closed-form expressions for the system outage probability and SEP were derived assuming Rayleigh fading channels. In addition, the system performance was studied at high SNR regime. It was proved that the proposed relaying schemes noticeably reduce the number

of channel estimations and hence, the system complexity compared to the opportunistic relaying, especially, when the switching threshold takes values that are comparable to the average SNR. Also, it was shown via the asymptotic analysis that the diversity order of the system with the two scheme is fixed at 2 and is not affected by the number of relays. In the case of DF relay systems, we derived exact closed-form expression for the system outage probability assuming Rayleigh fading channels. It was observed that the existence of interference in the considered system is severely limiting the gain achieved in performance when the SECps scheme is used compared to the conventional SEC scheme.

We also contributed in the area of opportunistic DF relay systems with interference at the relays and destination over Nakagami-m fading channels. Assuming this general fading model allowed for studying the effect of fading parameter on the system performance. We also studied the system behavior at the high SNR regime. It was observed that under the condition of finite number of interferers of finite powers, the system can still achieve full diversity order; whereas, a noise floor appears in the results and hence, a zero diversity gain is achieved when the interferers' powers scale with the SNR. Furthermore, it was shown that the interference effect at the destination is more severe on the system performance compared to the interference at the relay. It was also observed that having the fading parameter of the first hop better than that of the second hop gives better performance compared to the vise versa case.

As an effort to deal with the situation where the best relay is unavailable for

cooperation, we proposed the N^{th}-best relaying scheme where the second best or even the N^{th} best relay is selected to forward the source message to destination in case the best relay is busy. We derived exact closed-form expression and asymptotic high SNR approximation for the outage probability assuming Rayleigh fading channels. We observed that the outage probability increases as the order of relay increases. Also, it was shown that the diversity order linearly increases with the number of relays and linearly decreases with the order of the relay. Furthermore, we observed that the diversity order linearly increases with the number of active relays although one relay is being used only.

Our next contribution is in the area of fixed-gain AF relay systems with single relay and interference-limited destination. The proposed fading scenarios are applicable in micro-cellular mobile and indoor radio where a LOS propagation is existed between the BS and users in the desired cell. We derived approximate expressions for the outage probability and the SEP in addition to studying the performance at high SNR regime for some special cases of the proposed fading scenarios. We observed that with different fading models for interferers' channels, the interference is only affecting the system behavior through the coding gain while the diversity order remains constant. Also, we noticed that fading scenarios achieve zero diversity order when the power of one hop does not scale with the SNR. Finally, we illustrated that approximating the Rician fading model by the Nakagami-m does not give accurate results at least in our presented study.

7.2 Future Research

Cognitive networks is a hot area of research in these days. In such networks, an unlicensed user (secondary user) is allowed to share the spectrum of a licensed user (primary user) only if the later is found to be inactive. The issue of knowing whether the primary user is active or not is the responsibility of the secondary user. In situations where the secondary user fails in its decision, interference results between the transmissions of these two nodes. One research approach could be to study the performance of AF cognitive relay systems where a secondary user source and relays are interfering with a primary user. As a contribution over the existing work in this area is to utilize the low-complexity SEC and SECps relaying schemes presented in this dissertation to select among the relays in the secondary cell. In such systems, the issue that the statistics of the channels of the secondary cell nodes are being conditioned on that of the primary user is the most important issue to care of in the analysis.

Another relaying scheme that was presented in this dissertation and can be used in the aforementioned AF cognitive relay system is the N^{th}-best relay selection scheme. As mentioned before, this relaying scheme is very effective in situations where the best relay is busy in some scheduling and load balancing duties in other parts of the network. In such situations, the second-best or even the N^{th}-best relay could be selected to forward the source message to destination. With the SEC, SECps, and N^{th} relaying schemes, some performance measures like the outage probability and SEP can be derived and analyzed in addition to

evaluating the system behavior at high SNR values where more insights about system performance can be achieved.

Recently, the topic of channel estimation errors has become a hot area of research in relay networks. As known, in opportunistic relaying as an example, selecting the best relay among all relays requires estimating the channels of all relays. As a result to the fast variations in wireless channels and their quality, the channel coefficients could vary in a very fast manner. Therefore, the relay who is selected as the best at the time when relay channels are estimated could not be the best at the time of data transmission. A nice research avenue could be to study the channel estimation errors along with interference on the performance of DF relay systems with the SEC and SECps relay selection schemes. Also, the performance of N^{th} best DF relay systems with channel estimation errors and interference could be studied. For these systems, the outage probability and SEP can be evaluated and analyzed. Also, to have more about system insights, the system behavior can be studied at high SNR values where approximate expressions for the outage probability, SEP, diversity order, and coding gain can be derived and studied.

APPENDICES

APPENDIX A

APPENDIX FOR CHAPTER 2

A.1 Proof of Lemma 2.1 (for Section 2.4)

In this Appendix, we evaluate the outage probability for the case of i.n.d. relay paths of the proposed system. For i.n.d. relay channels, the CDF of γ_{SEC} in (2.5) can be written as [22]

$$F_{\gamma_{\text{SEC}}}(\gamma) = \begin{cases} \sum_{i=0}^{M-1} \pi_i F_{\gamma_i}(\gamma) \prod_{\substack{k=0 \\ k\neq i}}^{M-1} F_{\gamma_k}(\gamma_{\mathsf{T}}), & \gamma < \gamma_{\mathsf{T}}; \\ \sum_{i=0}^{M-1} \Bigg(\pi_i \prod_{k=1}^{M} F_{\gamma_k}(\gamma_{\mathsf{T}}) & \\ + \sum_{j=0}^{M-1} \pi_{((i-j))_M} \left[F_{\gamma_i}(\gamma) - F_{\gamma_i}(\gamma_{\mathsf{T}}) \right] & \\ \times \prod_{k=0}^{j-1} F_{\gamma_{((i-j+k))_M}}(\gamma_{\mathsf{T}}) \Bigg), & \gamma \geq \gamma_{\mathsf{T}}, \end{cases} \tag{A.1}$$

where M is the number of relays and γ_{T} is a predetermined switching threshold, $\pi_i, i = 0, \ldots, M-1$ are the stationary distribution of a M-state Markov chain and it is the probability that the i^{th} relay is chosen, and $((i-j))_M$ denotes $i-j$

modulo M. It is given by

$$\pi_i = \left[\sum_{j=0}^{M-1}\left(\frac{F_{\gamma_{M-1}(\gamma_\mathsf{T})}\left(1-F_{\gamma_j(\gamma_\mathsf{T})}\right)}{F_{\gamma_j(\gamma_\mathsf{T})}\left(1-F_{\gamma_{M-1}(\gamma_\mathsf{T})}\right)}\right)\right]^{-1}\frac{F_{\gamma_{M-1}(\gamma_\mathsf{T})}\left(1-F_{\gamma_i(\gamma_\mathsf{T})}\right)}{F_{\gamma_i(\gamma_\mathsf{T})}\left(1-F_{\gamma_{M-1}(\gamma_\mathsf{T})}\right)}. \tag{A.2}$$

For Rayleigh fading channels, the CDF and the PDF of the i^{th} relay path are respectively given by $F_{\gamma_i(\gamma)} = 1-\exp\left(-\frac{\gamma}{\bar{\gamma}_i}\right)$ and $f_{\gamma_i(\gamma)} = \frac{1}{\bar{\gamma}_i}\exp\left(-\frac{\gamma}{\bar{\gamma}_i}\right)$, where $\bar{\gamma}_i$ is the average power of the i^{th} path.

Differentiating (A.1) with respect to γ and upon taking the Laplace transform using $\int_0^\infty f_{\gamma_{\text{SEC}}}(\gamma)\ \exp(s\gamma)\,d\gamma$, and after some algebraic manipulations, the MGF of γ_{SEC} can be obtained as

$$\begin{aligned}\mathcal{M}_{\gamma_{\text{SEC}}}(s) = &\sum_{i=0}^{M-1}\pi_i\prod_{\substack{k=0\\k\neq i}}^{M-1}\left(1-\exp\left(-\frac{\gamma_\mathsf{T}}{\bar{\gamma}_k}\right)\right)\left[\frac{\left(1-\exp\left(-\left(\frac{1}{\bar{\gamma}_i}-s\right)\gamma_\mathsf{T}\right)\right)}{(1-\bar{\gamma}_i s)}\right]\\ &+\sum_{i=0}^{M-1}\sum_{j=0}^{M-1}\pi_{((i-j))_M}\prod_{k=0}^{j-1}\left(1-\exp\left(-\frac{\gamma_\mathsf{T}}{\bar{\gamma}_{((i-j+k))_M}}\right)\right)\left[\frac{\exp\left(-\left(\frac{1}{\bar{\gamma}_i}-s\right)\gamma_\mathsf{T}\right)}{(1-\bar{\gamma}_i s)}\right].\end{aligned} \tag{A.3}$$

As the MRC is used at the destination, the MGF of the total SNR at the MRC output is simply their multiplication $\mathcal{M}_{\gamma_{\mathsf{tot}}}(s) = \mathcal{M}_{\gamma_{\mathsf{S,D}}}(s)\mathcal{M}_{\gamma_{\text{SEC}}}(s)$.

Upon substituting the MGF of both the direct link $(1-\bar{\gamma}_{\mathsf{S,D}}s)^{-1}$ and that found in (A.3) in $\mathcal{M}_{\gamma_{\mathsf{tot}}}(s)$, and after using partial fraction operation, the MGF of the

total SNR at the output of SEC can be obtained as

$$\mathcal{M}_{\gamma_{\text{tot}}}(s) = \sum_{i=0}^{M-1} \pi_i \prod_{\substack{k=0 \\ k\neq i}}^{M-1} \left(1 - \exp\left(-\frac{\gamma_{\mathsf{T}}}{\bar{\gamma}_k}\right)\right) \left[\frac{(1-\bar{\gamma}_{\mathsf{S,D}} s)^{-1}}{\left(1-\frac{\bar{\gamma}_i}{\bar{\gamma}_{\mathsf{S,D}}}\right)} + \frac{(1-\bar{\gamma}_i s)^{-1}}{\left(1-\frac{\bar{\gamma}_{\mathsf{S,D}}}{\bar{\gamma}_i}\right)} \right.$$
$$\left. - \exp\left(-\left(\frac{1}{\bar{\gamma}_i} - s\right)\gamma_{\mathsf{T}}\right) \left\{ \frac{(1-\bar{\gamma}_{\mathsf{S,D}} s)^{-1}}{\left(1-\frac{\bar{\gamma}_i}{\bar{\gamma}_{\mathsf{S,D}}}\right)} + \frac{(1-\bar{\gamma}_i s)^{-1}}{\left(1-\frac{\bar{\gamma}_{\mathsf{S,D}}}{\bar{\gamma}_i}\right)} \right\} \right]$$
$$+ \sum_{i=0}^{M-1} \sum_{j=0}^{M-1} \pi_{((i-j))_M} \prod_{k=0}^{j-1} \left(1 - \exp\left(-\frac{\gamma_{\mathsf{T}}}{\bar{\gamma}_{((i-j+k))_M}}\right)\right)$$
$$\times \left[\exp\left(-\left(\frac{1}{\bar{\gamma}_i} - s\right)\gamma_{\mathsf{T}}\right) \left\{ \frac{(1-\bar{\gamma}_{\mathsf{S,D}} s)^{-1}}{\left(1-\frac{\bar{\gamma}_i}{\bar{\gamma}_{\mathsf{S,D}}}\right)} + \frac{(1-\bar{\gamma}_i s)^{-1}}{\left(1-\frac{\bar{\gamma}_{\mathsf{S,D}}}{\bar{\gamma}_i}\right)} \right\} \right]. \quad \text{(A.4)}$$

Taking the inverse Laplace transform of (A.4), the PDF of γ_{tot} can be obtained as

$$f_{\gamma_{\mathsf{tot}}}(\gamma) = \sum_{i=0}^{M-1} \pi_i \prod_{\substack{k=0 \\ k\neq i}}^{M-1} \left(1 - \exp\left(-\frac{\gamma_{\mathsf{T}}}{\bar{\gamma}_k}\right)\right) \left[\frac{\exp\left(-\frac{\gamma}{\bar{\gamma}_{\mathsf{S,D}}}\right)}{\bar{\gamma}_{\mathsf{S,D}}\left(1-\frac{\bar{\gamma}_i}{\bar{\gamma}_{\mathsf{S,D}}}\right)} + \frac{\exp\left(-\frac{\gamma}{\bar{\gamma}_i}\right)}{\bar{\gamma}_i\left(1-\frac{\bar{\gamma}_{\mathsf{S,D}}}{\bar{\gamma}_i}\right)} \right.$$
$$\left. - \exp\left(-\frac{\gamma_{\mathsf{T}}}{\bar{\gamma}_i}\right) \left\{ \frac{\exp\left(-\frac{1}{\bar{\gamma}_{\mathsf{S,D}}}(\gamma-\gamma_{\mathsf{T}})\right)}{\bar{\gamma}_{\mathsf{S,D}}\left(1-\frac{\bar{\gamma}_i}{\bar{\gamma}_{\mathsf{S,D}}}\right)} + \frac{\exp\left(-\frac{1}{\bar{\gamma}_i}(\gamma-\gamma_{\mathsf{T}})\right)}{\bar{\gamma}_i\left(1-\frac{\bar{\gamma}_{\mathsf{S,D}}}{\bar{\gamma}_i}\right)} \right\} U(\gamma-\gamma_{\mathsf{T}}) \right]$$
$$+ \sum_{i=0}^{M-1} \sum_{j=0}^{M-1} \pi_{((i-j))_M} \prod_{k=0}^{j-1} \left(1 - \exp\left(-\frac{\gamma_{\mathsf{T}}}{\bar{\gamma}_{((i-j+k))_M}}\right)\right)$$
$$\left[\exp\left(-\frac{\gamma_{\mathsf{T}}}{\bar{\gamma}_i}\right) \left\{ \frac{\exp\left(-\frac{1}{\bar{\gamma}_{\mathsf{S,D}}}(\gamma-\gamma_{\mathsf{T}})\right)}{\bar{\gamma}_{\mathsf{S,D}}\left(1-\frac{\bar{\gamma}_i}{\bar{\gamma}_{\mathsf{S,D}}}\right)} + \frac{\exp\left(-\frac{1}{\bar{\gamma}_i}(\gamma-\gamma_{\mathsf{T}})\right)}{\bar{\gamma}_i\left(1-\frac{\bar{\gamma}_{\mathsf{S,D}}}{\bar{\gamma}_i}\right)} \right\} \right]. \quad \text{(A.5)}$$

where $U(.)$ is the unit step function. The CDF of γ_{tot} can be obtained by integrating (A.5) with respect to γ using $\int_{-\infty}^{\gamma} f_{\gamma_{\mathsf{tot}}}(\lambda)d\lambda$, and after some algebraic manipulations, the outage probability for the case of i.n.d. relay paths can be

obtained in a closed-form expression as in (2.8).

A.2 Proof of Lemma 2.2 (for Section 2.4)

In this Appendix, we evaluate the SEP for the case of i.n.d. relay paths of the proposed system. The average SEP for BPSK signals in terms of the MGF is given by [22]

$$\mathsf{SEP} = \frac{1}{\pi}\int_0^{\pi/2} M_{\gamma_{\mathsf{tot}}}\left(-\frac{1}{\sin^2\phi}\right) d\phi. \tag{A.6}$$

Upon substituting (A.5) in (A.6), we get

$$\begin{aligned}
\mathsf{SEP} = \sum_{i=0}^{M-1}\pi_i \prod_{\substack{k=0\\k\neq i}}^{M-1}\left(1-\exp\left(-\frac{\gamma_{\mathsf{T}}}{\bar{\gamma}_k}\right)\right)\Bigg[&\frac{1}{\left(1-\frac{\bar{\gamma}_i}{\bar{\gamma}_{\mathsf{S,D}}}\right)}\underbrace{\frac{1}{\pi}\int_0^{\pi/2}\frac{\sin^2\phi}{\sin^2\phi+\bar{\gamma}_{\mathsf{S,D}}}\,d\phi}_{I_1}\\
+\frac{1}{\left(1-\frac{\bar{\gamma}_{\mathsf{S,D}}}{\bar{\gamma}_i}\right)}&\underbrace{\frac{1}{\pi}\int_0^{\pi/2}\frac{\sin^2\phi}{\sin^2\phi+\bar{\gamma}_i}\,d\phi}_{I_2}-\exp\left(-\frac{\gamma_{\mathsf{T}}}{\bar{\gamma}_i}\right)\Bigg\{\frac{1}{\left(1-\frac{\bar{\gamma}_i}{\bar{\gamma}_{\mathsf{S,D}}}\right)}\\
\times&\underbrace{\frac{1}{\pi}\int_0^{\pi/2}\frac{\sin^2\phi\exp\left(-\frac{\gamma_{\mathsf{T}}}{\sin^2\phi}\right)}{\sin^2\phi+\bar{\gamma}_{\mathsf{S,D}}}\,d\phi}_{I_3}+\frac{1}{\left(1-\frac{\bar{\gamma}_{\mathsf{S,D}}}{\bar{\gamma}_i}\right)}\underbrace{\frac{1}{\pi}\int_0^{\pi/2}\frac{\sin^2\phi\exp\left(-\frac{\gamma_{\mathsf{T}}}{\sin^2\phi}\right)}{\sin^2\phi+\bar{\gamma}_i}\,d\phi}_{I_4}\Bigg\}\Bigg]\\
+\sum_{i=0}^{M-1}\sum_{j=0}^{M-1}\pi_{((i-j))_M}\prod_{k=0}^{j-1}\left(1-\exp\left(-\frac{\gamma_{\mathsf{T}}}{\bar{\gamma}_{((i-j+k))_M}}\right)\right)\Bigg[&\exp\left(-\frac{\gamma_{\mathsf{T}}}{\bar{\gamma}_i}\right)\Bigg\{\frac{1}{\left(1-\frac{\bar{\gamma}_i}{\bar{\gamma}_{\mathsf{S,D}}}\right)}\\
\times&\underbrace{\frac{1}{\pi}\int_0^{\pi/2}\frac{\sin^2\phi\ \exp\left(-\frac{\gamma_{\mathsf{T}}}{\sin^2\phi}\right)}{\sin^2\phi+\bar{\gamma}_{\mathsf{S,D}}}\,d\phi}_{I_3}+\frac{1}{\left(1-\frac{\bar{\gamma}_{\mathsf{S,D}}}{\bar{\gamma}_i}\right)}\underbrace{\frac{1}{\pi}\int_0^{\pi/2}\frac{\sin^2\phi\ \exp\left(-\frac{\gamma_{\mathsf{T}}}{\sin^2\phi}\right)}{\sin^2\phi+\bar{\gamma}_i}\,d\phi}_{I_4}\Bigg\}\Bigg].
\end{aligned} \tag{A.7}$$

With the help of [22, Eq. (5A.9)], the integrals I_1 and I_2 can be respectively evaluated as follows

$$I_1 = \frac{1}{2}\left(1 - \sqrt{\frac{\bar{\gamma}_{\mathsf{S,D}}}{1+\bar{\gamma}_{\mathsf{S,D}}}}\right), \tag{A.8}$$

$$I_2 = \frac{1}{2}\left(1 - \sqrt{\frac{\bar{\gamma}_{i}}{1+\bar{\gamma}_{i}}}\right). \tag{A.9}$$

In evaluating the integral I_3, upon adding and subtracting $\bar{\gamma}_{\mathsf{S,D}}$ to and from its numerator, we obtain

$$I_3 = \frac{1}{\pi}\int_0^{\pi/2} \exp\left(-\frac{\gamma_{\mathsf{T}}}{\sin^2\phi}\right)\, d\phi - \underbrace{\frac{1}{\pi}\int_0^{\pi/2} \frac{\bar{\gamma}_{\mathsf{S,D}} \exp\left(-\frac{\gamma_{\mathsf{T}}}{\sin^2\phi}\right)}{\sin^2\phi + \bar{\gamma}_{\mathsf{S,D}}}\, d\phi}_{I_{3a}}, \tag{A.10}$$

where the first part in (A.10) is the well known Gaussian Q-function given by $Q\left(\sqrt{2\gamma_{\mathsf{T}}}\right)$.

In evaluating the integral I_{3a}, we apply the change of variables

$$w = \sqrt{\frac{\gamma_{\mathsf{T}}}{\sin^2\phi} - \gamma_{\mathsf{T}}} = \sqrt{\gamma_{\mathsf{T}}}\cot\phi. \tag{A.11}$$

Then, it can easily be shown that

$$dw = -\frac{(w^2+\gamma_{\mathsf{T}})}{\sqrt{\gamma_{\mathsf{T}}}} d\phi. \tag{A.12}$$

Upon substituting (A.11) and (A.12) in (A.10), and after few simple algebraic steps, we obtain

$$I_{3a} = \frac{\sqrt{\gamma_{\mathsf{T}}}\exp\left(-\gamma_{\mathsf{T}}\right)}{\pi}\int_0^{\infty}\frac{\exp\left(-w^2\right)}{w^2+\gamma_{\mathsf{T}}+\frac{\gamma_{\mathsf{T}}}{\bar{\gamma}_{\mathsf{S,D}}}}\,dw. \tag{A.13}$$

With the help of [42, Eq. 3.466.1], and after simple algebraic steps, we get

$$I_{3a} = \frac{1}{\sqrt{1+\frac{1}{\bar{\gamma}_{\mathsf{S,D}}}}}\exp\left(\frac{\gamma_{\mathsf{T}}}{\bar{\gamma}_{\mathsf{S,D}}}\right)Q\left(\sqrt{2\gamma_{\mathsf{T}}+\frac{2\gamma_{\mathsf{T}}}{\bar{\gamma}_{\mathsf{S,D}}}}\right). \tag{A.14}$$

Upon substituting $Q\left(\sqrt{2\gamma_{\mathsf{T}}}\right)$ and (A.14) in (A.10), the last result of I_3 becomes

$$I_3 = Q\left(\sqrt{2\gamma_{\mathsf{T}}}\right) - \frac{1}{\sqrt{1+\frac{1}{\bar{\gamma}_{\mathsf{S,D}}}}}\exp\left(\frac{\gamma_{\mathsf{T}}}{\bar{\gamma}_{\mathsf{S,D}}}\right)Q\left(\sqrt{2\gamma_{\mathsf{T}}+\frac{2\gamma_{\mathsf{T}}}{\bar{\gamma}_{\mathsf{S,D}}}}\right). \tag{A.15}$$

The integral I_4 can be evaluated by following the same steps as in the case of I_3. It can be obtained as

$$I_4 = Q\left(\sqrt{2\gamma_{\mathsf{T}}}\right) - \frac{1}{\sqrt{1+\frac{1}{\bar{\gamma}_i}}}\exp\left(\frac{\gamma_{\mathsf{T}}}{\bar{\gamma}_i}\right)Q\left(\sqrt{2\gamma_{\mathsf{T}}+\frac{2\gamma_{\mathsf{T}}}{\bar{\gamma}_i}}\right). \tag{A.16}$$

Finally, upon substituting (A.8), (A.9), (A.15), and (A.16) in (A.7), and after few simple manipulations, the SEP for the case of i.n.d. relay paths can be obtained in a closed-form expression as in (2.11).

APPENDIX B

APPENDIX FOR CHAPTER 3

B.1 Proof of Lemma 3.1 (for Section 3.4.1)

In this Appendix, we evaluate the first term $\mathrm{P_r}\left[\gamma_{\mathsf{d}} < u | C_L\right]$ in (3.7). The e2e SINR can be written as a ratio of two RVs $\gamma_{\mathsf{d}} = Y_1/Z_1$.

Proposition B.1 *The PDF of* $Z_1 = \sum_{i_d=1}^{I_d} \rho_I |h^I_{i_d,\mathsf{d}}|^2 + 1$ *is given by*

$$f_{Z_1}(z) = \prod_{i_d=1}^{I_d} \lambda^I_{i_d,\mathsf{d}} \exp\left(\lambda^I_{i_d,\mathsf{d}}\right) \sum_{g=1}^{I_d} \frac{\exp\left(-\lambda^I_{i_d,\mathsf{d}} z\right)}{\prod_{\substack{m=1 \\ m\neq g}}^{I_d} \left(\lambda^I_{m,\mathsf{d}} - \lambda^I_{g,\mathsf{d}}\right)}. \tag{B.1}$$

Proof. The RV Z_1 can be written as

$$Z_1 = \sum_{i_d=1}^{I_d} \rho_I |h^I_{i_d,\mathsf{d}}|^2 + 1 = X_1 + 1. \tag{B.2}$$

The PDF of X_1 is given by

$$f_{X_1}(x) = \prod_{i_d=1}^{I_d} \lambda^I_{i_d,\mathsf{d}} \sum_{g=1}^{I_d} \frac{\exp\left(-\lambda^I_{i_d,\mathsf{d}} x\right)}{\prod_{\substack{m=1 \\ m\neq g}}^{I_d} \left(\lambda^I_{m,\mathsf{d}} - \lambda^I_{g,\mathsf{d}}\right)}. \tag{B.3}$$

Using the transformation of RVs for $Z_1 = X_1 + 1$, the PDF of Z_1 can be obtained as in (B.1). ∎

Proposition B.2 *The PDF of* $Y_1 = \rho|h_{\mathsf{s},\mathsf{d}}|^2 + \rho|h_{\mathrm{SEC},\mathsf{d}}|^2$ *with* $\left|C_L\right| = L$, $L \geq 1$ *is given by*

$$f_{Y_1}(\gamma) = \sum_{i=0}^{L-1} \pi_i \prod_{\substack{k=0 \\ k\neq i}}^{L-1} \left(1 - \exp\left(-\lambda_{k,\mathsf{d}}\gamma_{\mathsf{T}}\right)\right) \left[\frac{\exp\left(-\lambda_{\mathsf{s},\mathsf{d}}\gamma\right)}{\left(\frac{1}{\lambda_{\mathsf{s},\mathsf{d}}} - \frac{1}{\lambda_{i,\mathsf{d}}}\right)} + \frac{\exp\left(-\lambda_{i,\mathsf{d}}\gamma\right)}{\left(\frac{1}{\lambda_{i,\mathsf{d}}} - \frac{1}{\lambda_{\mathsf{s},\mathsf{d}}}\right)} - \exp\left(-\lambda_{i,\mathsf{d}}\gamma_{\mathsf{T}}\right) \right.$$
$$\left. \times \left\{\Upsilon_3 + \Upsilon_4\right\} U(\gamma - \gamma_{\mathsf{T}}) \right] + \sum_{i=0}^{L-1} \sum_{j=0}^{L-1} \pi_{((i-j))_L} \prod_{k=0}^{j-1} \left(1 - \exp\left(-\lambda_{((i-j+k))_L,\mathsf{d}}\gamma_{\mathsf{T}}\right)\right)$$
$$\times \left[\exp\left(-\frac{\gamma_{\mathsf{T}}}{\bar{\gamma}_{i,\mathsf{d}}}\right) \left\{\Upsilon_3 + \Upsilon_4\right\} \right], \tag{B.4}$$

where $\Upsilon_3 = \exp\left(-\lambda_{\mathsf{s},\mathsf{d}}\left(\gamma - \gamma_{\mathsf{T}}\right)\right) \Big/ \left(\frac{1}{\lambda_{\mathsf{s},\mathsf{d}}} - \frac{1}{\lambda_{i,\mathsf{d}}}\right)$, $\Upsilon_4 = \exp\left(-\lambda_{i,\mathsf{d}}\big(\gamma - \gamma_{\mathsf{T}}\big)\right) \Big/ \left(\frac{1}{\lambda_{i,\mathsf{d}}} - \frac{1}{\lambda_{\mathsf{s},\mathsf{d}}}\right)$.

Proof. In finding this PDF, we use the MGF approach. The CDF of $\rho|h_{\mathrm{SEC},\mathsf{d}}|^2$ can be written as in (A.1). For Rayleigh fading channels, the CDF and the PDF of the i^{th} relay path are respectively given by $F_{\rho|h_{i,\mathsf{d}}|^2}(\gamma) = 1 - \exp\left(-\lambda_{i,\mathsf{d}}\gamma\right)$ and $f_{\rho|h_{i,\mathsf{d}}|^2}(\gamma) = \lambda_{i,\mathsf{d}} \exp\left(-\lambda_{i,\mathsf{d}}\gamma\right)$, where $\lambda_{i,\mathsf{d}}$ is the rate of the channel between the i^{th} relay and the destination.

Differentiating (A.1) with respect to γ and upon taking the Laplace transform us-

ing $\int_0^\infty f_{\rho|h_{\mathrm{SEC,d}}|^2}(\gamma)\ \exp(s\gamma)\,d\gamma$, and after some algebraic manipulations, the MGF of $\rho|h_{\mathrm{SEC,d}}|^2$ can be obtained as

$$\mathcal{M}_{\rho|h_{\mathrm{SEC,d}}|^2}(s) = \sum_{i=0}^{L-1}\pi_i \prod_{\substack{k=0\\k\neq i}}^{L-1}\left(1-\exp\left(-\lambda_{k,\mathsf{d}}\gamma_{\mathsf{T}}\right)\right)\left[\frac{\left(1-\exp\left(-\left(\lambda_{i,\mathsf{d}}-s\right)\gamma_{\mathsf{T}}\right)\right)}{\left(1-\frac{s}{\lambda_{i,\mathsf{d}}}\right)}\right]$$
$$+\sum_{i=0}^{L-1}\sum_{j=0}^{L-1}\pi_{((i-j))_L}\prod_{k=0}^{j-1}\left(1-\exp\left(-\lambda_{((i-j+k))_L,\mathsf{d}}\gamma_{\mathsf{T}}\right)\right)\left[\frac{\exp\left(-\left(\lambda_{i,\mathsf{d}}-s\right)\gamma_{\mathsf{T}}\right)}{\left(1-\frac{s}{\lambda_{i,\mathsf{d}}}\right)}\right]. \tag{B.5}$$

As the MRC is used at the destination, the MGF of the total SNR at the MRC output is simply their multiplication $\mathcal{M}_{Y_1}(s) = \mathcal{M}_{\rho|h_{\mathsf{s,d}}|^2}(s)\mathcal{M}_{\rho|h_{\mathrm{SEC,d}}|^2}(s)$.
Upon substituting the MGF of both the direct link $\left(1-\frac{s}{\lambda_{\mathsf{s,d}}}\right)^{-1}$ and that derived in (B.5) in $\mathcal{M}_{\rho|h_{\mathrm{SEC,d}}|^2}(s)$, and after using partial fraction operation, the MGF of Y_1 can be obtained as

$$\mathcal{M}_{Y_1}(s) = \sum_{i=0}^{L-1}\pi_i \prod_{\substack{k=0\\k\neq i}}^{L-1}\left(1-\exp\left(-\lambda_{k,\mathsf{d}}\gamma_{\mathsf{T}}\right)\right)\left[\Upsilon_1+\Upsilon_2-\exp\left(-\left(\lambda_{i,\mathsf{d}}-s\right)\gamma_{\mathsf{T}}\right)\left\{\Upsilon_1+\Upsilon_2\right\}\right]$$
$$+\sum_{i=0}^{L-1}\sum_{j=0}^{L-1}\pi_{((i-j))_L}\prod_{k=0}^{j-1}\left(1-\exp\left(-\lambda_{((i-j+k))_L,\mathsf{d}}\gamma_{\mathsf{T}}\right)\right)\left[\exp\left(-\left(\lambda_{i,\mathsf{d}}-s\right)\gamma_{\mathsf{T}}\right)\left\{\Upsilon_1+\Upsilon_2\right\}\right], \tag{B.6}$$

where $\Upsilon_1 = \left(1-\frac{s}{\lambda_{\mathsf{s,d}}}\right)^{-1}\Big/\left(1-\frac{\lambda_{\mathsf{s,d}}}{\lambda_{i,\mathsf{d}}}\right)$ and $\Upsilon_2 = \left(1-\frac{s}{\lambda_{i,\mathsf{d}}}\right)^{-1}\Big/\left(1-\frac{\lambda_{i,\mathsf{d}}}{\lambda_{\mathsf{s,d}}}\right)$.
Taking the inverse Laplace transform of (B.6), the PDF of Y_1 can be obtained as in (B.4).

Now, the CDF of γ_{d} can be obtained using

$$\mathrm{P_r}\left[\gamma_{\mathsf{d}} < u | C_L\right] = \int_1^{\infty} f_Z(z) \int_0^{uz} f_Y(y) dy dz. \tag{B.7}$$

Upon substituting (B.1) and (B.4) in (B.7), and with the help of [42, Eq. (3.351.2)] and after some algebraic manipulations, we obtain the result in (3.8). ∎

B.2 Proof of Lemma 3.2 (for Section 3.4.1)

In this Appendix, we evaluate the second term $\mathrm{P_r}\left[C_L\right]$ in (3.7). To evaluate this term, we first need to find the CDF of $\gamma_{\mathsf{s},k}$. This RV can be written as Y_a/Z_a, where Y_a has an Exponential distribution as given in Appendix B.1, and the PDF of Z_a is as derived in (B.1) with replacing i_d by i_k and d by k. The CDF of $\gamma_{\mathsf{s},k}$ can be obtained using the integration in (B.7). Upon substituting the PDF of Y_a and that of Z_a in (B.7), and with the help of [42, Eq. (3.351.2)] and after some algebraic manipulations, we obtain the result in (3.9).

APPENDIX C

APPENDIX FOR CHAPTER 4

C.1 Proof of Lemma 4.1 (for Section 4.4.1)

In this Appendix, we evaluate the first term $\mathrm{P_r}\left[\gamma_{\mathsf{d}} < u | C_L\right]$ in (3.7). The e2e SINR γ_{d} can be written as a ratio of two RVs $\gamma_{\mathsf{d}} = Y/Z$. The proof is carried out through the following series of results.

Proposition C.1 *The PDF of* $Z = \sum_{i_d=1}^{I_d} \rho_I |h_{i_d,\mathsf{d}}^I|^2 + 1 = X + 1$ *is given by*

$$f_Z(z) = -\sum_{i_d=1}^{I_d} (-1)^{m_{i_d,\mathsf{d}}^I} \exp\left(\alpha_{i_d,\mathsf{d}}^I\right) \sum_{i=1}^{m_{i_d,\mathsf{d}}^I} \frac{\beta_{i_d}^{i-1}}{(i-1)!} \sum_{g=0}^{m_{i_d,\mathsf{d}}^I - 1} \binom{m_{i_d,\mathsf{d}}^I - 1}{g} (-1)^g z^g \exp\left(-\alpha_{i_d,\mathsf{d}}^I z\right). \tag{C.1}$$

Proof. The PDF of X is given by

$$f_X(x) = \sum_{i_d=1}^{I_d} \sum_{i=1}^{m_{i_d,\mathsf{d}}^I} \frac{\beta_{i_d}^{i-1} x^{m_{i_d,\mathsf{d}}^I - 1}}{(i-1)!} \exp\left(-\alpha_{i_d,\mathsf{d}}^I x\right), \tag{C.2}$$

where $\beta_{i_d}^{i-1} = \frac{\prod_{l=1}^{I_d}\left(\alpha_{l,\mathsf{d}}^I\right)^{m_{l,\mathsf{d}}^I}}{(m_{i_d,\mathsf{d}}^I - i)!}\frac{d^{i-1}}{ds^{i-1}}\left[\prod_{\substack{n=1\\ n\neq i_d}}^{N}\left(\alpha_{n,\mathsf{d}}^I + s\right)^{-m_{n,\mathsf{d}}^I}\right]\Big|_{s=\alpha_{i_d,\mathsf{d}}^I}$.
Using the transformation of RVs for $Z = X + 1$, we get

$$f_Z(z) = \sum_{i_d=1}^{I_d}\sum_{i=1}^{m_{i_d,\mathsf{d}}^I}\frac{\beta_{i_d}^{i-1}(z-1)^{m_{i_d,\mathsf{d}}^I - 1}}{(i-1)!}\exp\left(-\alpha_{i_d,\mathsf{d}}^I(z-1)\right), \tag{C.3}$$

Now, using the Binomial formula, we can obtain the result in (C.1). ∎

Proposition C.2 *Let $Y = \rho|h_{\mathsf{s},\mathsf{d}}|^2 + \rho|h_{b,\mathsf{d}}|^2$ with $\left|C_L\right| = L$, $L \geq 1$. The PDF of Y is given by*

$$f_Y(y) = C_a\sum_{r=0}^{m_{\mathsf{s},\mathsf{d}}-1}\binom{m_{\mathsf{s},\mathsf{d}}-1}{r}(-1)^r\sum_{l=1}^{L}C_b(l)\Bigg[\frac{C_1(r,l)!}{C_2(l)^{m_{l,\mathsf{d}}+r}}y^{m_{\mathsf{s},\mathsf{d}}-r-1}\exp\left(-\frac{m_{\mathsf{s},\mathsf{d}}}{\Omega_{\mathsf{s},\mathsf{d}}}y\right)$$
$$-\sum_{k_1=0}^{C_1(r,l)}\frac{C_1(r,l)!}{k_1!C_2(l)^{m_{l,\mathsf{d}}+r-k_1}}y^{m_{\mathsf{s},\mathsf{d}}-r+k_1-1}\exp\left(-\frac{m_{l,\mathsf{d}}}{\Omega_{l,\mathsf{d}}}y\right) + \sum_{n=1}^{L}(-1)^n\sum_{j_1<\cdots<j_n,j_{(.)}\neq l}\ \sum_{q_1=\cdots=q_n=0}$$
$$\frac{\prod_{w=1}^{n}\left(\frac{m_{j_w,\mathsf{d}}}{\Omega_{j_w,\mathsf{d}}}\right)^{q_w}}{\prod_{p=1}^{n}q_p!}\Bigg\{\frac{C_6(r,l,q_i)!y^{m_{\mathsf{s},\mathsf{d}}-r-1}}{C_7(l,j_s)^{\sum_{i=1}^{n}q_i+m_{l,\mathsf{d}}+r}}\exp\left(-\frac{m_{\mathsf{s},\mathsf{d}}}{\Omega_{\mathsf{s},\mathsf{d}}}y\right) - \sum_{k_2=0}^{C_6(r,l,q_i)}\frac{C_6(r,l,q_i)!}{k_2!C_7(l,j_s)^{\sum_{i=1}^{n}q_i+m_{l,\mathsf{d}}+r-k_2}}$$
$$\times\, y^{m_{\mathsf{s},\mathsf{d}}-r+k_2-1}\exp\left(-\left(\sum_{s=1}^{n}\frac{m_{j_s,\mathsf{d}}}{\Omega_{j_s,\mathsf{d}}} + \frac{m_{l,\mathsf{d}}}{\Omega_{l,\mathsf{d}}}\right)y\right)\Bigg\}\Bigg], \tag{C.4}$$

where $C_a = \frac{m_{\mathsf{s},\mathsf{d}}^{m_{\mathsf{s},\mathsf{d}}}}{\Omega_{\mathsf{s},\mathsf{d}}^{m_{\mathsf{s},\mathsf{d}}}\Gamma(m_{\mathsf{s},\mathsf{d}})}$, $C_b(l) = \frac{m_{l,\mathsf{d}}^{m_{l,\mathsf{d}}}}{\Omega_{l,\mathsf{d}}^{m_{l,\mathsf{d}}}\Gamma(m_{l,\mathsf{d}})}$, $C_1(r,l) = m_{l,\mathsf{d}} + r - 1$, $C_2(l) = \frac{m_{l,\mathsf{d}}}{\Omega_{l,\mathsf{d}}} - \frac{m_{\mathsf{s},\mathsf{d}}}{\Omega_{\mathsf{s},\mathsf{d}}}$, $C_6(r,l,q_i) = \sum_{i=1}^{n}q_i + m_{l,\mathsf{d}} + r - 1$, and $C_7(l,j_s) = \sum_{s=1}^{n}\frac{m_{j_s,\mathsf{d}}}{\Omega_{j_s,\mathsf{d}}} + \frac{m_{l,\mathsf{d}}}{\Omega_{l,\mathsf{d}}} - \frac{m_{\mathsf{s},\mathsf{d}}}{\Omega_{\mathsf{s},\mathsf{d}}}$.

Proof. The PDF of $\rho|h_{b,\mathsf{d}}|^2$ given C_L can be written as

$$f_{\rho|h_{b,\mathsf{d}}|^2}(\tau) = \sum_{l=1}^{L}f_{\rho|h_{l,\mathsf{d}}|^2}(\tau)\prod_{\substack{i=1\\ i\neq l}}^{L}F_{\rho|h_{i,\mathsf{d}}|^2}(\tau). \tag{C.5}$$

For Nakagami-m fading, the PDF of $\rho|h_{l,\mathsf{d}}|^2$ and the CDF of $\rho|h_{m,\mathsf{d}}|^2$ are respectively given by $f_{\rho|h_{l,\mathsf{d}}|^2}(\tau) = \frac{m_{l,\mathsf{d}}^{m_{l,\mathsf{d}}}\tau^{m_{l,\mathsf{d}}-1}}{\Omega_{l,\mathsf{d}}^{m_{l,\mathsf{d}}}\Gamma(m_{l,\mathsf{d}})}\exp\left(-\frac{m_{l,\mathsf{d}}}{\Omega_{l,\mathsf{d}}}\tau\right)$, $F_{\rho|h_{i,\mathsf{d}}|^2}(\tau) = 1 - \sum_{q=0}^{m_{i,\mathsf{d}}-1}\frac{1}{q!}\left(\frac{m_{i,\mathsf{d}}}{\Omega_{i,\mathsf{d}}}\right)^q\tau^q\exp\left(-\frac{m_{i,\mathsf{d}}}{\Omega_{i,\mathsf{d}}}\tau\right)$. Upon substituting these statistics in (C.5) and after some algebraic manipulations, we get

$$f_{\rho|h_{b,\mathsf{d}}|^2}(\tau) = \sum_{l=1}^{L}\frac{m_{l,\mathsf{d}}^{m_{l,\mathsf{d}}}\tau^{m_{l,\mathsf{d}}-1}}{\Omega_{l,\mathsf{d}}^{m_{l,\mathsf{d}}}\Gamma(m_{l,\mathsf{d}})}\exp\left(-\frac{m_{l,\mathsf{d}}}{\Omega_{l,\mathsf{d}}}\tau\right)\left[1+\sum_{n=1}^{L}(-1)^n\sum_{\substack{j_1=1\\ j_1\neq l}}^{L-n+1}\sum_{\substack{j_2=j_1+1\\ j_2\neq l}}^{L-n+2}\cdots\sum_{\substack{j_n=j_{n-1}+1\\ j_n\neq l}}^{L}\right.$$
$$\left.\sum_{q_1=0}^{m_{j_1,\mathsf{d}}-1}\sum_{q_2=0}^{m_{j_2,\mathsf{d}}-1}\cdots\sum_{q_n=0}^{m_{j_n,\mathsf{d}}-1}\frac{\prod_{w=1}^{n}\left(\frac{m_{j_w,\mathsf{d}}}{\Omega_{j_w,\mathsf{d}}}\right)^{q_w}}{\prod_{p=1}^{n}q_p!}\tau^{\sum_{i=1}^{n}q_i}\exp\left(-\sum_{s=1}^{n}\frac{m_{j_s,\mathsf{d}}}{\Omega_{j_s,\mathsf{d}}}\tau\right)\right]. \tag{C.6}$$

We then can obtain the PDF of Y using $f_Y(y) = \int_0^y f_{\rho|h_{\mathsf{s},\mathsf{d}}|^2}(y-\tau)f_{\rho|h_{b,\mathsf{d}}|^2}(\tau)d\tau$ as in (C.4). ∎

Using the results of Proposition 1 and Proposition 2, we can obtain the CDF of $\gamma_{\mathsf{d}} = Y/Z$ as in (4.4) using (B.7).

C.2 Proof of Lemma 4.2 (for Section 4.4.1)

In this Appendix, we evaluate the second term $\mathrm{P_r}[C_L]$ in (3.7). The SINR $\gamma_{\mathsf{s},k}$ can be written as Y_1/Z_1, where the PDF of Y_1 is similar to $f_{\rho|h_{l,\mathsf{d}}|^2}(\tau)$ with replacing l by s and d by k, and the PDF of Z_1 is similar to that derived in (C.1) with replacing i_d by i_k and d by k.

Now, using the integral in (B.7) and with replacing Y by Y_1 and Z by Z_1, and after some algebraic manipulations, the CDF of $\gamma_{\mathsf{s},k}$ can be obtained as in (4.5).

C.3 Proof of Theorem 5.1 (for Section 5.4)

In this Appendix, we evaluate the first term in (3.7) $\mathrm{P_r}\left[\gamma_{\mathsf{d}} < u | C_L\right]$. The e2e SINR can be written as $\gamma_{\mathsf{d}} = Y_1/Z_1$. The CDF of γ_{d} given a decoding set C_L can be obtained using (B.7).

First, we evaluate the PDF of $Z_1 = \sum_{i_{d=1}}^{I_d} \rho_I |h_{i_d,\mathsf{d}}^I|^2 + 1 = X_1 + 1$, where the PDF of X_1 is given by $f_{X_1}(x) = \prod_{i_d=1}^{I_d} \lambda_{i_d,\mathsf{d}}^I \sum_{g=1}^{I_d} \frac{\exp\left(-\lambda_{i_d,\mathsf{d}}^I x\right)}{\prod_{\substack{m=1 \\ m\neq g}}^{I_d} \left(\lambda_{m,\mathsf{d}}^I - \lambda_{g,\mathsf{d}}^I\right)}$.

Using the transformation of RVs, we get

$$f_{Z_1}(z) = \prod_{i_d=1}^{I_d} \lambda_{i_d,\mathsf{d}}^I \exp\left(\lambda_{i_d,\mathsf{d}}^I\right) \sum_{g=1}^{I_d} \frac{\exp\left(-\lambda_{i_d,\mathsf{d}}^I z\right)}{\prod_{\substack{m=1 \\ m\neq g}}^{I_d} \left(\lambda_{m,\mathsf{d}}^I - \lambda_{g,\mathsf{d}}^I\right)}. \tag{C.7}$$

Now, we evaluate the PDF of $Y_1 = \rho|h_{\mathsf{s},\mathsf{d}}|^2 + \rho|h_{N_b^{\mathrm{th}},\mathsf{d}}|^2$ given $\left|C_L\right| = L$, $L \geq 1$. It is given by

$$f_Y(y) = \int_0^y f_{\rho|h_{\mathsf{s},\mathsf{d}}|^2}(y-\tau) f_{\rho|h_{N_b^{\mathrm{th}},\mathsf{d}}|^2}(\tau) d\tau. \tag{C.8}$$

The PDF of $\rho|h_{N_b^{\mathrm{th}},\mathsf{d}}|^2$ given C_L can be written as [12]

$$f_{\rho|h_{N_b^{\mathrm{th}},\mathsf{d}}|^2}(\tau) = \sum_{l=1}^{L} f_{\rho|h_{l,\mathsf{d}}|^2}(\tau) \sum_{\mathcal{P}} \prod_{j=1}^{L-N} F_{\rho|h_{i_j,\mathsf{d}}|^2}(\tau) \prod_{w=L-N+1}^{L-1} \left(1 - F_{\rho|h_{i_w,\mathsf{d}}|^2}(\tau)\right), \tag{C.9}$$

where $\sum_{\mathcal{P}}$ denotes the summation over all $n!$ permutations $(i_1, i_2, \ldots, i_L)$ of $(1, 2, \ldots, L)$. For Rayleigh fading, the PDF $f_{\rho|h_{l,\mathsf{d}}|^2}(\tau)$ and the CDF $F_{\rho|h_{i_j,\mathsf{d}}|^2}(\tau)$ are respectively given by $\lambda_{l,\mathsf{d}} \exp\left(-\lambda_{l,\mathsf{d}}\tau\right)$ and $1 - \exp\left(-\lambda_{i_j,\mathsf{d}}\tau\right)$. Upon substituting

these statistics in (C.9) and after some algebraic manipulations, we get

$$f_{\rho|h_{N_b^{\text{th}},\mathsf{d}}|^2}(\tau) = \sum_{l=1}^{L} \lambda_{l,\mathsf{d}} \sum_{\mathcal{P}} \exp\left(-\frac{m_{l,\mathsf{d}}}{\Omega_{l,\mathsf{d}}}\tau\right) \Bigg[\exp\left(-C_a\tau\right) + \sum_{q=1}^{L-N} (-1)^q \sum_{s_1<\ldots<s_q} \exp\left(-\left(C_a + C_b\right)\tau\right) \Bigg], \tag{C.10}$$

where $\sum_{s_1<\ldots<s_q} = \sum_{s_1=1}^{L-N-q+1} \sum_{s_2=s_1+1}^{L-N-q+2} \cdots \sum_{s_q=s_{q-1}+1}^{L-N}$, $C_a = \sum_{w=L-N+1}^{L-1} \lambda_{i_w,\mathsf{d}}$, and $C_b = \sum_{n=1}^{q} \lambda_{s_n,\mathsf{d}} + \lambda_{l,\mathsf{d}}$.

Having $f_{Z_1}(z)$ and $f_{Y_1}(y)$ being evaluated, the term $\mathrm{P_r}\left[\gamma_{\mathsf{d}} < u | C_L\right]$ can be obtained as in (5.2).

Now, in evaluating the second term in (3.7) $\mathrm{P_r}\left[C_L\right]$, the CDF of $\gamma_{\mathsf{s},k}$ is required to be obtained first. This SINR can be written as Y_a/Z_b. For Rayleigh fading channels, the PDF of Y_a is $\lambda_{\mathsf{s},k} \exp\left(-\lambda_{s,k}\tau\right)$ and the PDF of Z_b is similar to that found in (C.7) with replacing i_d by i_k and d by k. Having the CDF of $\gamma_{\mathsf{s},k}$ obtained as in (5.3), the term $\mathrm{P_r}\left[C_L\right]$ can be obtained.

C.4 Proof of Theorem 5.4 (for Section 5.5)

In this Appendix, we evaluate the asymptotic outage probability in (5.9). To obtain it, the terms $\mathrm{P_r}\left[\gamma_{\mathsf{d}} < u | C_L\right]$ and $\mathrm{P_r}\left[C_L\right]$ are required to be obtained first. For simplicity we consider the second hops of relays have identical CDFs ($\lambda_{1,\mathsf{d}} = \lambda_{2,\mathsf{d}} = \ldots = \lambda_{K,\mathsf{d}} = \lambda_{R,\mathsf{d}}$).

In deriving the term $\mathrm{P_r}\left[\gamma_{\mathsf{d}} < u | C_L\right]$, as $\rho \to \infty$ and with finite values of ρ_I, I_k, and I_d, the CDF and the PDF of the Exponential distribution can be respectively

approximated as $F_{\rho|h_{m,n}|^2}(\tau) \approx \lambda_{m,n}\tau$ and $f_{\rho|h_{m,n}|^2}(\tau) \approx \lambda_{m,n}$. Based on that, the PDF in (C.9) can be obtained in a closed-form expression as

$$f_{\rho|h_{N_b^{\text{th}},\mathsf{d}}|^2}(\tau) \approx L\binom{L-1}{N-1}\left(\lambda_{R,\mathsf{d}}\right)^{L-N+1}\sum_{k=0}^{N-1}\binom{N-1}{k}(-1)^k\left(\lambda_{R,\mathsf{d}}\right)^k(\tau)^{k+L-N}. \tag{C.11}$$

Now, following the same procedure as in Appendix C.3, the term $\mathrm{P_r}\left[\gamma_{\mathsf{d}} < u|C_L\right]$ in (3.7) can be obtained at high SNR as

$$\begin{aligned}\mathrm{P_r}\left[\gamma_{\mathsf{d}} < u|C_L\right] \approx -L\binom{L-1}{N-1}\frac{\left(\lambda_{\mathsf{d}}^I\right)^{I_d}(-1)^{I_d}\left(\lambda_{R,\mathsf{d}}\right)^{(L-N+1)}}{(I_d-1)!}\lambda_{\mathsf{s},\mathsf{d}}\exp\left(\lambda_{\mathsf{d}}^I\right)\sum_{g=0}^{I_d-1}\binom{I_d-1}{g}\\ \times(-1)^g\sum_{k=0}^{N-1}\binom{N-1}{k}\frac{(-1)^k\Gamma\left(g+k+L-N+3,\lambda_{\mathsf{d}}^I\right)}{(k+L-N+1)(k+L-N+2)}\left(\lambda_{\mathsf{d}}^I\right)^{-(g+k+L-N+2)-1}\left(\lambda_{R,\mathsf{d}}\right)^k\\ \times u^{k+L-N+2}.\end{aligned} \tag{C.12}$$

This expression can be further simplified due to the fact that it is still dominant when $k=0$ and $g=0$. Therefore, the result in (C.12) can be simplified as

$$\begin{aligned}\mathrm{P_r}\left[\gamma_{\mathsf{d}} < u|C_L\right] \approx -L\binom{L-1}{N-1}\frac{\left(\lambda_{\mathsf{d}}^I\right)^{I_d}(-1)^{I_d}\left(\lambda_{R,\mathsf{d}}\right)^{(L-N+1)}}{(I_d-1)!}\lambda_{\mathsf{s},\mathsf{d}}\exp\left(\lambda_{\mathsf{d}}^I\right)\\ \times\frac{\Gamma\left(L-N+3,\lambda_{\mathsf{d}}^I\right)}{(L-N+1)(L-N+2)}\left(\lambda_{\mathsf{d}}^I\right)^{-(L-N+2)-1}u^{L-N+2}.\end{aligned} \tag{C.13}$$

Now, the second term $\mathrm{P_r}\left[C_L\right]$ can be obtained after evaluating the CDF of $\gamma_{\mathsf{s},k}$ which can be approximated as

$$\mathrm{P_r}\left[\gamma_{\mathsf{s},k} < u\right] \approx \lambda_{\mathsf{s},k}\left(1 + \frac{I_k}{\lambda_k^I}\right) u. \tag{C.14}$$

Having (C.13) and (C.14) being evaluated, the asymptotic outage probability can be obtained as in (5.9).

APPENDIX D

APPENDIX FOR CHAPTER 5

D.1 Proof of Lemma 6.1 (for Section 6.4.1)

In this appendix, we derive the outage probability for the i.n.d. case of the Rician/Nakagami-m fading scenario.

To derive the outage probability of γ_{D}, conditioning on X_1 and Y, we first express the CDF of γ_{D} as

$$\begin{aligned} F_{\gamma_{\mathsf{D}}}(\gamma_{\mathsf{out}}) &= \Pr\left(\frac{X_1 X_2}{CY + Y + X_2} \leq \gamma_{\mathsf{out}}\right) \\ &= \int_0^{\infty} \Pr\left(X_2 \leq \frac{\gamma_{\mathsf{out}}\,(y(C+1))}{w - \gamma_{\mathsf{out}}}\right) f_{X_1}(w) f_Y(y) dw dy, \end{aligned} \tag{D.1}$$

where Pr(.) denotes probability, $f_{X_1}(w)$ and $f_Y(y)$ are the PDFs of X_1 and Y, respectively.

With change of variables, (D.1) can be rewritten as

$$F_{\gamma_{\mathsf{D}}}(\gamma_{\mathsf{out}}) = 1 - \int_0^{\infty} \Pr\left(X_2 \geq \frac{\gamma_{\mathsf{out}}(C+1)y}{z}\right) f_{X_1}(z+\gamma_{\mathsf{out}}) f_Y(y)\, dzdy. \quad \text{(D.2)}$$

To evaluate (D.2), the complement CDF of X_2, the PDF of X_1, and the PDF of Y are required, where X_1 and X_2 are non-central chi square distributed RVs with parameters K_1 and $\frac{N_0}{P_0\eta_1}$, K_2 and $\frac{1}{P_r\eta_2}$ respectively, and Y is a summation of independent gamma distributed RVs with parameters m_{I_i} and α_{I_i}.

The CDF of X_2 and the PDF of X_1 are respectively given by

$$F_{X_2}(x) = 1 - Q\left(\sqrt{2K_2}, \sqrt{\frac{2(1+K_2)}{\eta_2}x}\right), \quad \text{(D.3)}$$

$$f_{X_1}(x) = \frac{1+K_1}{\eta_1} \exp\left(-K_1 - \frac{(1+K_1)}{\eta_1}x\right) I_0\left(2\sqrt{\frac{(1+K_1)K_1}{\eta_1}x}\right), \quad \text{(D.4)}$$

where $Q(.,.)$ is the Marcum Q-function and $I_0(.)$ is the Modified Bessel function of first kind and order zero defined in [42, Eq. (8.431.1)]. The PDF of Y is given by (C.2).

Upon substituting the CCDF of X_2 and the PDFs of X_1 and Y in (D.2), we get

$$\begin{aligned} F_X(x) = 1 - \underbrace{\frac{1+K_1\exp(-K_1)}{\eta_1} \sum_{k=0}^{N} \sum_{i=1}^{m_{I_k}} \frac{\beta_k^{i-1} \exp\left(-\frac{1+K_1}{\eta_1}x\right)}{(i-1)!}}_{C_1} \int_0^{\infty} \exp\left(-\frac{1+K_1}{\eta_1}z\right) \\ \times Q\left(\sqrt{2K_2}, \sqrt{\frac{2(1+K_2)x(C+1)y}{\eta_2 z}}\right) I_0\left(2\sqrt{\frac{(1+K_1)K_1}{\eta_1}(z+x)}\right) \\ \times y^{m_{I_k}-1} \exp(-\alpha_{I_k} y)\ dzdy. \end{aligned} \quad \text{(D.5)}$$

Upon using the series representation of the Marcum Q-function in [22, Eq. (4.35)] and that of the Bessel function in [42, Eq. (8.447.1)], we get

$$\begin{aligned} F_X(x) =& 1 - C_1 \exp\left(-K_2\right) \sum_{n=0}^{\infty} K_2^n \sum_{j=0}^{\infty} \frac{K_2^j \left(\frac{(1+K_2)x(C+1)}{\eta_2}\right)^j}{j!\,\Gamma(n+j+1)} \sum_{l=0}^{\infty} \frac{x^l}{(l!)^2} \\ & \times \left(\frac{(1+K_1)K_1}{\eta_1}\right)^l \int_0^{\infty} y^{m_{I_k}+j-1} \exp\left(-\alpha_{I_k} y\right) \sum_{q=0}^{l} \binom{l}{q} x^{-q} \\ & \times \int_0^{\infty} z^{-j+q} \exp\left(-\frac{(1+K_2)x(C+1)y}{\eta_2 z} - \frac{1+K_1}{\eta_1} z\right) dz dy. \end{aligned} \tag{D.6}$$

Now, with the help of [42, Eq. (3.471.9)] and [42, Eq. (6.643.3)], and after some algebraic manipulations, we obtain the result in (6.4).

D.2 Proof of Lemma 6.2 (for Section 6.4.3)

In this appendix, we derive the outage probability and the SEP for the Rayleigh/Nakagami-m special case of the Rician/Nakagami-m fading scenario at high SNR values.

Upon letting $K_1 = K_2 = 0$ and taking only the first term of each summation as they are still dominant and using [53, Eq. (13.1.33)], the result in (6.6) can be rewritten in terms of the Tricomi hypergeometric function as

$$\begin{aligned} P_{\mathsf{out}} =& 1 - \Gamma(Nm_I + 1) \exp\left(-\frac{\gamma_{\mathsf{out}}}{\bar{\gamma}_1}\right) \left(\frac{\Omega_I(C+1)}{\bar{\gamma}_1 \bar{\gamma}_2} \gamma_{\mathsf{out}}\right) \\ & \times \Psi\left(Nm_I + 1, 2; \frac{\Omega_I(C+1)}{\bar{\gamma}_1 \bar{\gamma}_2} \gamma_{\mathsf{out}}\right), \end{aligned} \tag{D.7}$$

where $\Psi(.,;.)$ is the Tricomi hypergeometric function defined in [53, Eq. (13.1.6)]. Now, with the help of [53, Eq. (13.1.29)], the last result can be further simplified to

$$P_{\mathsf{out}} = 1 - \Gamma(Nm_I + 1) \exp\left(-\frac{\gamma_{\mathsf{out}}}{\eta_1}\right) \Psi\left(Nm_I, 0; \frac{\Omega_I(C+1)}{\eta_1\eta_2}\gamma_{\mathsf{out}}\right). \tag{D.8}$$

Upon letting $\eta_2 = \mu\eta_1$ and substituting the value of $(C+1) \approx C$ in (D.8), we get

$$P_{\mathsf{out}} = 1 - \Gamma(Nm_I + 1) \exp\left(-\frac{\gamma_{\mathsf{out}}}{\eta_1}\right) \Psi\left(Nm_I, 0; \frac{\Omega_I\sigma_{\mathsf{sr}}^2}{\mu\eta_1}\gamma_{\mathsf{out}}\right). \tag{D.9}$$

As $\eta_1 \to \infty$, by using the Taylor expansion of the exponential function $\exp(-x) \approx \left(1 - \frac{x}{1!} + o\left(x^2\right)\right)$ and the asymptotic expression of the Tricomi function $\Psi(b, 0; x) \approx \frac{1}{\Gamma(b+1)}\big(1 + b\left[\ln x + \psi(b+1) + 2c - 1\right] x + o\left(x^2\right)\big)$, where $\psi(\cdot)$ is the digamma function and $c = 0.577215$ is the Euler-Mascheroni constant. By ignoring the high power terms $o\left(x^2\right)$ in these approximations and after some algebraic manipulations, the outage probability at high SNR values can be obtained as in (6.10). Having the outage probability and hence, the CDF being evaluated, using (6.7), the SEP at high SNR values can be obtained as in (6.11).

Bibliography

[1] J. G. Proakis, *Digital Communications*, 5th Edition New York: McGraw- Hill, Inc., 2007.

[2] Z. Lin and E. Erkip, "Cooperative regions for coded cooperative systems," in *Proc. of IEEE Global Telecommun. Conf.*, 2004. Dallas, TX, USA.

[3] I. E. Telatar. (1995) Capacity of Multi-Antenna Gaussian Channels, Tech. Rep. Bell Labs, Lucent Technologies. [Online]. Available: http://mars.bell-labs.com/papers/proof/proof.pdf

[4] A. Narula, M. D. Trott, and G.W.Wornell, "Performance limits of coded diversity methods for transmitter antenna arrays," *IEEE Trans. Inf. Theory*, vol. 45, pp. 24182433, Nov. 1999.

[5] T. M. Cover and A. A. El Gamal, "Capacity theorems for the relay channel," *IEEE Trans. Inf. Theory*, vol. IT-25, pp. 572-584, Sept. 1979.

[6] J. N. Laneman, D. N. C. Tse and G. W. Wornell, "Cooperative diversity in wireless networks: efficient protocals and outage behavior," *IEEE Trans. Inf. Theory*, vol. 50, no. 12, pp. 3062-3080, Dec. 2004.

[7] A. Sendonaris, E. Erkip, and B. Aazhang, "Increasing uplink capacity via user cooperation diversity," in *Proc. IEEE Int. Symp. Inf. Theory (ISIT)*, Cambridge, MA, Aug. 1998, p. 156.

[8] A. Bletsas, A. Lippman, and D. P. Reed, "A simple distributed method for relay selection in cooperative diversity wireless networks based on reciprocity and channel measurements," in *Proc. 61st IEEE Semiannu. Veh. Tech. Conf.*, vol. 3, Stockholm, Sweden, May 30-Jun. 1 2005, pp. 1484-1488.

[9] I. Krikidis, J. Thompson, S. McLaughlin, and N. Goertz, "Amplify-and-forward with partial relay selection," *IEEE Commun. Lett.*, vol. 12, no. 4, April 2008.

[10] D. da Costa and S. Aïssa, "End-to-end performance of dual-hop semi-blind relaying systems with partial relay selection," *IEEE Trans. on Wireless Commun.*, vol. 8, no. 8, August 2009.

[11] V. Bao, L. Cuong, and H. Kong, "Performance analysis of threshold-based relaying with partial relay selection over Rayleigh fading channels," *Int. Conf. on Adv. Tech. for Commun.*, Vietnam, 20-22 Oct. 2010, pp. 172-177.

[12] S. Ikki and M. Ahmed, "On the performance of amplify-and-forward cooperative diversity with the Nth best-relay selection scheme," *IEEE Int. Conf. on Commun.*, Dresden, Germany, June 14-18 2009, pp. 1-6.

[13] H. Suraweera, D. Michalopoulos and G. Karagiannidis, "Semi-blind amplify-and-forward with partial relay selection," *Electronics Lett.*, March 2009, 45, (6), pp. 317-319.

[14] H. Lateef, M. Ghogho, and D. McLernon, "Performance analysis of Kth opportunistic relaying over non-identically distributed cooperative paths," *IEEE SPAWC*, Marakkech, Morocco, 2010, pp. 1-5.

[15] H. Yang and M. Alouini, "Performance analysis of multi-branch switched diversity systems," *IEEE Veh. Tech. Conf. (VTC'2002 Spring)*, Birmingham, England, May 2002, pp. 846-850.

[16] H. Yu, I. Lee, and G. Stüber, "Outage probability of decode-and-forward cooperative relaying systems with co-channel interference," *IEEE Trans. on Wireless Commun.*, vol. 11, no. 1, Jan. 2012.

[17] J. Kim and D. Kim, "Exact and closed-form outage probability of opportunistic decode-and-forward relaying with unequal-power interferers," *IEEE Trans. on Wireless Communs.*, vol. 9, no. 12, Dec. 2010.

[18] S. Ikki and S. Aïssa, "Impact of imperfect channel estimation and co-channel interference on regenerative cooperative networks," *IEEE Wireless Commun. Lett.*, Accepted for publication.

[19] R. Dohler, E. Lefranc, and H. Aghvami, "Space-time block codes for virtual antenna arrays," *Int. Conf. on Telecommun.*, France, 23 2003-March 1 2003, pp. 198-203.

[20] C. Zhong, S. Jin, and K. Wong, "Outage probability of dual-hop relay channels in the presence of interference," *IEEE Veh. Tech. Conf.*, Spring, 2009, pp. 1-5.

[21] F. Al-Qahtani, C. Zhong, K. Qaraqe, H. Alnuweiri, and T. Ratnarajah, "Performance analysis of fixed-gain AF dual-hop relaying systems over Nakagami-m fading channels in the presence of interference," *EURASIP J. on Wireless Commun. and Net.*, Dec. 2011.

[22] M. K. Simon and M.-S. Alouini, *Digital Communication over Fading Channels*, 2nd Edition, Wiley, 2005.

[23] G. L. Stüber, *Principles of Mobile Communications*. Norwell, MA: Kluwer Academic Publishers, 1996.

[24] A. Sendonaris, E. Erkip, B. Aazhang, "User cooperation diversity, Part I: System description," *IEEE Trans. on Commun.*, 2003, 51, (11), pp. 1927-1938.

[25] Y. Zhao, R. Adve and T. Lim, "Improving amplify-and-forward relay networks: optimal power allocation versus selection," *IEEE Int. Symp. on Inf. Theory*, Seattle USA, 9-14 July 2006, pp. 1234-1238.

[26] M. Torabi, D. Haccoun, and W. Ajib, "Performance analysis of cooperative diversity with relay selection over non-identically distributed links," *IET Commun.*, 2010, 4, (5), pp. 596-605.

[27] Y. Jing and H. Jafarkhani, "Single and multiple relay selection schemes and their achievable diversity orders," *IEEE Trans. on Wireless Commun.*, 2009, 8, (3), pp. 1414-1423.

[28] Y. Chen, C. Wang, and D. Yuan, "Novel partial selection schemes for AF relaying in Nakagami-m fading channels," *IEEE Trans. on Veh. Tech.*, 2011, 60, (7), pp. 3497-3503.

[29] F. Etezadi, K. Zarifi, A. Ghrayeb, and Sofiène Affes, "Decentralized relay selection schemes in uniformly distributed wireless sensor networks," *IEEE Trans. on Wireless Commun.*, 2012, 11, (3), pp. 938-951.

[30] Kyu-Sung Hwang and Young-Chai Ko, "An efficient relay selection algorithm for cooperative networks," in *IEEE Veh. Tech. Conf. (VTC Fall)*, Baltimore, USA, 30 Sep.-3 Oct. 2007, pp. 81-85.

[31] Kyu-Sung Hwang and Young-Chai Ko, and Mohamed-Slim Alouini, "A study of multi-hop cooperative diversity system," in *Asia-Pacific Conf. on Commun.*, Busan, Republic of Korea, 31 Aug.-2 Sep. 2006, pp. 1-5.

[32] A. Gharanjik K. Mohamed-pour, "Switch-and-stay partial relay selection over Rayleigh fading channels," *IET Commun.*, 2011, 5, (9), pp. 11991203.

[33] F. Gaaloul R. Radaydeh M. Alouini, "Switched diversity strategies for dual-hop amplifyand- forward relaying systems," *IET Commun.*, 2012, 6, (12), pp. 1651-1661.

[34] A. Bletsas, H. Shin, M. Z. Win, and A. Lippman, "A simple cooperative diversity method based on network path selection," *IEEE JSAC*, 2006, 24, (3), pp. 659-672.

[35] S. S. Ikki and M. H. Ahmed, "Performance analysis of adaptive decode-and-forward cooperative diversity networks with the best relay selection scheme," *IEEE Trans. on Commun.*, 2010, 58, (1), pp. 68-72.

[36] H. Mheidat and M. Uysal, "Impact of receive diversity on the performance of amplify-and-forward relaying under APS and IPS power constraints," *IEEE Commun. Lett.*, vol. 10, pp. 468-470, June 2006.

[37] T. A. Tsiftsis, G. K. Karagiannidis, P. T. Mathiopoulos, and S. A. Kotsopoulos, "Nonregenerative dual-hop cooperative links with selection diversity," *Eurasip J. Wireless Commun. and Networking*, pp. 1-8, 2006.

[38] D. Senaratne and C. Tellambura, "Unified performance analysis of two hop amplify and forward relaying," in *Proc. IEEE ICC 2009*, Dresdn, Germany, June 2009, pp. 1-5.

[39] H. A. Suraweera, H. K. Garg, and A. Nallanathan, "Performance analysis of two hop amplify-and-forward systems with interference at the relay," *IEEE Commun. Lett.*, vol. 14, no. 8, pp. 692694, Aug. 2010.

[40] N. Milošević, Z. Nikolić, B. Dimitrijević, "Performance analysis of dual hop relay link in Nakagami-m fading channel with interference at relay," *22nd Int. Conf. Radioelektronika*, April 2011, pp. 1-4.

[41] F. S. Al-Qahtani, T. Q. Duong, C. Zhong, K. A. Qaraqe, and H. Alnuweiri, "Performance analysis of dual-hop AF systems with interference in Nakagami-m fading channels," *IEEE Signal Proc. Lett.*, vol. 18, no. 8, August 2011.

[42] I. S. Gradshteyn and I. M. Ryzhik, *Tables of Integrals, series and Products*, 6th ed., San Diago: Acadamic Press, 2000.

[43] D. B. da Costa, H. Ding, and J. Ge, "Interference-limited relaying transmissions in dual-hop cooperative networks over Nakagami-m fading," *IEEE Commun. Lett.*, vol. 15, no. 5, May 2011.

[44] R. Prasad, A. Kegel, and M. Loog, "Cochannel interference probability for picocellular system with multiple Rician faded interferers," *Electronic Lett.*, Nov. 1992, vol. 28, no. 24, pp. 2225-2226.

[45] M. Hasna and M. Alouini, "Harmonic mean and end-to-end performance of transmission systems with relays," *IEEE Trans. on Commun.*, vol. 52, no. 1, Jan. 2004.

[46] W. Xu, J. Zhang, and P. Zhang, "Outage probability of two-hop fixed-gain relay with interference at the relay and destination," *IEEE Commun. Lett.*, to be published.

[47] D. B. da Costa and M. D. Yacoub, "Outage performance of two hop AF relaying systems with co-channel interferers over Nakagami-m fading," *IEEE Commun. Lett.*, vol. 15, no. 9, Sep. 2011.

[48] S. Chen, X. Zhang, Fa. Liu, and D. Yang, "Outage performance of dual-hop relay network with co-channel interference," in *IEEE Veh. Tech. Conf.*, Spring, 2010, pp. 1-5.

[49] S. S. Ikki and S. Aïssa, "Performance analysis of dual-hop relaying systems in the presence of co-channel interference," *IEEE Globecom Telecommun. Conf.*, Miami, Florida, Dec. 2010.

[50] A. Cvetković, G. Dordević, and M. Stefanović, "Performance of interference-limited dual-hop non-regenerative relays over Rayleigh fading channels," *IET Commun.*, vol. 5, iss. 2, pp. 135140, 2011.

[51] D. da Costa and M. Yacoub, "Dual-hop DF relaying systems with multiple interferers and subject to arbitrary Nakagami-m fading," *Electronics Lett.*, Aug. 2011, pp. 999-1001.

[52] H. A. Suraweera., D. S. Michalopoulos, R. Schober, G. K. Karagiannidis, and Arumugam Nallanathan, "Fixed gain amplify-and-forward relaying with co-channel interference," in *Proc. IEEE ICC 2011*, Kyoto, Japan, June 2011, pp. 1-6.

[53] M. Abramowitz and I. A. Stegun, *Handbook of Mathematical Functions with Formulas, Graphs, and Mathematical Tables*. New York, NY: Dover Publications, 9th Edition, 1970.

Vitae

- Name: Anas (M.A.) Ata Salhab
- Nationality: Palestinian
- Date of Birth: March 29, 1981
- Email: *salhab@kfupm.edu.sa*
- Permenant Address: Hebron, Palestine